RESPONSE OF STEEL AND COMPOSITE BEAMS SUBJECTED TO COMBINED SHEAR AND FIRE LOADING

By

Mohannad Zeyad Naser

A DISSERTATION

Submitted to
Michigan State University
in partial fulfillment of the requirements
for the degree of

Civil Engineering—Doctor of Philosophy

2016

ABSTRACT

RESPONSE OF STEEL AND COMPOSITE BEAMS SUBJECTED TO COMBINED SHEAR
AND FIRE LOADING

By

Mohannad Zeyad Naser

Civil infrastructures are built to last for several decades and hence, they are subjected to various types of loading during their service lives, including fire hazard. Thus, provision of fire safety measures to structural members is one of the primary considerations in the design of civil infrastructure. Since structural members, made of steel, exhibit lower fire resistance due to high thermal conductivity and rapid degradation of strength and stiffness properties of steel, they are vulnerable to fire-induced damage or collapse. Therefore, the behavior of steel and composite beams, under fire conditions, is of critical concern from fire safety point of view.

In contrast to current design philosophy at room temperature, where steel and composite beams are to be designed for flexural limit state and then checked for shear resistance, fire design of such beams is carried out based on flexural limit state only. This design philosophy for fire resistance evaluation may not be conservative or realistic under certain scenarios where shear forces are dominant or shear capacity degrades at a rapid pace under fire. Further, there is limited data and understanding in literature on the mechanism of shear failure in steel and composite beams under combined effects of shear and fire loading.

To overcome some of the limitations in current design philosophy with respect to shear limit state, a research program involving experimental and numerical studies on the fire response of steel and composite beams/girders is undertaken. Four composite beams were tested under simultaneous loading and fire exposure to study their flexural and shear behavior. Each of these composite beams is made of uninsulated standard hot-rolled steel section, compositely attached

to a concrete slab through shear studs. The main test variables included; level of composite action, type, and magnitude of loading. Results from fire tests indicate that composite beams can experience failure under standard fire conditions in about 30-50 minutes and their response is highly influenced by type of loading and development of sectional instability.

As part of numerical studies, a finite element model was developed in ANSYS for tracing thermal and structural response of beams under combined effects of structural loading and fire conditions. The developed model specifically accounts for geometric and material nonlinearities, temperature-dependent material properties, shear effect, sectional and global instability, composite action, and various failure limit states. This model was calibrated utilizing test data generated from fire experiments. The validated model was applied to carry out detailed parametric studies to quantify critical factors influencing response of steel and composite beams under dominant shear and fire loading such as, sectional instability; web slenderness; load level; fire severity; loading configuration (type); level of composite action; shear stud stiffness; and thickness of concrete slab.

Results from experimental and parametric studies are utilized to derive an approach for evaluating degrading shear capacity in fire-exposed steel and composite beams. This methodology accounts for temperature-induced degradation in materials, as well as sectional instability and level of composite action offered by concrete slab in evaluating shear capacity in beams. This methodology is combined with flexural capacity calculations, available in literature, to propose a unified approach for design (and analysis) of fire-exposed steel and composite beams. The proposed unified approach can be applied to fire design of steel and composite beams or girders subjected to wide ranging scenarios including dominant shear and fire loading.

To my parents, siblings and innocent souls lost to fire.

ACKNOWLEDGMENTS

Mohannad Zeyad Naser

2016

TABLE OF CONTENTS

LIST OF TABLES

LIST OF FIGURES

KEY OF SYMBOLS

A_c = Area of concrete slab

A_s = Area of steel section

A_{sc} = Shear stud cross sectional area

D_{slab} = Thickness of concrete slab

F_u = Minimum tensile strength of studs

$Q_{n,T}$ = Shear strength of shear studs at temperature, T

R_g, R_b = slab factors

V_c = Contribution of concrete slab to shear capacity

V_s = Contribution of steel beam to shear capacity

b_f = Width of steel flange

$f'_{c,T}$ = Compressive strength of concrete at temperature, T

f'_c = Compressive strength of concrete

A_w = Area of steel web = dt_w

C = Level of composite action

C_v = Web shear coefficient that depends on slenderness of web

$C_{v,T}$ = Temperature-dependent web shear coefficient

d = Overall depth for hot-rolled beams

f_y = Yield strength of steel section

$f_{y,T}$ = Yield strength of steel section at temperature, T

K = Stiffness of shear studs

t_w = Thickness of the web

Z_x = Plastic section modulus

β = Slenderness parameter

σ_1, σ_2 and σ_3 = Tensile and compressive stresses in the three principle directions that act in the three mutually perpendicular planes of zero shear

σ_y = Yield stress that to be compared with the uniaxial value yield stress f_y

τ_{yw} = Shear yield strength of the steel web ($\tau_{yw} = 0.6 f_{yw}$)

φ = Strength reduction factor at ambient conditions

φ_f = Strength reduction factor under fire conditions

y = moment arm of the couple formed by $A_s f_y$ and $0.85 f_c' A_c$

CHAPTER ONE

1. Introduction

1.1 General

Civil infrastructure, including buildings and bridges, are built to last for several decades. Over their life-span, these structures are subjected to various types of structural loading and hazards, such as fire. The increased number of fires in high-rise buildings and civil infrastructure, in recent years, due to rapid urbanization and increased use of combustible materials in buildings and other occupancies, makes fire to be a critical design parameter (Kodur et al., 2012; Garlock et al., 2012). This is because fire is a destructive event, and can threaten integrity and stability of structural systems, in addition to loss of life and property damage (Bajwa et al. 2012).

In high-rise buildings and bridges, structural framing typically comprises of steel beams/girders connected together by joints. Under fire conditions, steel structural members exhibit lower fire resistance due to rapid rise in steel temperatures (resulting from high thermal conductivity and low specific heat) as well as faster degradation of strength and modulus properties of steel at elevated temperatures. Thus, steel structural members can rapidly lose much of their load carrying capacity under fire conditions. Such rapid degradation in steel properties makes steel structural members to be highly vulnerable to fire-induced damage and collapse (Kodur and Naser, 2013; André Reis et al., 2015).

Flooring in steel framed buildings typically comprise of concrete slab (deck slab) overlaid on the steel beam (or girder) and connected via a number of shear studs and this type of system is referred to as composite beams throughout this thesis. These shear studs facilitate transfer of forces from steel beam to concrete slab. Thus, both steel beam and concrete slab act together as one unit through composite interaction. In such an arrangement, the steel beam is

designed to resist tensile forces and concrete slab is preferably designed to resist compressive forces. Since concrete possess better fire resistance than steel, due to its low thermal conductivity and high specific heat, the fire performance of a composite beam tends to be much higher than a bare steel beam under most fire conditions.

Steel and composite beams are subjected to bending moment and shear forces due to gravity loading. In typical building applications, the dominant loading on beams consist of bending moment and thus the primary consideration in room temperature design of beams is for flexure (bending moment). Thus, the flexural response of steel and composite beams under fire conditions is of primary concern and has been thoroughly investigated in the last five decades (Bletzacker, 1966; Wainman and Kirby, 1989; Shanmugam and Baskar, 2003; Alinia et al., 2009; Aziz et al., 2016). However, there has been little to limited research on steel and composite beams under dominant shear loading and fire exposure. Since shear loading can lead to sudden and brittle failure under shear limiting state, the current approach of designing fire-exposed steel and composite beams based on flexural limit state alone may not be conservative in situations where shear loadings are dominant or shear capacity degrades at a rapid pace with fire exposure time.

1.2 Response of Steel Beams under Fire Conditions

1.2.1 General

The response of a steel or composite beam (or girder) under fire conditions can vary significantly based on the geometry of steel section and concrete slab, rate of temperature progression in steel section under fire exposure, and type and magnitude of loading. Under fire conditions, most structural members including beams are typically subjected to a loading equivalent to 40-50% of their flexural capacity at room temperature. This magnitude of applied

loading remains same throughout fire exposure. Under fire exposure, capacity (both flexural and shear) of beams degrade due to temperature-induced strength and modulus degradation in steel and composite beams. Failure is said to occur when the flexural capacity drops below bending moment resulting from gravity loading present under fire condition. This is typically what occurs in most common scenarios and is what is considered in current practice.

However, under certain loading configurations, the effect of shear force can be much larger than that of bending moment. Shear capacity can degrade at a much faster pace than flexural capacity due to rapid rise in temperature in web due to web having larger (exposed) surface area resulting from larger slenderness of web. Failure of beams under such loading can occur when the shear capacity drops below the level of shear force which usually occur prior to attaining full flexural capacity (Kodur and Naser, 2013; Naser and Kodur, 2015; Reis et al., 2015). This type of behavior, where shear in beams failure can occur under fire conditions is quite complex and further articulated below.

1.2.2   Main Factors Governing Fire Response of Beams

The effect of various influencing factors such as geometric and material consediration, connection configuration, and restraint effects on the fire resistance of beams have been thoroughly studied (Chapman and Balakrishnan, 1964; Bailey et al., 1999; Franssen et al., 2009; Dwaikat and Kodur, 2010). However, critical factors such as type of loading, sectional instability (sectional characteristics) and composite action that develops between concrete slab and steel beam that affect the flexural or shear are not well studied. A detailed discussion on these factors is provided in the following sections.

1.2.2.1 Effect of Loading Type

The type of loading (i.e., loading configuration) can significantly affect the response of steel and composite beams at room and fire conditions. For instance, type of loading dictates the internal distribution of forces and resistance mechanism needed to resist such loading. A beam loaded with dominant flexural loading (representative of uniformly distributed loading on beams) with low shear effect is more likely to fail under fire conditions due to flexural capacity exceeding bending moment (since applied shear force is very small compared to shear capacity of the beam). Although bending moment can be predominant in most loading applications, shear effect can be predominant in some loading situations. Some of these situations where shear loading can be dominant is in transfer girders, beams with reduced cross-sectional area (coped beams), deep beams and plate girders (with slender webs).

The effect of loading type on response of a beam is illustrated by tracing response of a typical steel beam from loading stage to failure under fire exposure. Figure 1.1 shows a simply supported beam subjected to two different loading scenarios. In the first scenario, the beam is subjected to uniformly distributed loading (UDL), where the flexural effects (bending moment) are dominant. In the second case, the beam is subjected to two dominant point loads near end supports and minimal level of UDL. Under this loading configuration, shear force is dominant at support sections and the level of bending moment at mid-span may not be critical.

It is clear from Figure 1.1, that the bending and shear force distribution is different for each loading scenario (due to the different loading configuration) at room temperature. This distribution of bending and shear force, under fire exposure, is similar to that at room temperature but slightly reduced to account for the reduction of applied loading (which is 40-50% of room temperature capacity) at fire conditions. However, since moment and shear

4

capacity (i.e., resistance) that develops in the beam are independent of the type of loading, this beam develops similar (and a uniform) level of moment and shear capacity under both loading scenarios. This moment and shear capacity degrades with fire exposure time, as seen in Figure 1.1a and 1.1b.

In the case of a beam subjected to uniformly distributed loading (UDL), typically failure occurs when the applied bending moment exceeds the moment capacity at the mid-span section as shown in Figure 1.1a. Even under fire conditions, flexural effects govern the failure in this beam and; the beam fails when decreasing moment capacity at the critical section (mid-span) falls below that of the applied bending moment. This is mainly due to the fact that the beam has high reserve shear capacity (higher than applied shear force) even at 2 hours of fire exposure.

On the other hand, Figure 1.1b shows the same beam, but is subjected to high level of shear force (as compared to flexural forces) at end supports (i.e., critical sections). Thus, under fire conditions failure occurs due to shear capacity dropping below the applied shear force. As seen in Figure 1.1b, this occur prior to onset of flexural limit state. Since the beam has sufficient reserve moment capacity, the beam attains shear failure when the rapidly degrading shear capacity exceeds shear force at the critical section.

1.2.2.2 Effect of Sectional Instability

Steel beams/girders are usually made of I-shaped (W-shaped) sections, where webs in these sections are usually thinner and deeper (more slender) than flanges. These beams are optimized to attain higher flexural capacity, which is often the primary design consideration at room temperature, by providing much thicker flanges as compared to webs (to increase moment of inertia and related section modulus). Under fire conditions, such slender webs experience

rapid rise in temperature; since they are very thin and exposed to fire from two sides (larger surface area). Hence, strength and modulus properties of steel in the web degrade at a higher rate than that in flanges. In such scenario, shear capacity (i.e., shear resistance) of a steel beam will degrade at a higher rate than corresponding flexural capacity since web is the main contributor to shear capacity.

Because I-shaped steel sections are fabricated using welded thin plates (namely two flanges and a web), the response of such steel beams can be highly influenced by the onset of local buckling in flanges or web (at critical sections). This fact is well recognized in codes and standards and is taken into account while evaluating flexural and shear capacity at room temperature (AISC, 2011; Eurocode, 2003). For example, AISC (2011) design manual, classifies sections used in steel structures as compact, non-compact and slender based on sectional slenderness (width-to-thickness ratio (λ)) of flange and web as compared to their material characteristics (yield strength and elastic modulus). This slenderness ratio of flange or web is usually compared against two upper limits; compact (λ_p) and non-compact (λ_r) to determine the stability of the section against local buckling. If the sectional slenderness (λ) is less than compact limit, then the section is considered compact. However, if λ lies in between compact and non-compact limits, the section is classified as non-compact. Finally, a slender section is that with λ exceeding the limit of non-compactness.

Table 1.1 presents the compact (λ_p) and non-compact (λ_r) width-to-thickness limiting ratios under flexural and shear limit states for I-shaped steel sections at room temperature. It can also be seen from Table 1.1 that slenderness limits are a function of elastic modulus (E) and yield strength properties (f_y) of steel. Hence, in a steel beam exposed to fire, rise in temperature will induce loss of yield strength and elastic modulus in steel which starts to degrade at about

400 and 150˚C, respectively (see Figure 1.2 and Figure 1.3). Not only that, but these properties also degrade at different rates. It should be noted that current design provisions provide no recommendations for classification of steel beams based on compactness under fire conditions. In fact, local buckling (sectional instability) is not considered in the fire design of steel beams/girders due to the lack of research.

The effect of sectional instability on shear capacity of a steel beam subjected to fire loading is shown in Figure 1.4. It can be seen from this figure that the bending moment after 2 hours of fire exposure is lower than moment capacity of this beam, thus the beam does not fail in flexural mode. However, shear capacity after 2 hours of fire exposure falls below that of shear forces due to loading, leading to failure of this beam in shear limit state. Additionally, when instability effects are considered, shear capacity further reduces as a result of temperature-induced instability losses (web local buckling). Thus, degradation in shear capacity is governed by temperature-induced strength degradation as well as temperature-induced web local buckling. The combined effect of temperature-induced strength degradation and web local buckling can accelerate shear failure under fire conditions. Since elastic modulus properties starts to degrade earlier than yield strength properties (and at a faster pace), local buckling phenomenon in a steel section can start when steel temperature exceeds 150˚C. This further reduction in shear capacity can lead to earlier failure time (than that due to flexural effects).

1.2.2.3   Effect of Composite Action

In a composite beam, steel beam is typically attached to concrete slab via a number of shear studs. This number of shear studs can be varied to achieve a certain level of composite action. The addition of concrete slab can enhance flexural and shear capacity as well as stiffness of structural member at room temperature. Such enhancement to flexural and shear capacity can

be very beneficial under fire conditions as well, especially when strength and elastic modulus of steel start to degrade. Another benefit of adding a concrete slab is that it can act as a heat sink (due to low thermal conductivity and high specific heat of concrete) which draws heat from steel beam towards the slab (i.e., away from the top flange). This heat sink effect keeps the temperature in flange low and thus enhances flexural capacity and fire resistance of steel beam.

Unfortunately, in current fire design provisions, the positive contribution of concrete slab are only accounted for in evaluating flexural capacity of composite beams and neglected in shear capacity. For example, AISC design manual (2011) states that web of steel beam is assumed to provide the needed shear capacity in a composite beam. Hence, according to these provisions, the shear capacity of a composite beam is similar to that of a steel beam. It is clear that such assumption lacks rational and fundamental reasoning.

In order to illustrate the positive contribution of concrete slab to shear capacity of a composite beam, Figure 1.5 shows a comparative response between a steel beam and a composite beam at room and fire conditions. It is clear from Figure 1.5a that accounting for composite action (arising from concrete slab) can significantly enhance flexural and shear capacity in a composite beam at room temperature. Similarly, data plots in Figure 1.5, also show that shear capacity of a composite beam is much higher than that of in a steel beam (without slab). This improvement can also be seen when this beam is exposed to fire conditions where accounting for composite action can extend failure time.

1.3 Objectives and Scope of this Research

The main goals of this research is aimed at developing a fundamental understanding on the response of steel and composite beams (and girders) subjected to combined shear and fire

loading through comprehensive experimental, numerical and analytical studies. The following research objectives were undertaken to accomplish these goals:

- Carry out a detailed state-of-the-art literature review on the response of fire-exposed steel and composite beams/girders[*] and identify relevant knowledge gaps in literature. The comprehensive review will cover both experimental and numerical studies as well as current provisions in codes and standards.

- Undertake fire resistance experiments on typical composite beams (used in buildings and bridges) to generate needed data for tracing the behaviour of steel composite beams under fire conditions.

- Develop a numerical model to trace the response of a typical composite beam subjected to combined shear and fire loading using the commercially available finite element program, ANSYS. The developed model will account for temperature-dependent properties of constituent materials, geometric and material nonlinearities, various level of composite action, instability effects, as well as nonlinear contact interaction between steel and concrete slab.

- Validate the above developed numerical model by comparing response predictions from the model with test data obtained from fire resistance experiments on composite beams.

- Carry out parametric studies to quantify the effect of critical factors, such as sectional instability, web slenderness, type and magnitude of loading, fire severity, level of composite action, shear stud stiffness and thickness of concrete slab on the response of steel and composite beams under combined effect of shear and fire loading.

---

[*] The terms "beam" and "girder" are interchangeably used in this thesis

- Derive an approach that can be used for evaluating shear capacity of steel and composite beams. This approach needs to account for property degradation of constituent materials, temperature-induced sectional instability and level of composite action offered by concrete slab in evaluating shear capacity in beams.

- Develop a unified approach for optimum fire design of steel and composite beams taking into account fire-induced material degradation, fire-induced instability, level of composite action and all possible failure limit states. This approach considers flexural and shear effect and can be used to optimally design (and analyze) steel and composite beams especially when subjected to dominant flexural or shear loading and fire conditions.

Table 1.1: Width-to-thickness limiting ratios for flexural and shear strength evaluation of I-shaped sections

Element	Slenderness (λ)	Limiting value			
		Flexural capacity		Shear capacity	
		λ_p	λ_r	$\lambda_p{}^*$	$\lambda_r{}^{**}$
Flange	$b_f/2t_f$	$0.38\sqrt{\dfrac{E}{f_y}}$	$1.0\sqrt{\dfrac{E}{f_y}}$	-	-
Web	h/t_w	$3.76\sqrt{\dfrac{E}{f_y}}$	$5.70\sqrt{\dfrac{E}{f_y}}$	$1.10\sqrt{\dfrac{k_v E}{f_y}}$	$1.37\sqrt{\dfrac{k_v E}{f_y}}$

b_f is flange width; t_f is the flange thickness; h is the depth of section and t_w is the web thickness.

*limit of inelastic web buckling, ** limit of elastic web buckling, kv is 5 for unstiffened webs with $\lambda \leq 260$
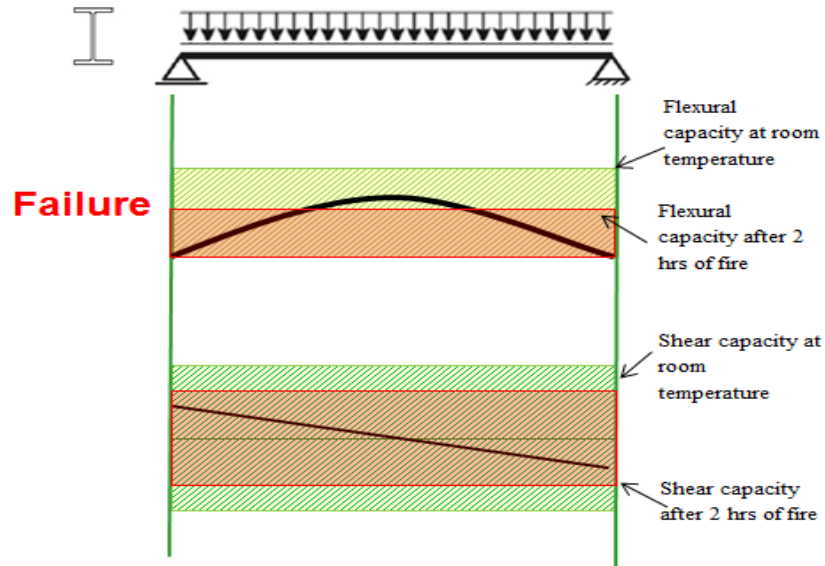
(a) Beam with low to moderate shear forces under ambient and fire
conditions
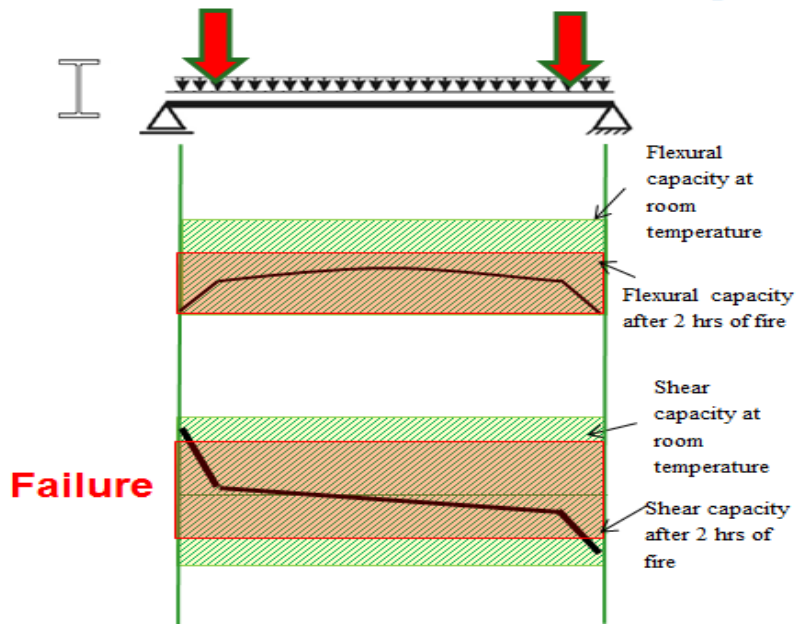
(b) Beam with high shear forces under ambient and fire conditions

(▨▨▨ Capacity at room temperature, ▭ Capacity under fire conditions)

Figure 1.1: Effect of temperature on flexural shear force in a steel beam under different loading
scenarios
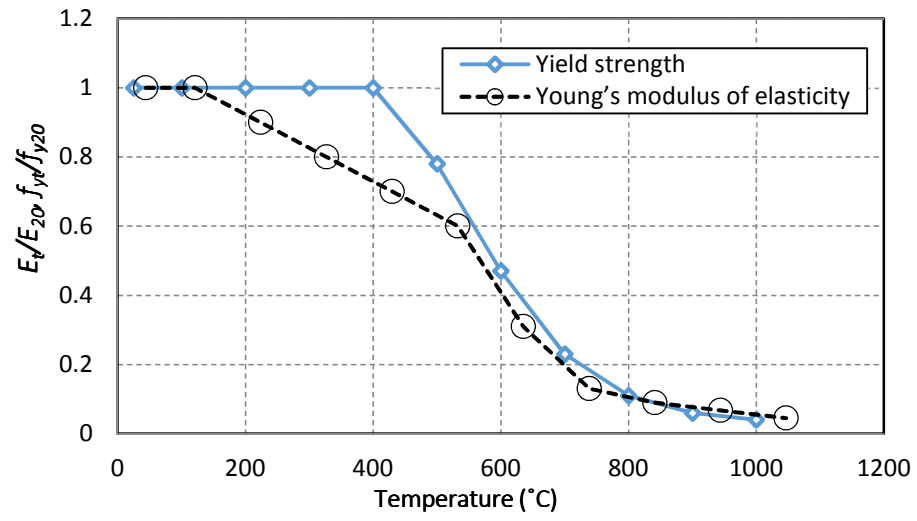
Figure 1.2: Degradation of strength and elastic modulus properties of steel at elevated temperatures
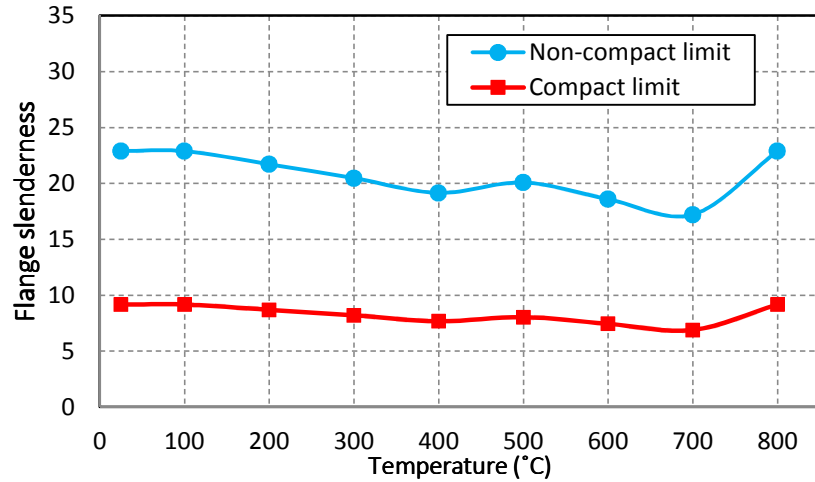
(a) flange slenderness limits for flexural calculation
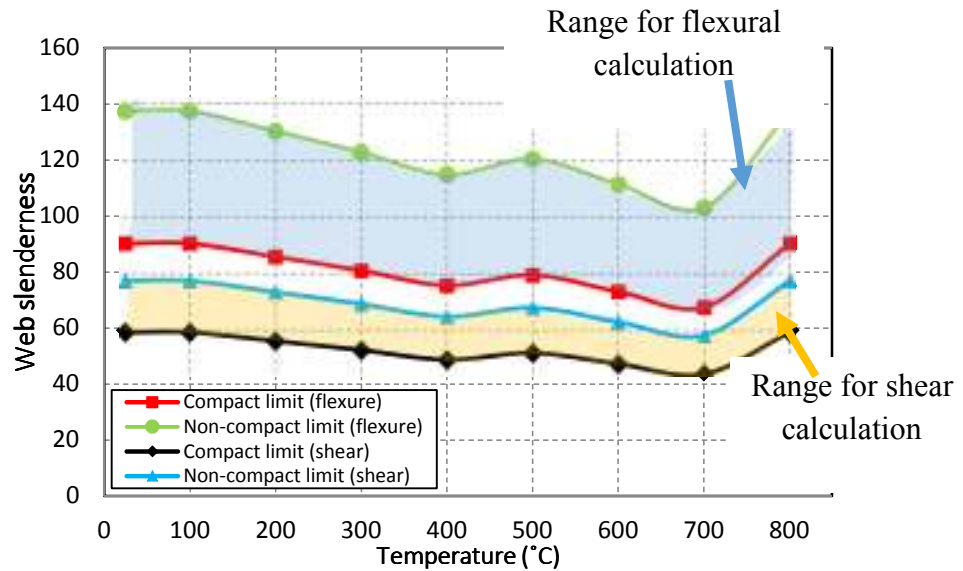
(b) web slenderness limits for flexural and shear calculations

Figure 1.3: Variation of slenderness limits adopted in flexural and shear design at elevated temperatures

(▨ Capacity at room temperature, ▬ Capacity under fire conditions (without local buckling), ▬ Capacity under fire conditions (with local buckling))
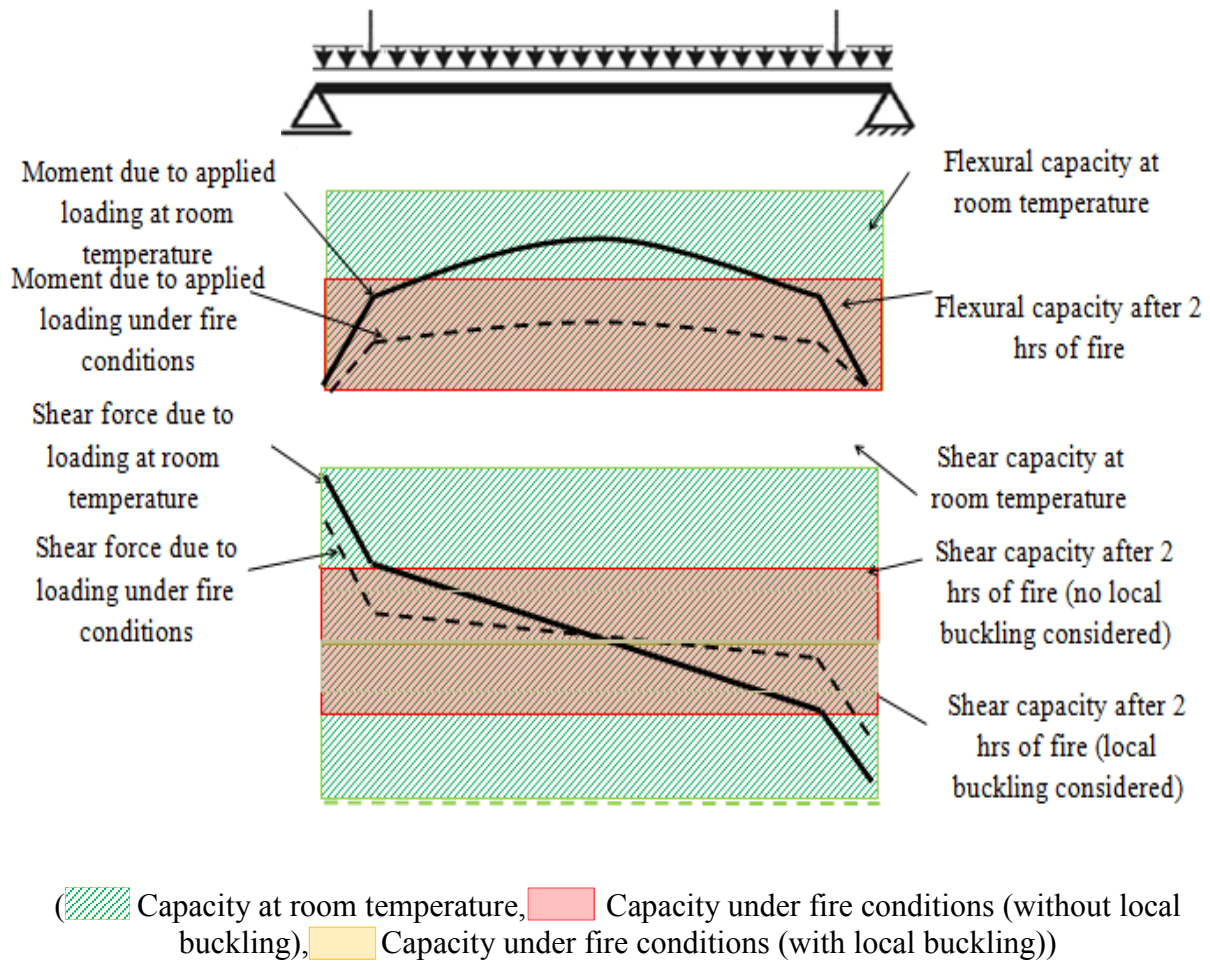
Figure 1.4: Effect of local buckling on variation of bending moment and shear force, as well as capacity in beams subjected to high shear forces

15

w/unit length

Concrete slab

Steel beam

Moment due to applied loading

Flexural capacity of composite beam

Flexural capacity of steel beam

Shear due to loading

Shear capacity of composite beam

Shear capacity of steel beam

Capacity at room temperature, Capacity under fire conditions)
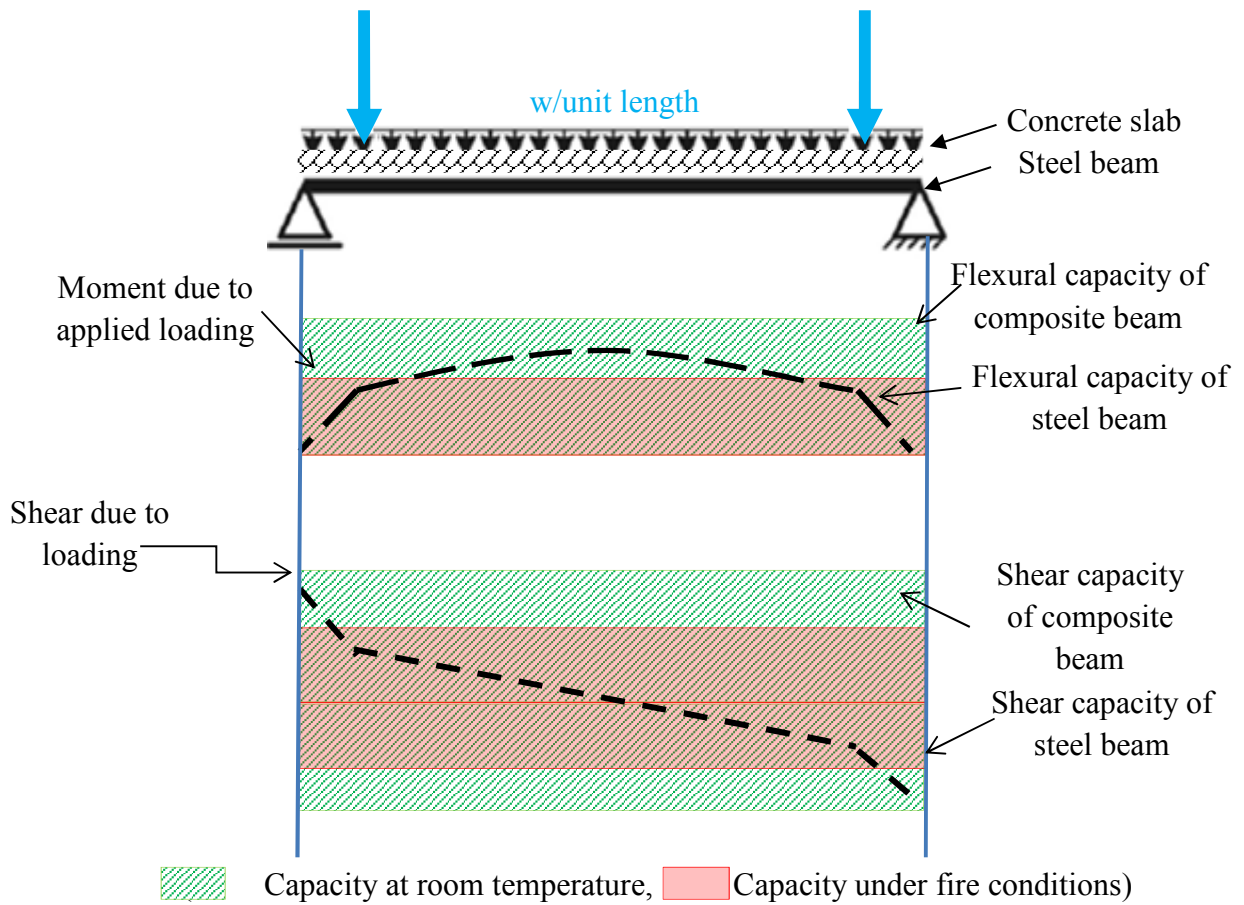
(a) Beam with high shear forces under ambient and fire conditions

Figure 1.5: Effect of composite action on flexural shear force in a steel and composite beams under different loading scenarios

16

Figure 1.5 (cont'd)

(b) Degradation of moment capacity with fire exposure time
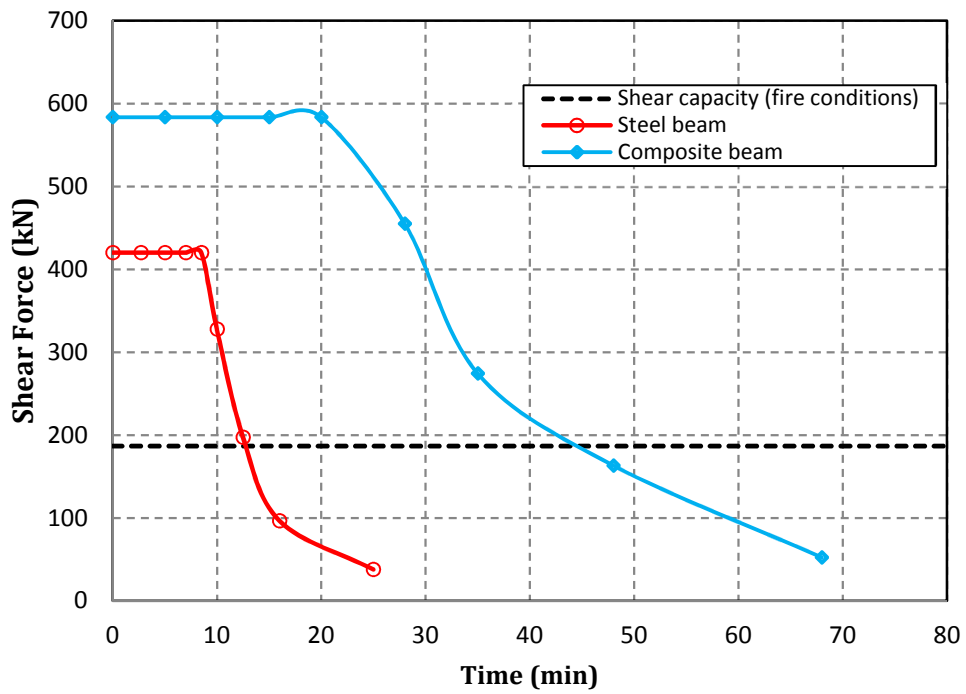
(c) Degradation of shear capacity with fire exposure time

1.4 Layout

The research presented as part of this dissertation is organized in to seven chapters. Chapter 1 presents background information on the magnitude of fire problem in buildings and infrastructure, various factors influencing fire resistance, and flexural and shear response of typical steel and composite beams subjected to different loading scenarios and fire conditions. Chapter 2 presents the state-of-the-art report on the fire performance of different types of structural members. In Chapter 2, recent fire incidents, previous experimental and analytical studies on fire-exposed steel beams, composite steel beams, and steel-concrete assemblies (thin floors) are reviewed and knowledge gaps in this area are identified. Chapter 3 presents details of fire resistance experiments on four composite beams subjected to different loading and fire severitys. Results from fire tests are utilized to discuss the comparative fire response of composite beams under dominant flexural and shear loading configurations. Chapter 4 presents the development of a finite element model to trace the overall behavior of steel and composite beams with special focus on tracing shear response under fire conditions. The validity of this numerical model is also established in Chapter 4, where response predictions from the model are compared against test data for different types of loading configurations and fire on beams. Chapter 5 presents results from parametric studies carried out to quantify the critical factors, such as sectional instability and level of composite action, governing the fire response of steel and composite beams. Chapter 6 presents derivations of expressions that can be used to evaluate shear capacity of steel and composite beams. The proposed design equations account for property degradation of constituent materials, temperature-induced sectional instability, and level of composite action offered by concrete slab in evaluating shear capacity in of steel and composite beams. In addition, Chapter 6 lays out a unified design approach that can be used for

design of steel and composite beams under fire conditions. This unified approach considers flexural and shear effects and can be used to optimally design (and analyze) steel and composite beams especially when subjected to dominant flexural or shear loading and fire conditions.

CHAPTER TWO

2. State of the Art Review

2.1 General

In current practice, beams at room temperature are to be designed to satisfy flexural limit state and then checked for shear limiting criteria. However, under fire conditions, beams are designed by considering flexural limit state only, with no consideration to shear limit state. Recent studies have indicated that this approach may not be fully valid in beams subjected to combined effects of high shear loading and fire exposure, and also for beams with slender webs exposed to fire. Failure in such beams, under fire conditions, can occur when shear capacity drops below level of applied loading, which can occur prior to reaching flexural limit state.

The effects of high shear loading, as well as degradation with shear capacity arising from local instability, is not accounted for in current design provision. In order to highlight the shortcomings in current design philosophy, a state-of-the-art review on fire resistance provisions for steel and composite beams, comprising of previous studies as well as fire design provisions in various codes and standards, is presented in this chapter. Based on this review, knowledge gaps in the area relating to fire performance of steel and composite beams/girders as well as composite beam-slab assemblies are identified.

2.2 Fire hazard to structures

Fire represents a significant hazard to built environment and can lead to damage or even collapse of structural members. Since fire is a random event, occurrence of fire in civil infrastructure can be defined using a stochastic (probabilistic) approach. The probabilistic nature of fire incidents is best described as a series of independent events that repeatedly occur over time. The nature of these events can also be statistically quantified using Poisson distribution

(Ramachandran, 1979; Rahikainen Keski-Rahkonen, 2004; Rutstein, 1979; Rychlik and Rydén, 2006; Rydén and Rychlik, 2006). In order to illustrate the magnitude of fire problem in buildings and bridges, statistical data, where shear effects can lead to failure in steel and composite beams/girders, is collected from past fire incidents is analyzed (Naser and Kodur, 2015). This needed data cover a wide range of influencing factors, such as, cause of fire, fire incident features (fire intensity, fuel type, duration of fire), building and bridge characteristics and overall building and bridge population etc.

The probability of a fire breaking-out and fire-induced collapse in buildings and bridges is calculated following rules of Poisson distribution shown in Eq. 2.1.

$$P = 1 - e^{-\rho t} \tag{2.1}$$

where,

ρ = fire intensity

t = time (in years)

From collected statistical data, approximately 480,500 fire incidents occurred in buildings out of 1,375,000 fire incidents in total (Karter, 2012). Hence, the probability of a fire occurring in a building is $P = 1 - e^{-\rho t} = 1 - e^{-0.35(1)} = 0.295(29.5\%)$, where $\rho = \dfrac{480,500}{1,375,000} = 0.35$ year^{-1}.

Compared to building fires, there have been a total of 195,600 vehicle fire incidents that occurred on all U.S. roadways in 2011 (NFPA, 2011). Out of these fire incidents, 90,000 occurred on highways, commercial roads and residential driveways. Since there is no specific statistical information available on the total number of fire incidents on bridges, a reasonable

fraction of the total highway fire incidents can be assumed to occur in the vicinity of bridges. Herein, 5% of total highway fire incidents is assumed to occur on/underneath bridges (Wardhana and Hadipriono, 2003; Sheer, 2010). Following the same approach described above, the probability of a fire breaking out on a bridge is $P=1-e^{-\rho t}=1-e^{-0.023(1)}=2.27\%$. It is clear that the probability of a fire breaking out in a building is almost thirteen times higher than that to occur in bridges

In order to arrive at the probable risk of fire-induced collapse of buildings and bridges, another set of data utilizing National Institute for Standards and Technology (NIST) survey on fire-induced collapses of buildings is analyzed. The outcome of this survey show that over a period of 32 years (1970-2002) there were a total of 22 fire–induced building collapses (in US), in addition to 7 buildings that suffered severe structural damage due to fire and had to be demolished (NIST, 2008). On the other hand, Wardhaua and Hadipriono (2003) reported that the total number of building failures (collapse) from various catastrophic events, including fire, is 225 in a period of 1989-2000. Hence, probability of fire-induced collapse of a building is $P=1-e^{-\rho t}=1-e^{-0.129(1)}=0.121$. Thus, the probability of fire-induced collapse of a building is estimated to be 12.1%.

Wardhana and Hadipriono (2003) also reported that there were 691,060 highway bridges in 2003. In addition, they stated that total number of bridge failures due to different extreme loading conditions was 503; out of which 16 bridges collapsed due to fire. Following the same assumptions discussed above, the estimated probability of at least one bridge collapsing due to fire is $P=1-e^{-\rho t}=1-e^{-0.032(1)}=3.1\%$. It can be seen that probability of a building to collapse is four times higher than that of a bridge.

The estimated fire and collapse probabilities are listed in Table 2.1 and plotted in Figure 2.1 to compare number of fire incidents and probability of collapse between bridges and buildings in USA. The tabulated data clearly show that the probability of fire occurring in a building, as well as fire-induced collapse of a building, is much higher than that of bridges. Further, the extent of fire-induced damages in buildings resulting is fire is also higher than that in bridges. For instance, U.S. Department of Homeland Security (2003) and Eldukair and Ayyub (1991) estimated fire-based economic consequences of damage to residential buildings and bridges to be 7,199 and 959 million dollars, respectively. This damage infers the vulnerability of structures (especially buildings) to fire damage. Such adverse consequences resulting from fire can be minimized to some extent in design of structural members by conserving all possible limitations under combined loading and fire.

2.2.1 Recent fire incidents in buildings and bridges

In high-rise buildings and bridges, structural framing (system) comprises of steel or composite beams/girders connected together by joints or connections. Under fire conditions, steel structural members can lose much of their strength and stiffness due to the rapid loss of strength and modulus properties. Thus, steel structures can be vulnerable to large scale fires. While occurrence of extreme fire conditions is rare, large scale fires can lead to human losses and partial/complete collapse of structures. To illustrate the vulnerability of steel structures to fire, examples of notable fire incidents which lead to substantial life loss and significant structural damage is presented below;

- The most notable collapse of steel framed buildings to fire would be the collapse of the Twin Towers of the World Trade Center on September 11, 2001, resulting from crashing of a jet airliner to each of the towers during terrorist attacks (Federal Emergency

23

Management Agency (FEMA), 2002). The twin towers were designed as "tube in tube" structure that had 59 perimeter columns made of steel along each face of the building. The floors consisted of 4 lightweight concrete slabs laid on a steel deck. This grid consisted of a network of lightweight bridging trusses and main trusses supported the floors and applied loadings. The trusses spanned 18 m along the long-span area and 11 m in the short-span area. According to the results of the joint investigation conducted by American Society of Civil Engineers (ASCE) and Federal Emergency Management Agency (Engineering News-Record, 2001), although the impact of the airliners caused extensive structural damage, including localized collapse of some of the floor systems and progressive collapse of some of the columns, still the towers were able to withstand such impact loading. However, the resulting fire at a number of floors along impact zones caused further (thermal) damage to steel trusses and columns and eventually leading to total collapse of buildings. When the fire-damaged structural system failed, it caused floors to sag, pulling perimeter columns inward. This resulted in a chain of events that ended with progressive collapse of towers. In total, the collapse of the towers claimed lives of 2,996 people and caused at least $10 billion in property and infrastructure damage (FEMA, 2002).

- On September 11, another 47 storey steel framed landmark building, World Trade Center Seven also experienced severe fire. The design of this building incorporated eight 14 m long cantilever transfer girders that spanned between building core and the north side at the 7th floor. The transfer girders, made of steel plate girders, varied in depth from 2.7 m at the north end, to a tapered portion in the middle, and to 1.37 m at the southern section closest to the core. Each transfer girder weighed approximately 52 tons and was

connected to steel beams through single-plate shear connection through thin web. The transfer girders were designed to carry significant levels of concentrated loads and resulting shear forces arising from upper floors. Rapid rise in temperature in these transfer girders has caused extensive structural damage to girders. Thus, transfer girders at the (5th and 7th floors) perimeter to became overloaded with vertical "shear" forces and then failed which led to the overall collapse of the building entirely due to fire (no impact of aircraft on this building) (FEMA, 2002; NIST, 2016).

- The above two fire incidents highlight the adverse effect of fire on high-rise building, specifically vulnerability of structural system under combined effects of fire and loading. In order to illustrate the hazardous nature of fire on structural systems in bridges, a noteworthy fire incident on a major bridge that is presented herein. On April 29, 2007, fire broke out at the two span bridge of the MacArthur Maze interchange in Oakland, CA, when a fuel tanker transporting 32,500 litters of fuel overturned under the bridge. The burning of highly combustible fuel lead to intense heat producing temperatures in the range of 1100°C in the uninsulated steel girders. The steel girders had no fire proofing, as per current practice where no fire protection measures is required for structural members in bridges. Due to rapid rise in steel temperatures, the strength and elastic modulus properties of steel beams/girders rapidly deteriorated. This rise in temperature accompanied with strength and stiffness degradation amplified local instability effects and resulted in large deflections in girders. The resulting deflections caused significant fire-induced tensile forces that overstressed the bolts and cause shear failure of shear tab connection used at end of girders (Bajwa et al. 2012). As a result, these connections failed and steel girders, which are highly vulnerable to shear effects under fire conditions,

collapsed in about 22 minutes. Fire-induced collapse of this bridge caused significant traffic detours, and the losses were estimated at $9 million and took weeks to repair (Garlock et al., 2012).

2.2.2 Current strategies for overcoming fire hazard

Codes and standards do recognize fire to be significant hazard from life safety point and require specific fire safety measures to be installed in the case of buildings. Fire safety in buildings is achieved through provisions of active and passive fire protection systems. Active fire protection systems alert or control fire by some external action (i.e., human or device); such as, water sprinklers, fire detectors, smoke control systems, and firefighting. On the other hand, passive protection systems are built into the structure to prevent spread of fire and subsequent collapse. Such systems include; fire barrier (walls), compartmentation, providing fire insulation material, and designing structural systems to maintain structural integrity/stability under fire conditions.

2.2.3 Fire resistance provisions in codes and standards

Model building codes set regulations for minimum requirements to ensure safety and serviceability of structural elements in buildings. For instance, in the United States there are two main building codes; the International Building Code (IBC, 2015) and the NFPA Building and Construction Code 5000 (NFPA, 2015). The intent of these regulations is to provide minimum standards to ensure public safety, health and structural integrity. IBC and NFPA codes specify fire resistance ratings following a prescriptive philosophy, i.e., minimum required fire endurance times (fire ratings) for building elements as well as for achieving fire ratings in structural members (beams, columns, slabs).

Steel structures in USA are to be designed as per AISC design manual as it is the main reference in IBC for design of steel and composite steel-concrete structures (AISC, 2011). Although this design manual provides a general discussion on overall fire design, it provides very limited information on "explicit" fire design provisions for steel structures. In addition to the AISC design manual, ASCE/SFPE 29 is a design standard that contains limited analytical approaches and empirical relations for determining fire resistance (and ratings) for steel structural members. Most of these analytical methods have been developed based on the results of fire tests carried out on steel structural members subjected to standard fire exposure.

On the other hand, European codes and standards provide sufficient information that can be used for fire design and analysis. For example, Eurocode 3 (2005) and Eurocode 4 (2003) gives simple and advanced calculation methods fire resistance calculation of steel and composite structural members (i.e., beams/girders).

2.3 Behavior of beams under fire conditions

Steel and composite beams (and girders) are horizontal members that are subjected to significant levels of bending moment resulting from gravity loads and thus failure typically occurs when the applied moment due to loading at the critical section exceeds the moment capacity. Therefore, under ambient conditions, beams are typically designed to satisfy flexural limit state and then checked for shear limiting criteria. This flexural behavior of steel and composite beams under fire conditions has been well studied (Kirby et al., 1986; Alexander et al., 2009; Huang et al., 2009; Payá-Zaforteza and Garlock, 2012; Kodur et al., 2013). Based on these studies, the flexural behavior of steel and composite beam can be governed by a number of factors including loading level, fire severity, thermal gradient and restraint conditions.

Beams and girders can experience significant loss of moment and shear capacity with fire exposure time when exposed to fire. However, as discussed in Chapter 1, failure in fire-exposed beams is evaluated by considering flexural strength limit state, with no consideration to shear limit state or associated local buckling limitations. This rationale may not be valid in certain situations such as the case of transfer girders or beams with slender webs. The shear response of steel and composite beams subjected to high shear loading and fire conditions can be influenced by various factors such as;

- Geometric features

- Loading level

- Temperature-induced instability

- Loading configuration

The adverse effects of these factors on fire performance of beams are illustrated in Chapter 1. There is very limited data on the extent of these factors on shear response of steel and composite beams.

2.4 Previous Studies on Fire Performance of Steel and Composite Beams

A review of the literature indicates that a number of fire resistance studies were conducted on simply supported hot-rolled steel beams (without slab), built-up beams/girders and/or web panels. In most of these studies, beams were often subjected to flexural loading and fire conditions. Further, in case of composite beams, fire tests and numerical studies evaluated fire resistance of composite beams with full composite (100%) action when subjected to dominant flexural loading. Thus, bulk of these studies did not investigate the effect of shear loading and instability on the fire performance of hot-rolled steel beams and/or fully/partially composite beams (See Table 2.2).

In order to identify knowledge gaps relating to flexural and shear response of fire-exposed steel beams, a review of previous studies were undertaken and findings from some of the notable studies are discussed in the following sections. These studies are presented under two categories i.e., experimental and numerical. Within each category, studies relating to isolated steel beams/girders (without slab), composite beams and composite beam-slab assemblies (floor systems) are discussed in detail.

2.4.1 Experimental studies

In the last four decades, extensive experimental studies have been conducted on behavior isolated hot-rolled and built-up steel beams under fire conditions. These studies mostly focused on investigating flexural behavior of such beams by subjecting the beams to dominant bending moment and fire loading. Only very few have studied the effects of shear, web buckling, and post-buckling shear capacity in steel beams (Alexander et al., 2009, Shanmugam and Baskar, 2003, Alinia et al., 2009). Based on the available studies, attempts have been made to quantify the influence of critical factors on fire performance of these structural elements; namely; end restraint, thermal gradients, and load level. Details of some of these studies are presented herein for steel and composite beams as well as beam-slab assemblies.

2.4.1.1 Steel beams (and web panels)

The notable experimental studies that recently investigated the fire response of steel beams (and web panels) are from Vimonsatit et al., (2007), Kodur and Fake (2009), and Dwaikat et al. (2011).

- Vimonsatit et al., (2007) tested numbers of small-scale isolated steel beams of 1.66 m span to evaluate shear effects on fire behavior of steel beams. Theses beams were grouped into five series, three of which were plate girders (built-up)

sections, while the rest were hot-rolled beam sections (UC 152x152x23 kg/m, and UC 203x203x52 kg/m) as shown in Figure 2.2. The plate girders were of 305 mm deep and web slenderness of 112, 152, and 203, while the hot-rolled beams had web slenderness of 26.3 and 25.6. The test specimens were loaded predominantly in shear loading under steady-state temperature conditions at 400°C, 550°C, and 700°C. The aim of this study was to investigate shear buckling behavior, diagonal web tensile field action, and development of plastic hinge mechanism in flange plates of girder panels. Failure of these girders (or beams) in bending mode was prevented by stiffening top and bottom flanges. The results indicated that shear capacity of steel beam/girder decreases significantly with increasing temperature and hence the authors concluded that shear limit state considered in evaluating failure of steel beams/girders under fire conditions.

- Kodur and Fike (2009) conducted a fire resistance test on a 4 m long W12×16 A992 steel beam (See Figure 2.3) subjected to ASTM E119 standard fire exposure. In this beam, the slenderness of flange and web were of 7.5 and 49, respectively. The beam was insulated with 50 mm thick spray applied vermiculite based fire insulation to achieve a 2-hr fire resistance rating. The beam was loaded with two point loads and this loading represented moderate bending effect of 31% and low shear effect of 5% of moment and shear capacity, respectively. Under fire conditions, the moment capacity in the beam remained intact for the first 75 minutes due to lower temperatures in flanges of steel beam. However, shear capacity started to degrade at 35 min due to relatively faster rise in web temperature. After 75 minutes, moment and shear capacity degraded further when

30

the temperature in steel section exceeds 350˚C. Degradation of moment capacity of steel section continues till 130 min at which point the beam failed since the capacity at mid-span falls below the moment due to applied loading. However, due to the low level of applied shear force, shear capacity did not fall below the shear force near the vicinity of support section, nor there was any signs of web local buckling.

- Dwaikat et al. (2011) tested four steel beam-columns that had a W8×48 cross-section and were made of A992 Grade 50 steel. The test specimen were 3.3 m long and were initially insulated with spray-on fire resistive material (SFRM) on all four sides along the majority of its length. Two beam-columns were insulated with 44 mm thick insulation and the other two were insulated with 38 mm thick insulation. In order to study the effect of thermal gradient on the response of these beam-columns, the insulation was removed in specific locations along the length of the specimens. These resulting gradients simulate the thermal gradients that would realistically emerge in perimeter columns and floor beams due to three-sided heating. From the conducted fire tests, it was evident that thermal gradients produced a change in plastic capacity to combinations of axial load and moment. Results from tests also showed that tested specimens all failed by plastic yielding under combined axial load and moment. Other factors including; Load level, fire scenario, and the direction of the thermal gradient were found to have a significant influence on the fire response of these beam–columns. Unfortunately, effect of shear loading, local buckling and moment-shear interaction were not investigated.

2.4.1.2 Composite beams

Some of the experimental studies on the fire response of composite beams presented in this section are from the work of Wainman and Kirby, (1987), Newman and Lawson (1991), Zhao and Kruppa (1993) and Aziz et al. (2015).

- Wainman and Kirby (1987) carried out fire resistance tests on two composite beams by exposing them to standard ISO834 fire exposure. These two beams comprised of a steel beam (UB 254x146x43) and normal weight concrete slab of 650 mm width and 130 mm thick. To achieve full composite interaction between the steel beam and the concrete slab, 32 shear studs (75 mm length and 19 mm diameter) were welded along the top flange in two rows. Experimental results indicated that the fire resistance of composite beams is influenced by load level, grade of steel, and composite action. Unfortunately, these composite beams were tested under flexural loading and effect of shear or local instability were not considered in this study.

- Newman and Lawson (1991) reported four tests on simply supported (and fire-insulated) composite steel beams. In these tests, the steel beams were of UB 305x102x33 section and were connected to concrete slabs using headed shear studs. These steel beams were connected to a slab of width and depth equal to 1125 mm and 125 mm, respectively. The composite beams spanned 4.50 m. They were subjected to similar mechanical loading consisting of four concentrated loads equal to 71.7 kN centered about the mid-span and exposed to standard fire exposure. The composite beams were protected with different fire insulation materials. The experimental results indicated that the failure was due to tensile

yielding of the steel beam. The effects of shear or sectional instability (local buckling) on performance of fire exposed steel structures were not considered since the main objective of this work was to investigate the flexural performance of fire-exposed steel beams. However, data from these tests is utilized by various researchers for validating computer models on tracing the response of steel framed structures under fire conditions.

- Similarly, Zhao and Kruppa (1993) conducted fire tests to study the flexural behavior of composite beams by subjecting them to ISO834 standard fire (ISO, 1975). The composite beams were of IPE 240 section that had web slenderness of 30. Although these composite beams were tested under flexural loading, the authors reported that these beams experienced signs of local buckling at interior supports (possibly due to shear loading). However, no further explanations were discussed, possibly because the effect of shear and fire-induced instability effects could not be isolated due to the nature of the flexural-loading test set-up.

- Aziz et al. (2015), conducted experiments on three composite steel girders subjected to gravity and fire loading. The objective of these experiments was to study the degradation of flexural capacity of one hot-rolled steel beam and two plate girders under fire conditions. Test variables included: load level, web slenderness, and spacing of stiffeners. The load level was varied between 30-50% of capacity at room temperature. The hot-rolled steel beam and plate girders had web slenderness of 52 and 123, respectively. Finally, spacing of stiffeners in plate girders was varied between 1.0 and 1.5. Results from fire tests indicated that typical steel beams can experience failure under standard fire conditions in about

30–35 min. The time to failure and mode of failure in fire exposed beams is highly influenced by web slenderness and spacing of stiffeners. It was also concluded that steel beams fail through flexural yielding when web slenderness is around 50; however failure mode changes to web shear buckling when web slenderness exceeds 100 (as in the case of plate girders).

2.4.1.3 Composite beam-slab assemblies

A review of the current literature indicates that there have been few experimental studies on the fire behavior of composite beam-slab (floor) assemblies. Experimental studies on fire behavior of composite floor assemblies began in 1990's after fire incidents in high rise buildings, such as the One Meridian Plaza (1991) and the Broad-gate Phase 8 fire (Kirby, 2000). The aforementioned experimental studies indicated that beam-slab composite action can be beneficial to achieve better fire performance through composite construction. These fire incidents stimulated researchers to evaluate the fire performance of steel-framed composite beam-slab assemblies under realistic gravity and real fire loading, along with different end restraint conditions. Some of these tests are discussed herein;

- Six fire tests on a full-scale steel frame building were conducted at Cardington, UK. Of these tests, four tests (Tests 3-6) involved measuring the fire response of composite floor systems. These tests were carried out on the seventh floor of the 8-storey frame and involved a single 305×165 mm beam and the surrounding concrete floor spanning 9 m between a pair of 254×254 mm columns. The columns and connections remained cool while the beam was subjected to heating from a fire furnace. The furnace was 8 m long × 3 m wide × 2 m high and was insulated with mineral wool and ceramic fibre. The test beam and surrounding

structure were extensively instrumented to measure temperatures, strains, deflections and rotations. Results from the tests showed that (a) the structural integrity of the composite system was maintained though the slab and the connected secondary beams underwent large deflections; (b) secondary beams and composite deck in the composite floor assembly experienced temperatures in excess of 900°C and 1100°C, respectively; (c) local buckling occurred near the ends of secondary beams due to the axial restraint imposed by the connecting steel members (beams, columns) and composite slab; and (d) although the peak steel temperature was 887°C measured on the bottom flange, steel beams did not fail undergo large deflections. Based on the experimental results, it was concluded that the interaction of the heated (fire-exposed) beams with the adjoining cooler concrete slab, enhanced the overall performance of the structural system (British Steel, 1998).

- Bailey et. al. (2000) designed an experimental program to simulate and study the development of tensile membrane action in composite slabs under fire conditions. To circumvent the complexities associated with testing and measuring the development of tensile membrane action under fire conditions, the authors have modified the room temperature test set-up to simulate the behavior of composite floor slab under fire conditions. To achieve this, the steel deck below the concrete was removed before the slab was loaded, leaving the concrete and anti-crack mesh unsupported. Thus, the slab was carried by four 305×165×40 beams. The rationale for adopting non-temperature testing, can be summarized based on the fact that in a fire test, the steel deck could reach temperatures above 1100°C thus

losing most of its original strength. Once the deck was removed, the composite slab was gradually loaded till failure. Upon failure of composite beam-slab assembly, the authors concluded that the tensile membrane action significantly enhances the performance of composite floor systems under fire conditions and need to be accounted for in fire design.

- Wellman et al. (2011) carried out tests to evaluate the fire behavior of slim composite floor slabs with different connection configurations, and fire protection by subjecting them to standard and realistic fire conditions. The composite floor assemblies consisted of concrete slabs placed on the top of two A992 steel W12×16 girders (3.96 m long) and three A992 steel W10×15 beams (2.13 m long). A 38.1 mm deep Vulcraft 1.5VLR metal deck was installed and fixed to the top of the steel girders and beams using 76.2 mm long, 15.9 mm diameter headed shear studs. The authors observed that no failure of shear studs occurred despite the fact that the slabs were designed to achieve low composite action (25-33%) by providing limited number of shear studs. Based on this observation, the authors concluded that the composite slab, through the development of tensile membrane action, plays a significant role in transferring loads from beams to girder under fire conditions. Unfortunately, effects of shear and web local buckling were not evaluated in these experiments.

- Fike and Kodur, (2011) carried out fire resistance experiment on a composite steel beam-concrete slab assembly to study the beneficial effect of adding steel fibers to concrete slab (as steel-fiber-reinforced concrete). The beam-slab assembly comprised of primary and secondary beams supporting a steel fiber reinforced

concrete used in the slab (SFRC) on a steel deck. Three W10x15 steel beams were connected to a pair of W12x16 beams with a composite deck (slab) incorporating shear studs. The two W12×16 steel beams were provided with external fire protection of 22 mm thickness to achieve a two-hour fire resistance rating, while the W10x15 secondary beams were left unprotected. The floor assembly was designed and fabricated based on AISC specifications. The beam-slab (floor) assembly was exposed to ASTM E119 fire. This study aimed to enhance the fire resistance of the composite assembly by using steel fiber reinforced concrete. Results from this study showed that the combined effect of composite construction, tensile membrane action, and improved properties of SFRC under realistic fire can provide sufficient fire resistance (1 to 2 hours) in steel beam-concrete deck slabs without the need for external fire protection to the secondary beams and steel deck of the slab. Similar to previous studies, effect of shear and local instability in steel beams/girders were not taken into account.

2.4.2   Numerical studies

A review of literature indicates that a number of numerical studies have been carried out on the fire behavior of steel and composite beams as an alternative to conducting full-scale fire tests which are often involves large costs and complexities. These studies reported results from finite element analysis, where different set of assumptions were made in each study to reduce the complexity of the problem. Following is a summary of some of these prominent studies on steel beams, composite beams and composite beam-slab assemblies.

2.4.2.1   Steel beams (and web panels)

Some of the notable numerical studies on the fire response of isolated steel beams (and

web panels) are from the work reported by Dharma and Tan (2007), Kodur and Naser (2013), Scandella et al. (2014) and André Reis et al. (2015);

- Dharma and Tan (2007) developed a finite element model (built in ANSYS) to evaluate inelastic rotational behavior of isolated steel beams subjected to fire conditions. They applied this model to study the effect of web and flange slenderness on fire response of steel beams. The authors reported a noticeable decrease in flexural and shear capacity with increase in flange and web slenderness. In addition, they reported that moment capacity of fire exposed steel beams decreases significantly in beams with slender webs due to occurrence of local buckling in webs. However, no specific observations were made with regard to the influence of web slenderness on shear capacity or instability of fire-exposed beams as the numerical model did not account for shear effects.

- In a recent study, Kodur and Naser (2013) applied a three dimensional finite element model to study shear response of steel beams (W16×31) exposed to fire. For tracing the realistic fire response of beams, several parameters such as geometric and material nonlinearities, temperature dependent material properties and various failure limit states are accounted for in the analysis. The effect of different loading pattern, web slenderness and presence of fire insulation on the behavior of fire exposed steel beams subjected to high shear loading was studied. Based on these studies the authors reported that under certain scenarios, the shear capacity can degrade at a higher pace than flexural capacity, thus failure can develop through shear effects. In addition, for slender beams, it was also shown that local buckling in web can cause temperature-induced instability losses and

further reduces shear capacity in beams. This phenomenon accelerates shear failure in fire-exposed steel beams.

- Scandella et al. (2014) applied a finite element model, built in ABAQUS, to study fire behaviour of steel plate girders. The numerical model was validated with results of an extensive experimental study on steel plate girders at ambient temperature performed by Basler et al. (1960). The steel plate girders had varying web slenderness between 76 and 230 and the girders spanned for 12.2 m. In this study, Scandella et al. showed that the non-uniform temperatures can impose additional thermally-induced forces and even change the failure mode in plate girders. In addition, they reported large differences between the flange and web thicknesses can lead to a faster heating in the web than flanges, resulting in the development of thermally-induced compressive stresses in the web, which will accelerate the local failure. Thus, a steel plate girder with a bending dominant failure at normal temperature may instead exhibit a shear dominant failure at elevated temperatures with non-uniform heating. Similar observations were noted during fire tests conducted by Aziz et al. (2016).

- Reis et al. (2015) developed a three dimensional model using SAFIR with the purpose of analyzing the lateral torsional buckling behaviour of steel plate girders for shear-moment interaction under fire conditions. The plate girders were tested in a simply supported manner and had a span of 1.8 m. In addition, web slenderness was varied in these girder between 100 and 200. As part of the analysis variables, two different end configurations were considered, rigid and non-rigid end posts. The authors found that the intentional low stiffness of the

flanges may precipitate the failure of plate girders, making the interaction between shear and bending an important phenomenon. A parametric study was also performed involving a wide range of cross-section's dimensions, plate girders' aspect ratios and steel grades. The analyzed plate girders had web slenderness of 115 and were numerically tested at both normal and elevated temperature, (steady-state conditions considering three temperatures (350°C, 500°C and 600°C). Unfortunately, the effect of web local buckling were not explicitly studied. However, predictions from numerical results were compared to the Eurocode 3 predictions for shear and shear–bending interaction and were found to be non conservative in certain conditions.

2.4.2.2 Composite beams

Some of the recent numerical studies on fire response of composite beams are from the work reported by Payá-Zaforteza and Garlock (2012), Glassman et al. (2015), and Kodur and Naser (2014, 2016). A brief summary of these studies is provided below;

- Payá-Zaforteza and Garlock (2012) developed a three dimensional numerical model (using ABAQUS) to study the response of a typical bridge of 12.2 m span length. This bridge consisted of five hot rolled steel girders of type W33×141 that support a reinforced concrete slab 200 mm depth not structurally connected to the girders with shear studs. Based on the validated model, the authors designed a parametric study that to investigate: (1) two possibilities for the axial restraint of the bridge deck, (2) four types of structural steel for the beams (carbon steel and stainless steel grades), (3) three different constitutive models for carbon steel, (4) four live loads, and (5) two alternative fire loads (the hydrocarbon fire defined by

Eurocode 1 and a fire corresponding to a real fire event). Results from this study show that restraint to deck expansion coming from an adjacent span or abutment should be considered in the numerical model. In addition, time to failure is low in the uninsulated composite girders (between 8.5 and 18 min). Despite the well-presented parametric study, the effect of shear, instability or composite action were not included in this work.

- Glassman et al. (2015), evaluated the web shear buckling response of two plate girders subject to fire conditions using a developed finite element in ABAQUS. In this model, three parameters were evaluated: flange boundary conditions, representation of thermal gradients, and composite action with the slab. To meet this objective, finite element models with varying parameters are compared to each other and to experimental results. Results show that the presence of a composite slab significantly increases the shear capacity of the plate girder by about 50%. Assuming simply supported boundary conditions for the flange can lead to lower estimates of post-buckling shear strength by about 20% and 30% than models that explicitly model the flange. Finally, modeling the girder with a uniform temperature equal to the temperature of the web leads to similar results as modeling with thermal gradients.

- Kodur and Naser (2014, 2016) developed a finite element model to study the fire response of composite steel beams by taking into consideration temperature-induced sectional instabilities. This model, developed in ANSYS, was applied to investigate the effect of sectional slenderness on the onset of local instability and capacity degradation in steel beams exposed to fire. Results from finite element

analyses were utilized to evaluate failure of beams under different limit states including flexure, shear, sectional instability and deflection criteria. These results show that under certain loading scenarios and sectional configurations, shear capacity in steel beams can degrade at a higher pace than that of moment capacity. In addition, results from numerical studies inferred that room temperature classification of steel beams, based on local instability, can change with fire exposure time; a compact section at ambient conditions can transform to a non-compact/slender section under high temperature effects. This could induce temperature-induced local buckling in steel sections and lead to failure prior to attainment of failure under flexural yield and/or shear limit state.

2.4.2.3 Composite beam-slab assemblies (floor systems)

Some of the notable numerical studies conducted on fire response of composite beam-slab assemblies are by Gillie et al. (2001), Lamont et al. (2007), and Kodur et al., (2012) and are described herein;

- Gillie et al. (2001) developed and validated a finite element subroutine (FEAST), in ABAQUS, to analyze the fire behavior of composite slab tested as part of first Cardington fire tests. The model accounted for material and geometrical nonlinearities, thermal expansion, thermal curvature and non-linear thermal gradients within the concrete slab. The concrete slab was discretized using shell elements while the beams and columns were modeled using beam elements, and the connections were assumed to be perfectly rigid. Based on the results of the analysis, it was concluded that the development of axial forces and deflections in the composite slab assembly are strongly influenced by the effects of thermal

expansion and strength (stiffness) degradation of steel and concrete. However, this study did not consider some of the important factors such as the shear and local buckling in beams, cracking of concrete and stress concentrations near cracked regimes in the concrete material, which influenced the behavior of the slab in the Cardington fire tests.

- Lamont et al. (2007) developed a numerical model to study the structural behavior of a steel-concrete composite frame subjected to a natural fire using two computer softwares, HADAPT and ABAQUS. The study was aimed at comparing the behavior of composite beam-slab assemblies with and without fire protected edge beams. Based on the results obtained from the numerical model, the authors concluded that (a) the behavior of the slab is dominated by the catenary action of the beam when the edge beams are unprotected, as opposed to tensile membrane action when the edge beams are protected; (b) when the edge beams are unprotected, the columns displace inwards towards the end of the fire indicating a possibility of runaway collapse; (c) the magnitude of tensile mechanical strains in the concrete slab are maximum when the edge beams are fire protected; (d) protected edge beams allow the development of tensile membrane action in the slab in addition to enhancing lateral support to the columns. Unfortunately, similar to other studies, the effect of shear and local buckling was not included in the analysis.

- Kodur et al., (2012) developed a three dimensional finite element models in ANSYS to evaluate the fire response of steel beam-concrete assembly. The finite element model was validated by comparing results obtained from the model with

experimental data from fire tests. In this study, critical factors that influence fire performance of beam-slab assembly namely, composite action, load level, fire scenarios and connection type were investigated. Results from the numerical studies indicated that the proposed model is capable of predicting the fire response of beam-slab assemblies with a good accuracy. Also, the authors concluded that the composite action arising from steel beam-concrete slab interaction significantly enhances the fire resistance of the composite beam-slab assembly. However, effect of shear and local buckling in steel beams was not considered as part of this study.

Table 2.1: Comparison of probability of fire incidents and fire-induced collapse in bridges and buildings (Naser and Kodur, 2015)

	Bridges (2000)	Buildings (2012[*], 2002[**])
Total number of structures	691,060	118,000,000
Reported fire incidents	4500	480,500
Probability of a fire breaking out (yearly)	2.27%	29.5%[*]
Number of collapsed structures	503	225
Number of collapsed structures due to fire	16	29
Probability of collapse due to fire (yearly)	3.1%	12.1%[**]

Table 2.2: List of recent studies conducted on steel beams under shear loading

Author(s)	Year	Shape of section	Parameters studied	Remarks
Tang and Evan	1984	Transversely stiffened plate beam	Differing web panel aspect ratios	Proposed a design method, compared with the design code for steel bridges, BS 5400
Herzog	1989	Unstiffened and stiffened beams	Different types of stiffeners	Proposed design formulas for stiffened and unstiffened beams loaded in shear
Shanmugam et al.	2001	Beams with centrally located web openings	Web plate slenderness, flange stiffness and openings shape and size	Compared FE results with the corresponding experimental results in which show close agreement with the experimental results
White and Barker	2008	Transversely stiffened beams	Shear loading	Investigated the analytical methods of beams
Romeijna et al.	2009	Beams with trapezoidally corrugated webs	Web height, length of parallel part, web configuration	Recommended design specifications in line with Eurocode 3
Sinur and Beg	2012	Rigid intermediate transverse stiffeners in longitudinally stiffened beams	Shear and bending moment	Proposed a design procedure for intermediate transverse stiffeners
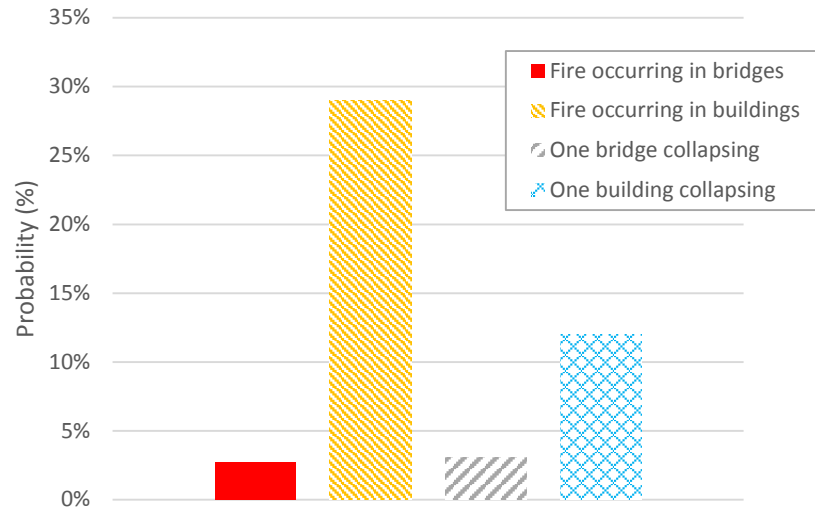
Figure 2.1: Probability of fire occurrence and fire-induced collapse in buildings and bridges (Naser and Kodur, 2015)

Applied loading

Flange   Stiffener   Flange stiffener

bf= 80 mm

Panel 1   Panel 2   d= 305 mm

tf= 6 mm
tw= 2.0 mm

240 mm   305 mm   810 mm   305 mm   240 mm

L= 1660 mm

(a) Plate girder TG3

Applied loading

Flange   Stiffener   Flange stiffener

bf= 80 mm

Panel 1   Panel 2   d= 305 mm

tf= 6 mm
tw= 2.7 mm

240 mm   305 mm   810 mm   305 mm   240 mm

L= 1660 mm

(b) Plate girder TG4

Applied loading

Flange   Stiffener   Flange stiffener

bf= 80 mm

Panel 1   Panel 3   Panel 4   Panel 2   d= 305 mm

tf= 6 mm
tw= 1.5 mm

240 mm   305 mm   810 mm   305 mm   240 mm

L= 1660 mm

(c) Plate girder TG5
Figure 2.2: Tested steel plate girders by Vimonsatit et al., (2007)
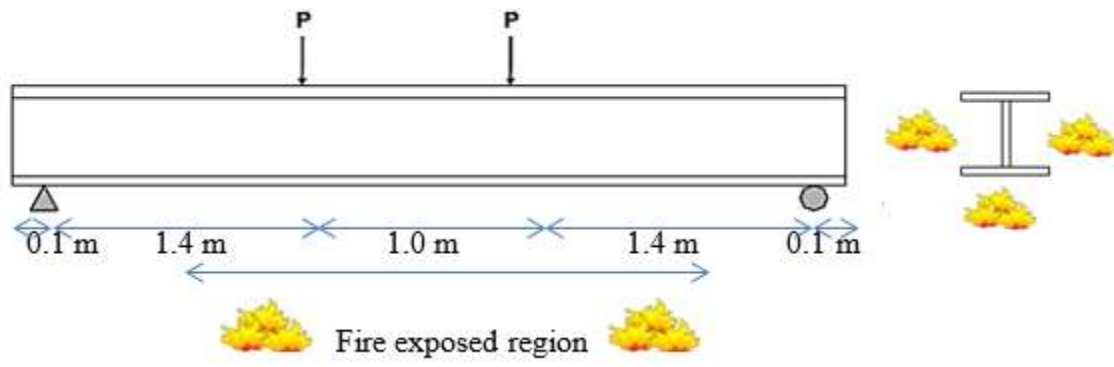
Figure 2.3: Geometric configuration of tested beam by Kodur and Fike (2009)

2.5 Knowledge Gaps

The above state-of-the art review clearly indicate that fire can be a major hazard to high-rise building and bridges. The failure of such steel beams can occur under flexural or shear, or deflection limit states. Such failure of members, not only leaves occupants and first responders with very short time to evacuate, and tackle fire but can also jeopardize their safety and integrity of the structure. Based on the literature review presented in this chapter, the following are some of the key knowledge gaps that require further research:

- There is lack of data on the behavior of steel beams especially under dominant shear effects and fire loading.

- Effect of composite action arising from concrete slab-steel beam interaction on shear and local buckling behavior of fire-exposed beams is not evaluated.

- There is no data from fire resistance experiment on the response of steel beams subjected to dominant shear forces and fire conditions. Data from such fire experiments are critical to validate finite element models that can trace structural response of fire exposed beams.

- Limited numerical models are available for tracing the shear response of steel and composite beams under fire conditions. Most of the current models do not fully account for shear and instability effects or composite action arise between steel beam and concrete slab.

- To date, there are no specific provisions in codes and standards to accounts for shear and instability effects in evaluating fire resistance of steel and composite beams/girders subjected to dominant shear forces and fire loading.

CHAPTER THREE

3.   Fire Resistance Experiments

3.1 General

The state-of-the-art review presented in Chapter 2 clearly indicates that there is lack of experimental data on the shear and instability behavior of fire-exposed composite beams (comprised of steel beam attached to a concrete slab via shear studs); especially incorporating the effect of composite action arising from concrete slab. To bridge this knowledge gap, an experimental study on fire performance of four uninsulated composite beams was carried out. In these tests, the main test variables are level of composite action, type and magnitude of loading. The composite beams were tested to failure by subjecting them to combined flexural and shear loading, and fire exposure. The main objective of these tests is to trace the response of composite beams under fire conditions and to generate test data for validation of finite element models. Full details of the fire resistance experiments, including specimen details, instrumentation, test set-up and procedure, and measured response parameters are presented in this chapter.

3.2 Experimental Details

3.2.1   Design of composite beams

Four composite beams were designed according to AISC specifications (AISC, 2011). These composite beams were not provided with any fire protection and were designed as composite beams to investigate the steel beam-concrete slab interaction under combined of thermal (fire) and structural (flexural and shear) loading.

3.2.2   Fabrication of composite beams

The tested composite beams, designated as CB1, CB2, CB3 and CB4, comprised of an uninsulated hot-rolled steel beam supporting a reinforced concrete slab. The four beams were made of the same hot-rolled section of W24x62 (taken from AISC, 2011). The steel sections

have flange width, and flange thickness of 179 and 15 mm, respectively. In addition, these sections have web depth and web thickness of 610 and 11 mm, respectively (see Fig 3.1). Thus, the web slenderness, defined as D/t_w (where D is the web depth and t_w is the web thickness), in this section is 55.1.

The steel sections were fabricated using A572 Grade 345 MPa (50 ksi) steel, which is a high strength, low-alloy steel commonly used in typical civil engineering applications. Composite beams CB1 and CB2 were designed to achieve full (100%) composite action with the concrete slab. For this purpose two rows of 19 mm diameter shear studs were placed to ensure full composite action between the steel beam and the concrete slab (see Fig. 3.1). Composite beams CB3 and CB4 had two rows of 19 mm diameter shear studs, placed at 230 mm apart to achieve partial (50%) composite action between the steel beam and the concrete slab (see Table 3.1). The layout of different shear stud arrangements in these composite beams are shown in Fig. 3.1a, b, c and d.

In order to maintain consistency between all four composite beams, the composite beams were fabricated at the same time using similar design and material batches (as that in CB1). Hence, composite beams CB2, CB3 and CB4 were designed and fabricated with one 9.5 mm thick stiffener at the supports and one 12.7 mm thick stiffener at the mid-span of the beam (to provide some level of lateral support to the beam). It has been shown in previous studies that addition of vertical stiffeners can enhance shear capacity of composite beams (especially in built-up plate girders) (Aziz, et al. 2015). However, in the tested composite beams, the added vertical stiffeners were not activated. This is due to the fact that in order for vertical stiffeners to contribute to the shear capacity, several conditions need to be met. Since,

1. $h/t_w > 1.1 \sqrt{k_v E/fy}$, for all tested beams; [$h/t_w = 55.1 < 1.1 \sqrt{k_v E/fy} = 59.23$], and also

2. $1 \le a/D \le 3$, for all tested beams [a/D = 1829/573 = 3.2 > 3.0]

Thus, vertical stiffeners provided in tested composite beams CB1, CB2, CB3 and CB4 will not contribute to shear capacity of these beams. Since the objective of this thesis is to study the comparative fire response of composite beams (made of standard hot-rolled sections and not built-up plate sections) when subjected to high level of flexural or shear loading, the effect of vertical stiffeners was not considered as a part of test variables.

The concrete slab used in composite beams was reinforced with a layer of tension steel rebars (as minimum reinforcement) at the bottom and a similar layer of compression steel reinforcement at the top as shown in Figure 3.1(d). The slab was cast with normal density concrete supplied from a local concrete batch mix plant. The batch proportions of concrete are shown in Table 3.2. After pouring the concrete, the concrete slab was covered with a vapor proof barrier and was cured with water for a week. After this, the slab was left to cure at ambient conditions for at least six months, before testing under fire conditions. The relative humidity of concrete was measured at different locations of the slab periodically during the three months of curing and on the day of testing.

It should be noted that no fire proofing was installed on any of the four composite beams since the main objective of fire tests was not to achieve fire rating of these beams but rather to compare their relative behavior once subjected to dominant flexural loading or dominant shear loading under fire conditions.

3.2.3 Instrumentation

The four tested composite beams were instrumented with thermocouples, strain gauges, and displacement transducers to monitor thermal and mechanical response during fire tests. Steel temperatures were measured using 0.91 mm thick Type-K Chromel-alumel thermocouples

installed on the lower and upper flanges, as well as on four vertical locations along the height of the web at quarter and mid-span locations (as shown in Fig. 3.4). Additional thermocouples were also attached on shear studs, at mid-depth and surface of concrete slab (at quarter and mid-span locations). Vertically and horizontally oriented linear variable displacement transducers (LVDT) were attached at distinct locations on the beams in order to measure axial, out-of-plane web displacement, and vertical deflections.

To measure out-of-plane displacement of the web, a well-insulated stiff threaded steel rod was attached to the center of the web panel and extended horizontally (i.e., parallel to the concrete slab). In order for this steel rod to vertically pass through a distinct opening in the furnace lid, the steel rod was bent as shown in Fig. 3.5. The vertical deflection was measured through two LVDTs that were attached to the top surface of the concrete slab beneath the loading actuators. The steel frame that carries the LVDT was installed on top surface of the concrete slab (outside the furnace zone). A schematic of the set-up that is used to measure the web out-of-plane displacement is shown in Figure 3.5.

Data collected from the above instrumentation network was recorded at five second intervals through central data acquisition system. Visual observations were also made through two windows in the furnace at five minute intervals to record significant changes (such as local buckling, spalling, etc.) throughout the duration of the test and also after the tests were terminated.

3.2.4 Test Equipment

The fire resistance tests on composite beams were carried out at the structural fire testing facility at Michigan State University (shown in Fig. 3.2). This fire test furnace has been specially designed to produce varying conditions of heating scenarios (temperature-time curves) and

structural loading, similar to that of a composite beam might experience during an actual fire incident.

The fire test furnace is comprised of a steel framework supported by four steel columns, with the furnace chamber inside the framework. This chamber is 2.44 m wide, 3.05 m long, and 1.78 m high and can produce a maximum heat energy of 2.5 MW using six gas burners located within the furnace. Inside of this furnace, six type-K Chromel-alumel thermocouples are mounted on the walls of the furnace to monitor actual progression of temperature. During the course of fire test, the gas supply is manually adjusted such that the furnace temperatures follow a pre-determined fire curve (standard or design (realistic)). This furnace is also designed with two small view ports provided on either side of furnace walls to facilitate visual observations of fire-exposed composite beams.

The fire test facility is primarily designed to test simply-supported horizontal members (i.e., beams and slab), as well as vertical members (columns). Vertical loading can be applied on columns, beams or slabs using an adjustable loading system. This system can be modified to apply one, two or five-point loadings. However, since this loading system is mounted above the fire zone, the adjustable loading system cannot be used to apply high magnitude of shear forces at end supports of beams (since end supports of beams are placed outside the furnace (see Fig. 3.6)).

In order to simulate high shear forces on composite beams during fire exposure, a new loading set-up was specially designed and fabricated as part of the current test program. The new loading set-up required addition of an intermediate support to be installed inside the furnace, such that high shear loading can be generated on the composite beam using two hydraulic

actuators placed on the sides of the intermediate support. This modification allows simply-supported composite beams to have an additional interior support (i.e., such beams can be tested as continuous beams). The needed internal support was designed to be in the form of a reinforced concrete (RC) column as shown in Fig. 3.2 and Fig. 3.3. This RC column is of a square cross section (204x204 mm) and is casted with a special concrete mix. This concrete mix is made of high strength concrete with embedded polypropylene fibers. The batch mix properties or this high strength concrete is shown in Table 3.3. During fire tests, this concrete column is insulated with 50 mm thick insulation to limit temperature rise in concrete column and also to avoid possible elongation of column.

3.2.5 Test conditions and procedure

For undertaking fire tests, each composite beam was placed inside the furnace as shown in Fig. 3.2 and Fig. 3.6. It should be noted that the furnace is designed for testing beams with a maximum depth of 406 mm, however, the test specimens have an overall depth of 750 mm. Hence, a new lid to the furnace, with increased overhead, was specially designed for these tests. The newly designed lid is made of reinforced concrete slab to accommodate the deep steel beams and allow three sides of beams and underneath of the slab to be exposed to fire during the fire test.

Prior to fire tests, a predefined load was applied vertically using hydraulic actuators and this load was kept constant throughout the fire test. This predefined load was about 33-40% of flexural and shear capacity of the tested beam. For instance, in the first test, composite beam CB1 was subjected to a single point load equivalent to 40% of its room temperature flexural capacity and to 27% of its shear capacity. However, composite beams CB2, CB3 and CB4 were subjected to two point loads placed at 430 mm from mid-span of the beam utilizing a different

set of actuators (smaller than the one used in testing of CB1). To simulate high magnitude of shear force, full capacity of these smaller actuators was utilized. The applied loading used in testing composite beams CB2, CB3 and CB4 was equivalent to 5% of room temperature flexural capacity and 33% of room temperature shear capacity of these beams.

Prior to fire exposure, each beam was gradually loaded by incrementing hydraulic pressure in the actuators. Once the target load was reached, it was allowed to stabilize for about 30 minutes. Then, the heating in the furnace was turned-on and furnace temperature was increased to follow ASTM E119 standard fire curve. Throughout the fire test, the loading on the composite beam was maintained at the specified load level. During fire test, cross sectional temperatures, vertical deflection, out-of-plane displacement of the web, and axial displacement of the beams was recorded at constant interval of 5 seconds. In addition to electronically recorded data points, visual observations were taken throughout the test until failure of composite beams.

The composite beams were considered to have failed and the tests were terminated when;

- The mid-span deflection exceeded L/30 (where L is the span length), in the case of CB1 which was tested as a simply-supported composite beam, or

- When the composite beams experienced loss of load bearing capacity and could no longer sustain the applied loading (Wainman and Kirby, 1989).

3.3 Material Properties

To evaluate mechanical properties of steel and concrete used in fabrication of composite beams, strength tests were carried out on steel coupons and concrete cylinders. For evaluating mechanical properties of steel, three coupons were cut from steel beams supplied by a local

fabrication company. Similarly, for evaluating compressive strength, concrete cylinders were cast from concrete batch mix during fabrication of concrete slab.

The selected steel coupons were tested in an MTS-810 testing equipment by subjecting them to incremental loading till failure and stress-strain response was recorded. The room temperature stress-strain response of a A572 steel coupon is shown in Figure 3.7. It can be seen that the general behavior of stress-strain relationship remained linear-elastic up to yielding, and then the response becomes nonlinear. No well-defined yield plateau was recorded in these tests. Once the peak stress is reached, steel undergoes plastic deformation through unloading phase up to rupture. The measured average tensile strength of steel coupons is 480 MPa.

Similarly, concrete cylinders were tested on 14, 28, and test days to evaluate compressive strength and tensile strength. A summary of strength properties of concrete used in concrete slab and interior column, as derived from room temperature tests, are tabulated in Tables 3.4 and 3.5. The average 28 day compressive strength of concrete used in slab is 30 MPa.

3.4 Experimental Results

Data generated from the above fire tests is utilized to trace the response of fire-exposed composite beams. Relative thermal and structural response, as well as failure modes, is compared to evaluate the effect of loading type and level of composite action on the fire response of composite beams.

3.4.1 Thermal response

As discussed above, composite beams CB1, CB2, CB3 and CB4 were exposed to ASTM E119 fire exposure. For evaluating thermal response of composite beams, cross-sectional temperatures were measured at different points in web, flanges, shear studs, and concrete slab at two traverse sections (as shown in Fig. 3.4). Since all four composite beams have similar

geometric characteristics (same steel section and concrete slab dimensions), made of same material batches and are subjected to same type of fire exposure (ASTM E119), all tested composite beams experienced similar thermal response. Therefore, cross-sectional temperatures at selected points on composite beam CB2 only are plotted as a function of fire exposure time in Fig. 3.8.

In general, temperatures at different points in steel beam increased at a much faster pace than that in concrete slab or shear studs. Within the steel beam, web temperature increased at a higher rate than that in top and bottom flanges (as shown in Fig. 3.8). This can be attributed to the fact that web is more slender (much deeper and has smaller thickness) than that of the flange, hence has a larger exposed surface area than that of flanges. Figure 3.8 also shows that measured temperatures in top flange of steel beams are much lower than that in bottom flange. This is due to insulating effect of the concrete slab which acts as heat sink. It should be noted that much of the heat from the top flange of beam gets dissipated to concrete slab due to high thermal capacity of concrete.

The temperature in shear studs remains much lower than that in top flange, despite the stud being welded to top flange of the beam. This is due to the better insulating properties of surrounding concrete in the slab which absorbs much of the heat from studs. Finally, the temperatures at mid-width of the slab (where steel beam connects with concrete slab) increase at a higher rate as compared to temperatures at the edge of the slab (406 mm from mid-width). This can be attributed to the fact that the concrete slab absorbs much of the heat from top flange of steel beams.

59

3.4.2 Structural response

The structural response of composite beams exposed to fire conditions can be assessed by tracing vertical deflection, out-of-plane web displacement, slip at concrete steel interface and failure modes. The following sub-sections provide further details on the comparative behavior of fire-tested composite beams when subjected to dominant flexural or high shear loading.

3.4.2.1 Vertical deflection

The flexural response of tested composite beams CB1, CB2, CB3 and CB4 during fire exposure time is illustrated in Fig. 3.9, where progression of vertical deflection is plotted as a function of fire exposure time. It can be seen from the figure that the response of composite beam CB1, with flexural loading, is significantly different than that of composite beams CB2, CB3 and CB4 that were tested under predominant shear loading. This is due to different loading type adopted in testing of composite beams. In general, the simply-supported composite beam (CB1) tested under high flexural loading undergoes large vertical deflection at mid-span accompanied by noticeable rotations near end supports. This response is different than that observed in composite beams CB2, CB3 and CB4, loaded with high shear forces, which experienced very little vertical deflection (with no signs of rotations at support regions). This infers that type of loading imposed on a beam can significantly impact the mechanism through which the beam resists the imposed loading.

To further illustrate the response of composite beam CB1, with flexural loading, can be grouped under three stages. During the first stage (Fig. 3.9a), the mid-span deflection in composite beam CB1 increases linearly up to about 10 min, when the temperatures in the bottom flange and web reaches about 300°C. The deflection at this stage of fire exposure is mainly due to significant temperature gradients that lead to high thermal stresses and curvature along the

beam section. The developed curvature at this stage of fire exposure is independent of loading on the composite beam, since this curvature results mostly from the effect of thermal gradients developed in the beam. In the second stage of fire exposure, the mid-span deflection starts to increase (between 10 min and 25 min) due to degradation of strength and modulus properties of the steel as the bottom flange and web temperatures exceed 400°C. In the final stage of fire exposure (after 30 min), when steel temperature exceeds 600°C, the mid-span deflection increases at a rapid pace due to spread of plasticity in the bottom flange, and high temperature creep effects, leading to formation of plastic hinge at the mid-span. The composite beam is said to attain failure when mid-span deflection exceeds L/30 limit (at 40 min) as the composite beam cannot sustain applied loading at this point.

As discussed earlier, composite beams CB2, CB3 and CB4, subjected to predominant under shear loading, were tested as continuous beams wherein a concrete column was used as an interior support at the mid-span of these beams (see Fig. 3.2). Since the structural loading was applied very close to the intermediate support (to simulate high shear loading), these composite beams experienced very low levels of vertical deflection and no rotations (at end supports) during fire exposure as shown in Fig. 3.9b. The vertical deflection of these composite beams is very similar in terms of magnitude and response. This vertical deflection starts to increase at the same rate throughout the fire exposure but remains very small (about 9-16.5 mm) and then stabilizes which is different than that shown in mid-span deflection in CB1. In composite beams CB2, CB3 and CB4, the maximum vertical defection ranged between 9 and 16.5 mm which corresponds to 7 and 13% of that of the BS-476 standard deflection limit criteria. Hence, it is clear that deflection in these composite beams is not clear representation for determining failure. Thus, failure in these composite beams occurs upon attaining their sectional load capacity.

3.4.2.2 Out-of-plane web displacement

The structural response of tested composite beams CB1, CB2, CB3 and CB4 with fire exposure time is further illustrated in Fig. 3.10, where progression of out-of-plane web displacement is plotted. The measured out-of-plane web displacement shown in Fig 3.10 is at a point located at the mid-height of the web and 430 mm away from mid-span (below the point of applied loading) as shown in Fig. 3.2. It can be seen that out-of-plane web behavior of tested composite beams varies significantly.

For instance, composite beam CB1, tested under flexural loading, did not experience any web lateral displacement as shown in Fig. 3.10. However, composite beams CB2, CB3 and CB4 experienced substantial levels of out-of-plane web displacement. It can be seen from Fig. 3.10 that out-of-plane web displacement in these three beams initiated within the first 10 min of fire exposure when web temperature reaches 150-220˚C range, which corresponds to start of temperature induced degradation of modulus of elasticity of steel.

In the case of composite beam CB2, the out-of-plane web displacement steadily increased to 5 mm from the start of fire test till about 22 min into fire exposure when average web temperature is 460˚C, then rapidly increased to 25.4 mm at 30 min of fire exposure when average web temperature is 500˚C. At this point, out-of-plane web displacement increased at a rapid pace to 35.6 mm (which corresponds to average web temperature of 590˚C) till failure occurs in the composite beam. At this point, the fire test was stopped and this composite beam (CB2) was left to cool down to room temperature. Upon cooling, further inspection was carried out and large amount of web buckling that occurred near the mid-span region was observed as shown in Fig. 3.11a. It was also noticed that the welding of stiffener located at mid-span was ruptured near the bottom flange region (shown in Fig. 3.11b).

In the case of composite beam CB3, the out-of-plane web displacement increased at a slightly faster pace than that in beam CB2 and reached up to 31 mm (at average web temperature of 505˚C). Then, the web displacement (readings) instantly increased indicating a change of displacement direction. Such sudden change of displacement direction was believed to be caused by temperature-induced instability of the web. Comparing the slenderness of the web ($\lambda = 55.1$) with slenderness limit ($\lambda_p = 51.5$) at that point in time (where average web temperature was 440˚C), it is clear that the web slenderness exceeded the slenderness limits, evaluated as per room temperature local buckling provisions. This leads to transforming of the web from a compact to non-compact web due to initiation of inelastic web local buckling. However, this sudden change lasted for few seconds before the web re-adjusted and continue to displace in the original direction as shown in Fig. 3.10. This is believed to be due to redistribution of stresses/forces in the composite beam.

Finally, the observed out-of-plane web displacement in composite beam CB4 was similar to that observed in composite beam CB2, but the extent of displacement was of higher magnitude since composite beam CB4 was designed with partial (50%) composite interaction. The out-of-plane web displacement in composite beam CB4 started to increase linearly until it reaches 20.3 mm. This displacement slightly decreases to 31 mm at about 30 min into fire exposure when average web temperature is 500˚C. Then, additional increase in out-of-plane web displacement continued until failure occurs in the composite beam. At the time of failure, the maximum horizontal displacement of web in composite beam CB4 was 36 mm and corresponding web temperature was 620˚C. The initiation of web local buckling in composite beam CB4, as well as buckling response at different times as observed during the fire test, is shown in Fig. 3.12. The

time and corresponding temperature at which web buckling initiates, together with maximum out-of-plane displacement in each composite beam is also summarized in Table 3.6.

3.4.2.3 Slip at beam-slab interface and cracking in slab

The contact state between the steel beams and concrete slab, in terms of slip at that interface and response of concrete slab, was closely monitored throughout the fire tests. In general, there was no slip at the steel-concrete interface in composite beams CB1 and CB2, but slip occurred in composite beams CB3 and CB4. This is mainly due to the fact that composite beams CB1 and CB2 were designed to achieve full composite action between slab and beam, while composite beams CB3 and CB4 were designed for partial composite interaction (50% of that provided in CB1 and CB2).

In the case of composite beam CB1, concrete slab experienced extensive cracking/crushing at failure of composite beam when the concrete slab achieved its flexural capacity. On the other hand, in the case of composite beam CB2, tested under shear loading, concrete slab in composite beam did not undergo any apparent cracking and remained intact throughout fire test. However, in composite beams CB3 and CB4, a relatively large shear crack appeared at the edge of the concrete slab after 30 min into fire exposure. This crack started from the location of the shear stud located at the end of the composite beam. Once this crack propagated through the thickness of the concrete slab and reached its surface, a large separation between the concrete slab and steel beam took place. This shear crack as well as complete interface separation between slab and beam are observed in composite beams CB3 and CB4 are shown in Fig. 3.13. It is clear from these observations that the level of composite action can affect response of fire-exposed composite beams when subjected to high shear loading.

64

3.4.2.4 Failure modes

Visual observations were made during and at the end of fire tests to capture state of tested composite beams and also to study development of failure mechanism in tested composite beams. Vertical deflection, out-of-plane web displacement, crack patterns in concrete slab, slip between slab and steel beam in the fire tested composite beams were utilized to identify failure limit states in each specimen.

For instance, test observations recorded in composite beam CB1 indicate that flexural behavior dominated response and failure of composite beam during the entire duration of fire exposure. This composite beam experienced significant degradation in flexural capacity and thus failed through yielding of bottom flange, with no signs of local buckling (instability) in the web. The condition and failure pattern of this composite beam after fire test is shown in Fig. 3.14a. The composite beam forms a "V" shape at failure due to large deflections, resulting from large rotations at the composite beam ends and also due to crushing of concrete at the mid-span region.

Figure 3.14 also shows failure and magnitude of deformation in composite beams CB2, CB3 and CB4. The failure of composite beams CB2 and CB4 was in shear mode in which web local buckling was prominent, while composite beam CB3 remains intact as discussed above. Both composite beams CB2 and CB4 failed early into fire exposure at 55 and 50 min, respectively. It is clear that shear action dominated structural response of these composite beams due to occurrence of large buckling of web and lack of flexural-related failure signs i.e., large mid-span deflection or significant rotation at end support regions. Furthermore, composite beam CB4 experienced larger torsional effects and cracking of slab than that observed in composite beam CB2. This is due to the fact that there was partial interaction (composite action) between

65

the concrete slab and steel beam since CB4 had half the number of shear studs as that in composite beam CB2.

Table 3.1: Summary of sectional dimensions, test parameters, and loading conditions of tested composite beams

Parameter	Description	CB1	CB2	CB3	CB4
Sectional geometry	Steel beam section	Rolled section W 24x62	Rolled section W 24x62	Rolled section W 24x62	Rolled section W 24x62
	Span (between supports), mm	3658	3658	3658	3658
	Total length (end to end), mm	4167	4167	4167	4167
	Flange plate (b_f x t_f), mm	177.8 x 12.7	177.8 x 12.7	177.8 x 12.7	177.8 x 12.7
	Web plate (D x t_w), mm	610 x 11.1	610 x 11.1	610 x 11.1	610 x 11.1
	Concrete slab (b_{eff} x t_s), mm	813 x 140	813 x 140	813 x 140	813 x 140
	End panel width (S), mm	254	254	254	254
	Web slenderness ratio (D/t_w)	52	52	52	52
	Composite action (%)	100%	100%	50%	50%
Stiffener	Bearing stiffeners- mid-span (w x t_{stf}), mm	76.2 x 12.7	76.2 x 12.7	76.2 x 12.7	76.2 x 12.7
	Bearing stiffeners- supports (w x t_{stf}), mm	76.2 x 9.5	76.2 x 9.5	76.2 x 9.5	76.2 x 9.5
Capacity at ambient temperature	Flexural (composite), kN.m	1569	1569	1569	1569
	Shear web buckling (V_{cr}), kN	1278	1278	1278	1278
	Total shear capacity (V_u), kN	1278	1278	1278	1278
Applied load	Applied load, kN	691	222	222	222
	Applied load/flexural capacity	40%	5%	5%	5%
	Applied load/shear capacity	27%	33%	33%	33%
	Fire exposure	ASTM E119	ASTM E119	ASTM E119	ASTM E119

Table 3.2: Mix proportions used in the tested composite beam-slab assembly

Components	NSC
Date Casted	08/06/14
No. of specimens (No. with TC)	30 (15TC)
Coarse Aggregate 3/8" Limestone, Kg/m^3	984.84
Natural sand, Kg/m^3	929.66
Cement, Kg/m^3	230.19
Silica fume, Kg/m^3	-
Fly Ash- Class C, Kg/m^3	76.53
Water, Kg/m^3	153.66
Superplastisizer, Kg/m^3	24.56
Water reducer, Kg/m^3	6.11
Accelerator, Kg/m^3	12.28
Air content admixture, Kg/m^3	3.08
Design Air content %	2.0
W/C ratio	0.50
Slump, mm	101.6
28 day $f'c$, MPa	30

Table 3.3: Mix proportions used in the concrete column (interior support)

Components	HSC-PP
Date Casted	07/16/14
No. of specimens (No. with TC)	30 (15TC)
Coarse Aggregate 3/8" Limestone, Kg/m^3	1089.256
Natural sand, Kg/m^3	640.74
Cement, Kg/m^3	560.65
Silica fume, Kg/m^3	41.53
Fly Ash- Class C, Kg/m^3	-
Water, Kg/m^3	150.69
Superplastisizer, Kg/m^3	
Water reducer, Kg/m^3	71.78
Accelerator, Kg/m^3	-
Air content admixture, Kg/m^3	-
Design Air content %	0-3.0
W/C ratio	0.30
Polypropelene fibers, Kg/m^3	1.66
Humidity during casting %	37
28 day $f'c$, MPa	100

Table 3.4: Properties of concrete used in fabrication of concrete

Age (days)	Compressive strength (f_c, MPa)	Indirect tensile strength (f_t, MPa)
14	22	3.0
28	30	3.8

Table 3.5: Properties of concrete used in fabrication of column (interior support)

Age (days)	Compressive strength (f_c, MPa)	Indirect tensile strength (f_t, MPa)
14	54	5.0
28	98	7.8

Table 3.6: Comparison of buckling behavior in composite beams CB1, CB2, CB3 and CB4

Composite beam	Time at initiation of web bucking (min)	Temp. at initiation of web bucking (˚C)	Max. out-of-plane displacement (mm)	Temp. at max. out-of-plane displacement (˚C)
CB1	-	-	-	-
CB2	9	220	35.6	590
CB3	5	150	31	530
CB4	5	153	36	620
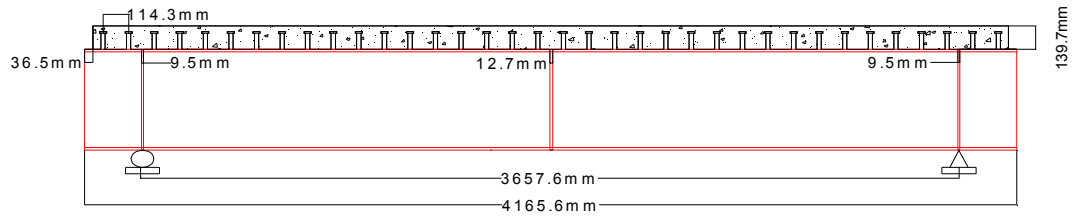
(a) Composite beams CB1 and CB2
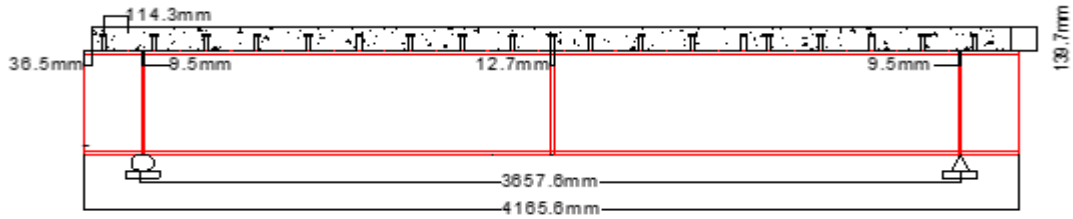
(b) Composite beams CB3 and CB4

(c) Steel beams with different shear stud arrangement
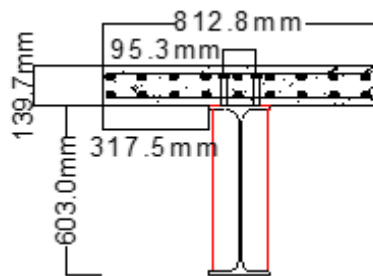
(d) Cross section of composite beams

Figure 3.1: Longitudinal and traverse sections for tested composite beams
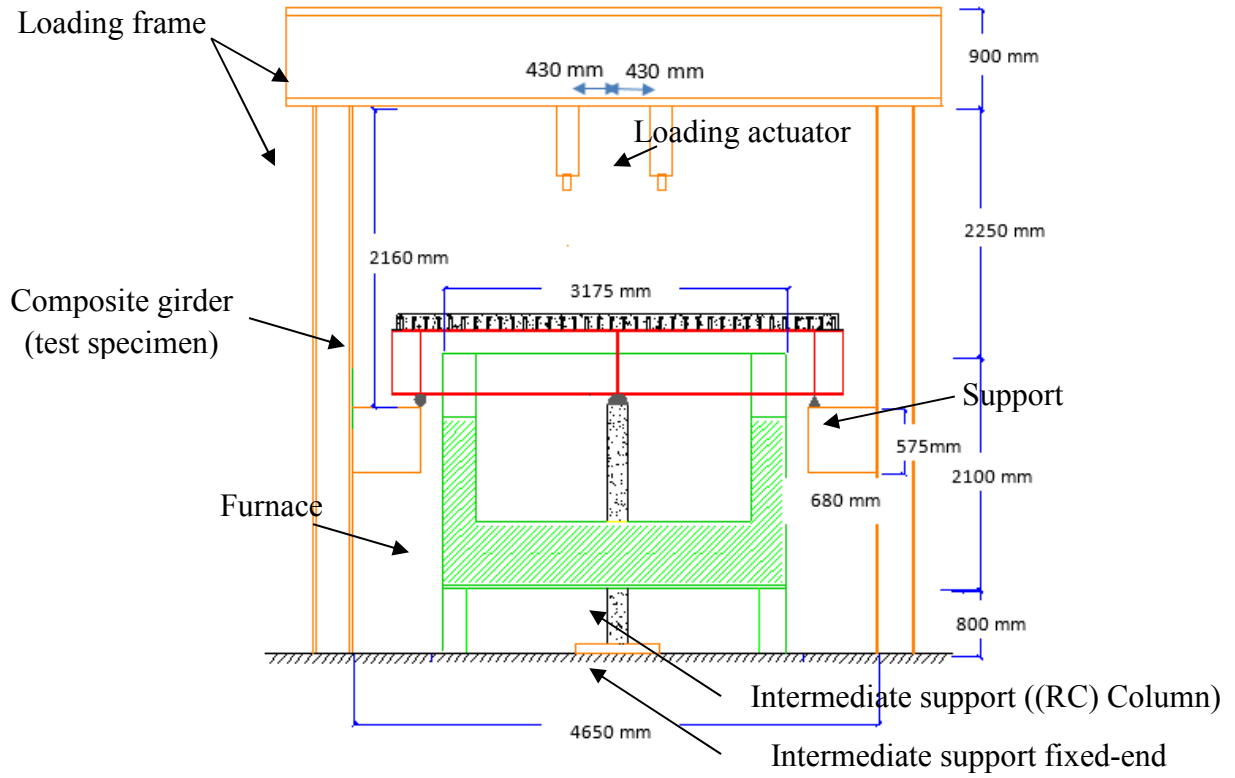
Figure 3.2: Fire testing facility and loading set-up
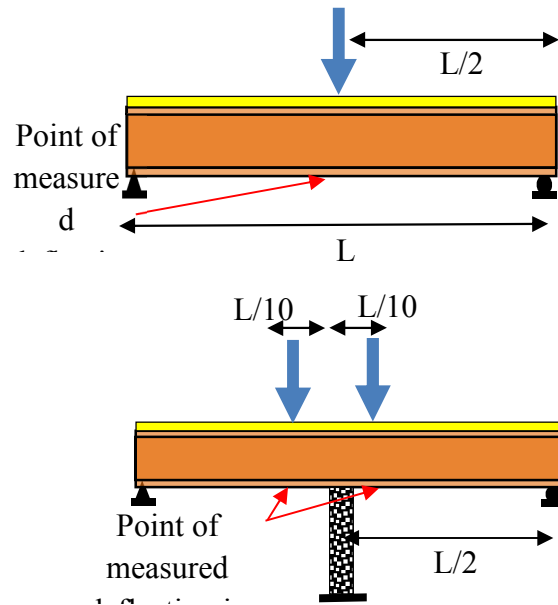
Figure 3.3: Schematic of test setup and steel-concrete beam placement in the furnace
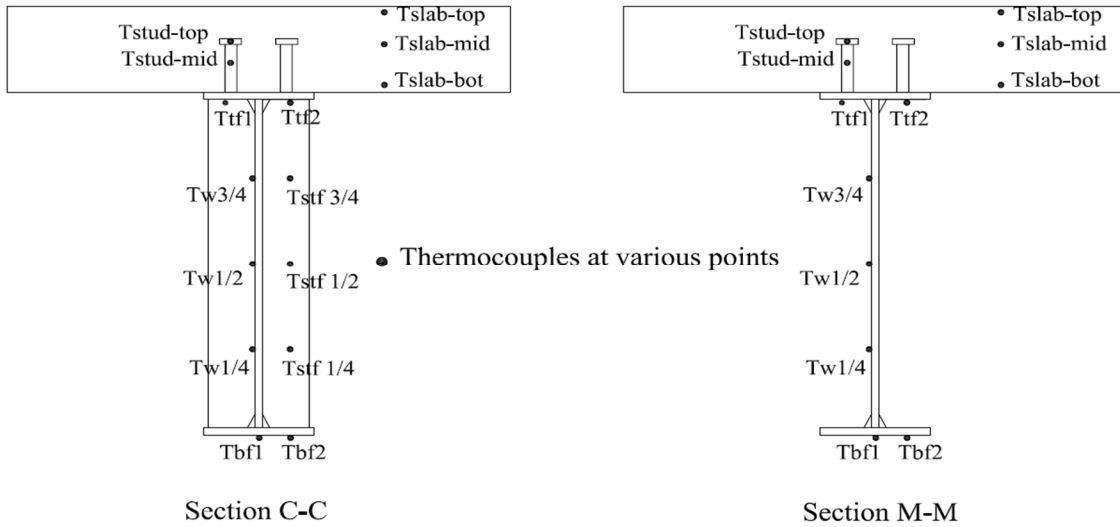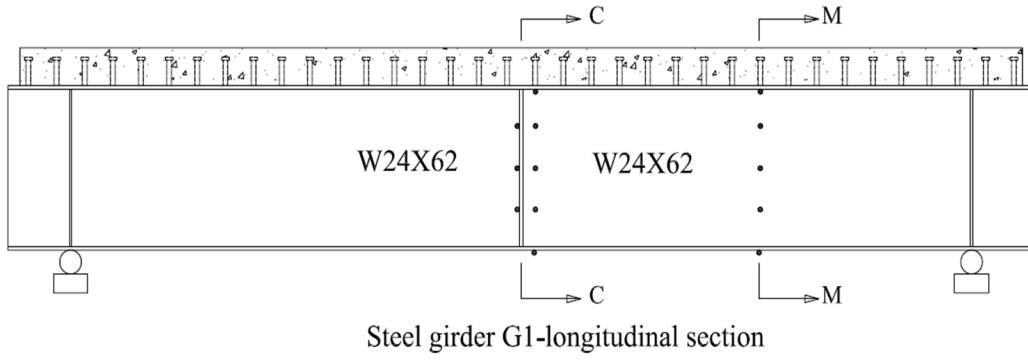
Figure 3.4: Layout of thermocouples on composite beam CB1 (Aziz et al., 2015)
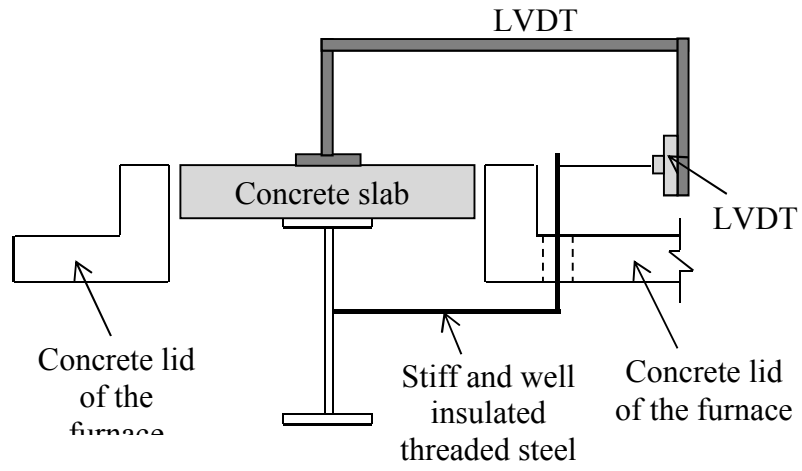
Figure 3.5: LVDT set-up to measure web out-of-plane displacement (Aziz et al., 2015)

(a) Longitudinal elevation
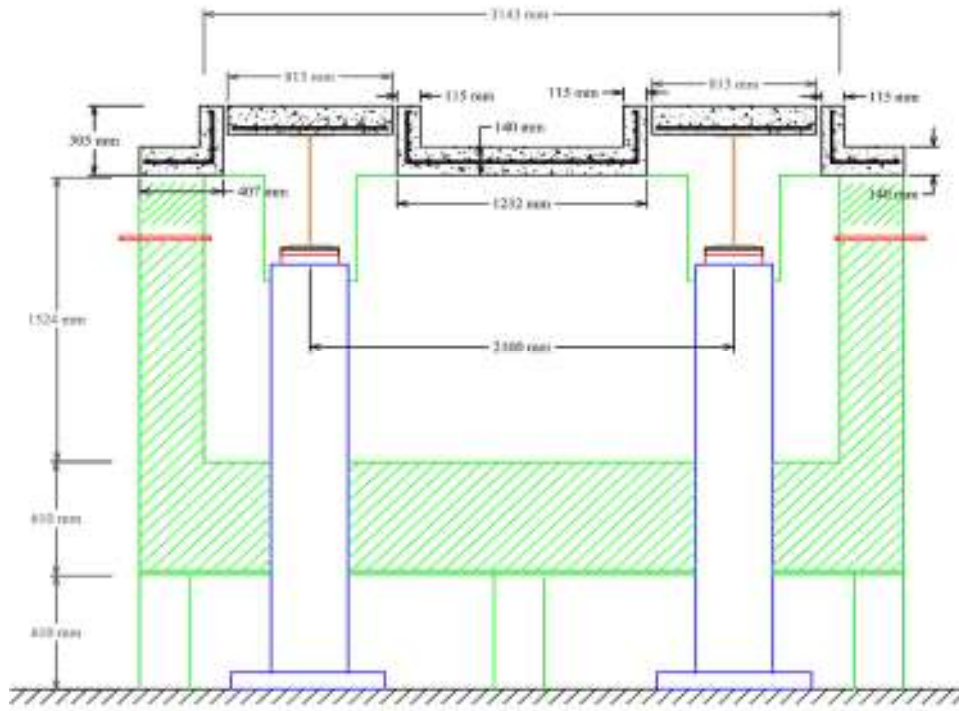
(b) Traverse section

Figure 3.6: Placement of composite beam in the furnace at the structural fire testing facility at Michigan State University
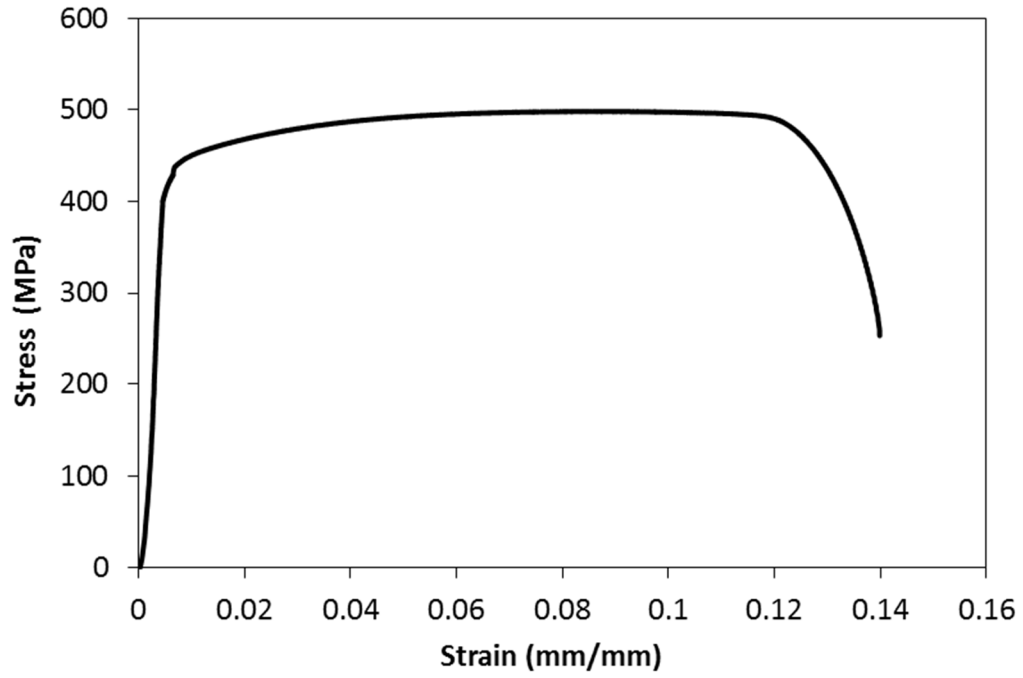
Figure 3.7: Room temperature stress-strain response of A572 Gr50 steel (Aziz et al., 2015)
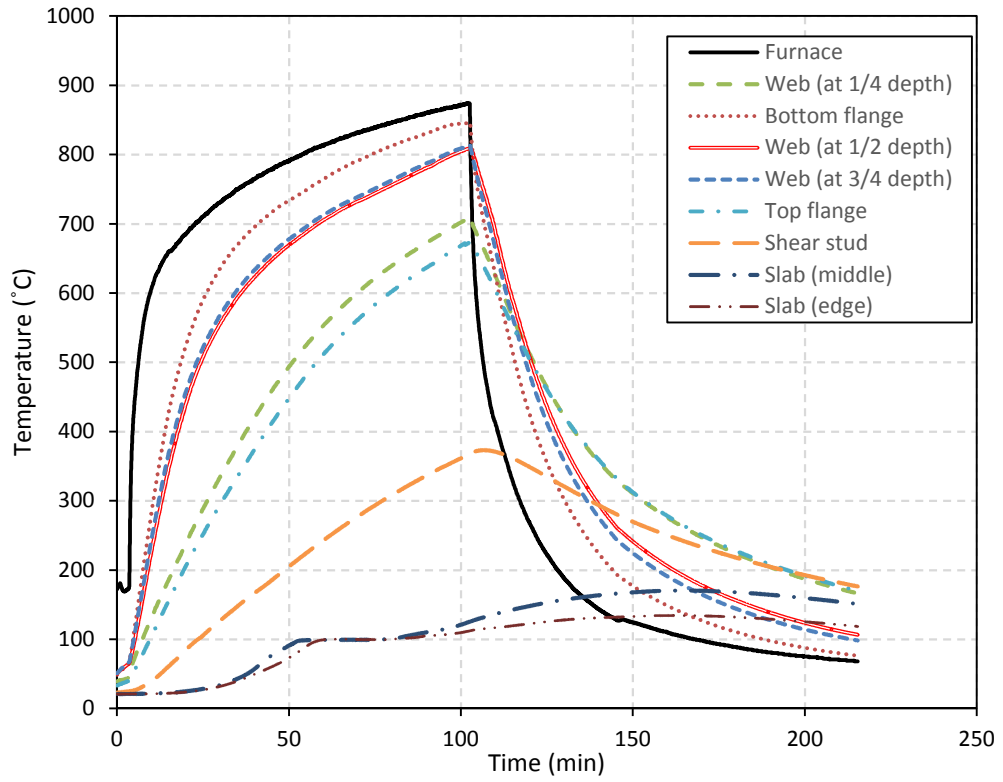
Figure 3.8: Measured temperature profiles in composite beam CB2 as a function of fire exposure time
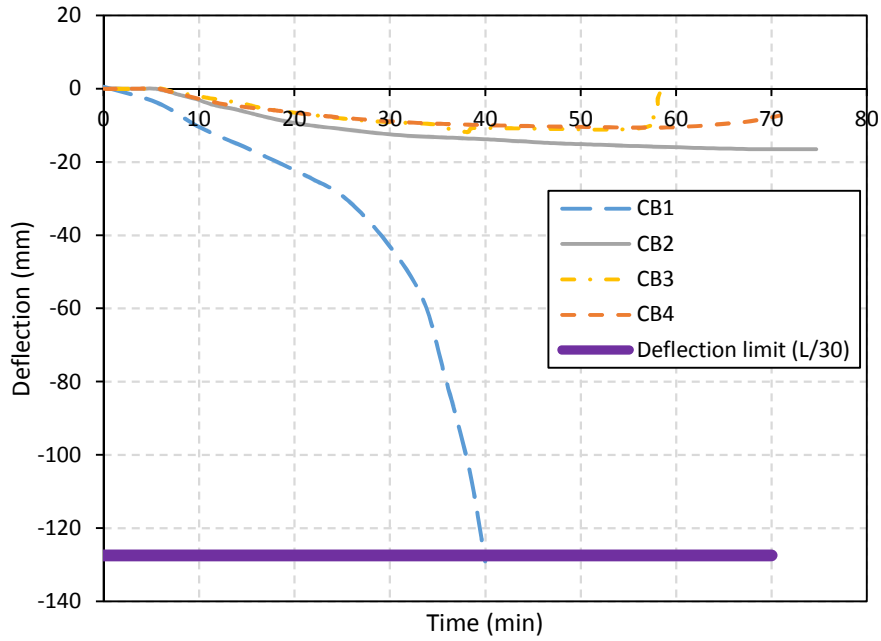
(a) Comparison of vertical displacement of CB1, CB2, CB3 and CB4
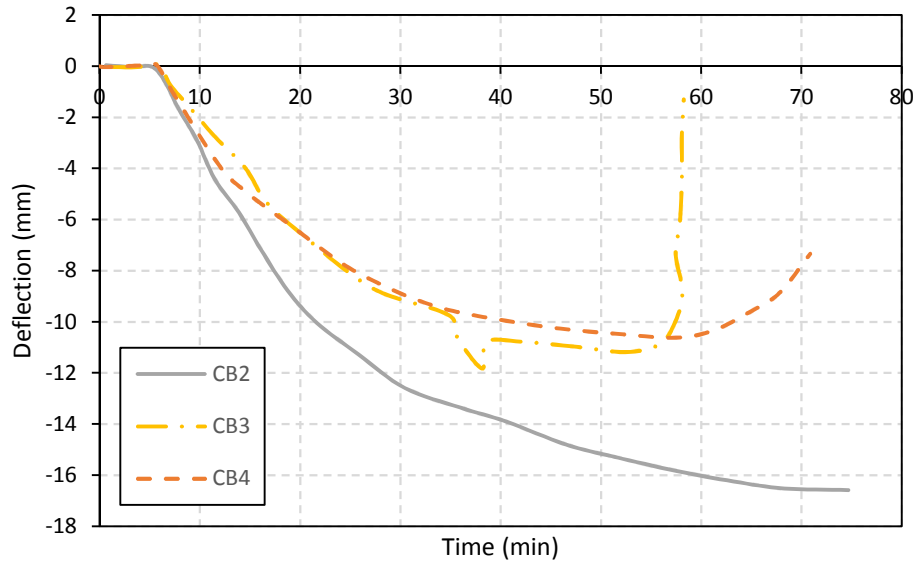
(b) Comparison of vertical displacement of CB2, CB3 and CB4

Figure 3.9: Vertical displacement in composite beams as a function of fire exposure time
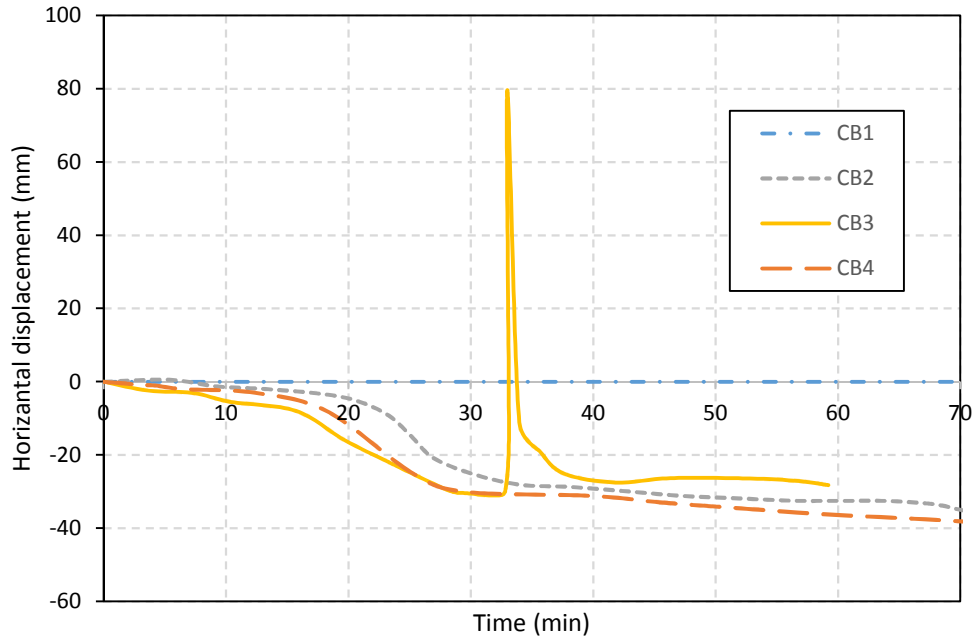
Figure 3.10: Variation of web out-of-plane displacement as a function of fire exposure
time in composite beams

(a) Local buckling of web   (b) Rupture of weld in stiffener

Figure 3.11: Web local buckling in composite beam CB2
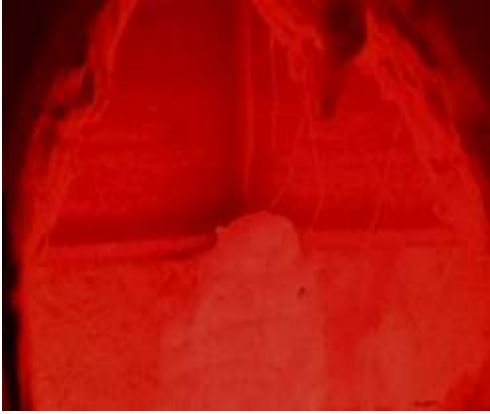
(a) Initiation of web local buckling at 48 min into fire exposure
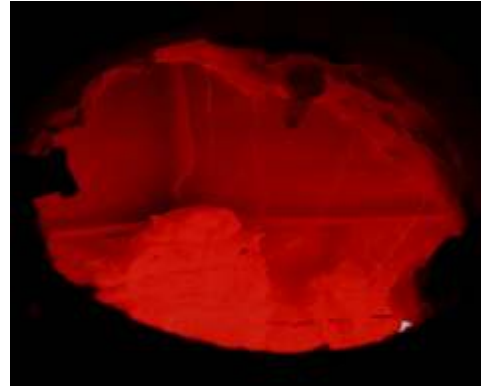
(b) Web local buckling at 55 min

Figure 3.12: Web local buckling in composite beam CB2 with fire exposure time

(a) Crack at end side of composite beam (CB3)

(b) Separation of concrete slab (CB4)

Figure 3.13: Cracking and separation of concrete slab in composite beam CB3 and CB4

(a) Failure mode of CB1 (Aziz et al.,
2015)

(b) Failure mode of CB2

(c) Intact state of CB3 (post fire test)

(d) Failure mode of CB4

Figure 3.14: Illustration of failure pattern in composite beams CB1, CB2, CB3 and CB4
after exposure to fire.

3.5 Summary

Fire resistance tests were carried out to study the fire behavior of four uninsulated, standard and hot-rolled composite beams under high flexural and shear loading. Test variables in the tests included; effect of loading type and level of composite action available between steel beam and concrete slab. Results from fire tests indicate that composite beams (when subjected to high flexural and/or shear loading) can experience early failure (in less than one hour) under standard fire conditions. The time to failure and mode of failure in these fire-exposed composite beams is highly influenced by effect of loading and level of composite action. These tests have showed that composite beams fail through flexural yielding when subjected to high flexural loading, however failure mode changes to shear failure (through web local buckling) when subjected to high shear loading.

CHAPTER FOUR

4. Numerical Model

4.1 General

Evaluating fire resistance of structural members through fire tests is quite expensive, complex, time consuming and requires sophisticated instrumentation and fire test facilities. Further, in such tests, only a limited number of governing parameters can be evaluated and interdependency of these parameters cannot be traced. The alternative to overcome many of the limitations in fire tests is to apply a numerical modeling approach for evaluating the fire response of structures. For this purpose, a three dimensional nonlinear finite element model was developed to evaluate fire resistance of isolated steel beams/girders and composite beams (steel beams attached to concrete slab via shear studs). This model takes into account geometric and material nonlinearities, temperature-dependent material properties, and various failure limit states. The validity of the finite element model in tracing thermal and structural response is established by comparing predictions from the analysis with results from fire tests presented in Chapter 3 and test data reported by other researchers (Kodur and Fike, 2009). Full details on the development of this model, as well as the validation process, is presented in this chapter.

4.2 Development of Finite Element Model

To study the effect of shear loading on the response of isolated steel beams and composite beams/assemblies under fire conditions, a finite element model was developed in ANSYS (2013). Fire response of such structural members is simulated through two stages of analysis, i.e. thermal and structural. For tracing the realistic fire response, critical parameters that influence fire response of such members, i.e. geometric and material nonlinearities, temperature-dependent material properties and various failure limit states are accounted for in the analysis. Details on elemental discretization, material properties input parameters, constitutive models,

simulation techniques and different failure limit states are also discussed in the following subsections.

4.2.1 General approach

Fire resistance analysis is generally carried out through two stages of analysis, namely thermal and structural analysis. In thermal analysis, cross-sectional temperature distribution in a structural member is generated as a function of fire exposure time. The output from the thermal analysis, i.e., nodal temperatures, is then applied as an input (i.e., thermal body load) to the structural model where a transient stress (structural) analysis is carried out. The structural analysis generates stresses, strains and deformations resulting from combined effect of structural loading and fire exposure. These steps, associated with fire resistance analysis of structural members, are illustrated through a the flowchart shown in Fig. 4.1.

4.2.2 Thermal analysis

In general, fire exposure along the beam span (length) is assumed to be uniform. This assumption has been verified by analyzing results of fire-tested composite beams presented in Chapter 3 as well as other researchers (Kodur and Fike, 2009). Thus, this assumption simplifies the heat transfer complex phenomenon and reduces its order from a three-dimensional problem into a two-dimensional problem. Therefore, the governing partial differential heat transfer equation within a structural member cross section can be written as:

$$\rho c_{(T)} \frac{dT}{dt} = \nabla . \left(k_{(T)} \nabla T \right) \tag{4.1}$$

where,

ρ = density,

c = specific heat,

∇ = is the spatial gradient operator

k = conductivity matrix,

T = temperature,

t = time,

Since the main mechanism of heat transfer at the fire-beam interface is through convection and radiation, the heat flux on this interface due to convection and radiation can be expressed through the following equation:

$$q_b = (h_{con} + h_{rad})(T - T_f) \qquad (4.2)$$

where,

h_{con} = the convective heat transfer coefficient, and equals 25 W/m^2.K for external, ASTM E119, and ISO 834 fires as recommended in Eurocode (EC1, 2002),

h_{rad} = the radiative heat transfer coefficients, and is defined as:

$$h_{rad} = 4\sigma\varepsilon(T^2 + T_f^2)(T + T_f) \qquad (4.3)$$

where,

T_f = fire temperature,

σ = Stefan-Boltzman constant = 5.67×10^{-8} (W/m^2.°K^4),

ε = emissivity factor which is related to the "visibility" of the exposed surface of structural member to the fire.

In numerical heat transfer analysis, fire is assumed to be originating from a point source (i.e., perfect black body) radiating heat equally in all spatial directions. Thus, to account for heat loss to surrounding environment as fire travels from its source to the structural member; it is assumed that only 70% of the radiant heat reaches the structural member surface. Therefore, an emissivity factor of 0.7 as specified in Eurocode (EC3, 2005) is assumed in the analysis.

According to Fourier's law, the governing heat transfer within a structural member is through conduction and can be expressed as:

$$k\left(\frac{\partial T}{\partial y}n_y + \frac{\partial T}{\partial z}n_z\right) = -q_b \qquad (4.4)$$

where, n_y and n_z are components of the vector normal to the boundary in the plane of the cross-section. The right hand side of Eq. [4.4] depends on the type of imposed boundary condition. As the structural member is exposed to fire from three sides, two types of boundary equations are to be considered in thermal analysis, namely:

- On fire exposed boundaries, the heat flux is governed by the following equation:

$$q_b = -h_f(T - T_f) \qquad (4.5)$$

- On unexposed boundary, the heat flux governed by:

$$q_b = -h_0(T - T_0) \qquad (4.6)$$

where, h_f and h_0 are heat transfer coefficient on fire side and the cold side, respectively, and T_f and T_0 are temperature at fire exposed and cold side, respectively.

Thus, the nodal temperatures of any element are related by shape function matrix (N) to arrive at the temperature in the element;

$$T = \{N\}^T . T_e \qquad (4.7)$$

Then, the heat transfer equation (Eq.[4.1]) subjected to appropriate boundary conditions (Eq.[4.4]) can be discretized as (Cook et al., 2002):

$$C_e^t \dot{T}_e + K_e^t T_e = Q_e \qquad (4.8)$$

where,

C_e^t = specific heat matrix,

K_e^t = thermal "stiffness" matrix, and is the sum of conductivity and convection matrices,

T_e = nodal temperature,

Q_e = applied nodal thermal load and is composed of the convective and radiative heat fluxes.

In order to simulate the thermal response of a composite beam subjected to a fire scenario, the composite beam is discretized with thermal elements available in ANSYS elemental library. These elements are SOLID70, SHELL131, LINK33 and SURF152 (shown in Fig. 4.2). SHELL131 is a layered shell element having in-plane and through-thickness thermal conduction capability and is used to simulate the steel beam. SOLID70 is a cubic thermal element with conduction capability and is used to discretize the concrete slab. LINK33 is a uniaxial element with the ability to conduct heat between its nodes and is used to simulate reinforcing steel embedded in the concrete slab. SURF152 is a surface thermal element capable of simulating heat conduction, convection and radiation. In the simulation environment, SURF152 is overlaid on top of SHELL131 and SOLID70 elements to simulate convection and radiation mechanisms of heat transfer from fire source to a composite beam.

4.2.3 Structural analysis

As discussed above, nodal temperatures generated in the thermal analysis are used as an input to the structural analysis. To perform a structural analysis, ANSYS utilizes virtual work principles. According to these principles, any virtual change of internal strain energy must be balanced by a change in the external work due to the applied loading.

$$\delta U = \delta V \tag{4.9}$$

where;

U = strain energy,

V = external work

The variation in strain energy (δU) can be evaluated as:

$$\delta U = \int_v \{\delta\varepsilon\}\sigma dv \tag{4.10}$$

For structural members subjected to fire conditions, the strain vector (ε) is the sum of thermal (ε_{th}), mechanical (ε_m), and creep (ε_{cr}) strains:

$$\varepsilon = \varepsilon_m + \varepsilon_{th} + \varepsilon_{cr} \tag{4.11}$$

Variation of external work (δV) due to the applied nodal forces (F_e^n) can be computed by assuming a variation of nodal displacement $\{\delta u\}$ as:

$$\delta V = \{\delta u\}^T \{F_e^n\} \tag{4.12}$$

The nodal displacements of the finite elements (u_e) are related to the nodal displacement field through shape functions matrix (N) as follows:

$$u_e = \{N\}^T \cdot u \tag{4.13}$$

Thus, the virtual work equation (Eq. [4.9]) can be rewritten in matrix form as:

$$K_e u_e - F_e^{th} = F_e^n \tag{4.14}$$

where,

K_e = element stiffness matrix,

F_e^{th} = element thermal load vector

Similar to the thermal analysis, and in order to simulate the structural response of a composite beam subjected to a fire scenario, the composite beam is discretized with structural elements available in ANSYS elemental library (2013). In the structural analysis, the different components of a composite beam or girder are steel beam, concrete slab, steel-concrete interface, and shear studs, are taken into consideration. These components are discretized using suitable elements available in ANSYS library, namely SHELL181, SOLID65, LINK8, BEAM188,

COMBIN39, COMBIN14, CONTA173 and TARGE170 (shown in Fig. 4.3).

SHELL181 element is formulated to capture local buckling of flanges and web so it is used to discretize the steel beam. SOLID65 is used to discretize concrete slab since this element is capable of accounting for cracking and crushing of concrete. LINK8 is used to simulate reinforcing steel embedded in concrete slab. COMBIN14 are spring element which are used to model the bond-slip behavior between steel reinforcement and surrounding concrete. In order to accurately simulate shear stud, BEAM188 element is used and assumed to be welded to top flange of steel beam. To simulate the bond-slip action at the interface between of shear studs and steel beam, COMBIN39 element is used.

Furthermore, to account for composite action between the concrete slab and the top flange of the steel beam, nonlinear surface-to-surface contact elements (CONTA174 and TARGE170) are used. The contact pair can be fully bonded to simulate the full composite action between the concrete slab and steel beam or it can be partially bonded to account for the slip that occurs between the concrete slab and steel beam in case of partial composite action.

It should be noted that the developed model can be extended to simulate thermal and structural response of isolated steel beams/girders, composite beams as well as thin composite floor systems. Further details and discussion of these structural members can be found elsewhere (Kodur and Naser, 2013; Naser and Kodur, 2015).

4.3 Selection of Material Models

In order to effectively simulate the response of composite beams under fire conditions, high temperature material properties of various constituent materials namely, structural steel, concrete, steel reinforcement (in slab), shear studs and fire insulation is required. The following

subsections provide further details on the appropriate material properties used as input to the developed finite element model.

4.3.1 High-temperature thermal material properties

High-temperature thermal properties of steel and concrete specified in Eurocodes (EC3, 2005) and (EC2, 2004) are used in numerical analysis. These temperature-dependent thermal properties relations of structural steel, reinforcing steel and concrete are presented in Tables 4.1 and 4.2. For an insulated section, the thermal properties of the fire insulation (thermal conductivity and specific heat) are also vary as a function of temperature.

4.3.2 High-temperature mechanical material properties

For fire resistance analysis, mechanical properties of structural steel, reinforcing steel, shear studs, and concrete are critical. These properties are stress-strain relationships and modulus of elasticity which vary with increasing temperature. Since the fire insulation material does not have significant mechanical properties, the strength contribution from insulation to the capacity of the beam is neglected. In the developed finite element model, the following material models were used in analysis:

- Steel

  To simulate the behavior of structural and reinforcing steel in compression and tension, multilinear stress-strain relationships with Von-Mises plasticity yielding criterion and isotropic hardening plasticity model were used in fire resistance analysis. The significant points on Eurocode 3 stress-strain curves at elevated temperatures are given in Tables 4.3 and 4.4 and are shown in Fig. 4.4. The nominal stress-strain curves were converted into true stress-strain curves using the following relations:

$$\sigma_{true} = \sigma_{nom}(1+\varepsilon_{nom}) \quad and \quad \varepsilon_{true} = \ln(1+\varepsilon_{nom}) \tag{4.15}$$

where; σ_{true}, ε_{true} represent true stress and strain, while σ_{nom}, ε_{nom} represent nominal stress and strain, respectively.

- Concrete

The behavior of concrete is modeled using Eurocode 2 stress-strain relations that is illustrated in Fig 4.5. Further, the constitutive relationships and high-temperature strength reduction factors specified in Eurocode 2 (EC2, 2004) is utilized to generate nominal stress-strain relations at various temperatures. The constitutive relations and the reduction factors for concrete are presented in Table 4.5.

The plastic behavior of concrete is simulated using Williams and Warnke (1975) constitutive material model adopted in ANSYS. This model takes into account the spread of plasticity of concrete in both compression and tension regimes. The compressive plastic behavior of concrete is defined using isotropic multi-linear compressive stress–strain curves that vary with temperature. The tensile behavior of concrete is modeled using a trilinear model. In this model, the concrete tensile strength is taken as $0.62\sqrt{(f'c)}$; where $f'c$ is the compressive strength of concrete. Once the concrete reaches its tensile stress, a tensile stiffness multiplier of 0.6 is used to simulate a sudden drop of the tensile stress to 60% of the initial rupture stress. Then, the drop is followed by a linearly descending response to zero at a strain value of six times the rupture strain. Upon the first crack, the concrete material is treated as an isotropic elastic material, then it transforms to an orthotropic material after the initiation of cracks. Once a concrete element cracks, the modulus of elasticity is set to zero in the direction parallel to the principal tensile stress direction.

The Williams and Warnke (1975) constitutive material model requires additional parameters identified as the open and close crack shear transfer coefficients, (β_t and β_c).

96

Shear transfer coefficients is taken as zero when there is a total loss of shear transfer (representing a smooth crack) and 1.0 when there is no loss of shear transfer (representing a rough crack). The values of β_t and β_c in the developed model are assumed to be 0.2 and 0.7, respectively.

- Shear stud

The horizontal shear force-slip that develops between shear studs and concrete slab, is simulated using force-slip relation based on a nonlinear constitutive relationship proposed by Ollgaard et al. (1971).

$$V_h = Q_u \left[1 - e^{-4.75S} \right]$$

(4.16)

where V_h is the shear force, Q_u is the strength of the studs calculated as

$Q_u = 0.43 A_s \sqrt{E_c f_c'} \leq 0.7 A_s f_u$; A_s, E_c, f'_c and f_u are cross sectional area of the shear studs, elastic modulus of the concrete taken as $4600\sqrt{f_c'}$ (in MPa), compressive strength of the concrete, and ultimate strength of the studs taken as 420 MPa, respectively. S is slip length and the maximum slip length was set to 1.27 mm (CEB-FIP model code, 1993).

4.3.3 Failure criteria

The failure of a composite beam, under fire conditions can occur in different modes. Thus, the evaluation of realistic failure requires applying all possible limiting failure criteria. In this analysis, different failure limit states, including thermal (limiting temperature), flexural, shear, local buckling and deflection, are considered in evaluating failure of structural member at each time step. Hence, failure is said to occur once any of these limiting states is exceeded.

For example, moment and shear capacity at each time step are evaluated utilizing internal bending and shear stresses generated from structural analysis. These stresses, generated at distinct elements across the length of the structural element, are integrated across the height of the section. Once the stresses across the height of the section are obtained, these stresses are input into an ANSYS Parametric Design Language (APDL) supplementary sub-routine. This sub-routine uses generated stresses to calculate associated sectional moment and shear capacity. To maintain equilibrium, the calculated moment and shear capacities are then compared against the bending moment and shear force due to applied loading level. Once the applied loading level exceeds that of the moment and/or shear capacity, the structural member is said to fail.

At any point during structural analysis, the generated internal stresses need to be equal to the level of stresses from applied loading. This is to satisfy principles of virtual work discussed in Sec. 4.2.3. However, increase in nodal temperature leads to degradation in material properties. Towards the end of fire resistance analysis, the equilibrium between generated internal stresses and level of stresses from applied loading cannot be maintained (due to the large degradation in material properties). Once internal stresses exceed that of the temperature-degraded strength and elastic modulus properties, failure occurs.

Similarly, local buckling limit state is also checked at each time step by comparing web and flange slenderness to that of the temperature-dependent slenderness limits. For instance, slenderness of flanges and web is checked against temperature-dependent flexural and shear slenderness limits at each load-step (i.e., at each temperature) using the above mentioned supplementary sub-routine. Once the sectional slenderness exceeds the degraded compactness or non-compactness slenderness limit (λ_p or λ_r), local buckling is said to occur and sectional

capacity (i.e., flexural and/or shear) is adjusted to account for the loss arising from local buckling.

Finally, a deflection limit state is also applied to evaluate failure of fire exposed structural members. When the structural member attains a deflection of *L/20* or rate of deflection reaches $L^2/9000d$, where *L* and *d* are the span and depth of the structural member, respectively, the structural member is said to attain failure (BS 476, 1987).

4.4 Model Validation

Figure 4.6 shows the above developed finite element model being validated by comparing predicted response parameters from the analysis with those measured in fire tests. The validation of the developed model was conducted on two types of structural members, namely isolated steel beams and composite beams. The validation process covered both thermal and structural response parameters, i.e. sectional temperatures, mid-span deflection, out-of-plane web displacement and failure modes. It should be noted that the developed model can be extended to model thin composite floor systems comprising of a number of steel beams attached to a steel deck and connected to a large concrete slab, as shown in Kodur et al. (2013) and can also be found elsewhere (Wellman, 2011).

4.4.1 Steel beams

The above finite element model was validated using data from tests on isolated steel beams subjected to combined flexural and shear loading. Kodur and Fike (2009) have conducted fire resistance test on a 4 m long W12×16 A992 steel beam subjected to ASTM E119 standard fire (shown in Fig. 4.7). The beam was insulated with 50 mm thick spray applied vermiculite based fire insulation to achieve a 2-hr fire resistance rating. Table 4.6 provides a summary of the geometric and material properties used as input into the developed model.

The tested beam is analyzed using the above developed model and various output parameters generated in the analysis, namely temperatures, mid-span deflection and failure mode are compared against measured data from tests. For instance, Fig. 4.8a shows a comparison of predicted and measured temperatures in the steel beam as a function of fire exposure time. In general, temperatures in steel section rise steadily and slowly due to the presence of fire insulation. It can be seen that there is a good agreement between predicted and measured temperatures up to first 45 minutes (till 350°C) in steel. Then, the predicted temperatures tend to be slightly higher than the measured ones; such variation can be attributed to differences in assumed and actual thermal properties of fire insulation at elevated temperatures. It can be also seen that both measured and predicted temperatures converged towards the later stages of fire exposure.

A comparison of predicted and measured mid-span deflection response of the tested steel beam is shown in Fig. 4.8b. The beam undergoes only small deflection and this remains constant in the first 90 min. This can be attributed to low temperature rise in the beam facilitated by the presence of fire insulation. It should be noted that steel does not experience significant degradation in strength in 20-400°C, but experiences low loss (of about 30% at 400°C) in elastic modulus and hence deflection remain moderate in this temperature range. However, as the temperature in steel beam reaches 550°C, at about 100 min, strength and stiffness properties of steel start to degrade at a faster rate leading to rapid rise in deflection. Finally, after two hours of fire exposure, steel loses most of its strength and stiffness as the temperature of the beam rise to 600°C. This leads to rapid rise in mid-span deflection and produces runaway failure of the beam at 122 min.

In order to further investigate the fire response of the tested steel beam, Fig. 4.9 shows the degradation of moment and shear capacity with fire exposure time at corresponding critical sections; mid-span section for moment and end support section for shear. It can be seen that the moment capacity in the beam remains intact for the first 75 minutes due to lower temperatures (much below 400°C) in flanges of steel beam. However, shear capacity starts to degrade at 35 min due to relatively faster rise in web temperature. Then, moment and shear capacity starts to degrade when the temperature in steel section exceeds 400°C. Degradation of moment capacity of steel section continues till 130 min at which point the beam fails when the capacity at the mid-span falls below the moment due to applied loading. However, due to the low level of applied shear force, shear capacity does not fall below the shear force near the vicinity of support section. Hence, failure of this beam occurs due to flexural effects at 130 min (as compared to reported failure time of this beam in fire test which occurred at 122 min). Overall, predicted mid-span deflections, time to failure, and failure modes from developed model compare well with the reported data in fire tests.

4.4.2   Composite steel beams from MSU fire resistance tests

To further validate the above developed model, measured data from fire tests conducted on composite beams, presented in Chapter 3, is utilized. These fire tests are considered to be unique experiments of which shear and instability effects were studied explicitly. In order to perform fire resistance analysis, the developed finite element model has the same geometry, material properties and boundary conditions of the tested composite beams and was subjected to similar loading and fire conditions (shown in Table 3.1). This model was validated by comparing the predicted response parameters from fire-tested composite beams CB1, CB2, CB3 and CB4 with measured test data, namely cross-sectional temperatures, mid-span deflection, out-of-plane

web displacement and failure mode. Full details on geometric and material properties of beams are given in Chapter 3 (see Table 3.1).

The comparison of thermal response is presented for composite beam CB2 only, since composite beams CB1, CB3 and CB4 experience similar temperature rise as that of composite beam CB1. This is due to the fact that these beams have similar cross-sectional geometry, material properties and are exposed to similar fire exposure conditions (as discussed in Chapter 3). Figure 4.10 shows a comparison of predicted and measured temperatures in composite beam CB1 as a function of fire exposure time. In general, temperatures in this composite beam rise in a rapidly due to lack of fire insulation. It can be seen that the top flange of the steel beam experienced much lower temperatures as compared to that at bottom flange which is mainly due to the heat-sink effect of concrete slab.

Throughput the fire test, the temperature in concrete at mid-depth of slab remains low, below 150°C, till the end of the fire test. Overall there is good agreement between predicted and measured temperatures, although there is slight mismatch at some points. These mismatches are due to variation of radiation and convection parameters (i.e., coefficient of convection, radiation and emissivity of fire) used as input in the model, as compared to actual values encountered in the fire test.

The comparison of predicted and measured mid-span deflection (in CB1), vertical deflection (in CB2, CB3 and CB4) and out-of-plane web displacement for the tested composite beams are shown in Figs. 11a, b and c, respectively. It can be seen that the deflections and out-of-plane web displacement in all composite beams gradually increase with fire exposure time especially at the early stage of fire exposure. The initial deflection in these composite beams are

mainly due to high temperatures resulting in steel section and associated reduction in elastic modulus and strength of steel resulting from increasing temperatures.

In general, vertical deflection of the composite beams under flexural (CB1) and shear (CB2, CB3 and CB4) loading varied significantly as shown in Figs. 11a and b. For instance, in composite beam CB1, once steel temperature exceeds 400°C, the mid-span deflections start to increase at a slightly higher pace due to temperature-induced degradation in strength and elastic modulus of steel and the rate of deflection increases at the final stage of fire exposure, prior to failure. Finally, this fully composite beam (CB1) experiences failure due to loss of load bearing capacity and associated excessive mid-span deflection with no signs of web buckling. In addition, CB1 did not experience any horizontal displacement in web or lateral torsional buckling due to the development of full composite action.

Results plotted in Fig. 11b show that composite beams CB2, CB3 and CB4, loaded with high shear loading, experienced very little vertical deflection (with no signs of rotations at support regions) since the applied loading was placed very close to the intermediate support. In addition, these composite beams experienced similar trend in out-of-plane web displacement throughout the fire test (see Fig. 4.11c). These three particular composite beams mainly failed due to loss of load bearing capacity as a result to web buckling at intermediate support region. As discussed earlier, deflection limit state can only be valid for flexurally-tested composite beam CB1. Failure of CB2, CB3 and CB4 is mainly governed by strength (shear) and stability limit states due to shear loading and web slenderness. Overall, there is a good agreement between measured and predicted deflections, out-of-plane web displacement and failure modes (shown in Fig. 4.11).

Table 4.1: High-temperature thermal properties of steel (EC3, 2005)

Thermal strain	$$\varepsilon_{ths} = \begin{cases} 1.2\times10^{-5}T + 0.4\times10^{-8}T^2 - 2.416\times10^{-4} & 20^oC \le T \le 750^oC \\ 1.1\times10^{-2} & 750^oC < T \le 860^oC \\ 2\times10^{-5}T - 6.2\times10^{-3} & 860^oC < T \le 1200^oC \end{cases}$$
Specific heat (J/kg K)	$$c_s = \begin{cases} 425 + 7.73\times10^{-1}T - 1.69\times10^{-3}T^2 + 2.22\times10^{-6}T^3 & 20^oC \le T < 600^oC \\ 666 + \dfrac{13002}{738-T} & 600^oC \le T < 735^oC \\ 545 + \dfrac{17820}{T-731} & 735^oC \le T < 900^oC \\ 650 & 900^oC \le T \le 1200^oC \end{cases}$$
Thermal conductivity (W/m K)	$$k_s = \begin{cases} 54 - 3.33\times10^{-2}T & 20^oC \le T < 800^oC \\ 27.3 & 800^oC \le T \le 1200^oC \end{cases}$$

Table 4.2: High-temperature thermal properties of concrete (EC2, 2004)

Thermal conductivity (W/m K)
All types :
Upper limit:
$k_c = 2 - 0.2451\ (T\ /\ 100) + 0.0107\ (T\ /\ 100)^2$
for $20°C \le T \le 1200°C$
Lower limit:
$k_c = 1.36 - 0.136\ (T\ /\ 100) + 0.0057\ (T\ /\ 100)^2$
for $20°C \le T \le 1200°C$

Specific heat (J/kg C)

$c = 900$,   for $20°C \le T \le 100°C$

$c = 900 + (T - 100)$,   for $100°C < T \le 200°C$

$c = 1000 + (T - 200)/2$,   for $200°C < T \le 400°C$

$c = 1100$,   for $400°C < T \le 1200°C$

Density change (kg/m^3)

$\rho = \rho(20°C) = Reference\ density$

for $20°C \le T \le 115°C$

$\rho = \rho(20°C)\ (1 - 0.02(T - 115)/85)$

for $115°C < T \le 200°C$

$\rho = \rho(20°C)\ (0.98 - 0.03(T - 200)/200)$

for $200°C < T \le 400°C$

$\rho = \rho(20°C)\ (0.95 - 0.07(T - 400)/800)$

for $400°C < T \le 1200°C$

Thermal Capacity $= \rho \times c$

Table 4.3: Constitutive relations for high-temperature mechanical properties of steel (EC3, 2005)

Stress-strain relationships	$\sigma_s = \begin{cases} \varepsilon_s E_{s,T} & \varepsilon_s \leq \varepsilon_{sp,T} \\ f_{sp,T} - c + (b/a)\left(a^2 - (\varepsilon_{sy,T} - \varepsilon_s)^2\right)^{0.5} & \varepsilon_{sp,T} < \varepsilon_s \leq \varepsilon_{sy,T} \\ f_{sy,T} & \varepsilon_{sy,T} < \varepsilon_s \leq \varepsilon_{st,T} \\ f_{sy,T}\left(1 - \dfrac{\varepsilon_s - \varepsilon_{st,T}}{\varepsilon_{su,T} - \varepsilon_{st,T}}\right) & \varepsilon_{st,T} < \varepsilon_s \leq \varepsilon_{su,T} \\ 0 & \varepsilon_s > \varepsilon_{su,T} \end{cases}$ Parameters $\varepsilon_{sp,T} = \dfrac{f_{sp,T}}{E_{s,T}} \quad \varepsilon_{sy,T} = 0.02 \quad \varepsilon_{ss,T} = 0.04 \quad \varepsilon_{st,T} = 0.15 \quad \varepsilon_{su,T} = 0.2$ Functions $a^2 = (\varepsilon_{sy,T} - \varepsilon_{sp,T})\left(\varepsilon_{sy,T} - \varepsilon_{sp,T} + \dfrac{c}{E_{s,T}}\right)$ $b^2 = c(\varepsilon_{sy,T} - \varepsilon_{sp,T})E_{s,T} + c^2$ $c = \dfrac{(f_{sy,T} - f_{sp,T})^2}{(\varepsilon_{sy,T} - \varepsilon_{sp,T})E_{s,T} - (f_{sy,T} - f_{sp,T})}$ Values of $f_{sp,T}$, $f_{sy,T}$ and $E_{s,T}$ can be obtained from Table 5.4
Stress-strain relationships (Strain-hardening region)	For temperatures below 400°C $\sigma_s = \begin{cases} 50(f_{su,T} - f_{sy,T})\varepsilon_s + 2f_{y,T} - f_{su,T} & 0.02 < \varepsilon_s \leq 0.04 \\ f_{su,T} & 0.04 \leq \varepsilon_s \leq 0.15 \\ f_{su,T}[1 - 20(\varepsilon_s - 0.15)] & 0.15 < \varepsilon_s < 0.2 \\ 0 & \varepsilon_s \geq 0.2 \end{cases}$ $f_{u,T} = \begin{cases} 1.25 f_{sy,T} & T < 300°C \\ f_{sy,T}(2 - 0.0025T) & 300°C \leq T < 400°C \\ f_{sy,T} & T \geq 400°C \end{cases}$

Table 4.4: Constitutive relations for high-temperature properties of concrete (EC2, 2004)

Stress-strain relationships	$$\sigma_c = \dfrac{3\varepsilon\, f'_{c,T}}{\varepsilon_{c1,T}\left(2+\left(\dfrac{\varepsilon}{\varepsilon_{c1,T}}\right)^3\right)} \quad, \varepsilon \le \varepsilon_{cu1,T}$$ For $\varepsilon_{c1(T)} < \varepsilon \le \varepsilon_{cu1(T)}$, the Eurocode permits the use of linear as well as nonlinear descending branch in the numerical analysis. For the parameters in this equation refer to Table 5.6
Thermal strain	Siliceous aggregates: $\varepsilon_{th} = -1.8\times10^{-4}+9\times10^{-6}T+2.3 \times 10^{-11}T^3$ *for* $20°C \le T \le 700°C$ $\varepsilon_{th} = 14 \times 10^{-3}$ *for* $700°C < T \le 1200°C$ Calcareous aggregates: $\varepsilon_{th} = -1.2\times10^{-4}+6\times10^{-6}T+1.4\times10^{-11}T^3$ *for* $20°C \le T \le 805°C$ $\varepsilon_{th} = 12 \times 10^{-3}$ *for* $805°C < T \le 1200°C$

Table 4.5: Values for the main parameters of the stress-strain relations of normal strength concrete at elevated temperatures (EC2, 2004)

Temp. (˚C)	Normal Strength Concrete					
	Siliceous Aggregate			Calcareous Aggregate		
	$\dfrac{f'_{c,T}}{f'_{c20}}$	$\varepsilon_{c1,T}$	$\varepsilon_{cu1,T}$	$\dfrac{f'_{c,T}}{f'_{c20}}$	$\varepsilon_{c1,T}$	$\varepsilon_{cu1,T}$
20	1	0.0025	0.02	1	0.0025	0.02
100	1	0.004	0.0225	1	0.004	0.023
200	0.95	0.0055	0.025	0.97	0.0055	0.025
300	0.85	0.007	0.0275	0.91	0.007	0.028
400	0.75	0.01	0.03	0.85	0.01	0.03
500	0.6	0.015	0.0325	0.74	0.015	0.033
600	0.45	0.025	0.035	0.6	0.025	0.035
700	0.3	0.025	0.0375	0.43	0.025	0.038
800	0.15	0.025	0.04	0.27	0.025	0.04
900	0.08	0.025	0.0425	0.15	0.025	0.043
1000	0.04	0.025	0.045	0.06	0.025	0.045
1100	0.01	0.025	0.0475	0.02	0.025	0.048
1200	0	-	-	0	-	-

Table 4.6: Geometric and material properties used in validating the developed model (for the cases of an isolated steel beam)

	Steel section	Steel properties		Failure time (min)		Failure mode	
		f_y (MPa)	E_s (GPa)	Exp.	FE	Exp.	FE
Isolated steel beam	W12×16	345	200	130	122	Flexural mode	
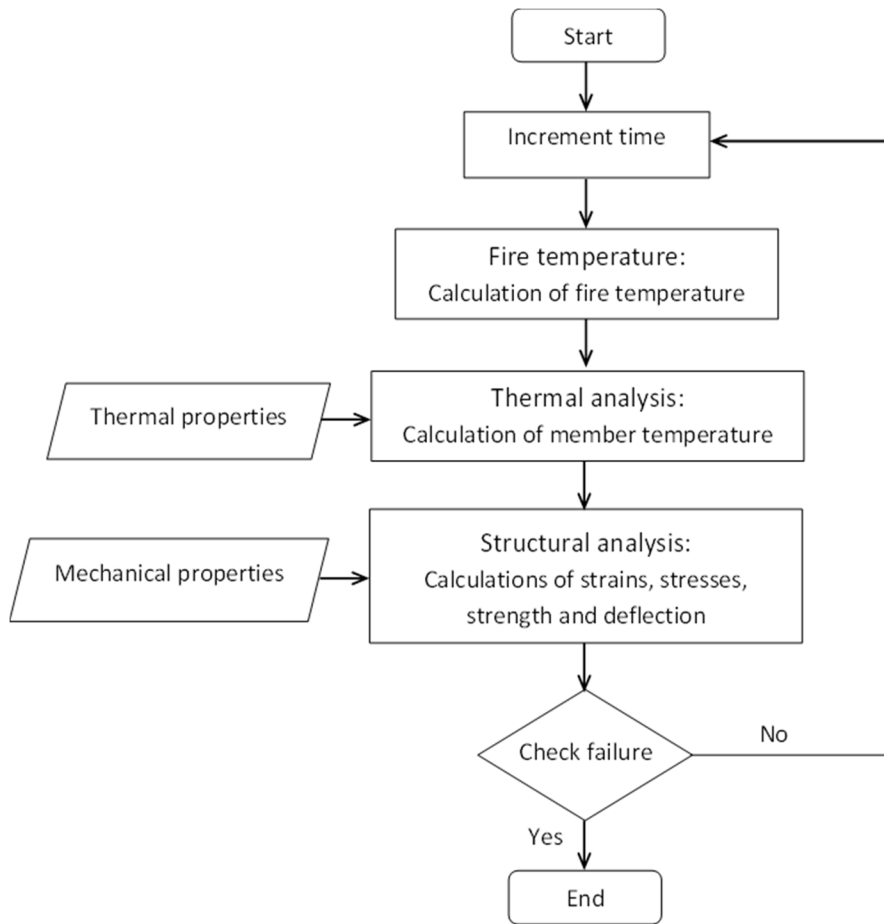
Figure 4.1: Flowchart for fire resistance analysis of structural members

SOLID70

SURF152

SHELL131

LINK33
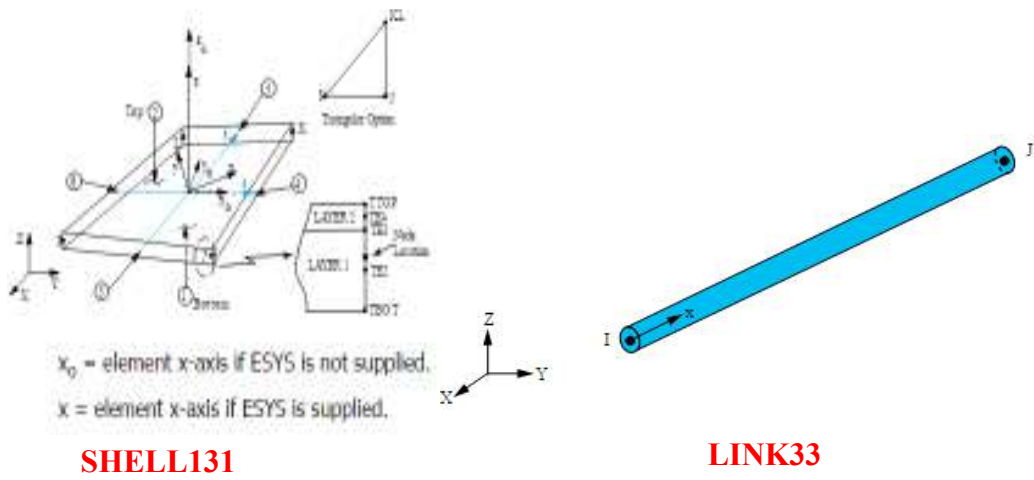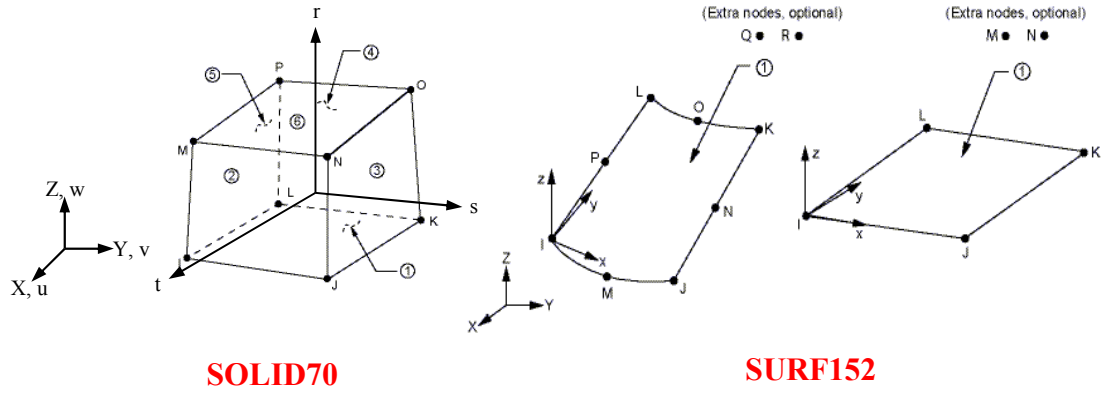
Figure 4.2: Element geometry used in thermal analysis (ANSYS, 2011)
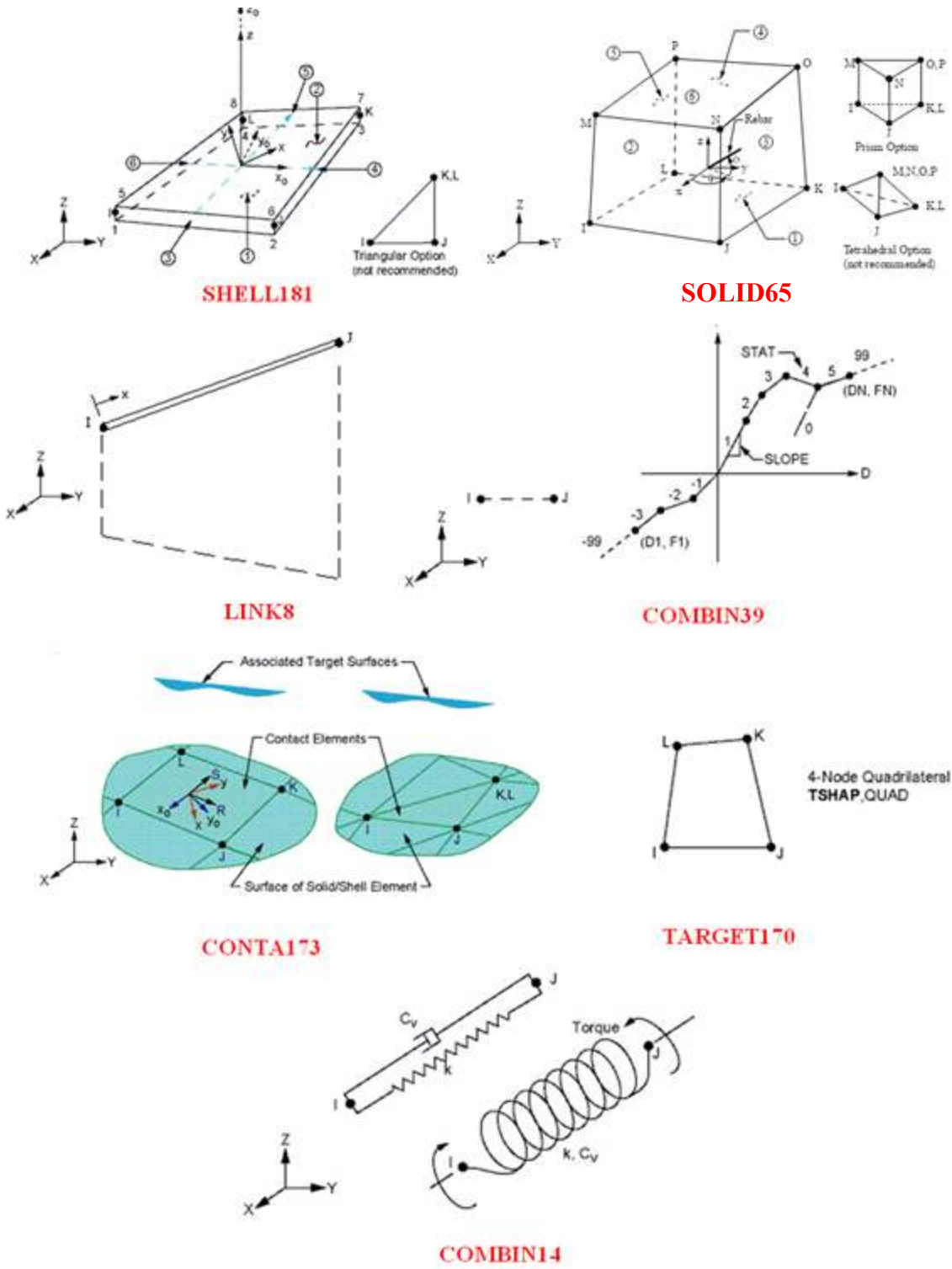
Figure 4.3: Element geometry used in structural analysis (ANSYS, 2011)
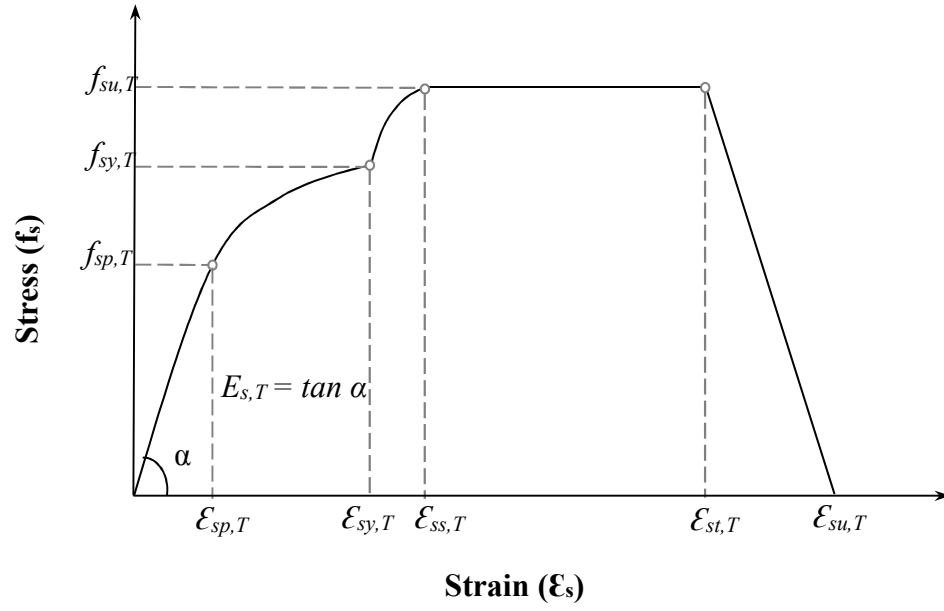
Figure 4.4: Eurocode stress-strain model for structural steel (EC3, 2003)
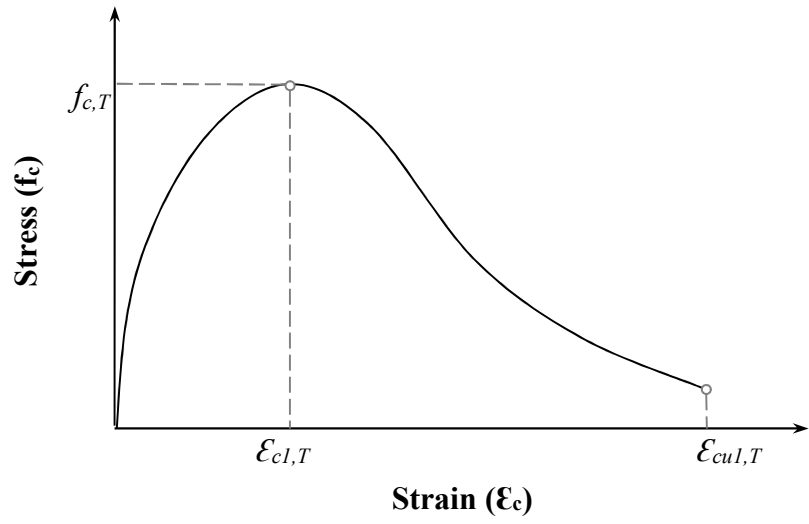
Figure 4.5: Eurocode stress-strain model for concrete (EC2, 2003)

Steel beam

(a) Test specimen and load set-up
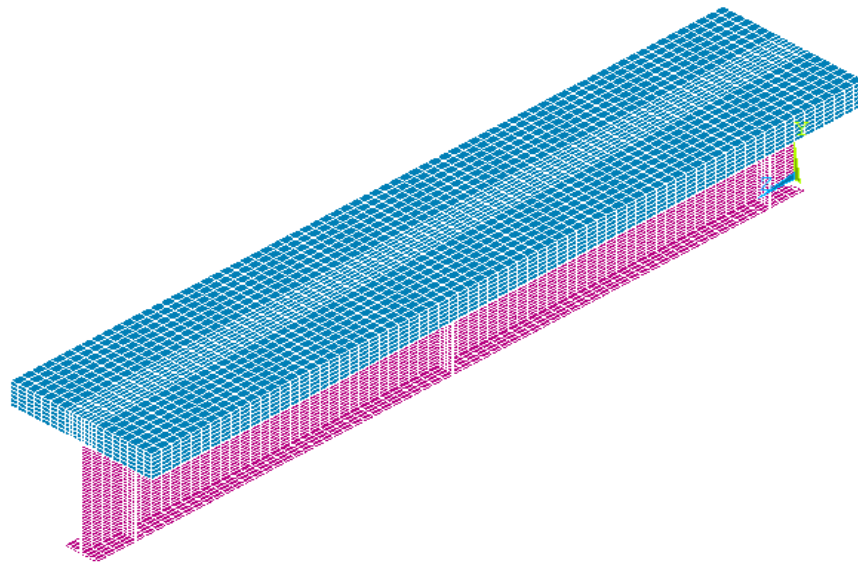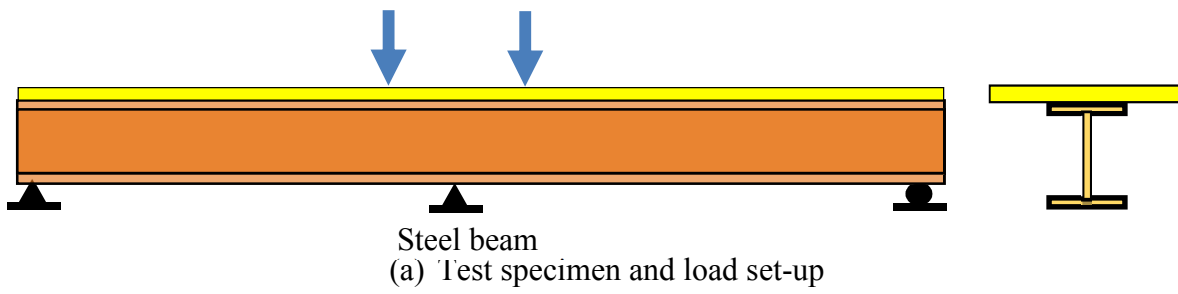
(b) Discretization of the developed finite element model

Figure 4.6: Loading set-up and discretized finite element model
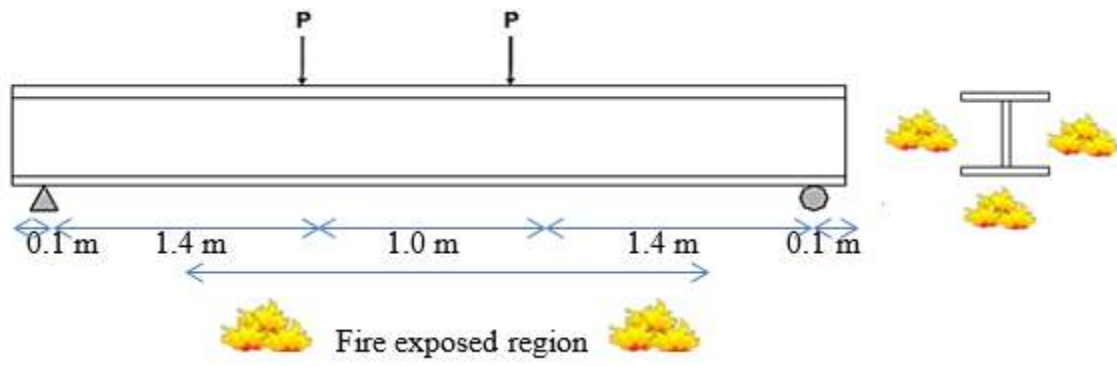
Figure 4.7: Tested beam used in validating the developed finite element model
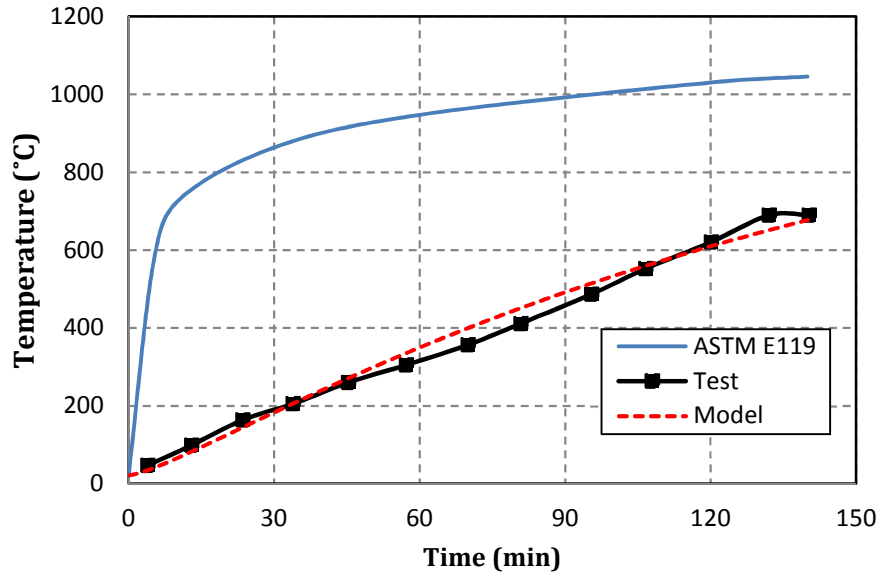
(a) Thermal response
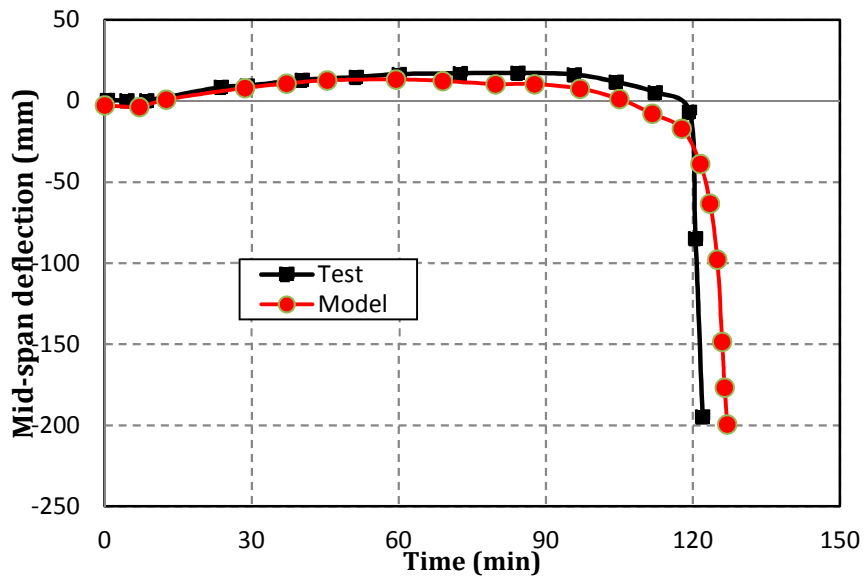
(b) Structural response

Figure 4.8: Comparison of predicted and measured temperature and deflections as a function of fire exposure time
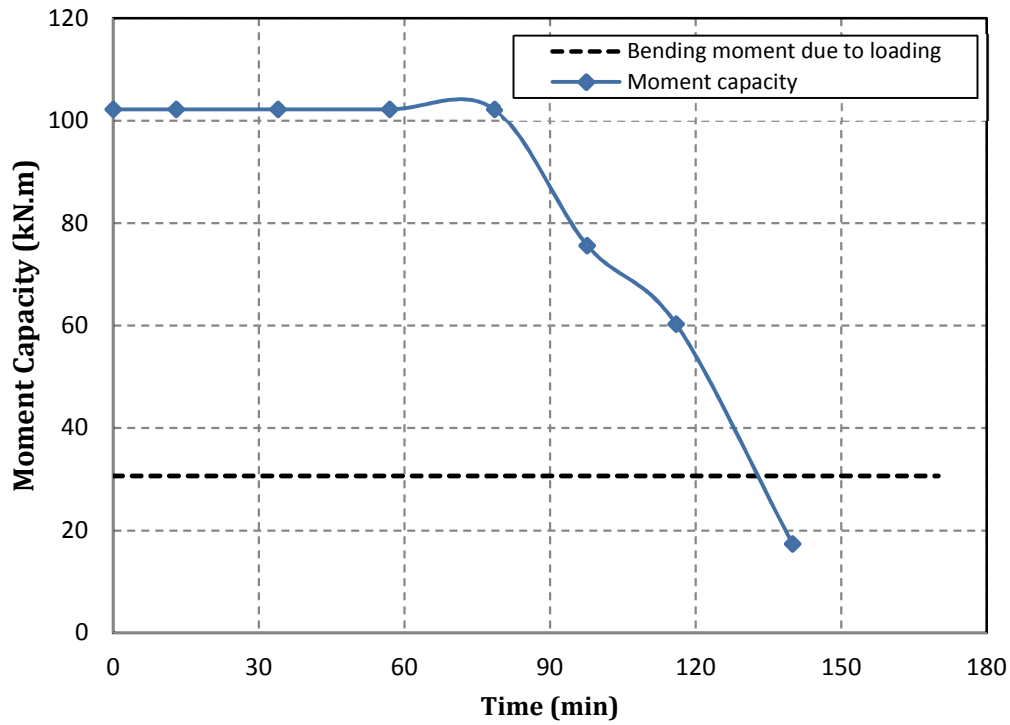
(a) Moment capacity
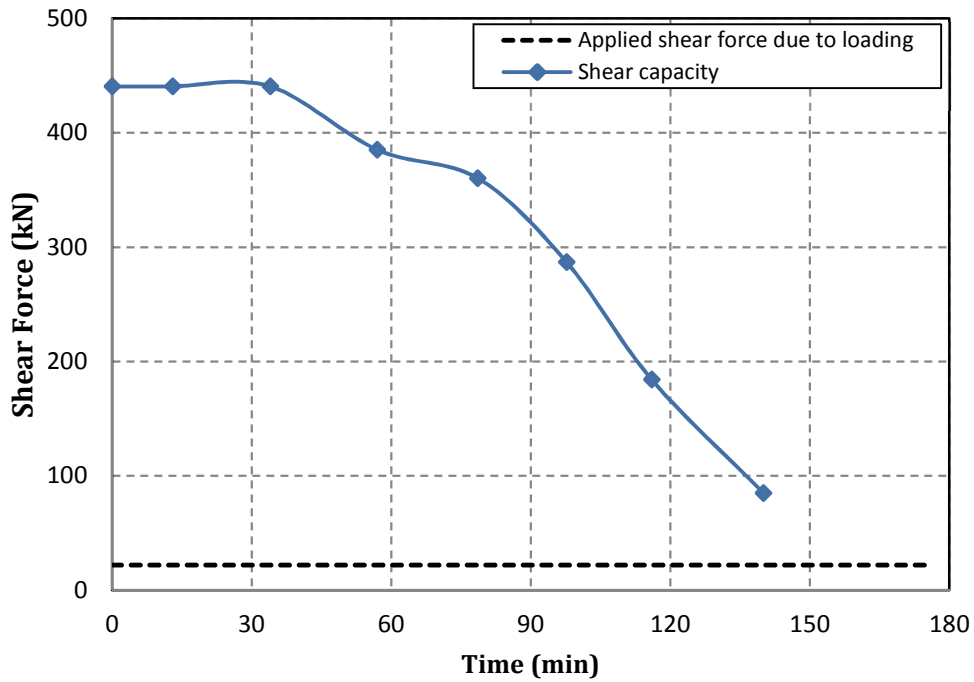
(b) Shear capacity

Figure 4.9: Degradation of moment and shear capacity in the tested beam (Kodur and Fike, 2009)
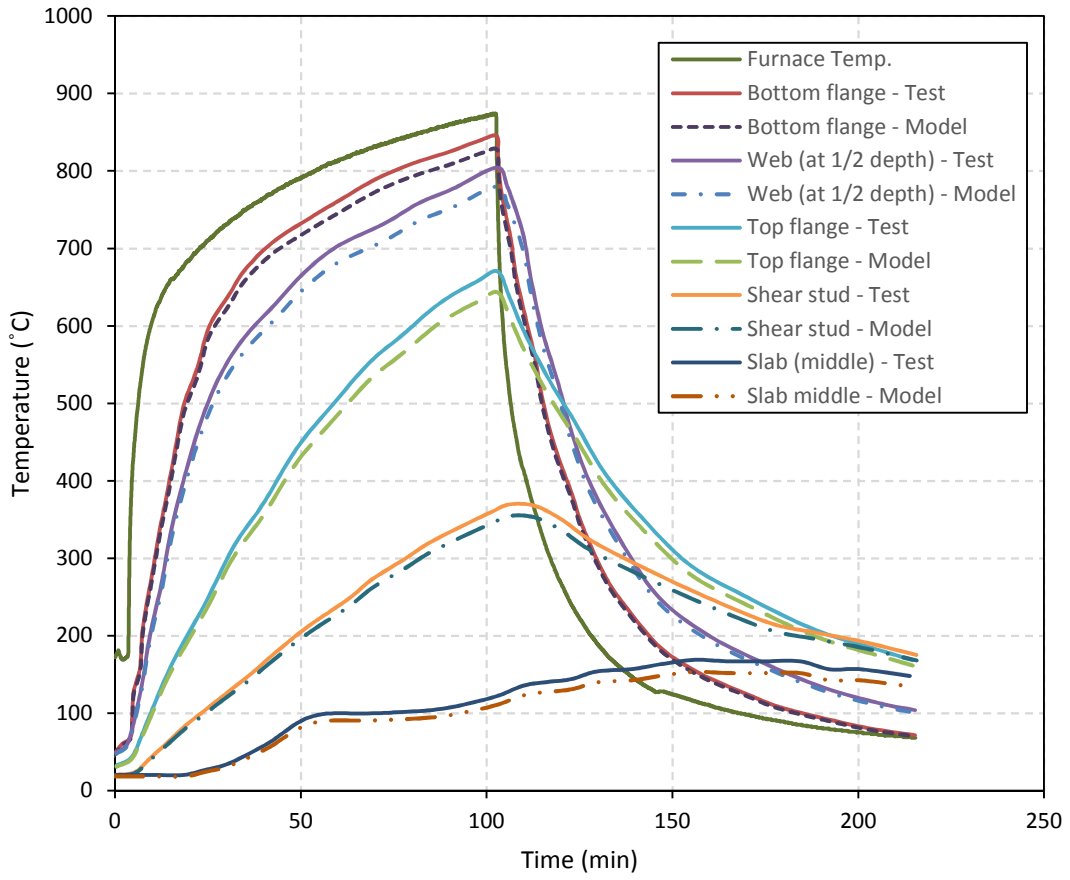
Figure 4.10: Comparison of predicted and measured cross-sectional temperatures in composite beam CB1
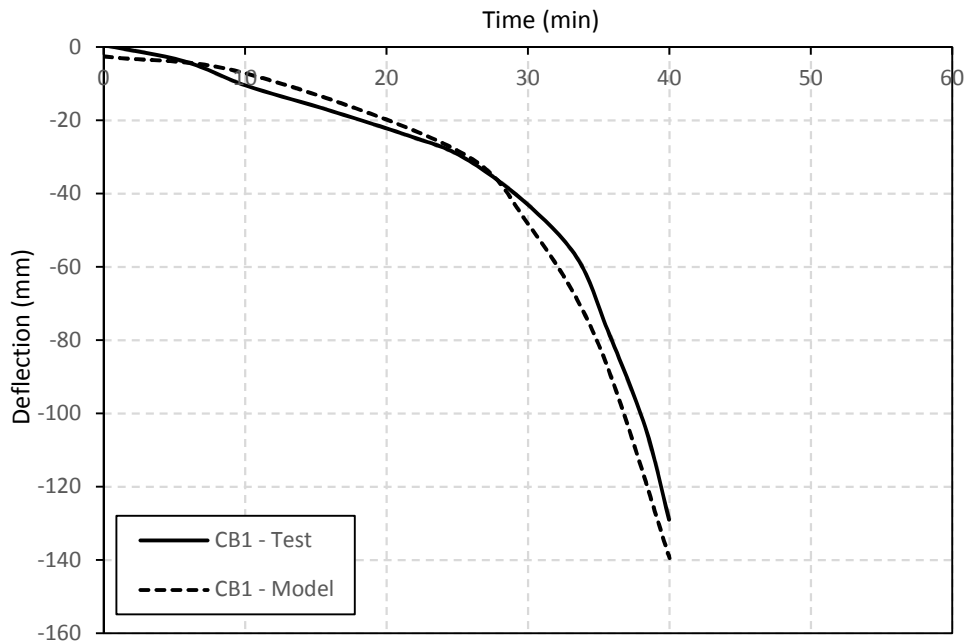
(a) Mid-span deflection for composite composite beam CB1
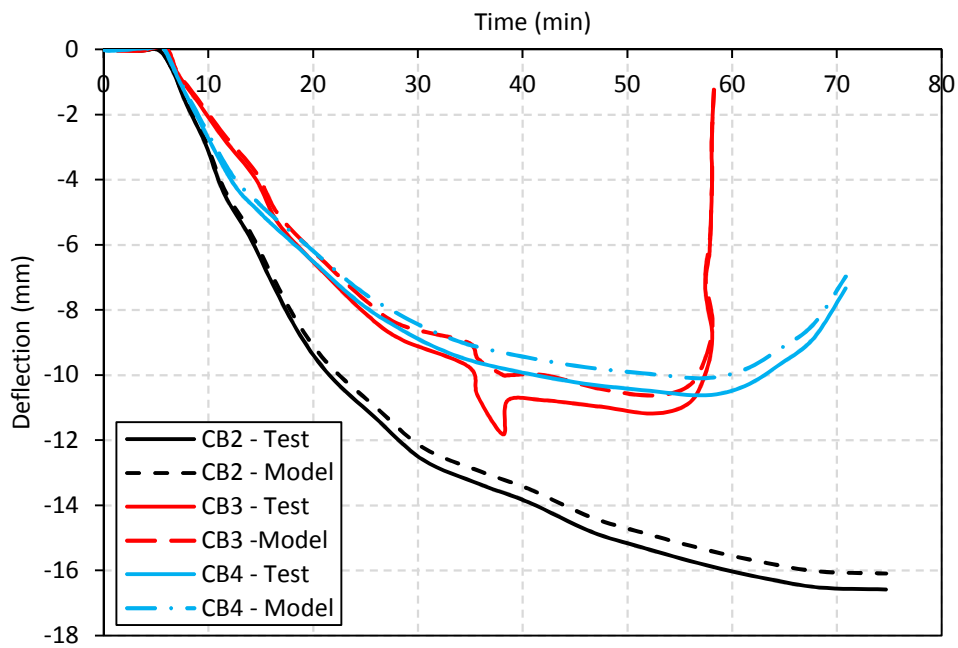
(b) Vertical deflection for composite composite beams CB2, CB3 and CB4
Figure 4.11: Comparison of predicted and measured mid-span deflections and out-of-plane web displacement in composite beams CB2, CB3 and CB4

Figure 4.11 (cont'd)
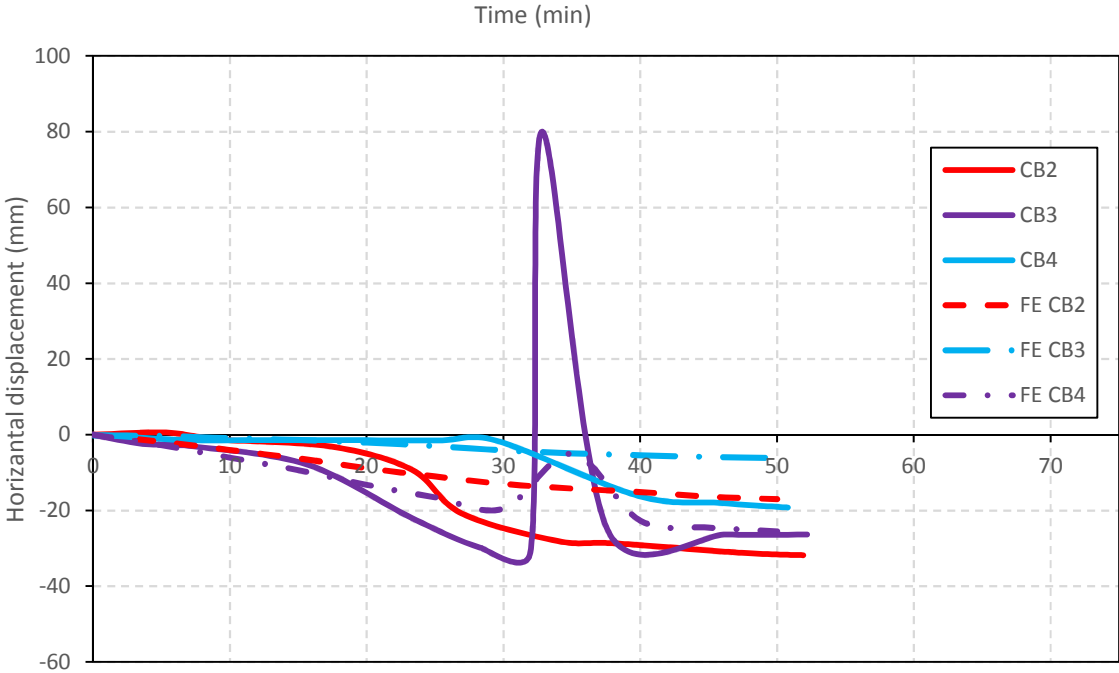
(c) Out-of-plane web displacement
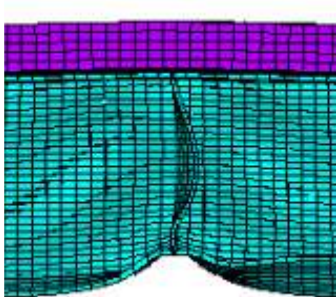
(d) Failure mode

4.5 Summary

This chapter presents the development and validation of numerical model for tracing the response of isolated steel beams and composite beams exposed to fire. The numerical model, comprising of thermal and structural finite element sub-models, are developed using commercially available finite element software ANSYS. The fire resistance analysis was carried out in two stages namely: thermal and structural analyses. The developed model accounts for geometric and material nonlinearities, high temperature thermal and mechanical properties, composite action arising from steel beam and concrete slab interaction, and various failure limit states.

The validity of the thermal and structural sub-models is established by comparing the predicted response parameters from fire resistance tests on isolated steel beams and also on composite beams. The close agreement of predicted results with measured data indicates that the developed model is capable of tracing the fire response of isolated or composite beams and thus can be used for undertaking detailed numerical studies. In Chapter 5, this validated model will be applied to carry out a set of parametric studies on the effect of critical parameters influencing fire response of different configuration of composite beams.

CHAPTER FIVE

5. Parametric Studies

5.1 General

Fire tests, such as the ones provided in Chapter 3, can provide good insight into the overall behavior of steel and composite beams under fire conditions. However, it is not feasible to undertake large number of fire experiments due to huge costs and time constraints involved in preparing and undertaking fire tests. Furthermore, under fire conditions, shear and instability related failure occurs in a brittle/sudden manner and may not be possible to track as it requires sophisticated instrumentations. Therefore, use of numerical modeling can be an effective alternative to trace the fire behavior of structural members. Numerical modeling can be used specifically to track the complex (and unique) behavior under the combined effects of shear, instability and fire exposure.

Such numerical models, once validated, can be applied to carryout parametric studies to evaluate the influence of various factors on fire resistance of steel and composite beams. As part of such an exercise, the numerical model, presented in Chapter 4, is applied to quantify the effect of critical parameters including: sectional instability (geometric imperfections), web slenderness, load level, fire severity, load configuration (type of application), level of composite action, shear stud stiffness and concrete slab thickness on fire response of different configuration of beams.

5.2 Definition and Range of Parameters

Fire response of beams, specifically flexural response, is influenced by a number of factors such as material degradation at elevated temperatures, load level, fire intensity, and restraint conditions. These factors have been well studied in literature (Kirby et al., 1986; Huang et al., 2009; Aziz et al., 2015). However, the main parameters that influence shear response of steel and composite beams, namely: sectional instability (geometric imperfections), web

slenderness, load level, fire severity, load application, level of composite action, shear stud stiffness and concrete slab thickness are not evaluated. The range of variations of these parameters in realistic and practical scenarios is tabulated in Table 5.1 and discussed below.

5.2.1 Sectional stability (geometric imperfections)

Due to the complex nature of fabrication process of steel beams and girders, actual geometric properties (dimensions) are usually different than the nominal values listed in standardized design manuals and listings. Hence, newly fabricated beams (which are made of thin plates) may have initial geometric imperfections. These imperfections can affect buckling behavior and strength of steel plates under fire conditions.

Initial geometric imperfections are typically neglected in numerical analysis due to complexity. However, in order to illustrate the effect of these geometric imperfections on temperature-induced local buckling of steel beams, a parametric study is needed (Klasson et al., 2016). To account for the effect of initial geometric imperfections on the structural behavior of fire-exposed beams, the geometry of the steel beam in the finite element analysis is updated using various scaled deformation as shown in Table 5.1. These scaled deformations ranged from L/10, L/100, L/1000, L/5000 to L/10000, where L is the total length (span) of the beam.

5.2.2 Web slenderness

I-shaped hot-rolled steel sections are often used as flexural members in most civil engineering applications. I-shaped sections are designed to have thicker flanges, deeper web to increase sectional stiffness ($EI^{\dagger}$) of beams. This can significantly increase their bending capacity which is favorable in bending application. However, I-shaped hot-rolled steel sections can be very vulnerable to shear effects due to higher slenderness of web as compared to flanges

---

† E = Modulus of elasticity, I = Moment of Inertia

124

(especially under fire conditions as shown in Chapters 1, 2 and 3). Hot-rolled steel sections typically used in buildings have web slenderness (D/t_w) in the range of 40 to 55 as compared to flange slenderness (which has a range of 6-15). On the other hand, typical built-up sections (plate girders) used in bridges have web slenderness up to 100-150 for girders with traverse stiffeners. In order to study the effect of web slenderness on fire-induced degradation in shear capacity of beams, a parametric study was carried out by varying web slenderness from 50 to 150 as shown in Table 5.1.

5.2.3   Load level

The load level (LL), corresponding to shear limit state, can be defined as the ratio of the maximum shear force (V_{max}) induced due to the applied gravity loading present during a fire to the shear capacity ($V_{capacity}$) of the steel or composite beam at room temperature, i.e.

$$LL = \frac{V_{max}}{V_{capacity}} \times 100\%$$
(5.1)

The load level can have significant influence on fire response. For example, heavily loaded beams generate higher internal stresses to counter-balance (resist) the applied loading. Thus, a steel beam loaded with higher loads can reach yield limit of steel (and plastification) much faster. This can accelerate failure of such beams under fire condition when strength properties degrade rapidly. To account for the effect of load level on the shear behavior of fire-exposed steel and composite beams, various load levels are applied on the beam analyzed, ranging from 15 to 75% of beam shear capacity as shown in Table 5.1.

5.2.4   Fire severity

Fire scenarios to be considered in structural fire design can be grouped under two categories, namely: standard and design (realistic/actual) fire scenarios. In the case of a standard

fire, used in most prescriptive design standards, the heat generated from the fire source to the exposed structural members is assumed to increase throughout the duration of fire exposure. In the case of a design fire, the heat generated from fire source is assumed to increase till maximum temperature is reached, then the temperature is assumed to decrease gradually (in what is referred to as decay or cooling phase). The decay phase usually reflects the limited availability of fuel or ventilation and/or actions of sprinklers or firefighters.

Another key characteristic of fire is its intensity. Fire intensity refers to the rate at which a fire produces heat (or total heat flux) and is generally dependent on the type and amount of combustible/flammable material (gasoline, wood, etc.) available in a building. Fire intensity can also govern temperature rise in beams and can dictate the degradation rate of sectional capacity (especially shear capacity). Hence, to illustrate the effect of fire scenario (severity), different temperature-time curves including ASTM E119, ASTM E1529, Hydrocarbon modified (HCM), RWS "RijksWaterStaat" and two compartment (reaslitic) fires are studied. Table 5.2 lists the maximum temperature and heat flux generated in each of the aforementioned fire scenarios.

5.2.5 Loading configuration

To illustrate the effect of different loading patterns, three configurations of load application are chosen and studied in this parametric study. The three configurations reflect cases in which the beam is subjected to dominant flexural or shear effects as shown in Fig. 5.2. In this figure, two concentrated loads equivalent to 50% of shear capacity were applied at 0.25L, 0.50L and 0.80L along the span (of the beam "L"). it can be seen in Fig. 5.3 that varying location of concentrated loads changes bending moment and shear force distribution along the span of the beam. For example, applying concentrated loads at 0.25L, amplifies shear effects at interior support, while applying concentrated loads at 0.50L, amplifies flexural effects at mid-span. It is

clear that this can change distribution of internal forces which in turn has to trigger different resistance mechanisms (i.e., flexural or shear) to resist applied loading. It should be noted that flexural and shear capacity of a beam is independent of the magnitude and type of loading, flexural and shear capacity is constant for any given beam since they are a function of the geometric and material properties. Table 5.2 lists different loading patterns in each of the aforementioned loading scenarios.

5.2.6   Level of composite action

The level of composite action that develops at the interface of top flange of beam and soffit of concrete slab is dependent on the number of shear studs in a composite beam. Shear studs are typically welded to the top flange of beam and help in transferring horizontal (axial) forces from steel beam into concrete slab. It is well established in literature that a fully composite beam, which requires sufficient number of shear studs to transfer all of the forces developed at flange-slab interface exhibit better fire performance than partially composite beams, where the number of studs is less than that in a fully composite beam.

In current practice, the beneficial effect of composite action is not often taken into consideration in evaluating shear capacity under fire conditions. This can be attributed to lack of understanding on the shear behavior of fire-exposed composite beams. As part of this parametric study, the effect of composite action on shear capacity in composite beams is studied under different levels of composite action. Table 5.1 lists the extent of composite action varied in beams; namely from 0, 10, 25, 33, 50, 75 to 100%.

5.2.7   Shear stud stiffness

As discussed above, shear studs (shear connectors) play key role in achieving certain level of composite action between a steel beam and concrete slab. This is due to the fact that

transfer of forces between steel beam and concrete slab occur through shear studs. Although the number of available shear studs dictates the level of achieved composite action, the rigidity (i.e., stiffness) of these shear studs can also affect the distribution of shear flow which indirectly, affect the shear capacity. For instance, a stiffer shear stud can resist higher level of shear flow without bending, breaking or pulling out. To quantify the effect of shear stud stiffness, multiple values of stud stiffness are varied as shown in Table 5.1, and these values include 0, ¼, ½, 1, 2 and 5 times the amount of actual stiffness in a stud.

5.2.8 Concrete slab thickness

Along with the level of composite action and shear stud stiffness, concrete slab thickness also influences the level of shear capacity in a composite beam. To illustrate this effect, previous studies, through room temperature tests, have concluded that for the same slab width, a thicker concrete slab can have larger shear capacity than that of a thinner slab (Vasdravellis and Uy, 2014; Nie et al., 2004; Liang et al., 2005). In order to quantify the effect of concrete slab thickness on the shear response (and capacity) of fire-exposed composite beams, thickness of slab is varied as 50, 100, 150, 200, 250, 300, 350 and 400 mm (See Table 5.1).

5.3 Analysis Details

The validated numerical model presented in Chapter 4 is applied to carry out parametric studies on a typical steel and composite beam/girder. The developed finite element model has the same geometry, material properties and boundary conditions of the tested composite beams (in Chapter 3) and was subjected to shear and fire loading simultaneously. In the numerical analysis, the selected beam is discretized for thermal and structural analysis using described elements in Chapter 4. In addition, material properties and constitutive models used in the analysis of various

key factors considered as part of this parametric study are the same as those discussed in Chapter 4 (Sec. 4.3).

Since evaluation of realistic failure requires applying all possible limiting failure criteria, different limit states are considered in the numerical analysis (at each time step). The considered failure limit states, are, namely: thermal, flexural, shear, and deflection (which generally correlated to flexural limit state). When studying each parameter, failure is said to occur once any of the above mentioned limit states is exceeded. Figure 5.5 presents a flow chart illustrating the systematic numerical procedure followed in this study.

In this parametric study, thermal and structural response, as well as failure patterns, is compared to evaluate the effect of sectional stability (geometric imperfections), web slenderness, load level, fire severity, loading configuration, level of composite action, shear stud stiffness, and concrete slab thickness on the shear response of fire-exposed steel and composite beams. The parametric study matrix and corresponding fire resistance factors for the 45 analysis cases on steel or composite beams are presented in Table 5.1.

5.4 Results from Parametric Studies

Results from parametric studies are utilized to quantify the influence of critical factors on the shear response of fire-exposed steel and composite beams.

5.4.1 Effect of sectional stability (Geometric imperfections)

To quantify the effect of sectional stability on fire response of beams, the pattern of initial imperfections is often chosen to be the worst case scenario in order to account for instability effects. For example, ASTM A6/A6M (2011) specifies an imperfection magnitude of L/960 (where L is the span length) to be applied to the geometry of the structural member. This level of imperfection is to be taken into consideration in the finite element analysis to evaluate the effect

of global imperfections. Similarly, cross-sectional imperfections are usually input as a fraction of individual plate thickness (i.e., 10% of web thickness) to generate effect of cross-sectional imperfections (Zeinoddini and Schafer, 2012).

In order to apply geometric imperfection to the developed model, a two-step approach was followed. In the first step, an elastic buckling analysis (modal analysis) was performed on a perfect (straight) steel beam to obtain its first buckling mode. In the second step, scaled global and sectional deformations, obtained from the first buckling mode, were introduced to the steel beam (model) used in the thermal-stress analysis. In order to study the effect of initial geometric imperfections on structural behavior of fire-exposed beams, the geometry of the structural model was updated using the scaled deformation of L/10, L/100, L/1000, L/5000 and L/10000.

Figures 5.6 and 5.7 shows the predicted response of beams with different initial imperfections as well as their deformed shape at failure. It can be seen that the magnitude of initial geometric imperfections can significantly affect the structural response of beams when subjected to high shear loading and fire conditions. For instance, composite beams with initial imperfections of L/100 and L/1000 provide the best response as compared with the experimentally tested beam CB2 which was assumed to have L/960 imperfection. Applying initial imperfections of L/100 and L/1000 can accurately capture buckling behavior of web and produce deformation close to those experienced in fire tests.

On the other hand, predicted results from beams with scaled initial imperfections of L/10, L/5000 and L/10000 do not seem to agree well with meatus results from fire tests. It was noticed that large magnitude of initial imperfections (i.e., L/10) causes numerical instability that affect numerical convergence. However, the use of much smaller values of imperfection (in the range

of L/5000 and L/10000) causes unpredictable (invalid) localized stress concentrations (localized plastification of part of plates) at critical sections of the beam (i.e., near supports and under applied loadings). Such stress concentrations do not reflect actual behavior of a composite beam and can lead to localized failure (through crushing at web/flange interface).

5.4.2 Effect of web slenderness

To quantify the effect of web slenderness on response of beams, five beams with varying web slenderness of 50, 75, 100, 125 and 150 were analyzed. From flexural limit state consideration, all five sections have compact flanges (with flange slenderness of 5.97) as per room temperature classification in AISC design manual (2011). However, webs in these sections were varied from compact, non-compact, to slender depending on the level of web slenderness. A beam with web slenderness of 50 is a compact section as it is expected to develop its full plastic moment capacity at room temperature. However, section with web slenderness of 75 has a non-compact web and sections with web slenderness of 100, 125 and 150 are classified as slender sections. In the absence of provisions to classify these sections under fire conditions, these sections are assumed to maintain the same status as classified at room temperature throughout fire exposure duration.

In order to study the effect of web slenderness on response of beams subjected to shear and fire loading, the variation of web slenderness limits with temperature under shear limit state is evaluated by applying temperature-induced reduction in yield strength and elastic modulus to room temperature slenderness classification limits. For instance, Fig. 5.8 shows the evolution of web slenderness of tested sections when compared to the temperature-dependent slenderness limit. It is clear that web classification of a beam that has a web slenderness of 50 changes to non-compact at temperature of 500°C. Further details on the transformation of sectional

131

slenderness (for shear limit state) at fire conditions can be found in Chapter 1 and elsewhere (Kodur and Naser, 2013).

Figure 5.9 illustrates the degradation of shear capacity in the selected beams with fire exposure time. Since shear capacity is a function of yield strength and web area, at room temperature, shear capacity in beams with web slenderness of 75, 100, 125 and 150 are significantly lower than that of the beam with web slenderness of 50 due to reduced web thickness. Reduction in web thickness causes rapid rise in temperature (in web). This rapid rise in web temperature leads to significant deterioration in strength property which causes large degradation in shear capacity. Degradation of shear capacity is also influenced by the onset of local buckling (instability) in web, as can be seen in Fig. 5.9, where variation in shear capacity is plotted under two scenarios of accounting for local buckling of web (LB) and not considering local buckling (no LB). The rate of degradation in shear capacity is seen to be different in these beams due to variation in temperature rise resulting from different web thicknesses. It can be also seen that the effect of local buckling is high when a compact section (for $\lambda = 50$) transforms into a non-compact section but can be significant when a non-compact section transforms into a slender section.

The variation of vertical deflection in beams with varying slenderness is plotted in Fig. 5.10 as a function of fire exposure time. The vertical deflection in these beams is compared against deflection limits to determine failure as recommended in British Standard BS-476 (1987). In all beams, deflections are quite small at the initial stage of fire, then increases steadily with fire exposure time. Just prior to failure, deflections rapidly increase due to rise in steel temperature. In general, composite beams with higher web slenderness (more than 50), experience much larger deflections throughout fire exposure duration; of about 16.2, 25.7, 33.2,

and 38.1% for web slenderness of 75, 100, 125 and 150, respectively. These results infer that web slenderness not only influence shear capacity of composite beams but also deflection response under fire conditions.

5.4.3 Effect of load level

In current codes of practice, fire resistance in structural members is generally evaluated based on a load level (load ratio) of 40-50%. This is based on the fact that structural members at room temperature are designed with various load factors and load combination factors and during a fire event the probability of all such combinations of loading be present at the same time is low. In order to evaluate response under a wide range of loading for comparison purposes, the effect of load level on a composite beam is varied from 15, 30, 40, 65, and 75% of shear capacity of beams. This range can cover most scenarios, experienced in practice, on fire response of beams subjected to high shear loading.

To further illustrate the effect of varying load level on shear response of fire-exposed beams, Fig. 5.11 shows a comparison between vertical deflection in beams loaded with 15, 30, 40, 65, and 75% of their shear capacity. It can be seen that higher load levels cause additional stresses within the beam which accelerates rate of deflections and failure time. These large deflections reflect the fact that beams loaded with high load levels undergo rapid degradation in shear capacity at fire conditions. For instance, beams loaded with 15, 30, 40, 65, and 75% of their shear capacity fail at 800, 700, 640, 600 and 580°C, respectively.

5.4.4 Effect of fire severity

To quantify the effect of applying different fire severity on the shear response of beams, fire resistance analysis was carried out under different fire exposure scenarios as represented in

133

Fig. 5.13. Temperature rise in a beam is significantly influenced by the amount of heat absorbed by the beam which in turn affects degradation of shear capacity. Thus, beams subjected to high intensity fires (i.e., HCM and RWS) experienced larger deformations as compared to beams subjected to moderate fires (ASTM E119) or low intensity fires (compartment fires). In general, high intensity fires can cause rapid rise in web temperature (and rapid degradation in shear capacity) which causes higher deformations and lead to early failure of beams.

From trends shown in Fig. 5.13, it can be seen that deflection response follows that of the fire exposure scenario. For example, when a beam is subjected to a standard fire, its rate of deflection (and response) tend to follow that of the fire intensity associated with standard fire scenario. Similarly, a beam exposed to compartmental fire scenarios undergoes large amount of deflection (initially). This amount and rate of deflection reduces once the beam regains some of its initial shear capacity back (at the decay phase of fire).

5.4.5   Effect of loading configuration

As discussed in Section 5.2.5, the location of the applied loading (along the span of a beam) can significantly affect the resulting magnitude of bending moment and shear force. In order to study this effect, response under three configurations of load application are studied as shown in Fig. 5.2. High shear loading was applied at locations equivalent to 25, 50 and 80% of the composite beam span. Applying point loading at these locations leads to apparent changes in bending moment and shear force as shown in Fig. 5.3.

For instance, applying two shear point loadings at 0.25L results in high shear force at intermediate support and low bending moment. On the other hand, applying two high shear point loadings at 0.50L results in high bending moment (at mid-span) and lower shear force (at

intermediate support) when compared to that in the case of applying high shear loading at 0.25L. In order to quantify the net effect of both shear and moment, an interaction of both of these forces need to be accounted for as follows:

$$\frac{M_n}{M_u} + \frac{5}{8}\frac{V_n}{V_u} < 1.0 \qquad (5.2)$$

Using the interaction relationship shown in Eq. 5.2, it can be inferred that applying two loadings at 0.25L results in high interaction effects as compared to that of applying two high concentrated loadings at 0.50 and 0.80L. Thus, a beam subjected to a larger shear force- moment interaction undergoes higher deflections as shown in Fig. 5.14. This can also be seen from data plotted in Fig. 5.15. Failure in beams subjected to high shear forces at locations equivalent to 0.25, 0.50 and 0.80L occurs at 635, 680 and 780°C, respectively.

5.4.6   Effect of level of composite action

To quantify the effect of level of composite action on response of composite beams, seven beams with varying level of composite action from 0, 10, 25, 33, 50, 75 and 100% are analyzed. Predictions from the analysis show that the extent of composite action determine magnitude of forces that can be transferred between steel beam and slab. High level of composite action leads to transferring higher magnitude of forces from fire-weakened steel beam to the cool and resilient concrete slab. This enhances shear capacity and delays failure of composite beam as shown in Fig. 5.16. These predicted results agrees well with the measured results from the experimental results presented in Chapter 3 (i.e., CB3 with 50% composite action experienced lower deflection than that in CB2 with full composite action).

Higher levels of composite action also limits horizontal slippage between concrete slab and steel beam. For example, the maximum slip at the interface of steel beam and concrete slab

is predicted to be 5, 9, 11 and 15 mm for composite beams with 10, 25, 50 and 100% composite action, respectively. This has been also seen in the contact status (at the interface of concrete slab and steel beam) generated in finite element analysis shown in Fig. 5.17. From contact status plots, this is apparent by the reduction in the "sticking" area predicted by the contact behavior.

The effect of composite action can also affect failure mode (shape) of the beam towards the end of fire exposure. For instance, Fig. 5.18 draws a comparison of failure mode (shape) in an isolated steel beam and composite beam at end of fire resistance analysis. It is clear from predicted results that presence of concrete slab provided significant lateral support (and bracing) to the steel beam by limiting the amount of buckling in flanges and web as can be seen from plotted failure shape in Fig. 5.18c. In this figure, top flange and top-portion of web buckled due to the large compressive forces while flange and web in the composite beam did not experience local buckling. This can be attributed to transferring of compressive forces from fire-weaked steel beam into the cooler concrete slab through composite action.

5.4.7   Effect of shear stud stiffness

As discussed in Sec. 5.2.7, shear studs are key component in achieving cohesive action and transferring forces between the steel beam and concrete slab. One of the most important characteristics of shear studs is their rigidity (i.e., stiffness/flexibility). The stiffness of shear studs can affect the distribution of horizontal shear flow which affect the amount of force transferred compositely between different components in a composite beam, especially under fire conditions. For example, stiffer shear studs can increase level of force transmission between concrete slab and steel beam, especially under fire conditions.

To further illustrate this effect, Fig. 5.19 shows the amount of horizontal slippage that concrete slab can undergo when attached to steel beam with various cases of shear stud stiffness.

136

As expected, shear studs with lower stiffness are prone to being more flexible (vulnerable to bend). For instance, in a composite beam designed with flexible shear studs (of 0.25K, where k is a typical stiffness of shear stud of value equals to 125.2 kN/mm), the slab can slide and move a distance of 7.43 mm as compared to 0.025 mm when shear stud stiffness increases to 5K.

Further, deflection response plots shown in Fig. 5.20 show that composite beams with stiffer shear studs achieve better fire performance than those with lower shear stud stiffness. This is due to the fact that effectiveness of shear studs starts to be more apparent when temperature rise in steel beam reaches 300-400°C. At this point, steel beam starts to lose some of its initial strength and stiffness and more forces are to be transferred into the concrete slab (to maintain stability and equilibrium).

Results plotted in Fig. 5.20 also infer that shear studs with stiffness of more than 2K, seem to slightly enhance the overall performance of the composite beam by (1-5%). On the same note, fully composite beams designed with flexible shear studs (with lower stiffness <1K), achieved poor structural response; equivalent to that of a partially composite beam (similar to tested beam that is presented in Chapter 3 (CB4)). Thus, the use of shear studs of stiffness in the range of 1-2K seem to achieve a more economical and practical performance.

5.4.8   Effect of concrete slab thickness

Along with shear stud stiffness, thickness of concrete slab is another key factor that can contribute to shear capacity in fire-exposed composite beams. In order to investigate the effect of different concrete slab thickness on shear capacity of composite beams, especially under fire conditions, concrete slab thicknesses of 50, 100, 150, 200, 250, 300, 350 and 400 mm was varied on a steel beam. Predicted structural response of composite beams with different slab thicknesses is shown in Figs. 5.21 and 5.22.

Figures 5.21 and 5.22 show that the overall structural response of composite beam with varying concrete slab thickness is a function of the interaction of the vertical and horizontal displacement of the beam (web). These figures illustrate that horizontal web displacement in composite beams with thin concrete slab thickness (of 50 and 100 mm), undergo a different response than that of the webs in composite beams with thicker slabs. In composite beams with thin slabs, the web tends to translate in an "in-and-out of plane" manner due to the overall flexibility of the composite beam. Hence, it can be inferred that thicker concrete slabs can effectively brace and laterally restraint the composite beam and hence limit the movement of web.

Table 5.1: Summary results of test parameters from parametric studies

Case	Varied Parameter	Parameters variation and scenarios	Constant parameters
Case 1	Geometric imperfections	L/10	ASTM E119, Load level=30%, D/t_w =50
Case 2		L/100	
Case 3		L/1000	
Case 4		L/5000	
Case 5		L/10000	
Case 6	Web slenderness	50	ASTM E119, Load level=30%,
Case 7		75	
Case 8		100	
Case 9		125	
Case 10		150	
Case 11	Load level	15%	ASTM E119, D/t_w =50
Case 12		30%	
Case 13		40%	
Case 14		65%	
Case 15		75%	
Case 16	Fire severity	ASTM E119	Load level=30%, D/t_w =50
Case 17		ASTM E1529	
Case 18		Hydrocarbon	
Case 19		RWS	
Case 20		Compartment 1	
Case 21		Compartment 2	
Case 22	Loading configuration	0.25L	ASTM E119, Load level=30%, D/t_w =50
Case 23		0.50L	
Case 24		0.80L	
Case 25	Level of composite action	0%	ASTM E119, Load level=30%, D/t_w =50
Case 26		10%	
Case 27		25%	
Case 28		33%	
Case 29		50%	
Case 30		75%	
Case 31		100%	
Case 32	Shear stud stiffness	0	ASTM E119, Load level=30%, D/t_w =50
Case 33		¼K	
Case 34		½K	
Case 35		K	
Case 36		2K	
Case 37		5K	

Table 5.1 (cont'd)

Case 38		50 mm	
Case 39		100 mm	
Case 40		150 mm	
Case 41	Concrete slab thickness	200 mm	ASTM E119, Load level=30%, D/t_w =50
Case 42		250 mm	
Case 43		300 mm	
Case 44		350 mm	
Case 45		400 mm	

Table 5.2: Maximum temperature and heat flux in fire scenarios (Beyler et al., 2007)

Fire scenario	Max. temperature (°C) [*]	Max. Heat flux (kW/m^2)
ASTM E119	1000[*]	110
ASTM E1529	1180	158
HCM	1300	347
RWS	1350	393
Compartment 1	1150	-
Compartment 2	875	-

[*] After 2 hours of fire exposure
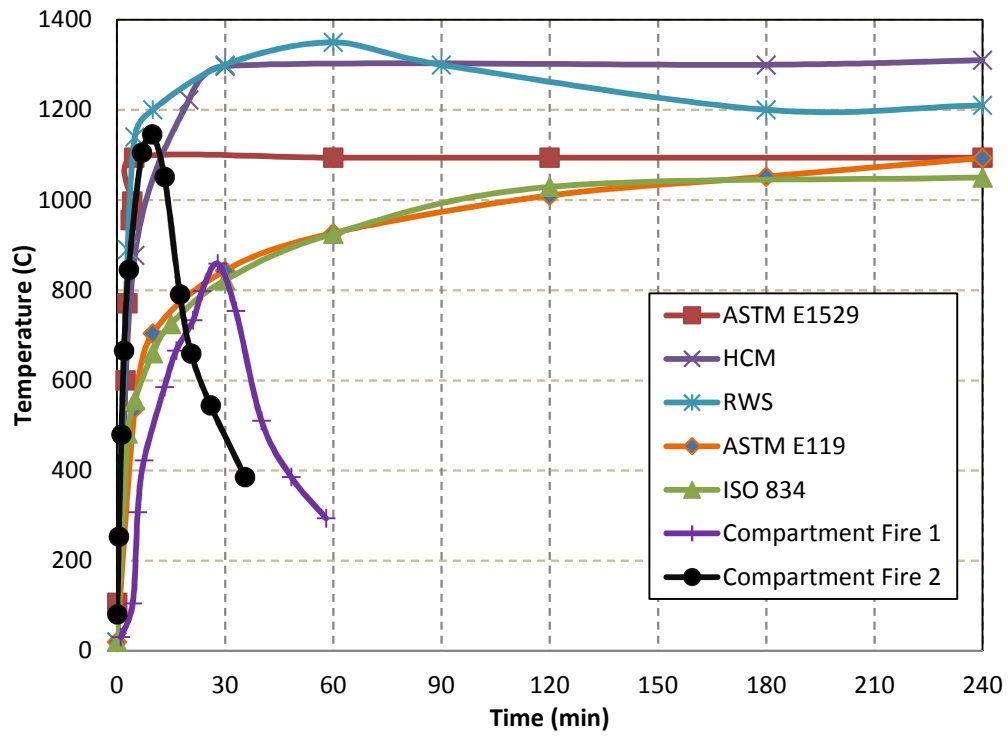
Figure 5.1: Temperature-time curves in different scenarios
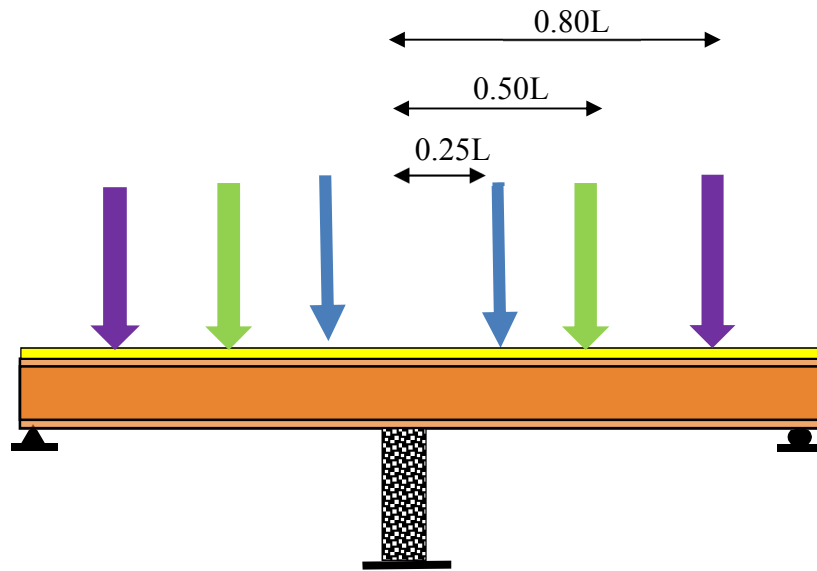
Figure 5.2: Composite beam configuration and applied loading points
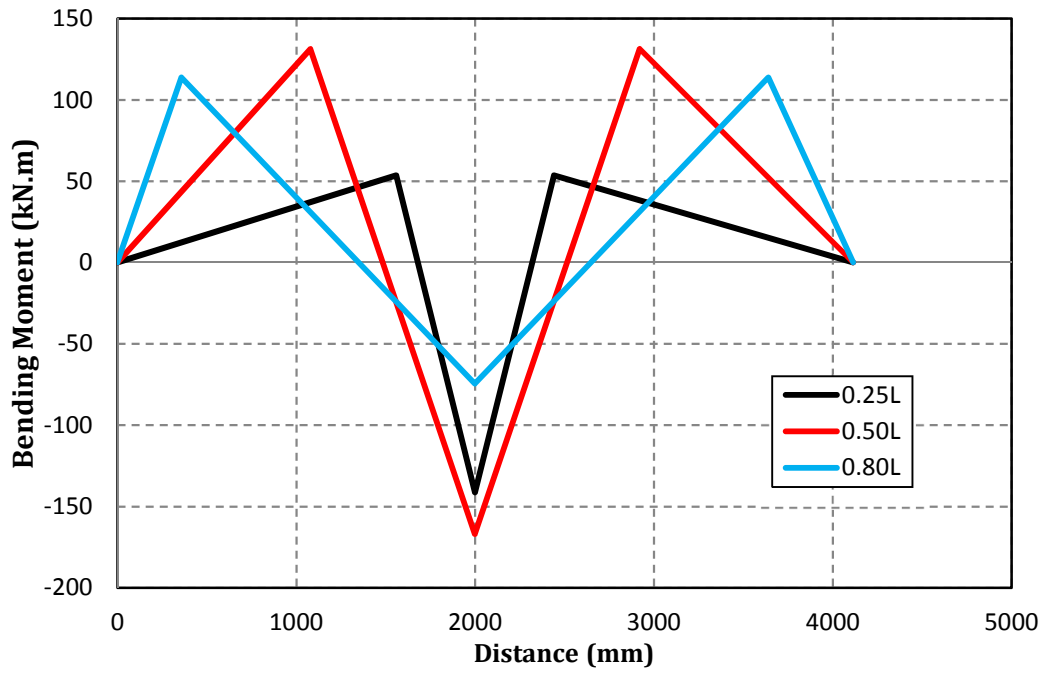
(a) Bending moment of applied loading at 0.25L, 0.50L and 0.80L
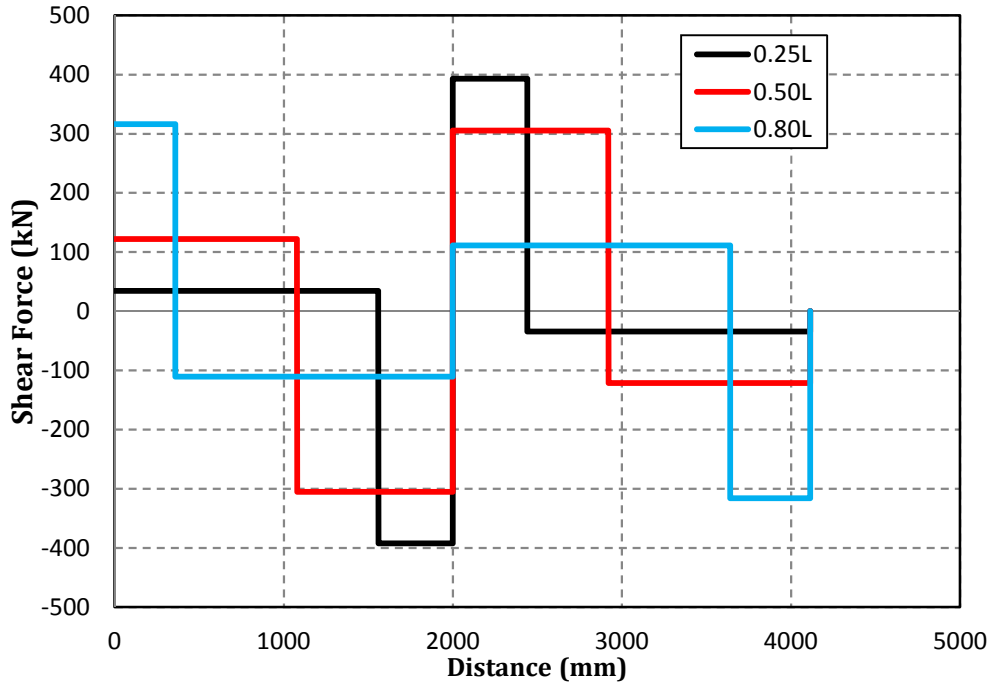
(b) Shear force of applied loading at 0.25L, 0.50L and 0.80L

Figure 5.3: Applied loading scenarios and associated bending moment and shear forces

Steel beam

(a) Test specimen and load set-up

(b) Discretization of the developed finite element model

Figure 5.4: Loading set-up and discretized finite element model of composite beam

```
                                    ┌─────────┐
                                    │  Start  │
                                    └─────────┘
                                         │
                                         ▼
┌──────────────────────────┐   ┌──────────────────────────┐
│ Input room and           │   │ Discretization of beam   │
│ temperature-dependent    │──▶│ for thermal analysis     │
│ properties               │   │                          │
└──────────────────────────┘   └──────────────────────────┘
                                         │
                                         ▼
                                ┌──────────────────────────┐
                                │ Evaluate thermal response│
                                │ (i.e., temperature       │
                                │ distribution)            │
                                └──────────────────────────┘
                                         │
                                         ▼
                                ┌──────────────────────────┐
                                │ Discretization of beam   │
                                │ for structural analysis  │
                                └──────────────────────────┘
                                         │
                                         ▼
                                ┌──────────────────────────┐
                                │ Evaluate structural      │◀───────┐
                                │ response (i.e., stress,  │        │
                                │ strain, deflection)      │        │
                                └──────────────────────────┘        │
                                         │                          │
                                         ▼                          │
                                ┌──────────────────────────┐      ◇
                                │ Check for failure (i.e., │      ╱ ╲
                                │ compare against flexural,│────▶│ No │
                                │ shear, and deflection    │      ╲ ╱
                                │ limit states)            │       ◇
                                └──────────────────────────┘
                                         │
                                         ▼
                                        ◇
                                      ╱   ╲
                                     │Failure│
                                      ╲   ╱
                                        ◇
                                         │
                                         ▼
                                    ┌─────────┐
                                    │  Stop   │
                                    └─────────┘
```
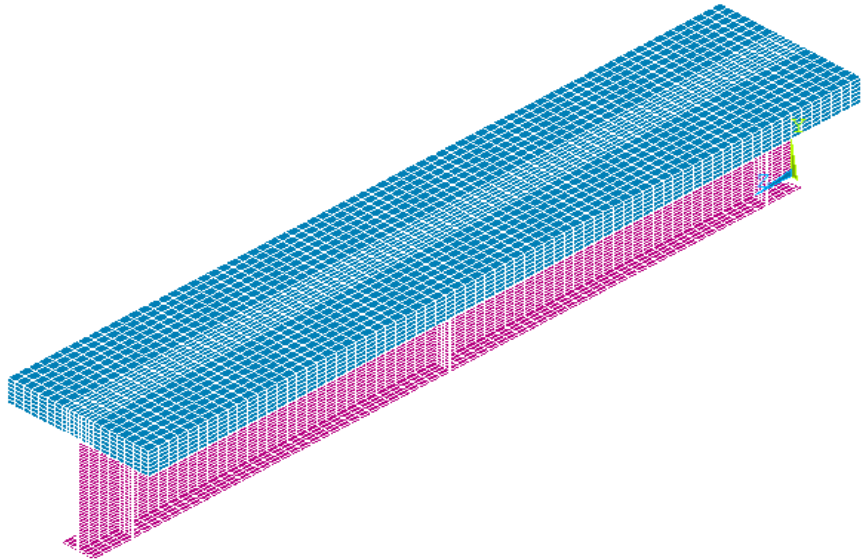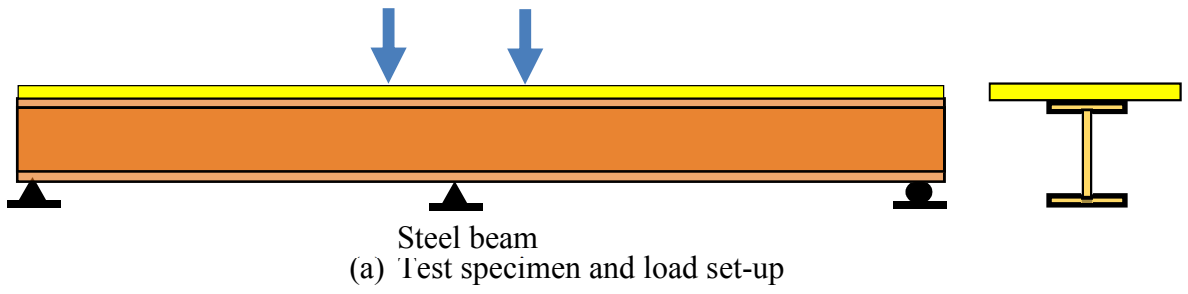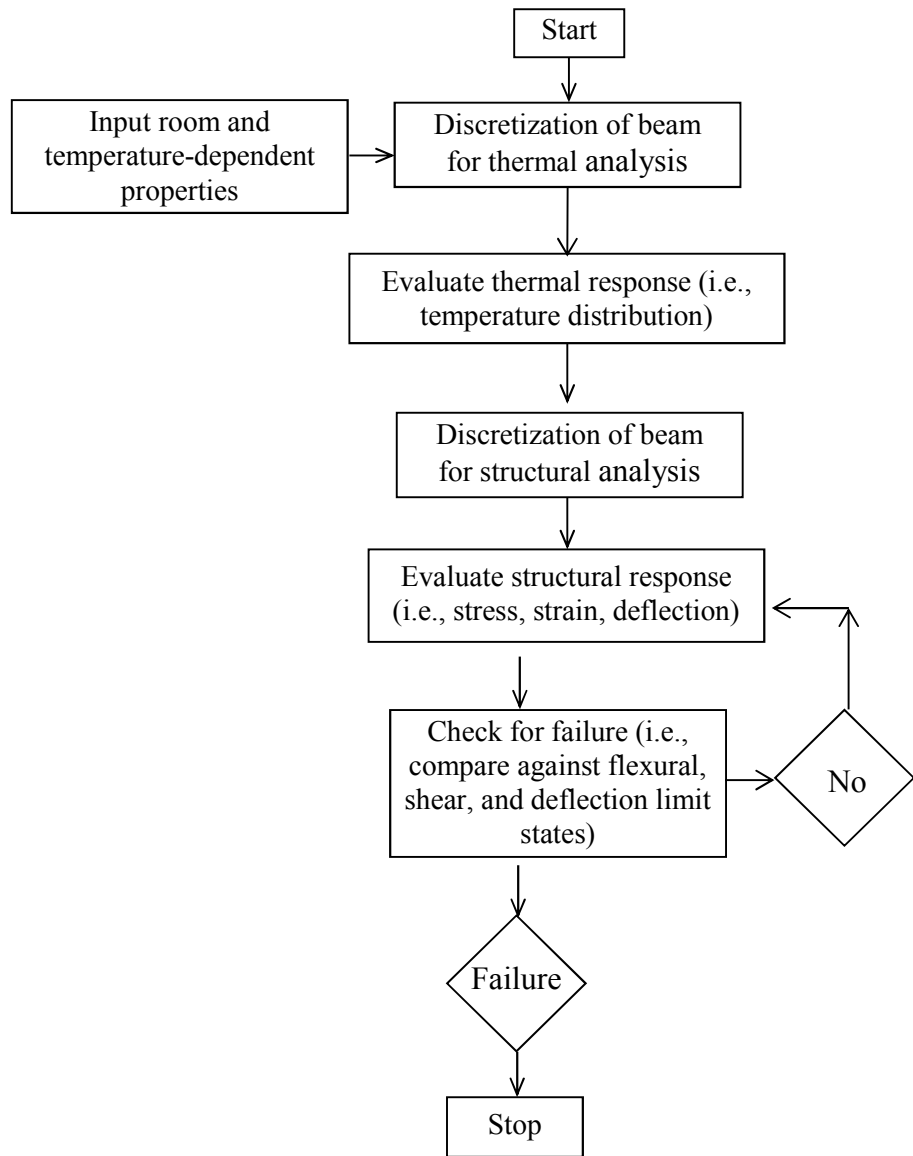
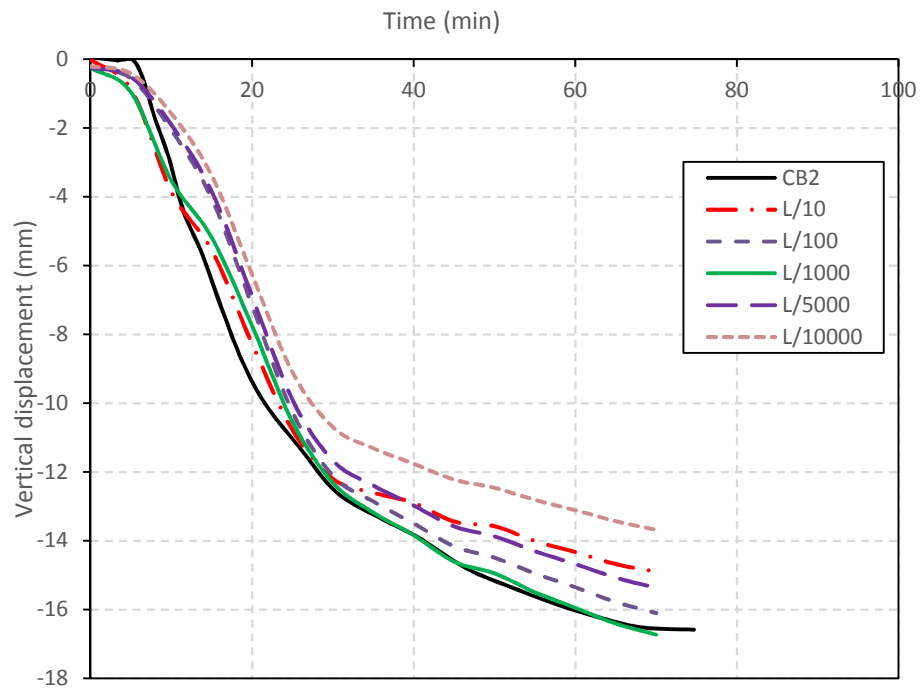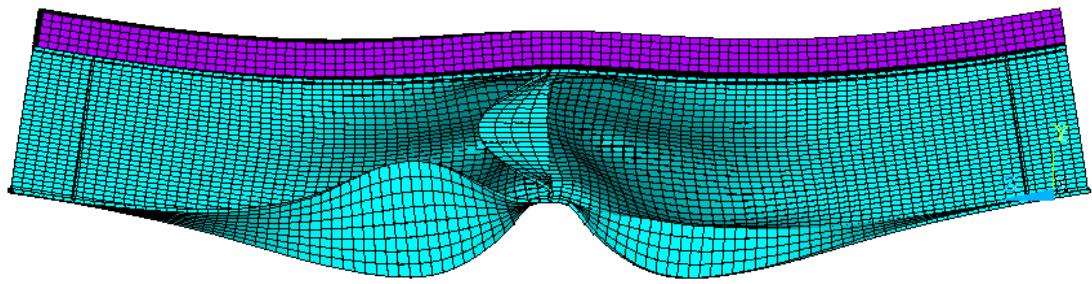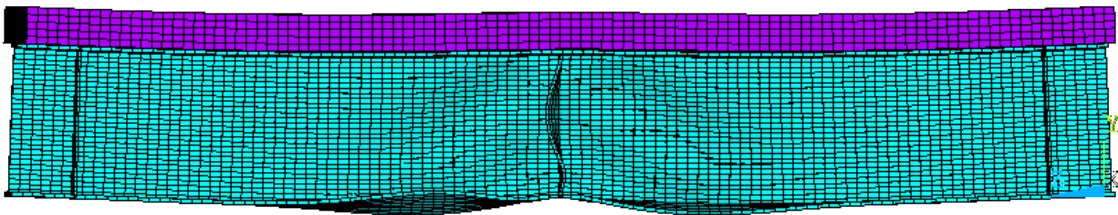Figure 5.5: Flow chart illustrating various stages in undertaking fire resistance analysis
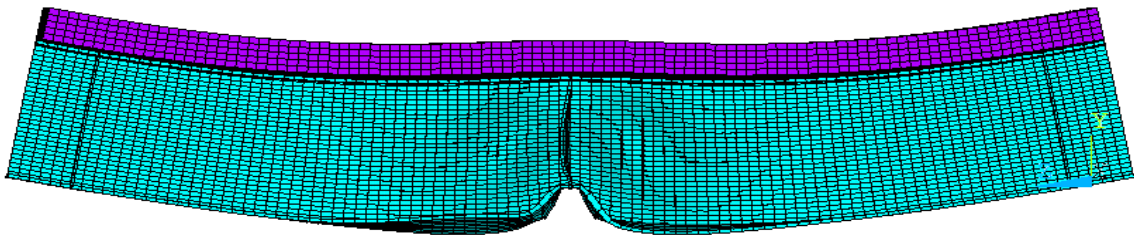
Figure 5.6: Predicted deflection response of composite beams with different magnitude of initial imperfections
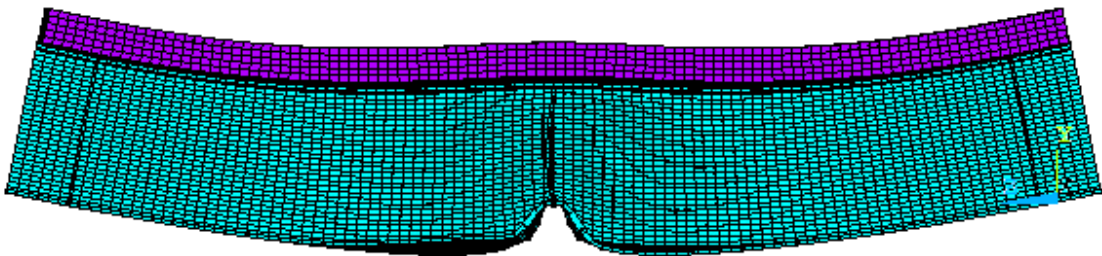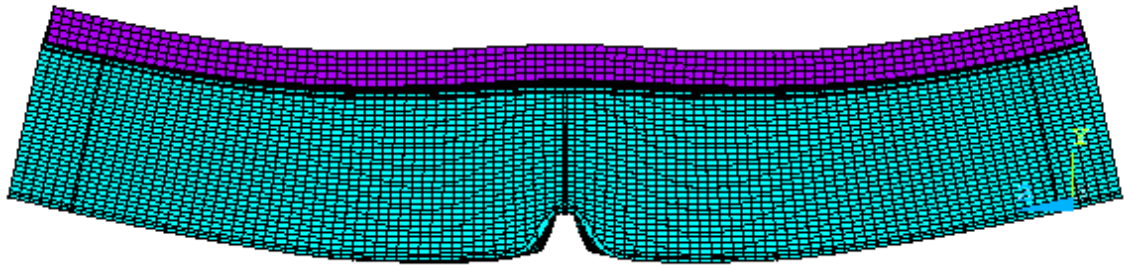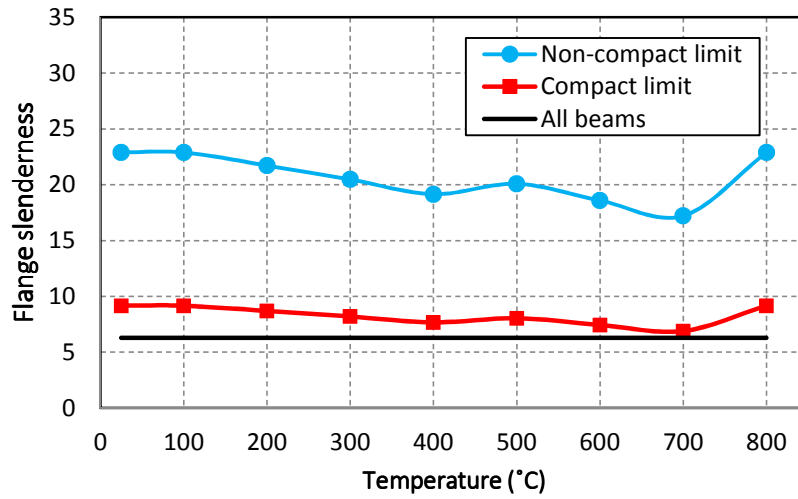
(a) L/10

(b) L/100

(c) L/1000

(d) L/5000

Figure 5.7: Predicted deformed shape at failure of composite beams with different initial imperfections
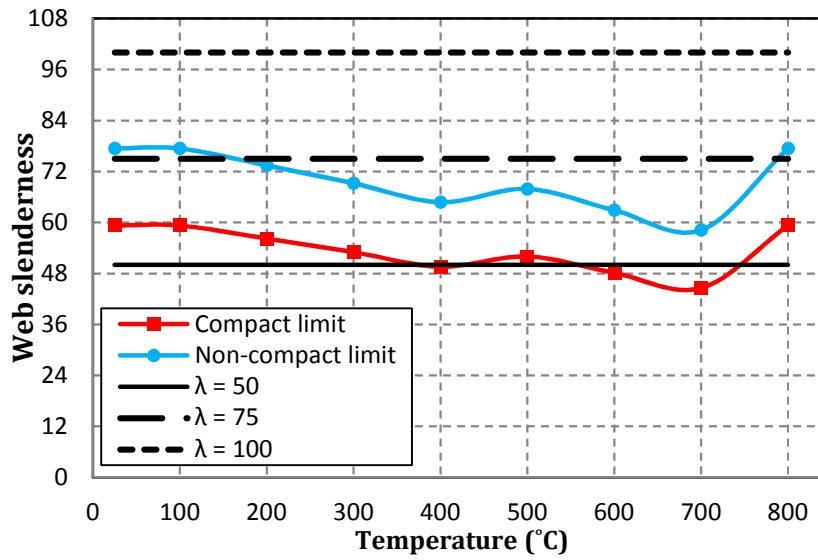
148

Figure 5.7 (cont'd)

(e) L/10000

(a) flange slenderness limits under flexural limit state

(b) web slenderness limits under shear limit state

Figure 5.8: Variation of flange and web sectional slenderness limits under flexural and shear limit states at elevated temperatures
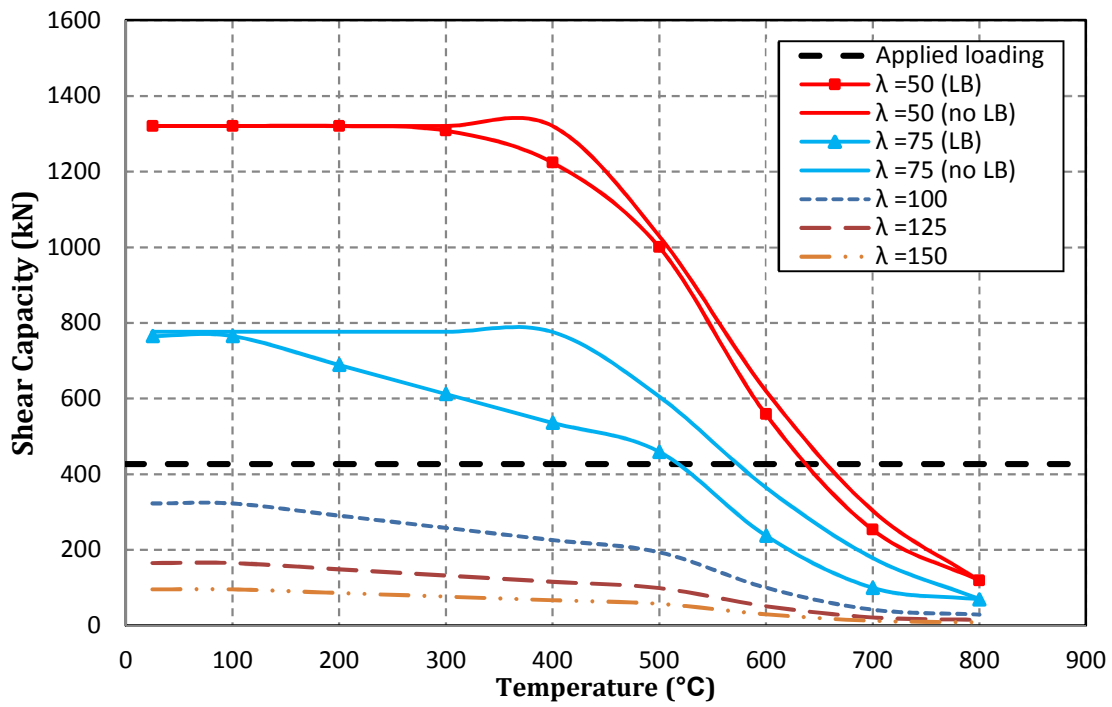
Figure 5.9: Degradation of shear capacity in the selected composite beams with fire exposure time
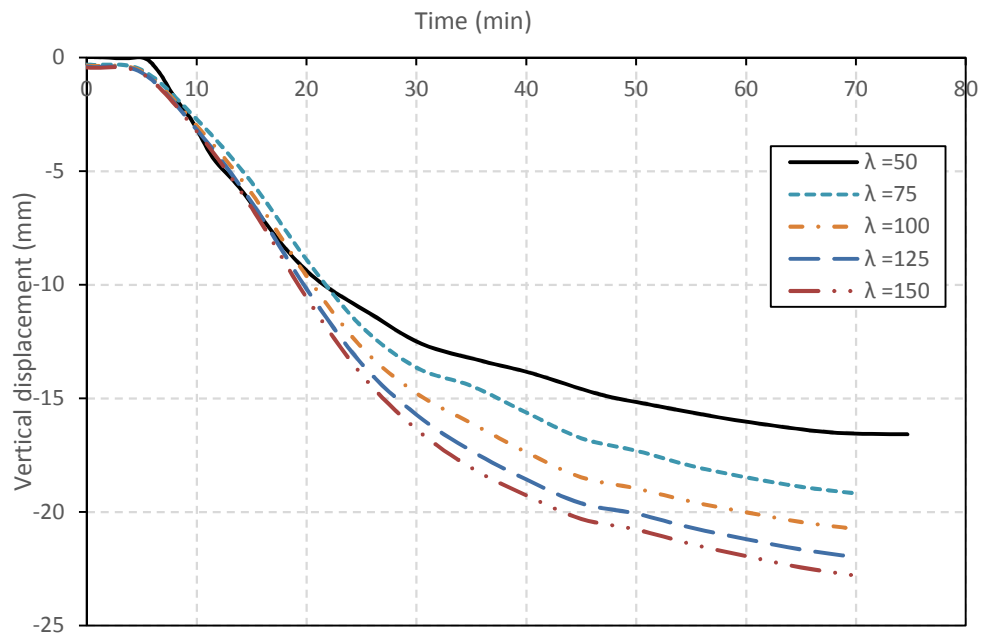
Figure 5.10: Comparison of vertical deflection in composite beams with different web slenderness during fire resistance analysis

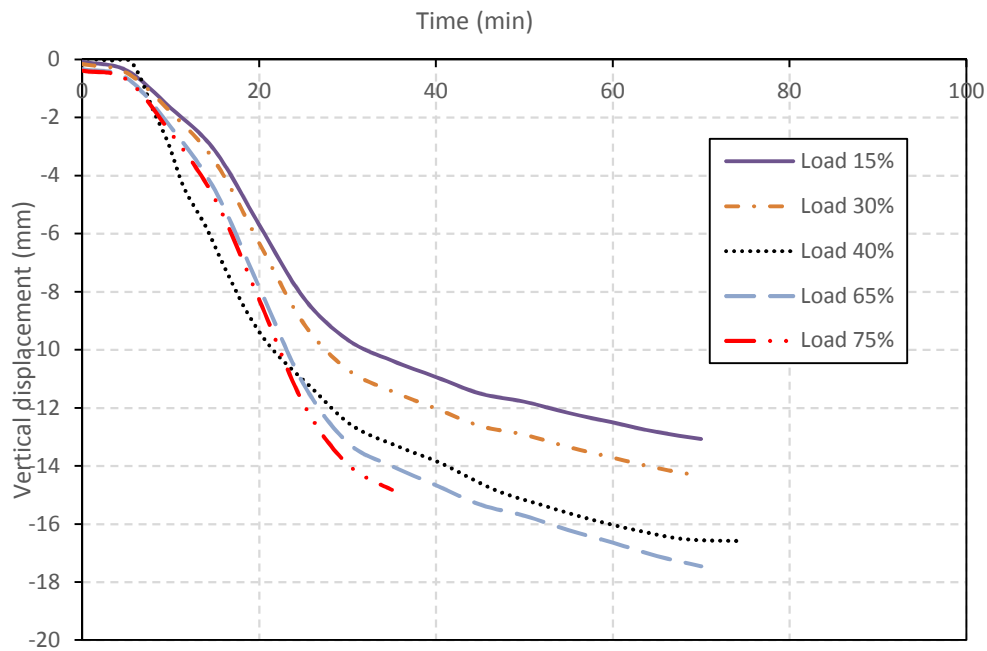Figure 5.11: Predicted vertical deflection in composite beams loaded with load level ot
15, 30, 40, 65 and 75% of sectional capacity
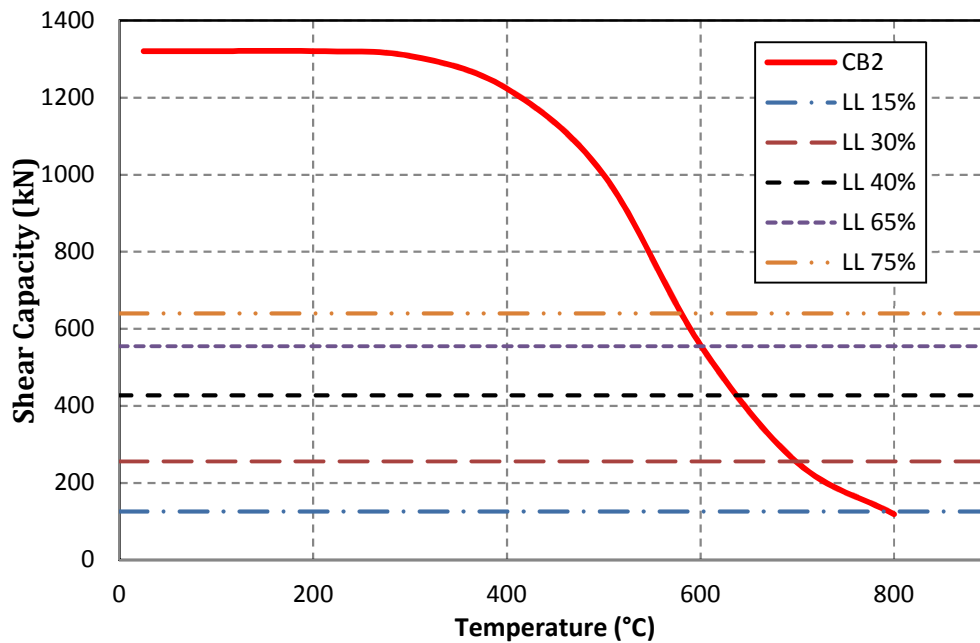
Figure 5.12: Degradation of shear capacity with fire exposure time in composite beams
with varying load levels

153
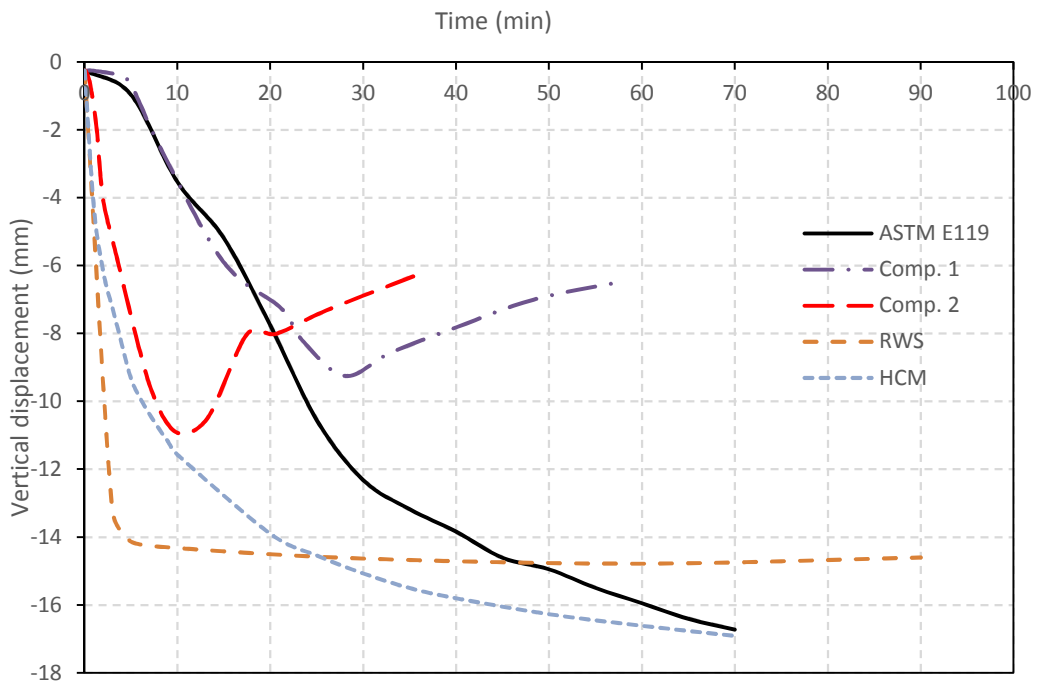
Figure 5.13: Deflection in composite beams subjected to different fire exposures
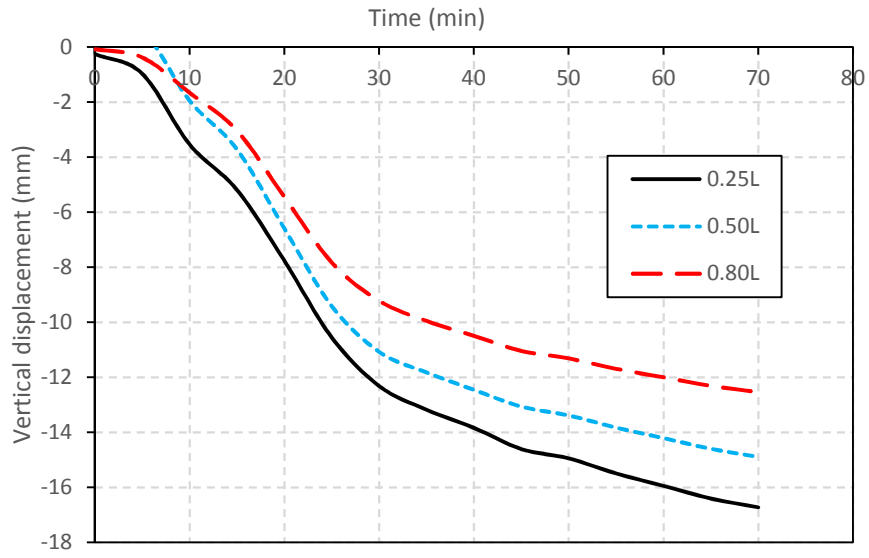
Figure 5.14: Deflection in composite beams loaded with high shear loading at 0.25L, 0.50L and 0.80L
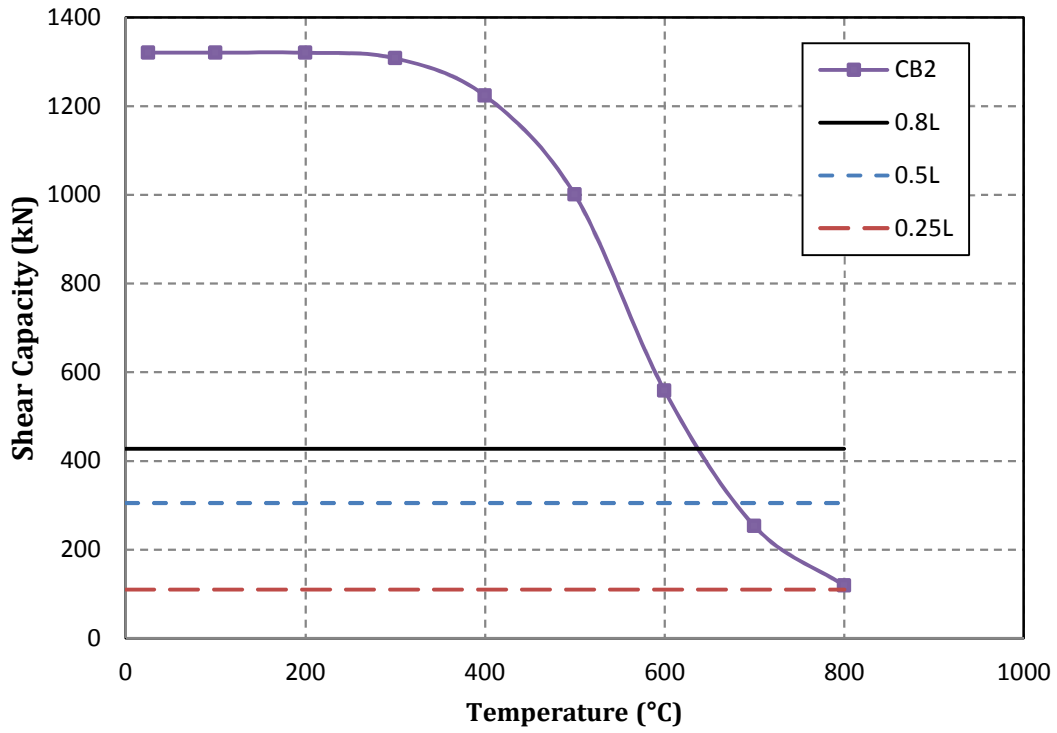
Figure 5.15: Degradation of shear capacity in composite beams loaded with high shear
loading at 0.25L, 0.50L and 0.80L under fire exposure
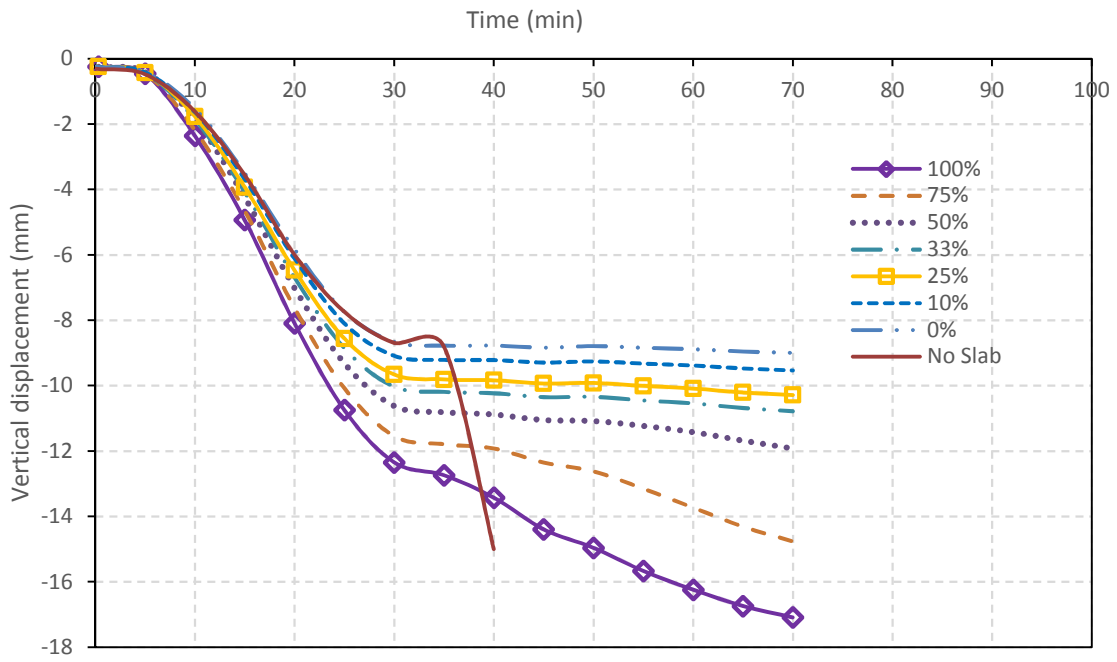
Figure 5.16: Progression of vertical deflection in beams with different level of composite action
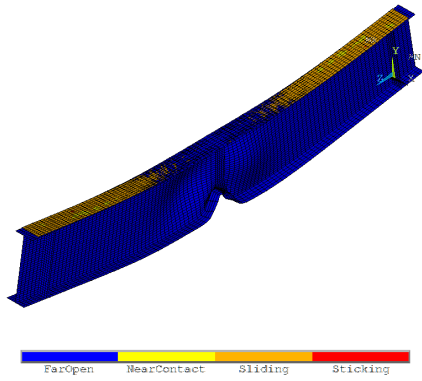
(i) Composite action of 100%
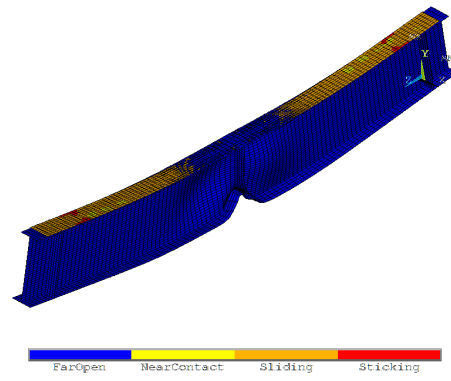
(ii) Composite action of 75%
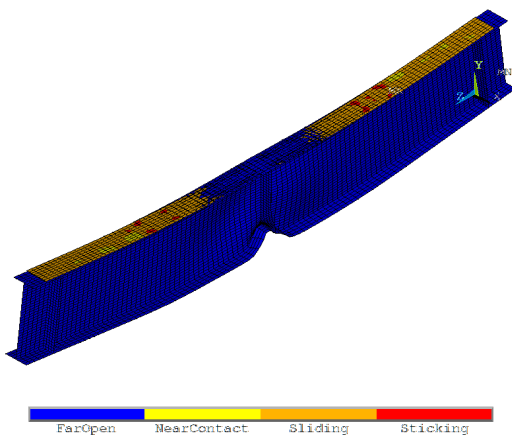
(iii)Composite action of 50%
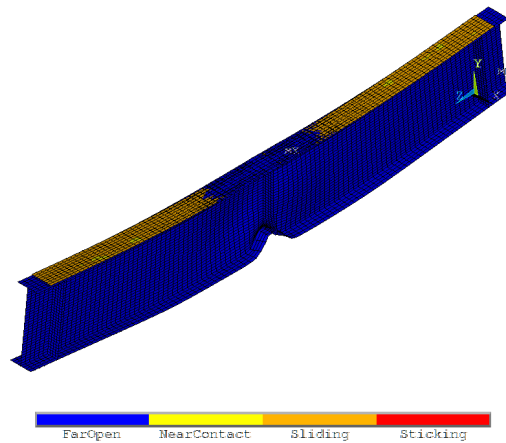
(iv)Composite action of 30%
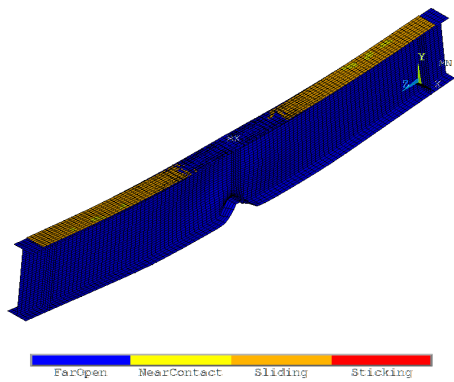
(v) Composite action of 25%
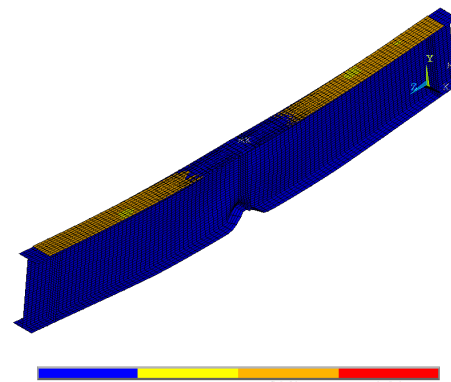
(vi)Composite action of 10%

Figure 5.17: Variations in contact status at failure in composite beams with different level of composite action
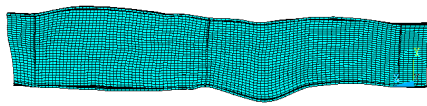
a) No slab (side view)
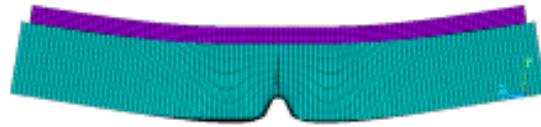
b) Composite beam (side view)
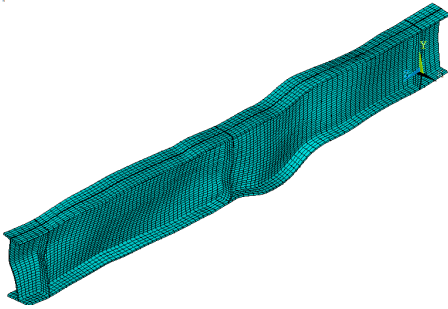
c) No slab
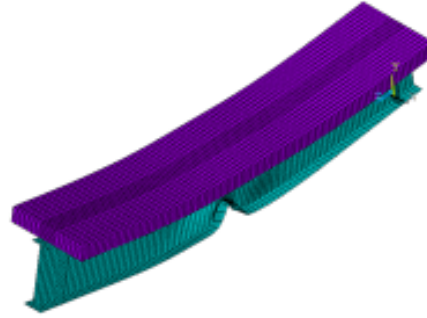
d) Composite beam

e) Buckling of steel beam (from (d))

Figure 5.18: Effect of concrete slab on failure mode of fire-exposed isolated and composite beams
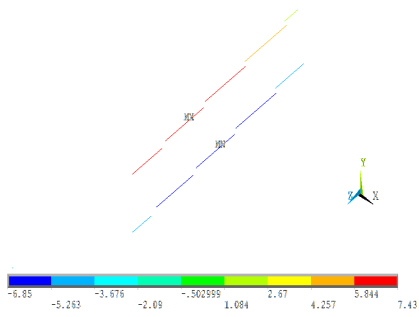
(i) 0.25K
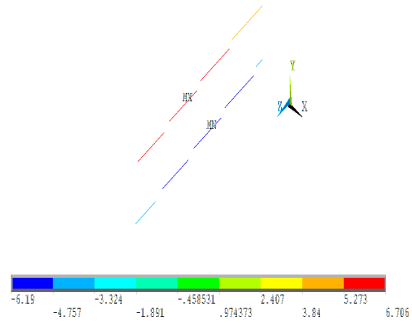
(ii) 0.5K
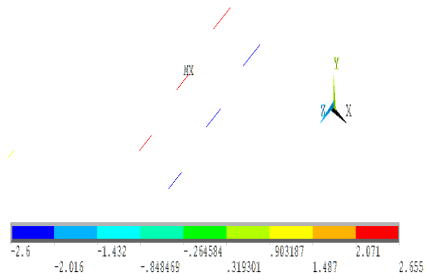
(iii)K
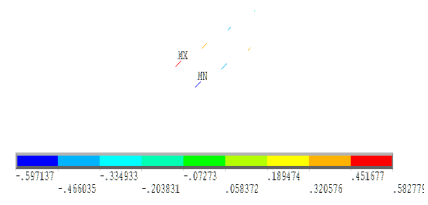
(iv)2K
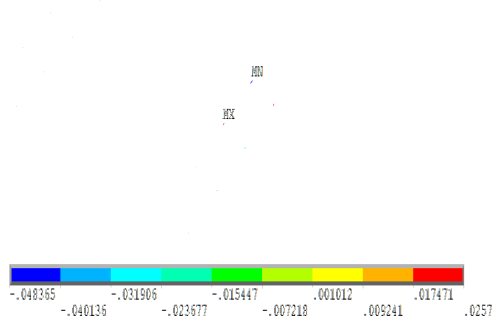
(v) 5K

Figure 5.19: Slippage at slab-beam interface in composite beams with varying shear stud stiffness
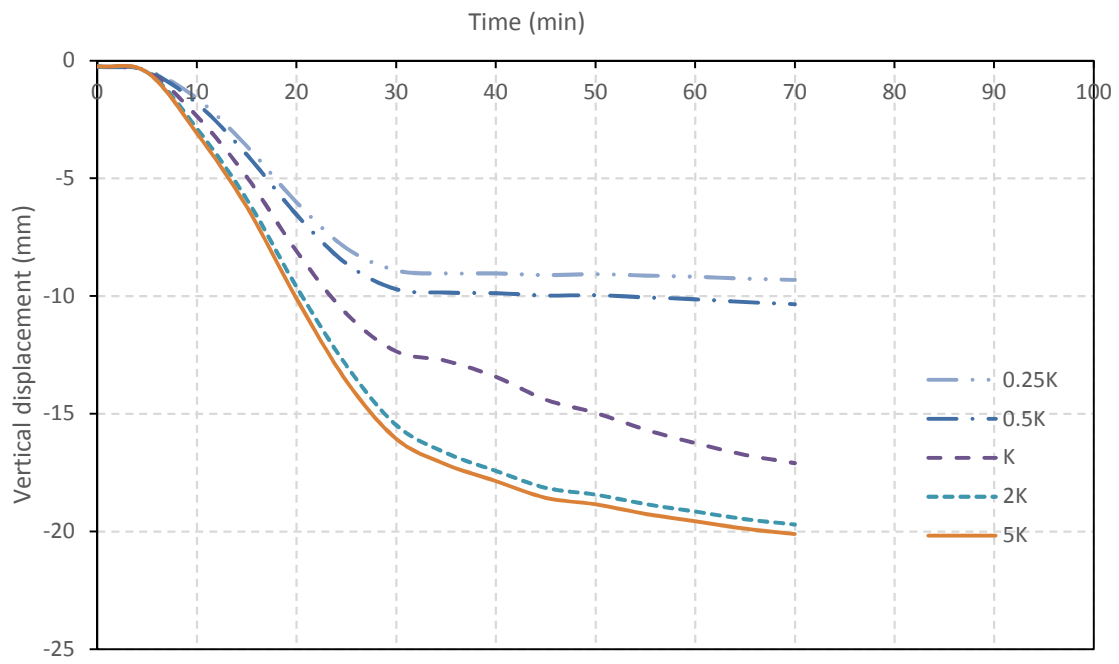
Figure 5.20: Progression of deflection in beams with varying shear stud stiffness
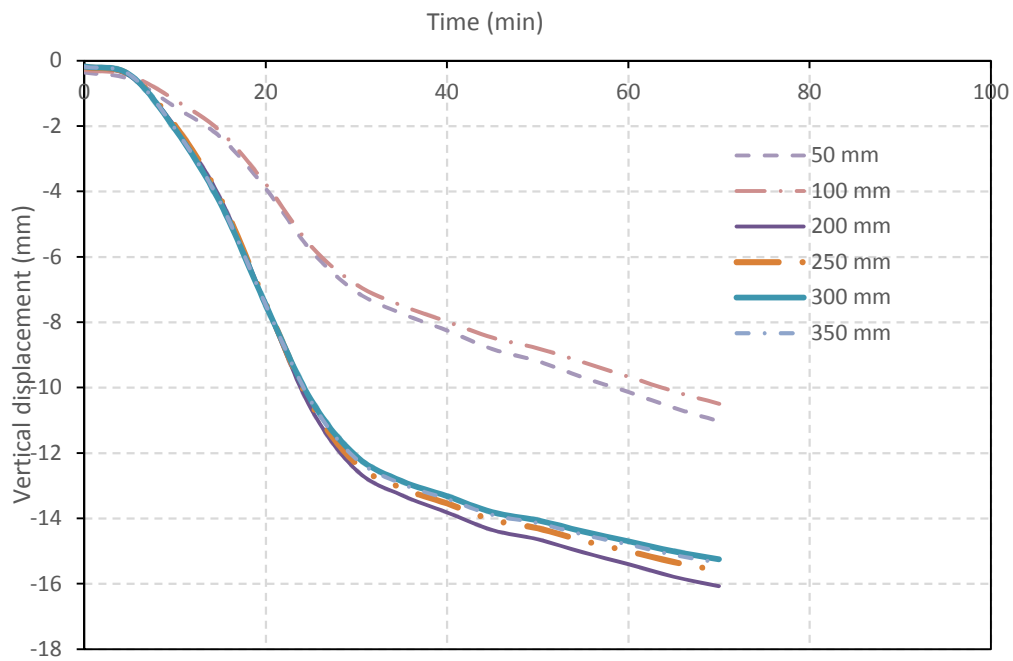
Figure 5.21: Progression of vertical deflection in composite beams with varying concrete slab thicknesses
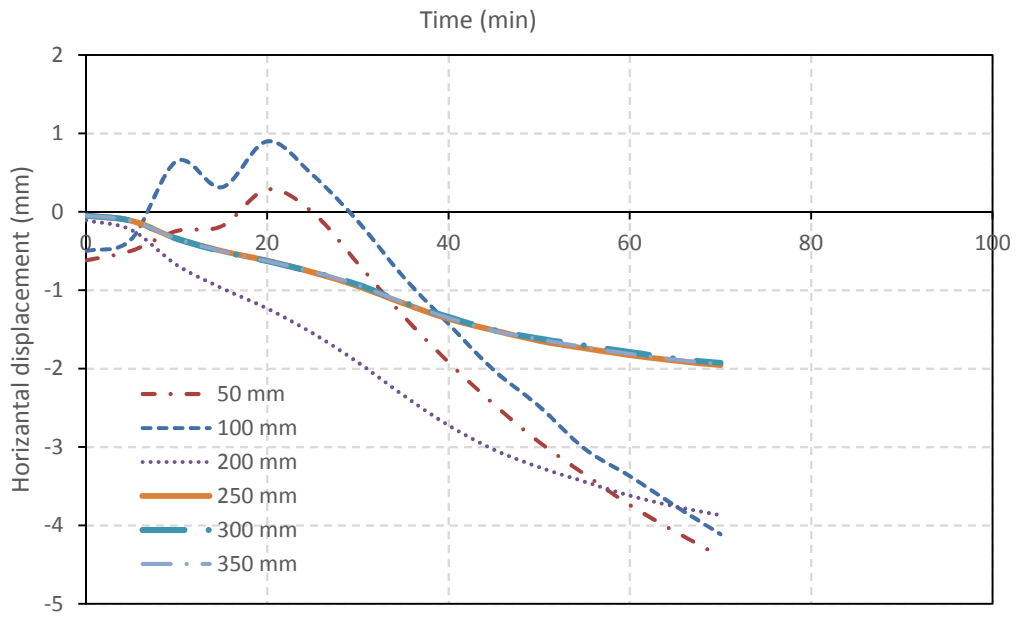
Figure 5.22: Horizontal web-displacement in composite beams with varying concrete slab thicknesses

5.5 Summary

The influence of various factors on the fire response of composite beams this chapter. The varied parameters included: sectional stability (geometric imperfections), web slenderness, load level, fire severity, loading configuration, level of composite action, shear stud stiffness and concrete slab thickness. Results from parametric studies indicate that composite beams loaded with high shear loading can experience failure in less than 50-60 minutes of fire exposure. The time to failure (and temperature at failure) in fire-exposed composite beams is highly influenced by web slenderness, instability of the web, and available level of composite action. Some of the main findings from the parametric study are:

- Applying moderate levels of initial imperfections (in the range of L/100 - L/1000) in the finite element analysis can effectively capture buckling mode and deformed shaped of fire-exposed steel and composite beams especially under combined shear and fire loading.

- Local buckling effects need to be accounted for when evaluating fire-response of beams especially those subjected to high shear loading.

- Higher load levels can cause beams to fail pre-maturely (especially under shear limit state through brittle failure mode.

- Type of loading configuration dictates the internal distribution of forces and resistance mechanism developed in structural member (i.e., steel and composite beams).

- Number of shear studs, stiffness of shear stud and thickness of concrete slab are key parameters that determine level of composite action in a composite beam. Composite beams with high level of composite action develop higher shear and deformation capacity.

CHAPTER SIX

6. Rational Design Methodology

6.1 General

In spite of clear indication that shear is a dominant loading (and failure) mechanism under ambient conditions and that shear effects can influence response of structural members under fire conditions, the adverse effects of shear parameters on the response of fire-exposed steel and composite beams is not accounted for in current design provisions (AISC, 2011; Eurocode, 2003). Further, the influence of concrete slab and associated composite action, on shear response of composite beams is also not considered in current fire design provisions (AISC, 2011).

To be more specific, current fire design requirements for steel structures in standards such as AISC 360 (2011), Eurocode 3 and 4 (2003), and AS 2327.1 (2003) do not explicitly account for shear failure, temperature-induced local buckling or contribution of concrete slab (i.e., composite action) to shear capacity of steel and composite beams. But rather, these standards often refer designers to specified requirements for design of steel structural members at room temperature. As a result, composite beam (made of steel beam attached to concrete slab) are currently designed following the assumption that applied shear force is resisted by the web of the steel beam alone; and neglecting any contribution from composite action.

It is clear that current design provisions lacks fundamental understanding and do not provide realistic evaluation of response (and behavior) of steel and composite beams subjected to high shear and fire loading. In order to overcome such limitations, this chapter presents the development of an approach for evaluating shear capacity of steel and composite beams. This methodology specifically accounts for property degradation of constituent materials, temperature-induced sectional instability and level of composite action offered by concrete slab

165

in evaluating shear capacity in beams. The proposed approach is combined with flexural capacity provisions available in literature to develop a unified approach for design (and analysis) of fire-exposed beams that can account for all possible failure limit states. The validity of the proposed approach is established and the applicability of this approach to design situations is illustrated through a numerical examples.

6.2 Approach for Evaluating Flexural Capacity under Ambient and Fire Conditions

At ambient conditions, beams are to be designed to satisfy strength and serviceability limit states. The ultimate limit states (i.e., flexural or shear) are to check for load carrying capacity under maximum loading conditions and prevent yielding or buckling at critical sections. On the other hand, the serviceability limit state prevent excessive vibration and deflection of beams under service loads).

The limit state criterion for evaluating flexural capacity of steel and composite beams under fire conditions specified are only available in some codes and standards (AISC, 2011; Eurocode, 2003). In general, these provisions extend room temperature design equations by taking into consideration appropriate strength degradation factors of materials. This approach[‡] of using material degradation factors simplifies capacity calculations at elevated temperature. In this section, a summary of the available design equations for evaluating flexural capacity of steel and composite beams is presented.

6.2.1 Steel beams (without concrete slab)

Beams, under fire conditions, can experience failure under flexural, or shear limiting states or due to a combination of different failure modes. The current provisions for evaluating flexural capacity of beams under fire conditions are through an extension of same principles as

---

[‡] It should be noted that current design provisions do not account for buckling due to flexural effects (i.e., flange buckling and torsional-flexural buckling).

that of room temperature and relevant equations available is AISC (2011) and Eurocode 3 (2003). In current room temperature design provisions, the flexural capacity of an I-shaped section is given by;

$$\varphi M_n = \varphi\, M_p = \varphi\, f_y\, Z_x \tag{6.1}$$

where,

φ = Strength reduction factor at ambient conditions[§]

f_y = Yield strength of steel section

Z_x = Plastic section modulus

In this case, flexural failure can occur when a beam becomes fully plastic (reaching plastic moment capacity, M_P) and this capacity falls below the bending moment resulting from factored loading (See Fig. 1.2). It should be noted that these provisions have been widely accepted and well validated (AISC, 2011; EC3, 2003).

For evaluating flexural capacity under fire conditions, room temperature flexural capacity equation (Eq. 6.1) is extended to account for temperature-induced degradation in strength properties. All that is needed is the appropriate reduction to yield strength of steel at a specified temperature to be implemented in to Eq. 6.1. Following this procedure, flexural capacity can be evaluated at a given temperature in steel. The moment capacity-fire exposure response curve can be used to evaluate failure temperature (and/or time) once moment capacity drops below level of bending moment. In order to account for these factors, Eq. 6.1 can be re-written as (AISC, 2011; EC3, 2003):

$$\varphi_f\, M_f = \varphi_f f_{y,T}\, Z_x \tag{6.2}$$

where,

[§] Usually $\varphi = 0.9$ (AISC, 2011)

φ_f = Strength reduction factor under fire conditions[**]

$f_{y,T}$ = Yield strength of steel section at temperature, T

In order to illustrate the applicability of these two equations, the flexural capacity of a typical steel beam is evaluated at room and fire conditions in Appendix A. In addition, the degradation in moment capacity of this beam is also plotted (as a function of fire exposure).

6.2.2 Composite beams (steel beams connected to a concrete slab)

Often concrete slab is overlaid on a steel beam and connected through a number of shear studs, thus forming a composite beam. The flexural capacity in a composite beam is the sum of the strength contributions from steel beam and that of concrete slab. The extent of flexural capacity also depends on the level of composite action that develops between concrete slab and steel beam which is mainly governed by number of shear studs. Similar to a steel beam, flexural capacity (in a composite beam) can be reached when the entire steel section yields (plastifies) followed by crushing of concrete slab, as shown in failure mode of composite beam CB1 (Fig. 3.14a).

The distribution of internal stresses at critical sections in a composite beam can follow any of the three distributions developing on the extent of composite sections that develops at slab-beam interface as shown in Fig. 6.1 (and Table 6.1). In these three cases, concrete stress is shown to have a uniform compressive distribution of $0.85 f'_c$; where f'_c is the compressive strength of concrete. This stress distribution, referred to as Whitney equivalent stress block, is a simplified version of average stress block. Whitney stress block has a resultant that matches actual stress distribution and extends from the top of the slab to a depth equals to or lesser than the thickness of slab (Sagui, 2013).

[**] Usually $\varphi_f = 1.0$ to reflect the fact that fire is an accidental limit state and that extremes of fire and extremes of load are unlikely to occur simultaneously.

In the case shown in Fig. 6.1a, the plastic neutral axis lies in the concrete slab and the corresponding stress distribution resembles full tensile yielding of steel beam and partial compression of the concrete. If the plastic neutral axis lies in the flange or web of steel beam, the concrete stress block extends to full depth of the slab and the plastic neutral axis lies in the steel flange (or web as shown in Figs. 6.1b and 6.1c). When the plastic neutral axis lies in flange or web, the part of steel section above plastic neutral axis is in compression which supplements the compression force in the slab. In all three cases, if sufficient number of shear studs is provided, full composite action develops in the beam. If not, only partial composite action develops in the composite beam. The nominal moment capacity at section in a composite beam can be calculated by computing the moment of the tensile and compressive resultants as shown in Fig.6.1.

The extent of composite action is a function of horizontal shear force (V_h) that develops at the interface between the steel and concrete. In order to maintain equilibrium within the composite cross-section, this horizontal shear force (V_h) need to be resisted by the available shear studs. The capacity of these shear studs is taken to be the lowest of compressive force developed in slab (either $A_s f_y$ or $0.85 f_c' A_c$), or resistance of all studs at the slab-beam interface (ΣQ_n).

where,

ΣQ_n is taken as the lesser of $0.5 A_{sc} \sqrt{f_c' E_c}$ or $R_g R_b A_{sc} F_u$,

A_{sc} is shear stud cross sectional area

F_u minimum tensile strength of studs

R_g, R_b are slab factors $= 1.0$ for solid slab.

Thus, for a composite beam the nominal flexural capacity can be evaluated by Eq. 6.3;

$$\varphi M_n = \min \text{ of } \varphi \{A_s f_y, 0.85 f_c' A_c \text{ or } \Sigma Q_n\} \times y \tag{6.3}$$

where,

A_s= Area of steel section

f_c'= Compressive strength of concrete

A_c= Area of concrete slab

y = moment arm of the couple formed by $A_s f_y$ and $0.85 f_c' A_c$

Similar to Eq. 6.1, Eq. 6.3 is also well established for evaluating for flexural capacity of composite beams at room temperature. Equation 6.3 can be extended to evaluate flexural capacity under fire conditions if an iterative procedure that accounts for temperature-induced degradation in strength properties of steel and concrete is accounted for (AISC, 2011; EC3, 2003). Thus, Eq. 6.3 can be re-written as;

$$\varphi_f M_n = min \ of \ \varphi \left\{ A_s f_{y,T}, 0.85 f_{c,T}' A_c \ or \ \sum Q_{n,T} \right\} \times y \qquad (6.4)$$

$f_{c,T}'$= Compressive strength of concrete at temperature, T

$f_{y,T}$= Yield strength of steel section at temperature, T

$Q_{n,T}$= Shear strength of shear studs at temperature, T

In order to illustrate the use of Eqs. 6.3 and 6.4, the flexural capacity of a typical composite is evaluated at room and fire conditions in Appendix B.

6.3 Approach for Evaluating Shear Capacity under Ambient and Fire Conditions

As discussed in Chapters 1, 2 and 3, failure in steel and composite beams can occur under flexural or shear limit states. From discussion provided in Secs. 6.2.1 and 6.2.2, it is clear that flexural limit state is well established. However, knowledge gaps from literature review provided in Chapter 2, along with findings from experimental and numerical results presented in Chapters 3 and 5, infer that current provisions for evaluating shear capacity of steel and composite beams lack fundamental understanding and may not be representative under fire conditions.

For instance, current design provisions neglect the development of sectional instability arising from local buckling, in evaluating shear (or flexural capacity) under fire conditions. Furthermore, current fire design provisions of composite beams also neglects the contribution of concrete slab to shear capacity. In this approach, composite beams are assumed to have same shear capacity as that of steel beam at room temperature. Under current provisions, shear capacity of a steel and/or composite beam at room temprature can be evaluated using Eq. 6.5,

$$\varphi_v \, V_n = \varphi_v \, 0.6 f_{yw} \, A_w \, C_v \tag{6.5}$$

where,

φ_v = Strength reduction factor at ambient conditions ($\varphi_v = 0.9$)

t_w = Thickness of the web

d = Overall depth for hot-rolled beams

A_w = Area of steel web = $d t_w$

C_v = Web shear coefficient that depends on slenderness of web

One of the major knowledge gaps identified in Chapter 2 is the lack of an approach to evaluate shear capacity of steel and composite beams, while taking into account temperature-induced instability effect as well as contribution of concrete slab. To overcome this limitations, a new approach is proposed as part of this research.

The following sections provide insights into the development of a new approach that accounts for the occurrence of temperature-induced instability in steel and composite beams as well as derivation of new equations that can take into account contribution of concrete slab (i.e., level of composite action) to shear capacity in composite beams. This approach can be used to evaluate shear capacity of steel and composite beams at room and under fire conditions. Later

on, the derived approach is combined with flexural capacity provisions available in literature to propose a unified approach for design (and analysis) of fire-exposed beams.

6.3.1 Procedure to evaluate shear capacity of steel beams

As shown through results from experimental studies in Chapter 3 and parametric study in Chapter 5, the key factors that influence shear capacity developed in a steel beam are web area (slenderness), temperature level in web and temperature-induced web local buckling (which is a function of web slenderness). Hence, these three factors are to be taken into account when deriving an expression for evaluating shear capacity of a steel beam. The derived approach will follow the same principles applicable to room temperature design calculations.

The basis of evaluating concrete shear capacity at room temperature can be derived from principles of Energy of Distortion Yield Theory (Huber-von Mises-Hencky, 1904). In this theory, the uniaxial yield stress in terms of the three principal stresses is given by;

$$\sigma_y{}^2 = \tfrac{1}{2}\left[(\sigma_1 - \sigma_2)^2 - (\sigma_2 - \sigma_3)^2 - (\sigma_3 - \sigma_1)^2\right] \tag{6.6}$$

where,

σ_1, σ_2 and σ_3 = Tensile and compressive stresses in the three principle directions that act in the three mutually perpendicular planes of zero shear,

σ_y = Yield stress that to be compared with the uniaxial value yield stress f_y

According to Huber (1904), in typical civil engineering applications, one of these three principal stresses is either zero or small enough to be neglected. Hence, Eq. 6.6 reduces to;

$$\sigma_y{}^2 = \sigma_1{}^2 + \sigma_2{}^2 - \sigma_1\sigma_2 \tag{6.7}$$

Since pure shear occurs on 45° plane to the principle planes, when $\sigma_2 = -\sigma_1$, then corresponding shear stress equals principle stress ($\tau = \sigma_1$). Substitution of $\sigma_2 = -\sigma_1$ into Eq. 6.7 gives;

$$\sigma_y{}^2 = \sigma_1{}^2 + \sigma_1{}^2 - \sigma_1 (-\sigma_1) = 3\sigma_1{}^2 \tag{6.8}$$

$$\sigma_1 = \tau = \sigma_y/\sqrt{3}$$

which indicates that the yield state for shear stress acting alone is;

$$\tau = \sigma_y/\sqrt{3} = 0.58f_{yw},$$

This can be approximated to be equals to $0.6f_{yw}$ (AISC, 2011). Thus, nominal shear capacity at room temperature can be evaluated using the following equation specified in AISC (2011);

$$\varphi_v\, V_n = \varphi_v\, \tau_{yw}\, dt_w\, C_v \tag{6.9}$$

where,

τ_{yw} = shear yield strength of the steel web ($\tau_{yw} = 0.6f_{yw}$)

t_w = thickness of the web

d = overall depth for hot-rolled beams

C_v = web shear coefficient that depends on slenderness of web

As shown above, this shear stress equals $0.6f_{yw}$. Thus, Eq. 6.9 can be re-arranged to be equivalent to Eq. 6.5 shown in Sec. 6.3;

$$\varphi_v\, V_n = \varphi_v\, 0.6f_{yw}\, A_w\, C_v$$

Equation 6.5 clearly shows that shear capacity in steel beams at room temperature is a function of the web area ($d \times t_w$) which constitute of depth of web and its thickness. These two parameters are also used to classify web slenderness through slenderness ratio ($\lambda = d/t_w$). In order to illustrate the effect of web slenderness on shear capacity of a steel beam, relative shear capacity as obtained from Eq. 6.5 is graphically represented in Fig. 6.3a for various web slenderness ratios. It can be seen that there are three distinct zones, in the response plot, i.e., shear yielding (plastic), inelastic buckling and elastic buckling. These zones can be utilized to

explain structural behavior of webs, and in turns development of sectional instability. In the plastic zone, ($d/t_w < 1.10\sqrt{\frac{E}{f_y}}$), web is not susceptible to any local buckling and this state represent a "compact" section phenomenon. In other words, a web with slenderness less than of that of the inelastic slenderness limit will achieve its full shear capacity.

On the other hand, a web with slenderness ratio of that in between $1.10\sqrt{\frac{E}{f_y}}$ and $1.37\sqrt{\frac{E}{f_y}}$, lie in the inelastic buckling zone. In this range, web buckling will occur after some part of web have yielded due to summation of applied stresses and preexisting residual stresses. A web in this zone will lose some of its shear strength due to occurrence of inelastic buckling. Finally, a web that lie in the elastic buckling zone, with sectional slenderness higher than that of $1.37\sqrt{\frac{E}{f_y}}$, are considered to be of slender webs and can fail prematurely: "elastically".

Web slenderness ratio is a geometric property of steel section independent of its strength and type of applied loading. This ratio is of a constant value even under fire conditions. However, slenderness limits are a function of ($\sqrt{\frac{E}{f_y}}$) which degrade under fire conditions as shown in Chapter 1. Currently, there are no provisions to classify steel webs in hot-rolled standard steel sections under fire condition although, temperature-induced loss in material properties changes (shifts) the three distinct zones in the response plot shown in Fig. 6.3a. Figure 6.3b shows the response plot of normalized shear capacity as a function of various web slenderness at temperatures of 200, 400, and 600°C. It can be seen from this figure that web stability in steel beam is a function of temperature rise in web, as well as web slenderness.

In general, rise of temperature softens web stiffness (i.e., web has more flexibility to move laterally or buckle) due to the large reduction in the degrading elastic modulus of steel

174

which starts at 150°C (as opposed to yield strength of steel which starts at higher temperature of 400°C). For example, a web with slenderness of 50 is considered to be "compact" at room temperature. However, the same web can transform into a "slender" web (and undergoes 20% reduction in capacity) once it reaches a temperature of 600°C. It is clear that in order to accurately evaluate shear capacity of steel beams, temperature rise in web, and web transformation (i.e., temperature-induced instability) need to be account for.

In order to account for these two factors, a new approach is proposed. This proposed approach requires an iterative procedure to evaluate sectional slenderness of a web and this to be checked against that of temperature-dependent slenderness limits during fire exposure (i.e., at a given temperature, ex: 100, 200, 300, 400°C... etc.). This iterative procedure can track status of web throughout exposure duration to account for web transformation due to temperature-induced effects. At each iteration, if web slenderness exceeds the compactness or non-compactness limits, appropriate reduction factors to account for web buckling is applied to evaluate in shear capacity. The reduction in shear capacity is accounted for through a temperature-dependent web shear coefficient ($C_{v,T}$).

The temperature-dependent web shear coefficient ($C_{v,T}$) can be grouped under three ranges. These ranges follows that of room temperature principles discussed above. Three limiting values are;

(i) $C_{v,T} = 1.0$, when $\dfrac{h}{t_w} \leq 1.10 \sqrt{\dfrac{E_T}{f_{yT}}}$

(ii) $C_{v,T} = \dfrac{1.10 \sqrt{\dfrac{k_v E_T}{f_{yT}}}}{\dfrac{h}{t_w}}$, when $1.10 \sqrt{\dfrac{k_v E_T}{f_{yT}}} \leq \dfrac{h}{t_w} \leq 1.37 \sqrt{\dfrac{k_v E_T}{f_{yT}}}$

(iii) $\quad C_{v,T} = \dfrac{1.37\sqrt{\dfrac{k_v E_T}{f_{yT}}}}{\dfrac{h}{t_w}}$, when $1.37\sqrt{\dfrac{k_v E_T}{f_{yT}}} \leq \dfrac{h}{t_w}$

where,

k_v = is shear buckling coefficient ($k_v = 5$, for webs without transverse stiffeners such as those in standard hot-rolled sections).

It can be seen that web shear coefficient ($C_{v,T}$.) can vary due to degradation in strength and modulus of steel at elevated temperature. Thus, this factor need to be evaluated at each target temperature through an iterative procedure shown in flow chart in Fig. 6.5. This analytical procedure comprises of three steps. In the first step, a steel section of web slenderness (d/t_w) in the range of 50-60 is selected (since these sections are more prone to transform into slender section under fire conditions) . For this section, web shear coefficient is evaluated, at different temperatures ranging from (ex. 25-800°C) to arrive at $C_{v,T}$ (i.e., $C_{v,25°C}$, $C_{v,100°C}$, $C_{v,200°C}$ etc.). Then, in the next step, the average of these web shear coefficients (i.e., $C_{v,25°C} - C_{v,800°C}$) is calculated to arrive at $C_{v,T,section}$ for the selected section.

In order to simplify this analytical procedure and reduce the number of steps involved in calculation of $C_{v,T}$ (or $C_{v,T,section}$). The above discussed steps are repeated for all other steel sections of web slenderness (d/t_w) of 50-60. Finally, web shear coefficients of selected sections are averaged to arrive at the average of web shear coefficient ($C_{v,Tave}$). Since this factor ($C_{v,Tave}$) is arrived at by averaging web shear coefficient of all steel sections, this factor (of a known value[††]) now can be applied to any steel section selected as follows.

$$\varphi_f V_n = 0.6 f_{yw,T}\, t_w^2 C_{v,Tave} \tag{6.10}$$

[††] For instance, for steel grade of 345 MPa, $C_{v,Tave} = 0.89$.

As discussed earlier, web shear coefficient ($C_{v,T}$ or $C_{v,Tave}$) tracks the transformation of web from one state to another under fire conditions. Currently, this web transformation, arising from local buckling is not recognized although web buckling can lead to significant reduction in shear capacity (of 20% or more). In order to limit (or minimize) web transformation, as well as associated reduction in strength due to buckling of web, a limitation on shear capacity of web is not to exceed a maximum boundary limit is specified. This boundary limit is dictated by a slenderness parameter (β), reflects web slenderness at which a compact or non-compact web transforms into a slender web. In other words, shear capacity of a steel web cannot exceed that of its non-compactness limit ($1.37\sqrt{\frac{E_T}{f_{yT}}}$) which allows for a safer design at fire conditions.

In order to further illustrate the effect of slenderness parameter (β) on temperature-induced instability, the compactness and non-compactness slenderness limits for a typical steel grade is plotted in Fig 6.4. It can be seen from plotted response that a web of slenderness of 57 is classified to be "compact" at room temperature. However, this web can transform into a "slender"[‡‡] web at 700°C. Hence, the slenderness parameter β equals 57[§§]. This factor is applied into Eq. 6.5 to arrive at a newly derived Eq. 6.11 as follows:

$\beta = d/t_w$

thus,

$d = \beta\, t_w$

since,

$A_w = dt_w$

[‡‡] Same procedure can be used to limit shear capacity of web so that it cannot exceed that of compactness limit
[§§] For illustrative purposes, $\beta = 57$ is applicable for steel grade of 345 MPa. Same procedure can be used to arrive at boundary factor β of other steel grades.

then,

$A_w = (\beta \ t_w) \ t_w$

Hence, the simplified design equation to calculate shear capacity in standard hot-rolled steel section is;

$$\varphi_f \ V_n = \varphi_f \ 0.6 f_{yw,T} \ \beta \ t_w{}^2 C_{v,Tave} \tag{6.11}$$

In order to summaries the proposed approach, Fig. 6.6 outlines various steps needed to evaluate nominal shear capacity of steel beams taking into account the effect of temperature-induced degradation in strength property as well as temperature-induced instability. It should be noted that the derived equations need to be used at temperatures higher than 150°C since modulus of elasticity properties starts to degrade at that temperature.

6.3.2 Procedure to evaluate shear capacity in composite beams

Steel beams are often designed as part of slab to achieve beneficial effects of composite action. In this type of construction, a concrete slab is usually attached to a steel beam through a number of shear studs. As discussed in Chapters 2, 3, 4 and 5, level of composite action, arising from beam-slab interaction can increase available shear stress (flow) along the depth of the composite beam which translate into producing higher shear capacity (as well as bracing and stiffness) as shown in Fig. 6.7 (Vasdravellis and Uy, 2014; Nie et al., 2004; Liang et al., 2005).

The presence of concrete slab can also be beneficial under fire conditions. For instance, concrete slab acts as a heat sink in a composite beam exposed to fire. This is due to the higher specific heat (and low thermal conductivity) of concrete which attracts much of heat of top flange and top portion of web which lowers average temperature rise in steel beam. This can reduce rate of degradation in strength and modulus properties and delays failure of composite beam under fire conditions. Despite the above mentioned advantageous, presence of concrete

slab and associated level of composite action is not taken into account in the evaluation of shear capacity of composite beams.

It is clear that in order to achieve a realistic evaluation of shear capacity in a composite beam, contribution of concrete slab to shear capacity need to be quantified. Hence, to develop a methodology for the evaluation of shear capacity in composite beams, it is assumed that shear capacity of a composite beam comprises of shear capacity of steel beam, V_s, and shear capacity of concrete slab, V_c, i.e.,

$$\varphi_v V_n = \varphi_v V_s + \varphi_v V_c \tag{6.12}$$

where,

V_s is the contribution of steel beam to shear capacity (calculated as shown in Eq. 6.11)

V_c is the contribution of concrete slab to shear capacity

Since Eq. 6.12 accounts for the contribution of concrete slab to shear capacity, this contribution need to be quantified at room and elevated temperatures. In order to quantify the beneficial contribution of concrete slab, results from the analysis on a large number of beams (presented in Chapters 3, 4 and 5) are utilized. For example, Fig. 6.8 shows the contribution of induvial steel beam to applied shear loading. In addition, this figure also shows the individual contribution of a steel beam and concrete slab to shear capacity in two composite beams made of same steel section as that used in individual steel beam.

In the case of an individual steel beam, it is clear that the applied loading is being resisted with the actions (shear capacity) of the steel beam alone (since the beam is not attached to a concrete slab). However, in the case of a composite beam made of concrete slab of 100 and 200 mm thickness, it is clear that both steel beam and concrete slab work as one unit in resisting the applied loading. In the latter case, the concrete slab can carry as much as 50% of the applied

shear loading. This observation is also shown in Fig. 5.16 and has been well reported in previous studies (Vasdravellis and Uy, 2014; Nie et al., 2004; Liang et al., 2005).

To illustrate the contribution of concrete slab to shear capacity under fire conditions, Fig. 6.9 shows individual contribution of steel beam and concrete slab (in carrying shear loading) at 10 minutes of fire exposure. It is clear that with increase in fire exposure time, the contribution of steel beam to shear capacity decreases as steel properties (f_y and E) degrade with rise in web temperature. At the same time, the contribution of concrete slab to overall shear capacity increases and this compensate, to some extent, to the degrading shear capacity of steel beam. This compensation can be explained by continuous shift of neutral axis upward (towards the cooler slab) to maintain structural equilibrium.

This positive contribution of concrete slab can be quantified by a closer examination to measured and predicted results shown in Chapters 3 and 5. The positive contribution of concrete slab can be influenced by the effective area of concrete under shear (which includes concrete slab thickness (D_{slab})), level of composite action (C), and stiffness of shear studs (K). Hence, in order to derive an accurate expression that can be used to evaluate available shear capacity of a concrete slab. This expression needs to account for variation of slab thickness (D_{slab}), level of composite action (C), and stiffness of shear studs (K).

In order to arrive at such an expression, data on shear force carried by slab were collected from analysis of experimental and numerical results presented in Chapters 3, 4 and 5 and as well as results from other studies reported by Vasdravellis and Uy (2014), Nie et al. (2004), and Liang et al. (2005), represent maximum shear capacity carried by the slab. Once these values are collected, a linear regression analysis was carried out to compile these values and derive an expression to evaluate concrete slab contribution to shear capacity ($\varphi_v V_c$) as shown in Eq. 6.13.

$$\varphi_v V_c = \varphi_v [0.16\sqrt{f_c'}\, b_f + 0.95 D_{slab} + 89C - 4.7K - 179] \tag{6.13}$$

where,

$\sqrt{f_c'}$ = Measure of concrete tensile strength (ACI, 2011)

b_f = Width of the top steel flange

D_{slab} = Thickness of concrete slab

C = Level of composite action

K = Stiffness of shear studs

Based on these results, the shear capacity of a composite beam under fire condition can be evaluated taking into account strength degradation, instability effect, shear strength of the concrete slab, stiffness of shear studs and level of composite action by Eq. 6.14;

$$\varphi_v V_n = \varphi_v\, V_s + \varphi_v\, V_c$$

$$\varphi_v V_n = \varphi_v\, [0.6 F_{yw,T}\, \beta t_w{}^2 C_{v,Tave} + 0.16\sqrt{f_{c,T}'}\, b_f + 0.95\, D_{slab} + 89C - 4.7K - 179] \tag{6.14}$$

Figure 6.10 shows a flow chart that illustrates the procedure evaluating shear capacity in steel and composite beams under fire conditions.

6.4 Unified Approach for Evaluating Flexural and Shear Capacity

From earlier discussion provided in Secs. 6.2 and 6.3 as well as knowledge gaps present in recent studies, current design provisions in codes and standards only accounts for flexural limit state when evaluating failure of steel and composite beams exposed to fire conditions. However, from measured and predicted results presented in this thesis, it is clear that failure in steel and composite beams can occur under flexural or shear limit states. In order to derive a rational design procedure (that is complete and thorough), a unified approach that accounts for all possible limit states in evaluating failure of steel and composite beams is needed.

From the derived equations in Sections 6.2 and 6.3, a unified approach to evaluate flexural and shear capacity of steel and composite steel beams at room and under fire conditions is proposed. This approach accounts for effects of temperature-induced material degradation and instability, shear strength of the concrete slab, stiffness of shear studs and level of composite action. The validity of this approach along with detailed numerical example is presented in this section. In addition, the limitations of this approach are also discussed.

6.4.1 General procedure

The proposed approach comprises taken into account both limit states, flexural and shear, to evaluate failure as shown in flow chart present in Fig. 6.11. The analysis can be carried out for a steel or composite beam. If a steel beam is selected, then web slenderness is compared against that of slenderness limit to check if this web is prone to temperature-induced local buckling. If web local buckling is to be imminent, then the procedure lied out in Sec. 6.3.1 is followed and the shear capacity of this beam is evaluated utilizing Eq. 6.11.

Similarly, the flexural capacity of steel or composite beam can be also evaluated following current design provisions discussed in Sec. 6.2.1. The evaluated flexural and shear capacity are compared against bending (moment) and shear (force) effects arising from applied loading. Through this comparison, failure mode and temperature (or time) at failure of beam can be determined. For instance, if the shear capacity drops below shear force before flexural capacity drops below bending moment, then the beam is to fail due to shear effects.

On the other hand, if the selected beam is a composite beam, then similar consideration to that described above are applied to the steel beam. In addition, the flexural and shear contribution of concrete slab is evaluated as discussed in Secs. 6.2.2 and 6.3.2 and added to the corresponding flexural and shear capacity of steel beam. In this procedure, the flexural and shear

capacity (of steel beam and concrete slab) is compared against effects of applied bending moment and shear force. Once flexural and/or shear capacity drops below level of bending moment and/or shear force, failure occurs.

The proposed procedure provides a unified approach for evaluation of flexural and shear capacity of steel and composite beams (at ambient and fire conditions). This approach accounts for all possible failure limit states and can evaluate flexural and shear capacity in steel and composite beams. This proposed approach is easy to apply, and can be systematically programmable into a simple and robust computer code (excel macro or Matlab code).

6.4.2 Validation of unified approach for steel beams

Since current design provisions for flexural evaluation have been well validated and established (as shown in Sec. 6.2), the applicability of the proposed unified approach in fire design of steel beams, predicted shear response of several standard steel sections is investigated and plotted in Fig. 6.12 and compared against predictions from AISC room temperature design provisions (when extended to elevated temperatures). To validate the shear response of selected steel beams, shear capacity of various steel sections of I-shaped (W-shaped) W18×40, W12×14, W16×26, W21×50, W24×55, W27×84, W30×90, W33×130, and W40×167 is compared in Fig. 6.12. It is clear that the predicted response is in close agreement with that predicted following current AISC design provisions at room temperature. However, since the proposed equations take into account effect of temperature-induced instability, the adverse effect of local instability is apparent especially at temperatures of more than 150 and 400°C.

Figure 6.12 also shows the temperature at failure in the selected beams when the shear capacity drops below an assumed level of applied loading (of 40% of shear capacity). Table 6.2 also lists the predicted temperature at failure in these sections along with the geometric and

material properties used in this analysis. It can be seen from presented results that predicted temperature at failure can be significantly different between predicted results from the proposed approach and that of predictions obtained from AISC extended equations as shown in Table 6.2.

Since all beams are subjected to shear force of 40% of their shear capacity, these beams fail at the same temperature when predictions from AISC extended equations is applied. The temperature at failure in these beam corresponds to 640°C, since these equations only account for temperature-induced strength degradation. However, due to occurrence of temperature-induced instability along with strength degradation, failure of these beams occurs at lower temperatures than that predicted by AISC extended equations. These temperatures are also different in each section which reflect that fact that temperature-induced instability effects are mainly influenced by sectional slenderness of web.

6.4.3   Validation f of unified approach or composite beams

In order to validate the applicability of the proposed unified approach in fire design of composite beams, the shear capacity (and response) of fire-exposed composite beams is compared against current AISC design provisions as well as predictions from equations proposed by other researchers (based on room temperature tests)[***]. In order to study a wide range of geometric and material parameters, these beams are analyzed by varying concrete compressive strength, stiffness of shear studs and composite action as shown in Table 6.3. The predicted shear capacity of composite beams tested in Chapter 3 (of W24×62) along with other composite beams of various steel sections W18×40, W12×14, W16×26, W21×50, W24×55, W27×84, W30×90, W33×130, and W40×167 and concrete slab configurations are analyzed. The shear capacity of these composite beams was evaluated and plotted in Fig. 6.13 as a function of fire exposure time.

[***] Vasdravellis and Uy (2014), Nie et al. (2004) and Liang et al. (2005)

These predictions (and temperature at failure) were also compared against predictions from AISC equations and other researchers such as Vasdravellis and Uy (2014), Nie et al. (2004) and Liang et al. (2005).

As discussed earlier, equations derived by these other researchers were derived based on room temperature tests. These equations do not account for the level of composite action, shear stud stiffness or local buckling of web. Thus, these equations were extended to fire conditions by accounting for temperature-induced degradation in strength properties. It can be seen from Fig. 6.13 that the predicted shear capacity of composite beams from the proposed approach and predictions of other researchers is higher than that predicted following the AISC provisions. This is due to the fact that AISC design provisions do not account for presence of concrete slab and assumes the shear capacity of a composite beam to carried by the web of steel section.

6.4.4 Numerical Example

A 4 m long composite beam comprises of a W18×40 section of A992 steel with a 140 mm thick reinforced concrete slab at the top. Assume full composite action between steel beam and concrete slab provided through sufficient number of stiff shear studs. The strength of the concrete is $f_c' = 45$ MPa. Determine the flexural and shear capacity of the composite beam at ambient conditions. Then, evaluate the flexural and shear capacity of this composite beam at fire conditions (500°C). In addition, the following parameters are needed;

Steel beam:

$b_f = 153$ mm, $b_t = 13.3$ mm, $d=454.6$ mm, $t_w = 8$ mm, $f_y = 345$ MPa, $f_{y,500°C} = 269.1$ MPa, $Z = 1280$ mm^3

Concrete slab:

$D_{slab} = 140$ mm, $K = 1$, $C = 100\%$, $b = 1320$ mm, $D_{stud} = 18.4$ mm, $F_{y,stud} = 450$ mm

The flexural capacity of this composite beam can be evaluated at room and fire conditions (500°C)[†††] using Eq. 6.15:

In this composite beam;

- $0.85 f'_c A_c = 4076 \ kN$

- $A_s f_y = 2691 \ kN$

- $\sum Q_n = 2781 \ kN$

It is clear that steel beam ($A_s f_y$) controls the design of this section and the neutral axis lies within the slab (at room temperature). Thus, the flexural capacity of this composite beam can be evaluated by:

$$\varphi \, M_n = min \ of \ \varphi \{A_s f_y, 0.85 f'_c A_c \ or \ \sum Q_n \} \times y$$

$$\varphi \, M_n = 0.9 \times 2691 \times 279 = 675.8 \ kN.m$$

Similarly, when steel beam temperature reaches 500°C, the average rise in concrete slab and shear stud is much lower than their critical temperature (of 400°C). Thus,

- $0.85 f'_{c,500°C} A_c = 4076 \ kN$

- $A_s f_{y,500°C} = 2043 \ kN$

- $\sum Q_{n,500°C} = 2781 \ kN$

Again, steel beam ($A_s f_{y,500°C}$) controls the design of this section and the neutral axis needs to shift upward to account for degradation in steel strength. Thus,

$$\varphi_f \, M_n = min \ of \ \varphi \{A_s f_{y,T}, 0.85 f'_{c,T} A_c \ or \ \sum Q_{n,T} \} \times y$$

[†††] The reduction factor for yield strength of steel at 500°C = 0.78 (EC 3, 2003)

$$\varphi_f\, M_{n,500°C,} = 1.0 \times 2043 \times 288 = 610\ kN.m$$

Similarly, the shear capacity of this composite beam can be evaluated at room and fire conditions (500°C) as:

$$\varphi_v\, V_n = 0.9\,[\ 0.6 f_{yw}\, d\, t_w\, C_v + \left\{0.16\sqrt{f'_{c,20°C}}\ b_f + 0.95\, D_{slab}\ +\ 89C - 4.7K - 179\right\}]$$

$$\varphi_v\, V_n = 0.9\,[\ 752 + \left\{0.16\sqrt{45}\ (177.8) + 0.95(177.8)\ +\ 89(1) - 4.7(1) - 179\right\}]$$

$$\varphi_v\, V_n = 0.9\,[\ 752 + 218.1] = 970.1\ kN$$

This predicted shear capacity, which includes the presence of the concrete slab, is much larger than the shear strength predicted using AISC provisions (which equals 752 kN) because it neglects the presence of concrete slab and level of composite action.

And the shear capacity of this composite beam at fire conditions (500°C) is:

$$\varphi_f\, V_n = 1.0\,[\ 30.4\ f_{yw,T} t_w{}^2 + \left\{0.16\sqrt{f'_{c,20°C}}\ b_f + 0.95\, D_{slab}\ +\ 89C - 4.7K - 179\right\}]$$

$$\varphi_f\, V_n = 1.0\,[\ 523.4 + 218.1] = 741\ kN$$

The predicted shear capacity of this composite beam under fire exposure can be seen in Fig. 6.13c.

6.4.5   Limitation of proposed approach

Due to the large variability in the cross-sectional configurations of steel sections, the proposed approach is derived for hot-rolled standard steel beams with I-shaped (W-shaped) sections since it is not possible to develop a unified approach or model that covers all possible shapes of steel sections. However, the same methodology can be applied for M, S and built-up sections (plate girders) as well as non-standard sections if special attention is paid to the derivation of the slenderness parameter (β) and temperature-dependent web shear buckling

$(C_{v,Tave})$. The following are the limitations under which the proposed approach may not be fully applicable:

(e) The proposed approach does not account for buckling due to flexural effects (i.e., flange buckling and torsional-flexural buckling).

(f) Flexural-shear interaction is not considered in evaluating shear capacity.

(g) The proposed approach may not be applicable for beam-columns.

(h) The proposed approach has not been verified for use in temperatures higher than 800°C.

(i) The proposed approach has not been verified for special concrete types including fiber-reinforced concrete (steel fibers, polypropylene), high strength concrete and ultra-high performance concrete.

(j) The flexural and shear capacity prediction obtained from proposed approach does not account for uncertainty factors such as fire-induced spalling and cracking of concrete.

Table 6.1: Classification of composite beam based on relative strength of its components

|		$\sum Q_n > S^*$	$\sum Q_n = S^*$	$\sum Q_n < S^*$
I.	$0.85 f_c' A_c < A_s f_y$	Fully composite; Inadequate slab; PNA in steel	Fully composite; Inadequate slab; PNA in steel	Partially composite; Inadequate slab; PNA in steel
II.	$0.85 f_c' A_c = A_s f_y$	Fully composite; Adequate slab; PNA in top flange	Balanced design; Adequate slab; PNA in top flange	Partially composite; Adequate slab; PNA in steel
III.	$0.85 f_c' A_c > A_s f_y$	Fully composite; Adequate slab; PNA in slab	Fully composite; Adequate slab; PNA in slab	Partially composite; Adequate slab; PNA in steel

$S^* = \min(0.85 f_c', A_s f_y)$

Table 6.2: Geometric and material properties of steel beam used in the validation of the proposed approach

Steel section	t_w (mm)	D (mm)	d/t_w	T_{PA} (°C)	T_{AISC} (°C)
W12×14	4.9	292	59.5	602	640
W16×26	6.1	385	62.8	592	640
W18×40	7.7	439	56.8	613	640
W21×50	9.3	510	54.7	618	640
W24×55	9.6	578	59.8	600	640
W27×84	11.3	654	58	608	640
W30×90	11.5	773	62.8	593	640
W33×130	14.2	811	57	611	640
W40×167	16	946	59.4	603	640

Table 6.3: Geometric and material properties of composite beams used in the validation of the proposed approach

Steel section	t_w (mm)	D (mm)	d/t_w	D_{slab} (mm)	f'_c (MPa)	K	C (%)	T_{PA} (°C)	T_{AISC} (°C)	T_{Nie} et al. (°C)	T_{Liang} et al. (°C)	$T_{Vasdrave}$ llis and Uy (°C)
W12×14	4.9	292	59.5	100	30	1	100	780	640	-	-	-
W16×26	6.1	385	62.8	140	25	1	75	750	640	720	-	800
W18×40	7.7	439	56.8	125	40	1	50	710	640	680	755	700
W21×50	9.3	510	54.7	175	27	2	25	703	640	650	740	700
W24×55	9.6	578	59.8	150	45	1	100	715	640	645	790	670
W24X62	11	581	55.12	140	54	1	100	720	630	630	735	650
W27×84	11.3	654	58	75	42	3	80	685	640	570	650	570
W30×90	11.5	773	62.8	180	48	1	100	715	640	638	800	660
W33×130	14.2	811	57	180	37	0.5	100	700	640	600	700	620
W40×167	16	946	59.4	250	60	1	30	680	640	620	800	665
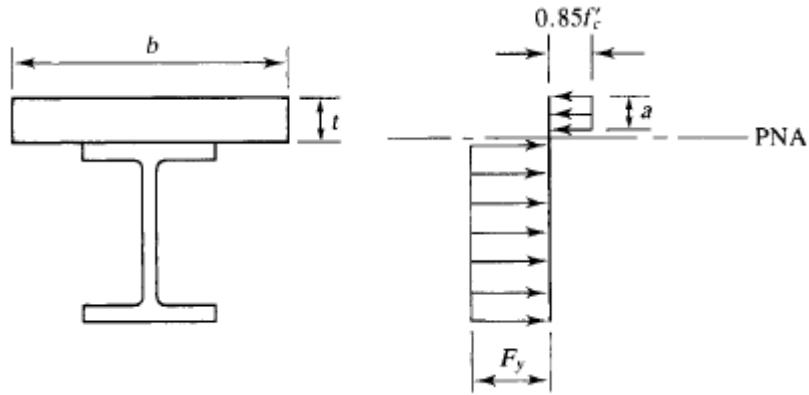
(a) Plastic nuetral axis in slab
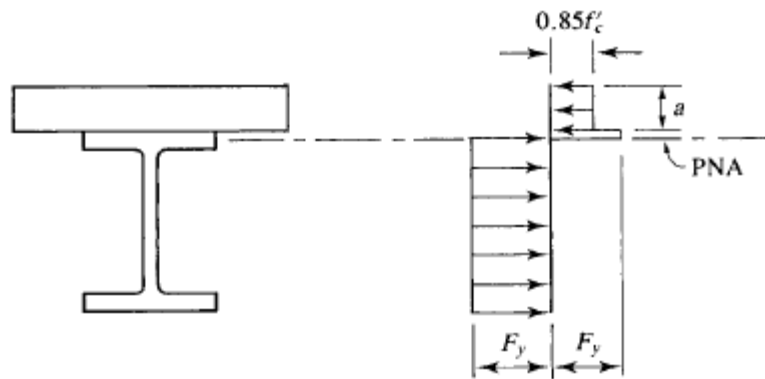
(b) Plastic nuetral axis in flange
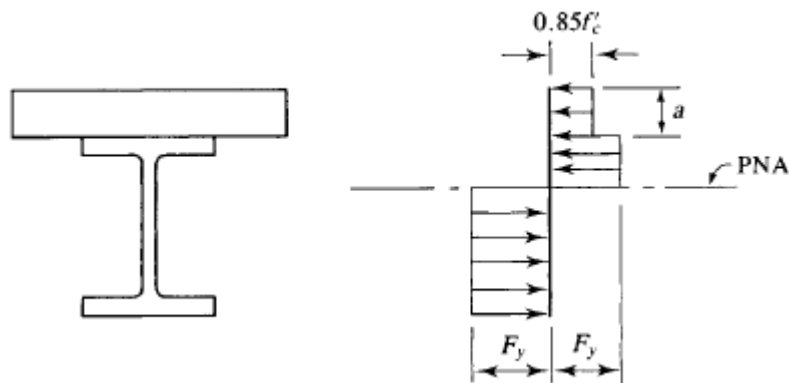
(c) Plastic nuetral axis in web
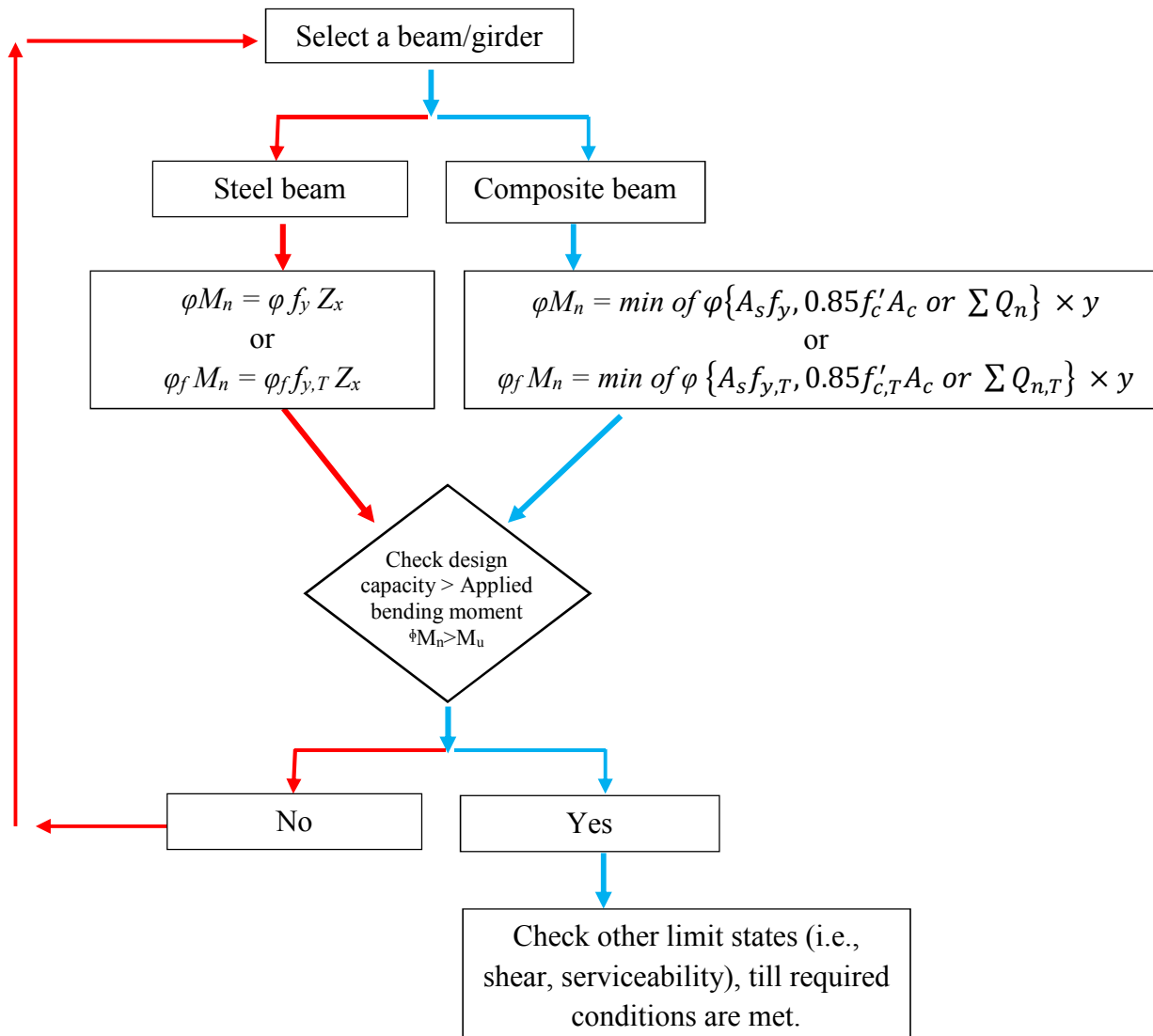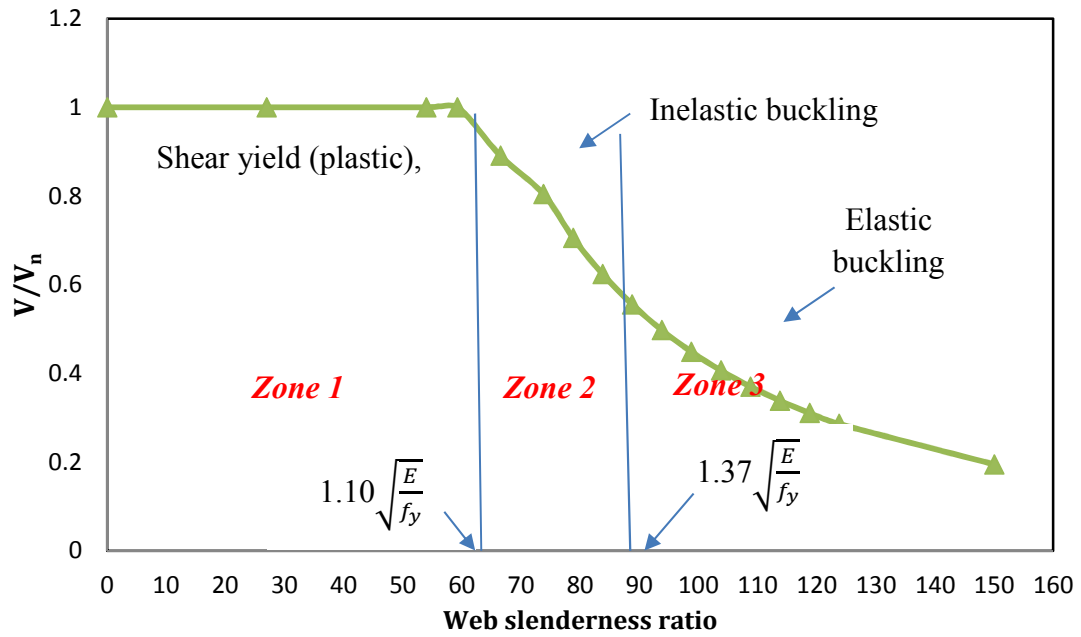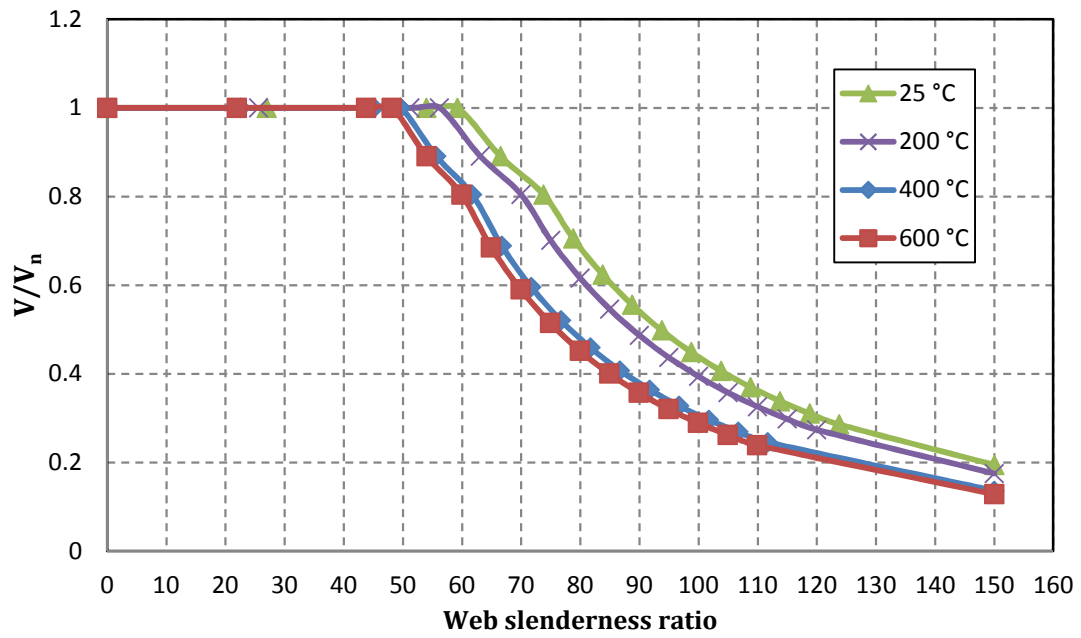Figure 6.1: Stress distibutionin in a composite section (Sagui, 2013)

Figure 6.2: Analytical procedue to evalute flexural capacity in steel and composite beams

Select a beam/girder

Steel beam

Composite beam

$\varphi M_n = \varphi \, f_y \, Z_x$
or
$\varphi_f M_n = \varphi_f f_{y,T} \, Z_x$

$\varphi M_n = min \; of \; \varphi \{A_s f_y, 0.85 f_c' A_c \; or \; \sum Q_n\} \times y$
or
$\varphi_f M_n = min \; of \; \varphi \{A_s f_{y,T}, 0.85 f_{c,T}' A_c \; or \; \sum Q_{n,T}\} \times y$

Check design capacity > Applied bending moment
$\Phi M_n > M_u$

No

Yes

Check other limit states (i.e., shear, serviceability), till required conditions are met.

(a) Room temperature

(b) under fire conditions

Figure 6.3: Classification of web in fire-exposed beams subjected to shear loading

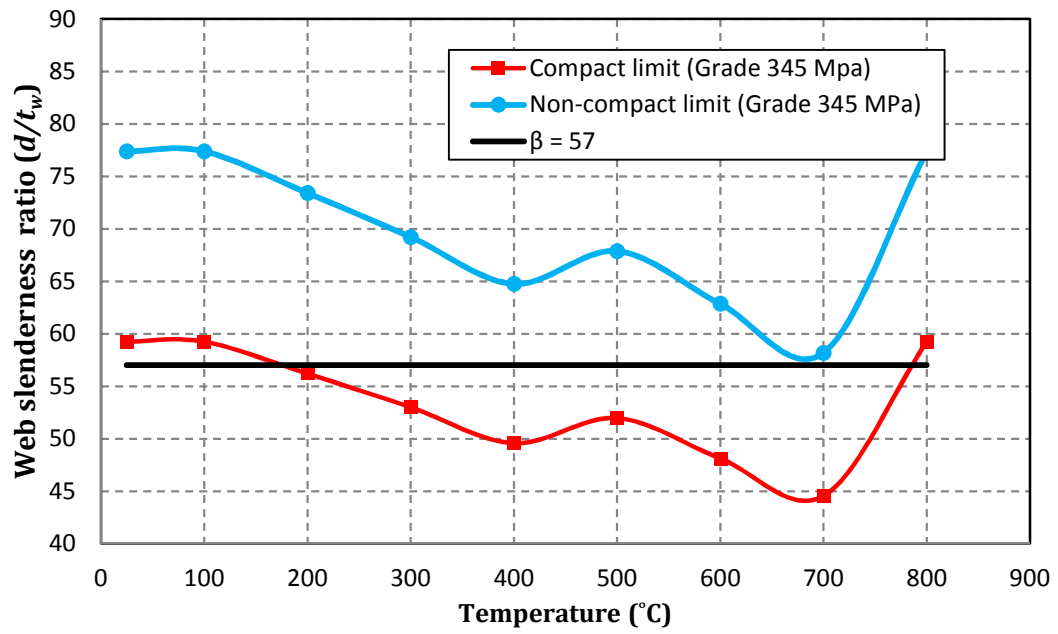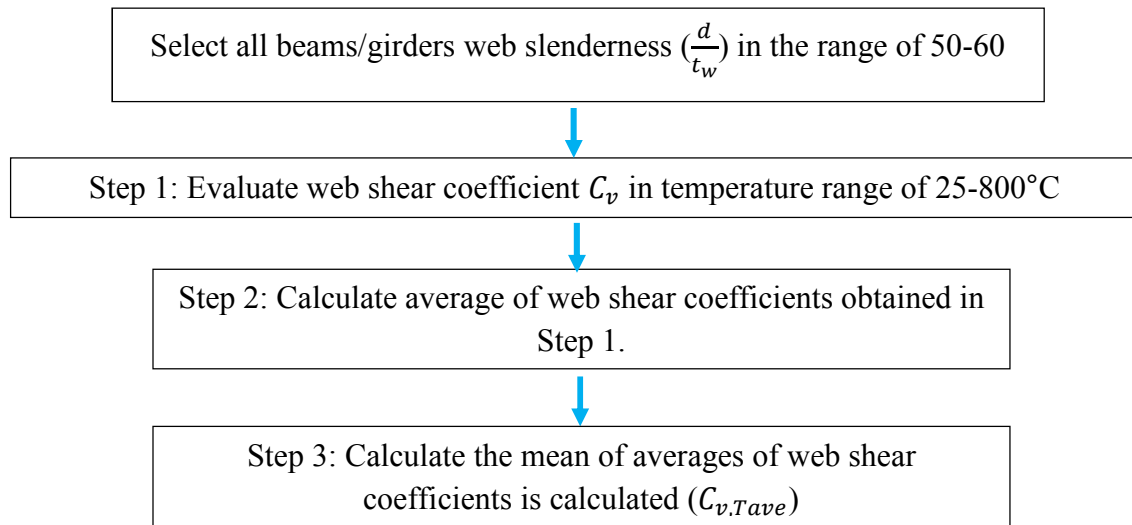Figure 6.4: Illustration of slenderness parameter (β)

Select all beams/girders web slenderness ($\frac{d}{t_w}$) in the range of 50-60

Step 1: Evaluate web shear coefficient C_v in temperature range of 25-800°C

Step 2: Calculate average of web shear coefficients obtained in Step 1.

Step 3: Calculate the mean of averages of web shear coefficients is calculated ($C_{v.Tave}$)

Figure 6.5: Analytical procedure to calculate the average temperature-dependent web shear coefficient ($C_{v,Tave}$)
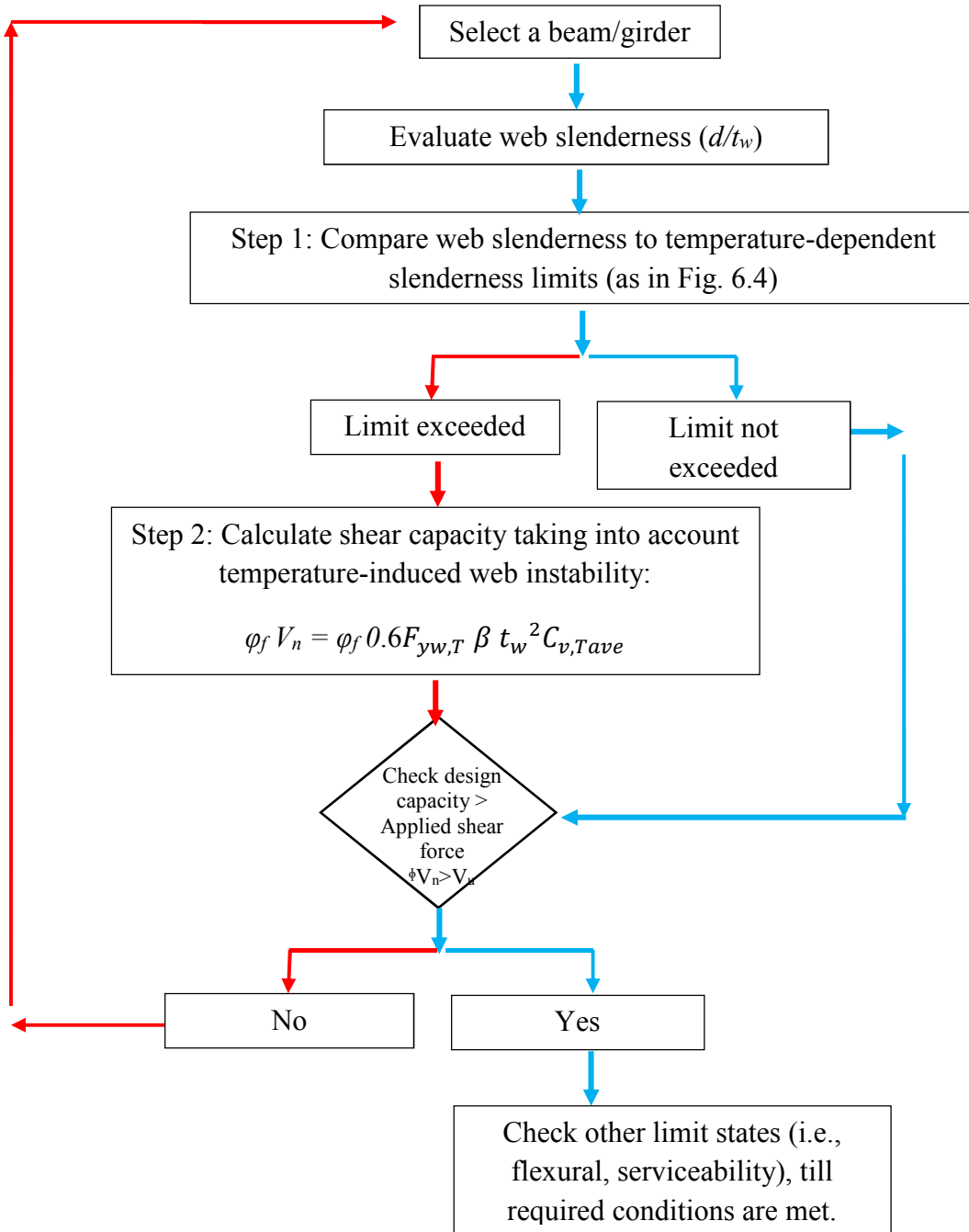
Figure 6.6: Flow chart illustrating steps for evaluating shear capacity of steel beams under fire conditions

The flow chart contains the following elements:

Select a beam/girder

Evaluate web slenderness (d/t_w)

Step 1: Compare web slenderness to temperature-dependent slenderness limits (as in Fig. 6.4)

Limit exceeded

Limit not exceeded

Step 2: Calculate shear capacity taking into account temperature-induced web instability:

$$\varphi_f \, V_n = \varphi_f \, 0.6 F_{yw,T} \, \beta \, t_w{}^2 C_{v,Tave}$$

Check design capacity > Applied shear force $\phi V_n > V_u$

No

Yes

Check other limit states (i.e., flexural, serviceability), till required conditions are met.

(i) Strain   (ii) Shear stress

(a) No interaction

(i) Strain   (ii) Shear stress

(b) Partial interaction

(i) Strain   (ii) Shear stress

(c) Full interaction

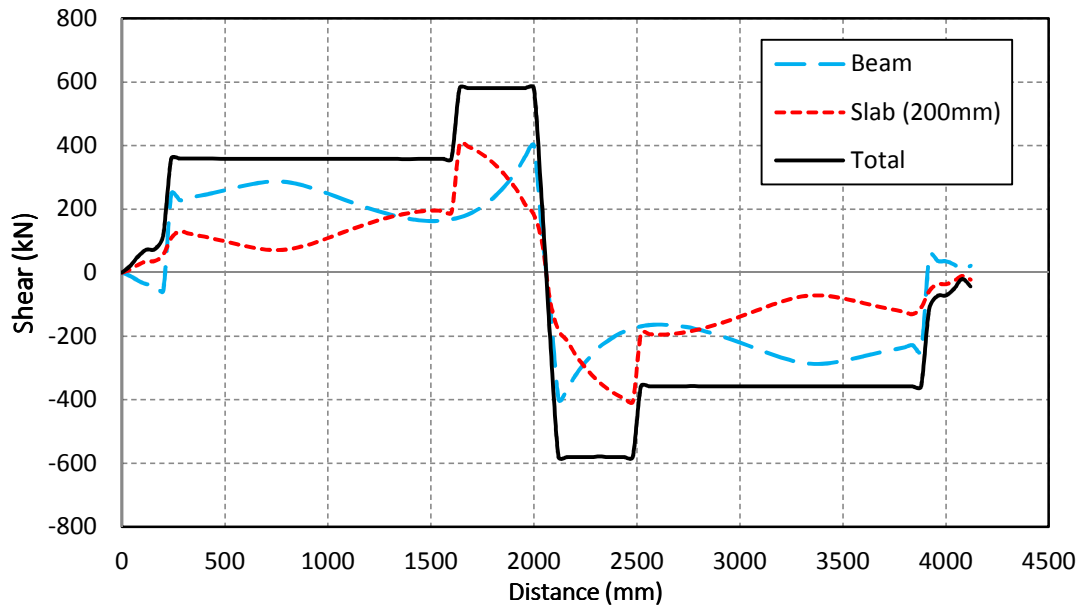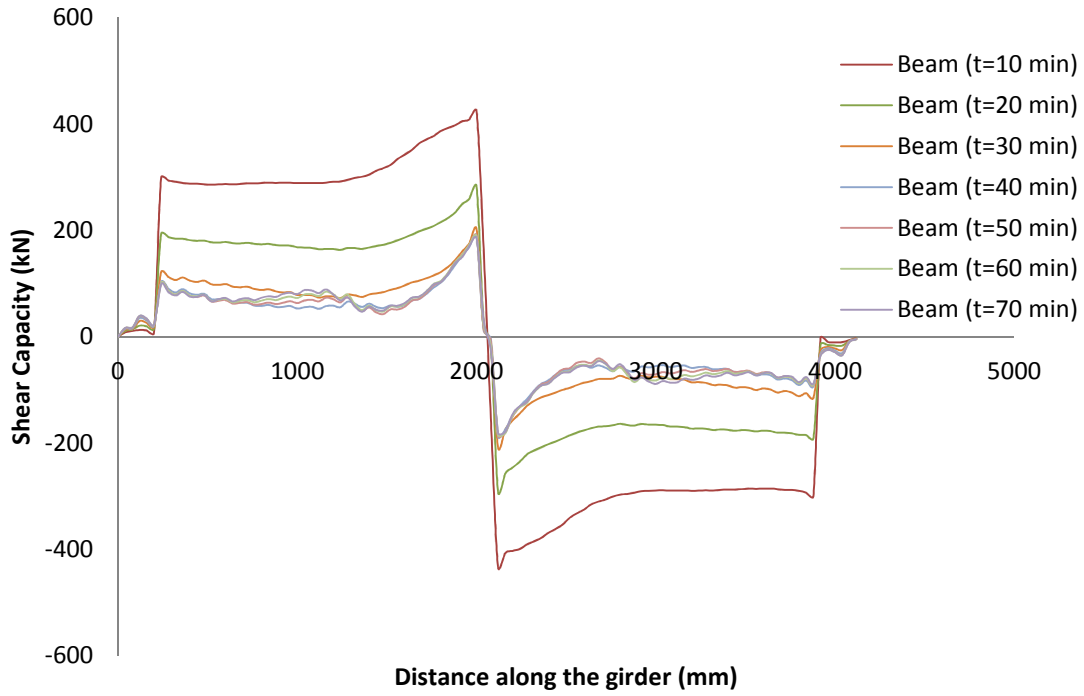Figure 6.7: Strain and shear stress distibutionin of a composite beam
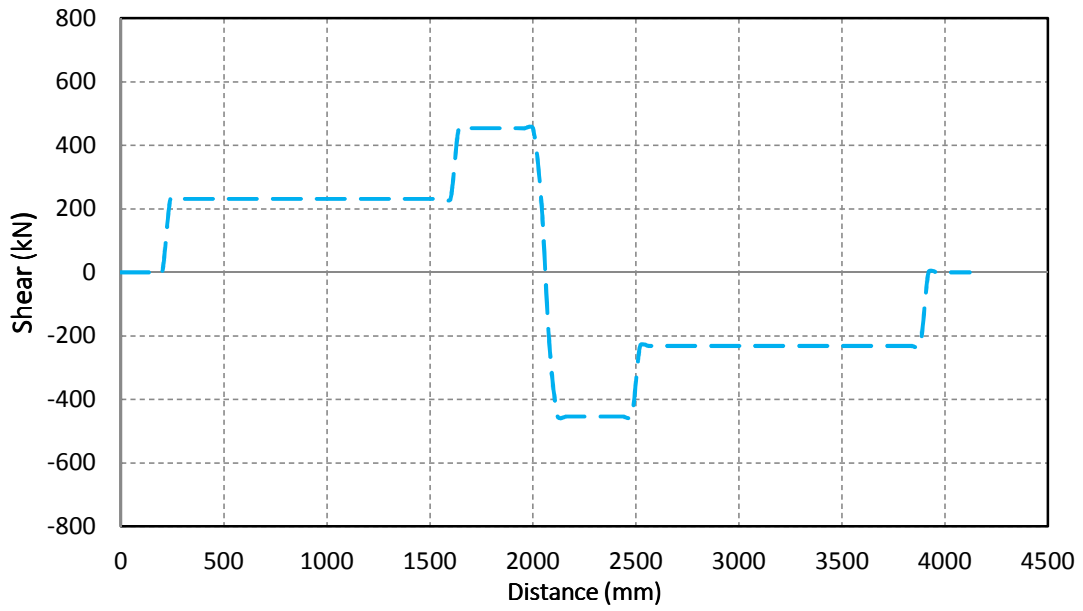
(a) Steel beam
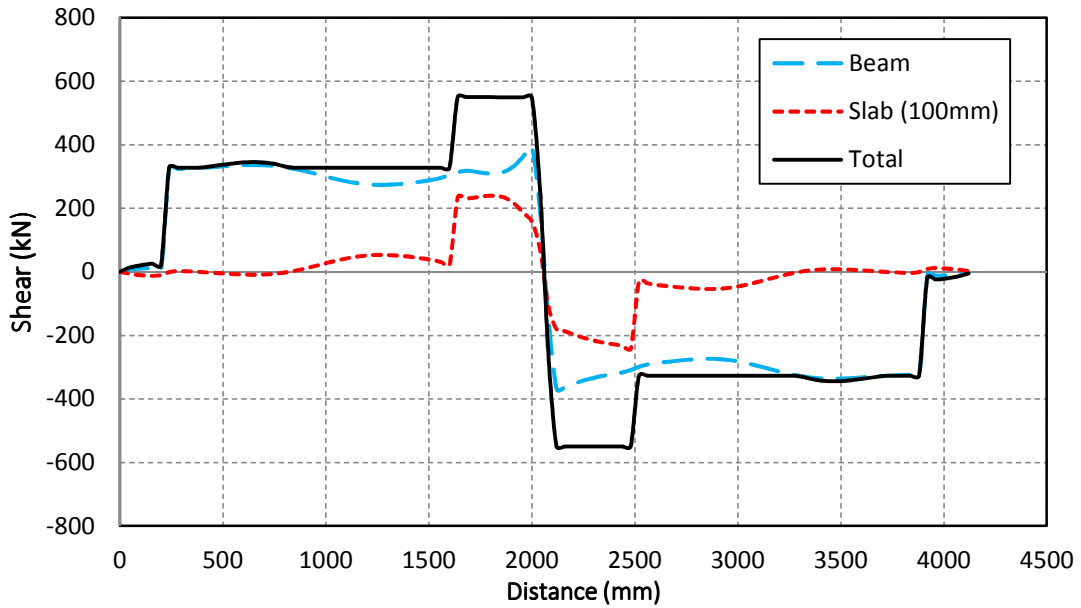
(b) Composite beam (with slab thickness of 100 mm)

Figure 6.8: Contribution of steel beam and concrete slab to shear capacity
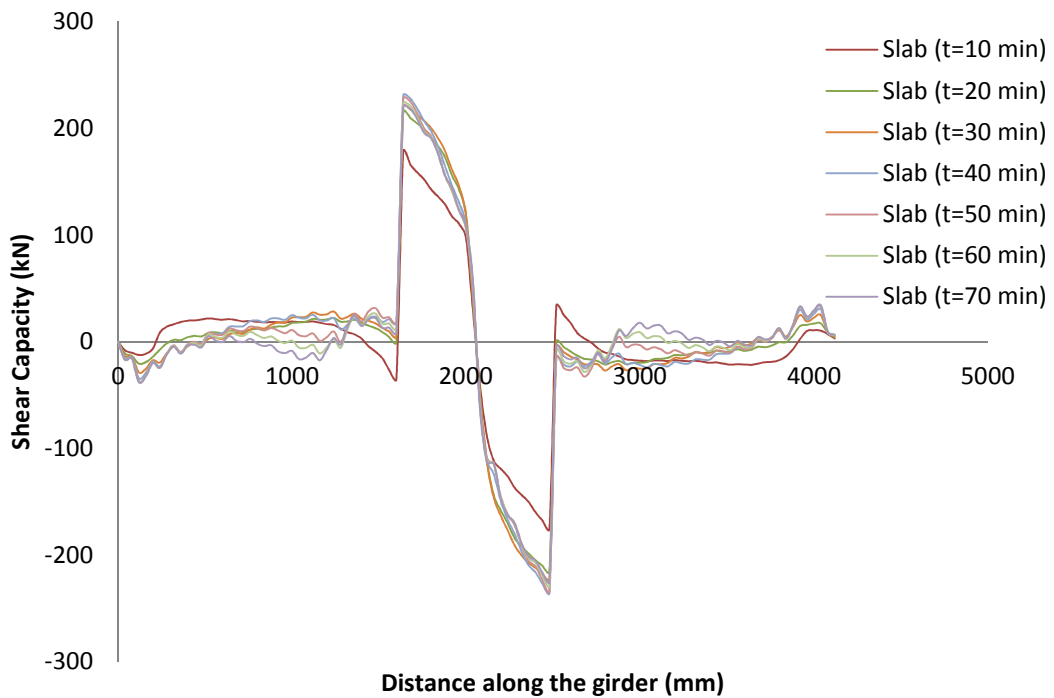
Figure 6.8 (cont'd)

(c) Composite beam (with slab thickness of 200 mm)

(a) Steel beam

(b) Concrete slab

Figure 6.9: Contribution of Steel beam and concrete slab to shear capacity during fire exposure
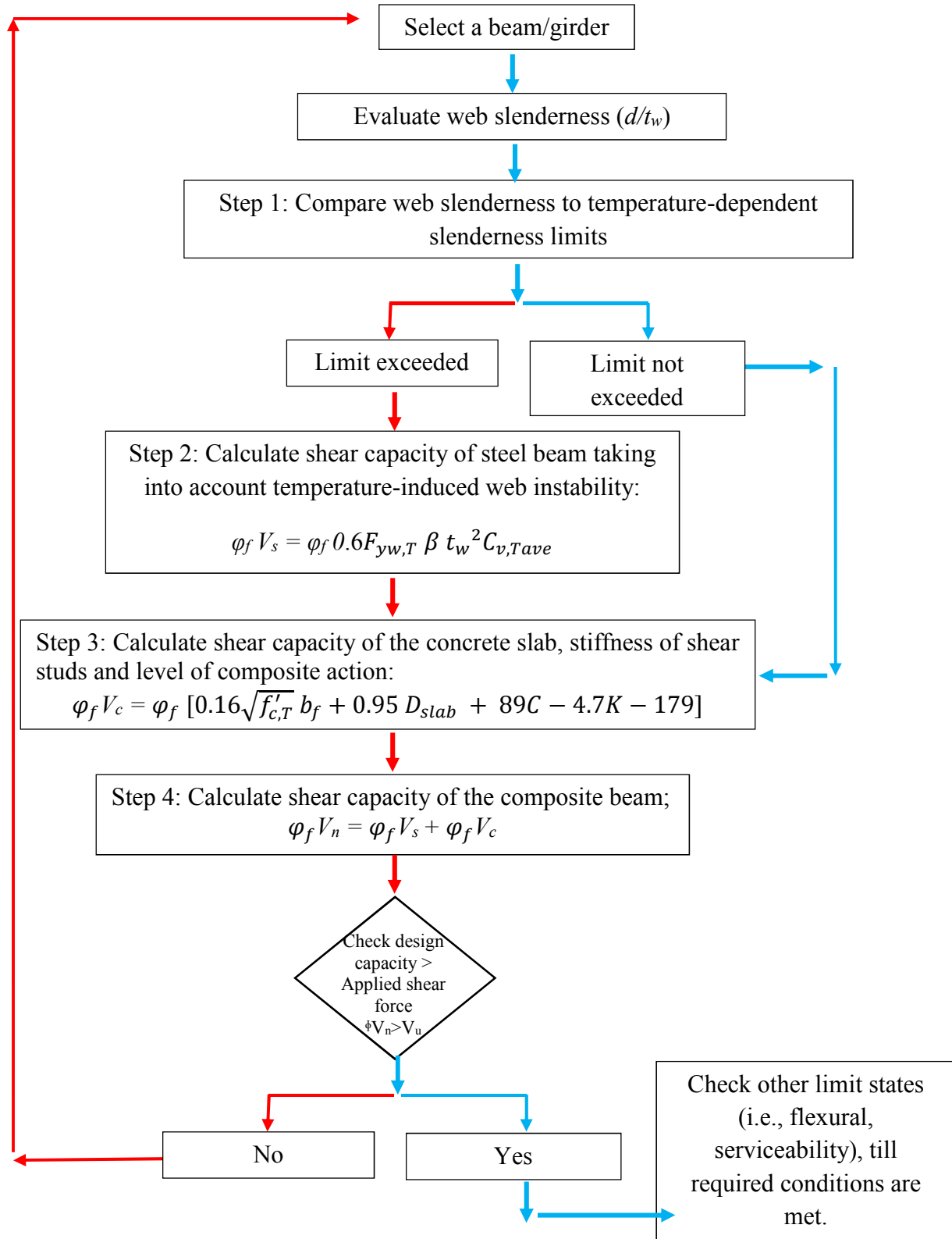
Select a beam/girder

Evaluate web slenderness (d/t_w)

Step 1: Compare web slenderness to temperature-dependent slenderness limits

Limit exceeded

Limit not exceeded

Step 2: Calculate shear capacity of steel beam taking into account temperature-induced web instability:

$$\varphi_f \, V_s = \varphi_f \, 0.6 F_{yw,T} \, \beta \, t_w{}^2 C_{v,Tave}$$

Step 3: Calculate shear capacity of the concrete slab, stiffness of shear studs and level of composite action:

$$\varphi_f V_c = \varphi_f \left[0.16\sqrt{f'_{c,T}} \, b_f + 0.95 \, D_{slab} + 89C - 4.7K - 179 \right]$$

Step 4: Calculate shear capacity of the composite beam;

$$\varphi_f V_n = \varphi_f V_s + \varphi_f V_c$$

Check design capacity > Applied shear force $\phi V_n > V_u$

No

Yes

Check other limit states (i.e., flexural, serviceability), till required conditions are met.

Figure 6.10: Flow chart for proposed methodology of calculating shear strength of steel and composite beams at fire conditions
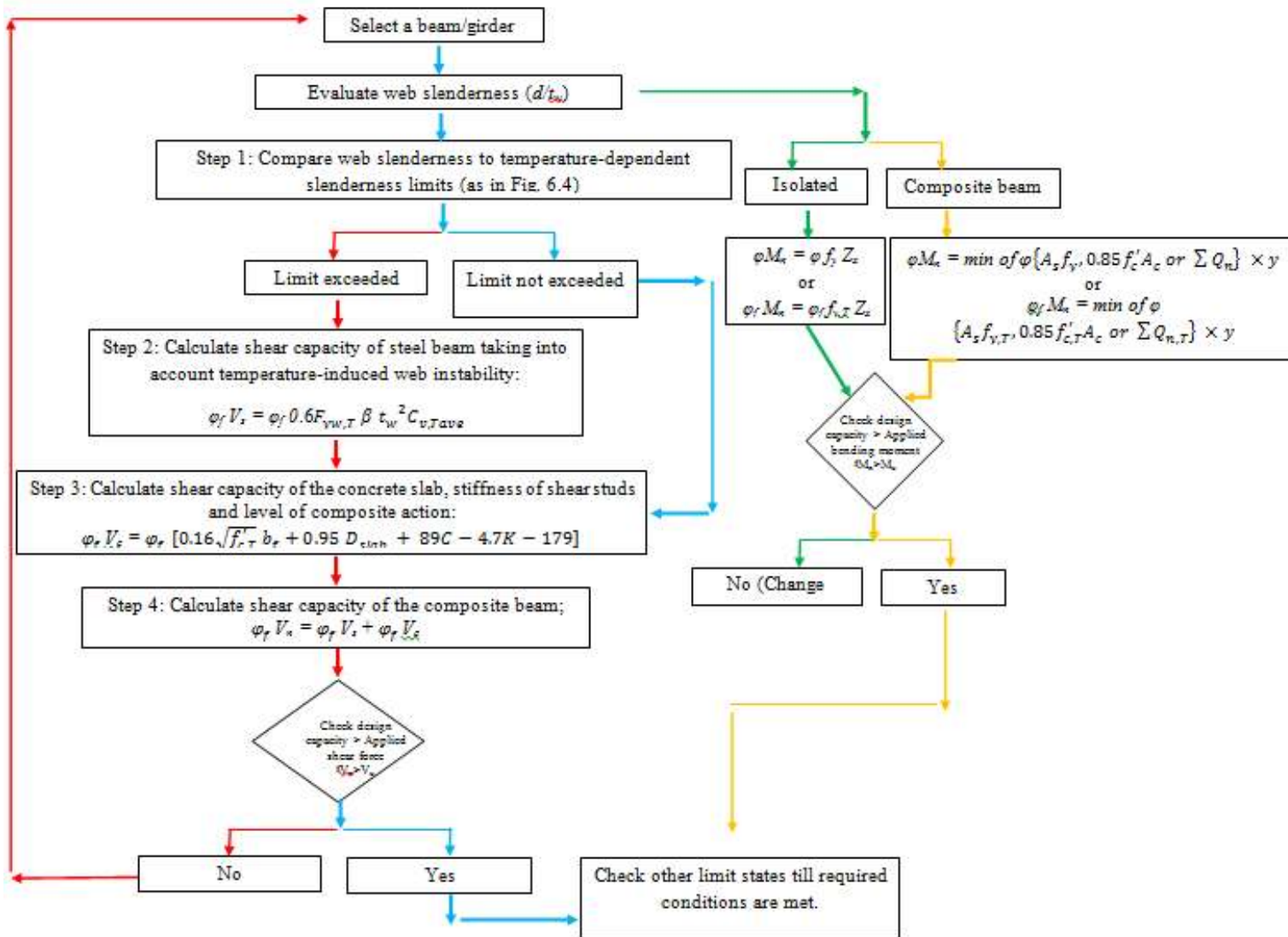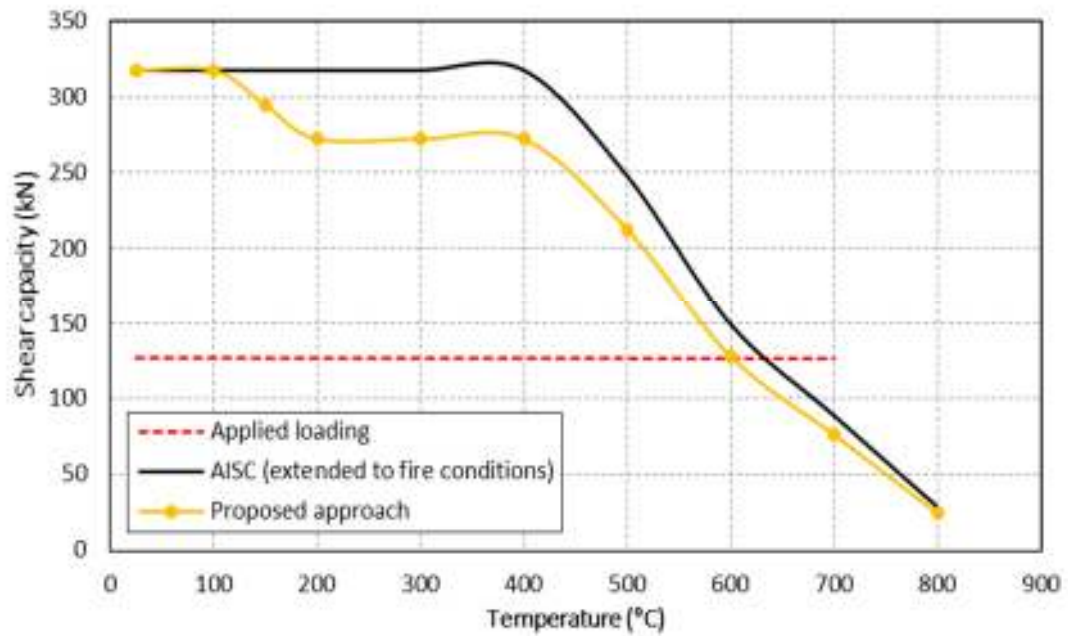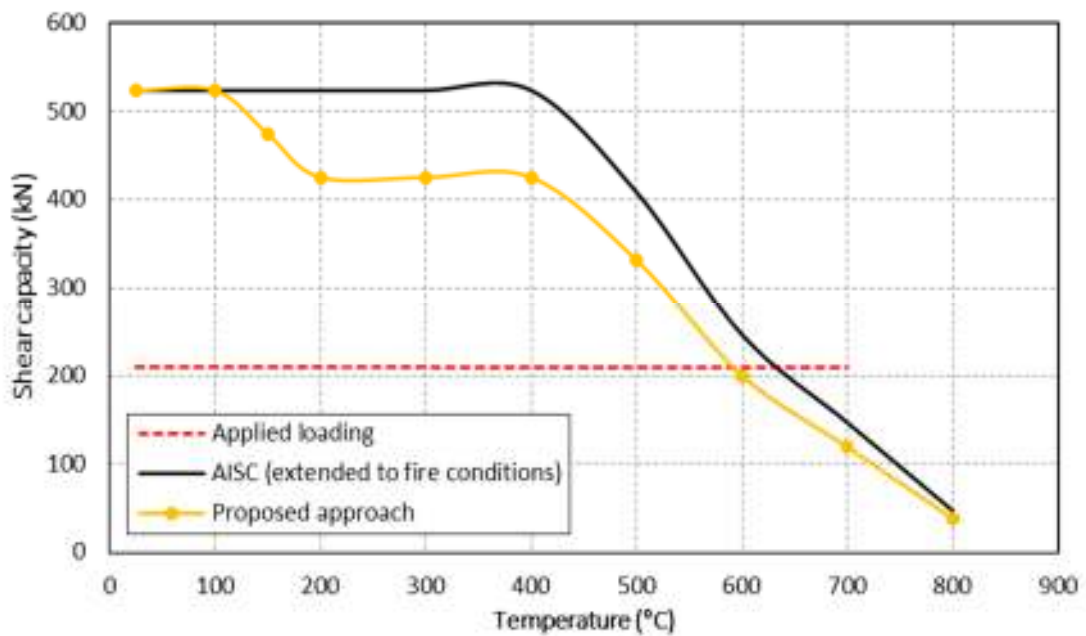
Figure 6.11: Unified approach to evaluate flexural and shear capacity in steel and composite beams
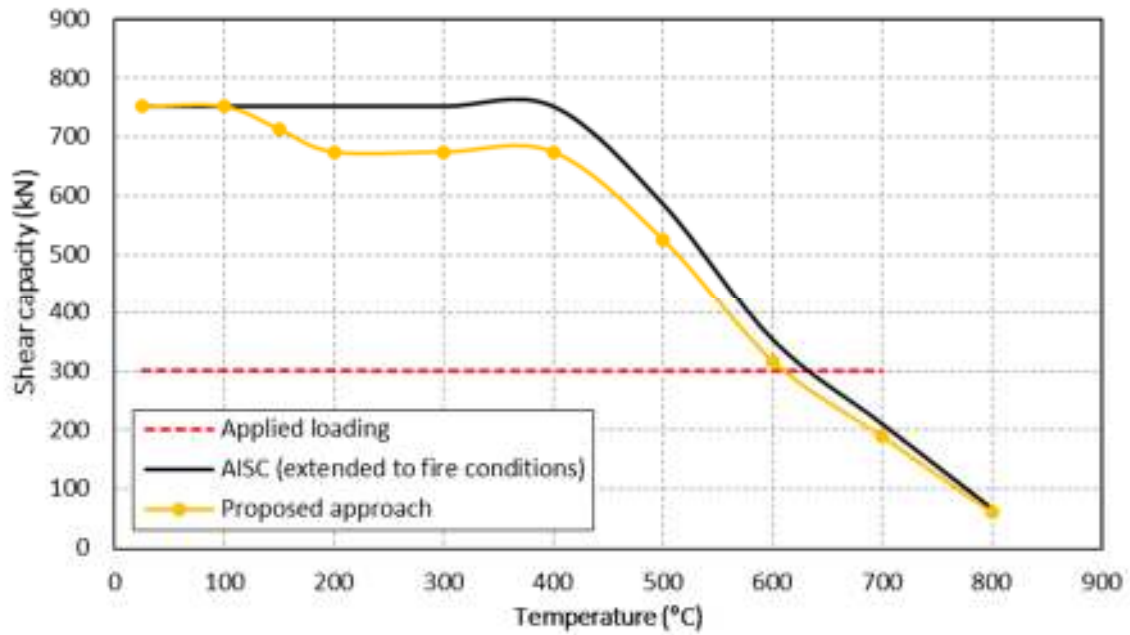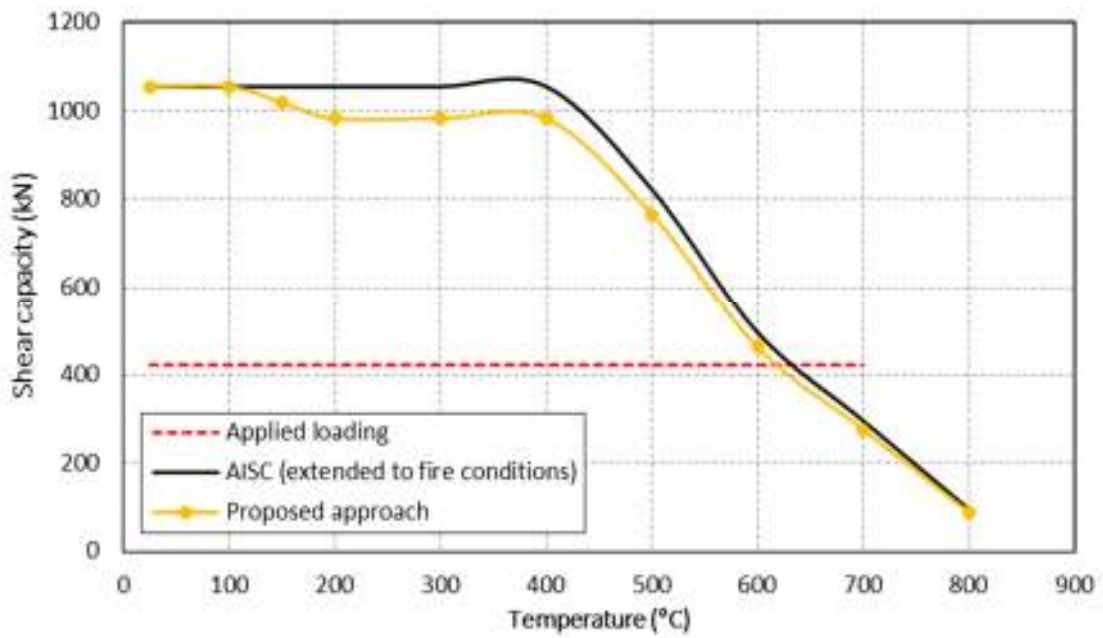
(a) W12×14

(b) W16×26

Figure 6.12: Comparison between predicted shear capacity of hot-rolled sections using proposed and AISC approaches
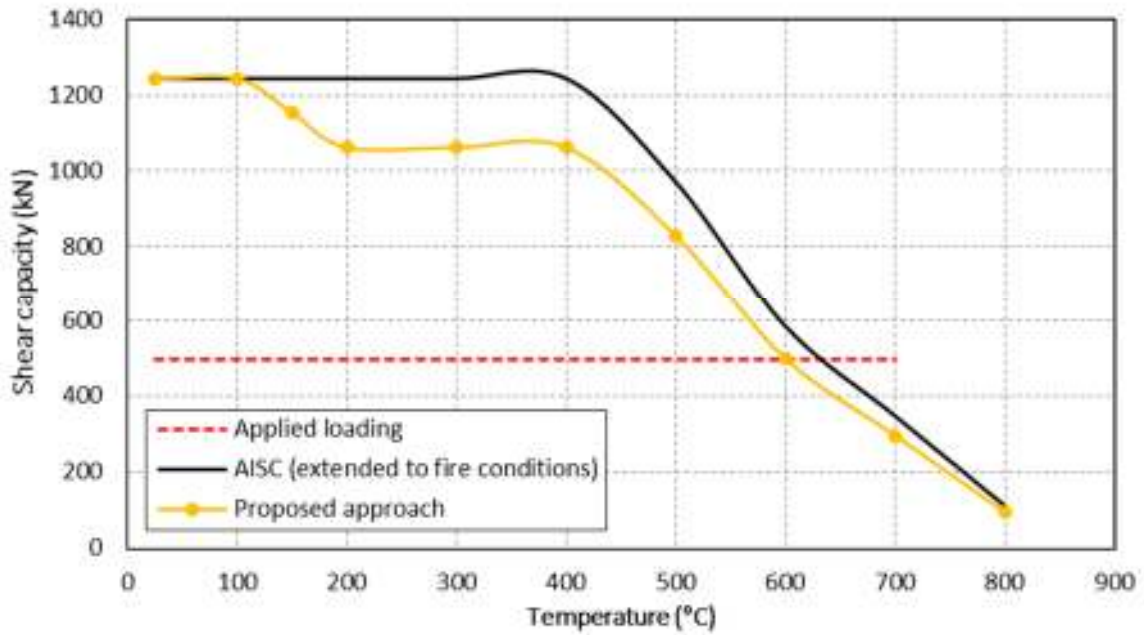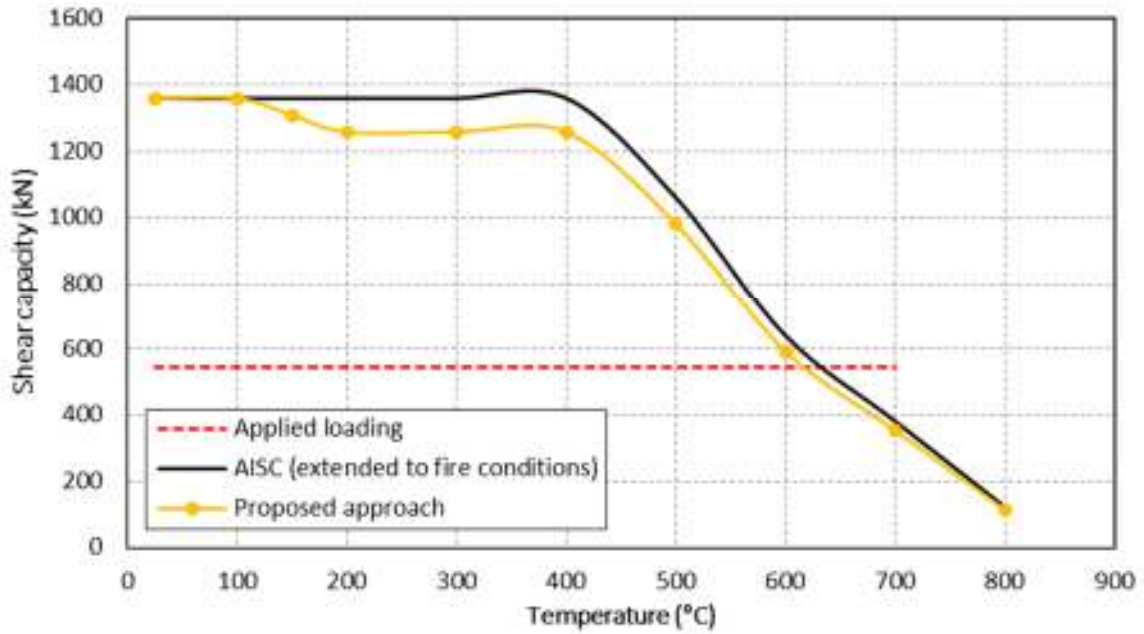
Figure 6.12 (cont'd)
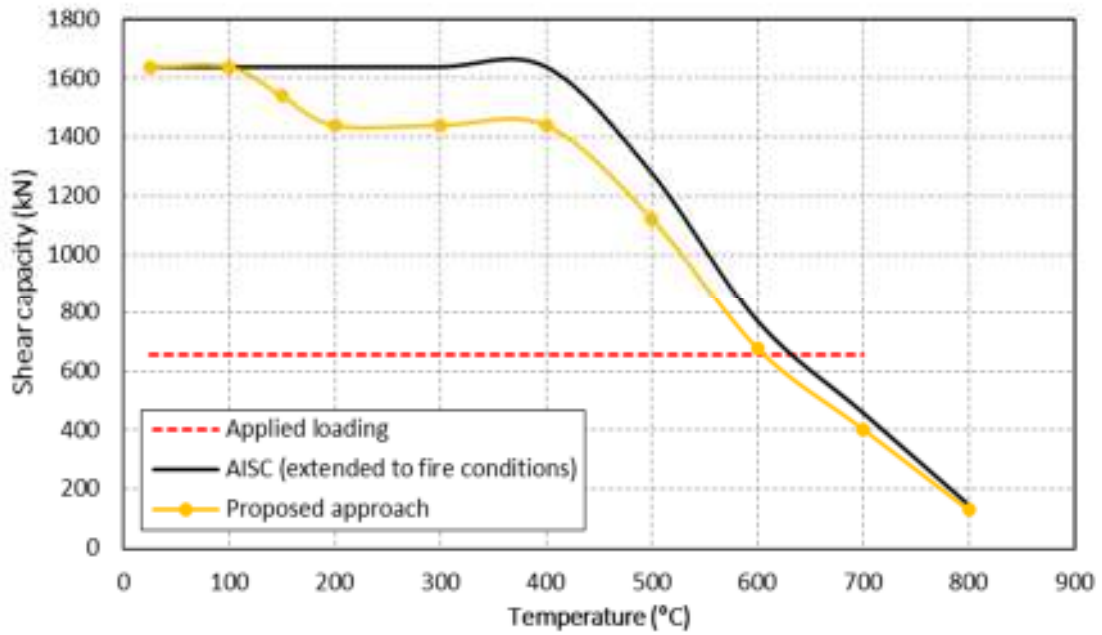

(c) W18×40

(d) W21×50

Figure 6.12 (cont'd)

(e) W24×55

(f) W24×62

Figure 6.12 (cont'd)

(g) W27×84

(h) W30×90

Figure 6.12 (cont'd)

(i) W33×130

(j) W40×167

208

(a) W12×14

(b) W16×26

Figure 6.13: Comparison between proposed approach and current design provisions

Figure 6.13 (cont'd)

(c) W18×40
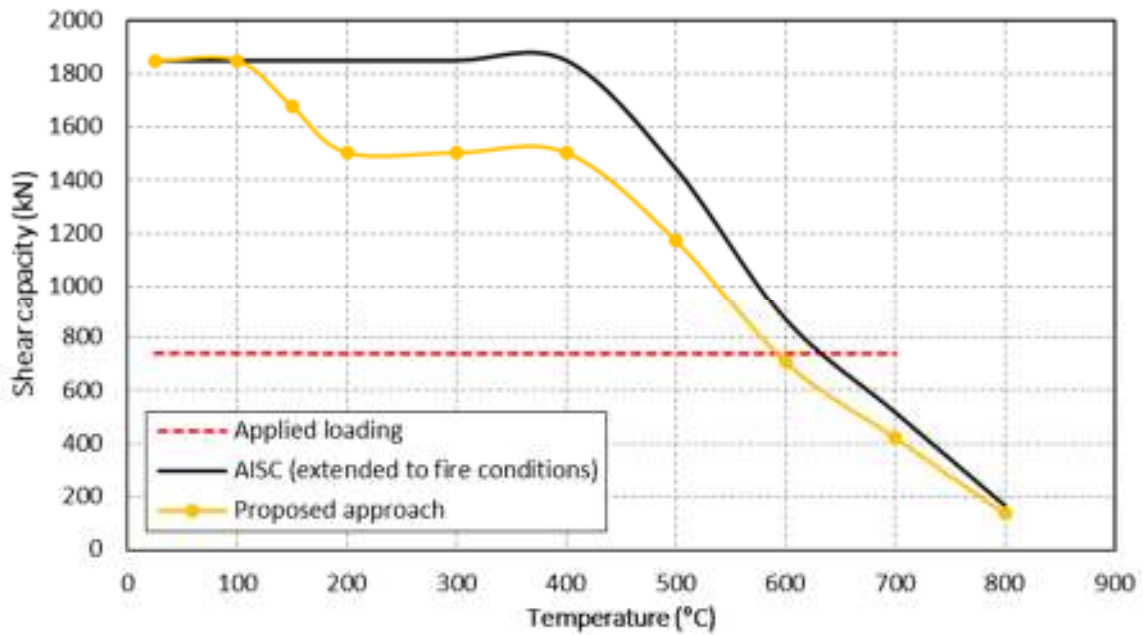

(d) W21×55

Figure 6.13 (cont'd)
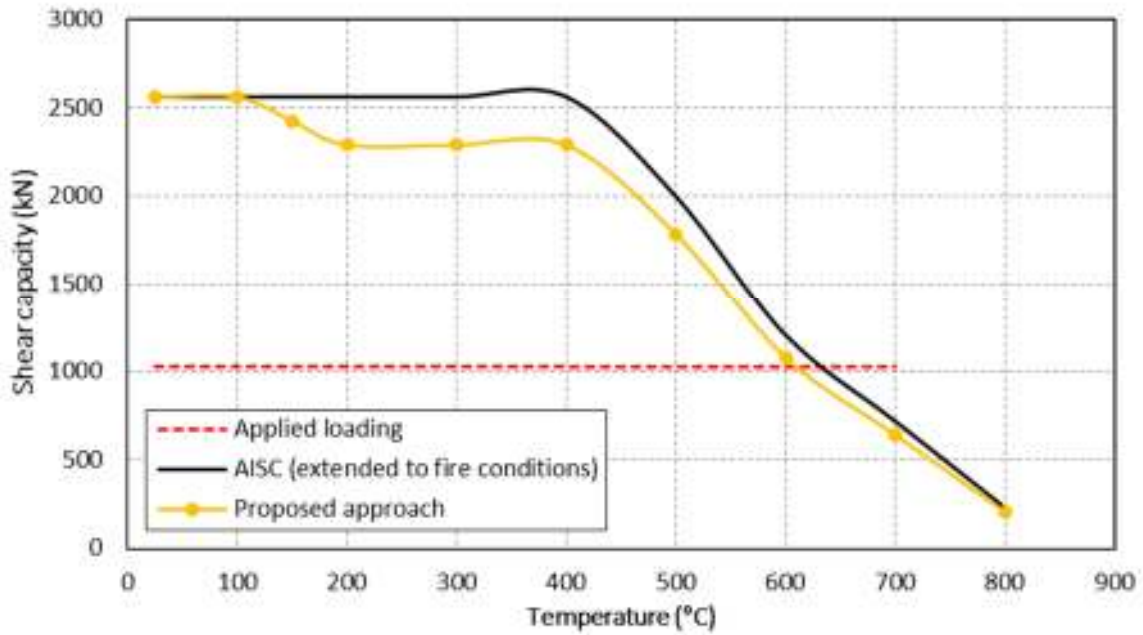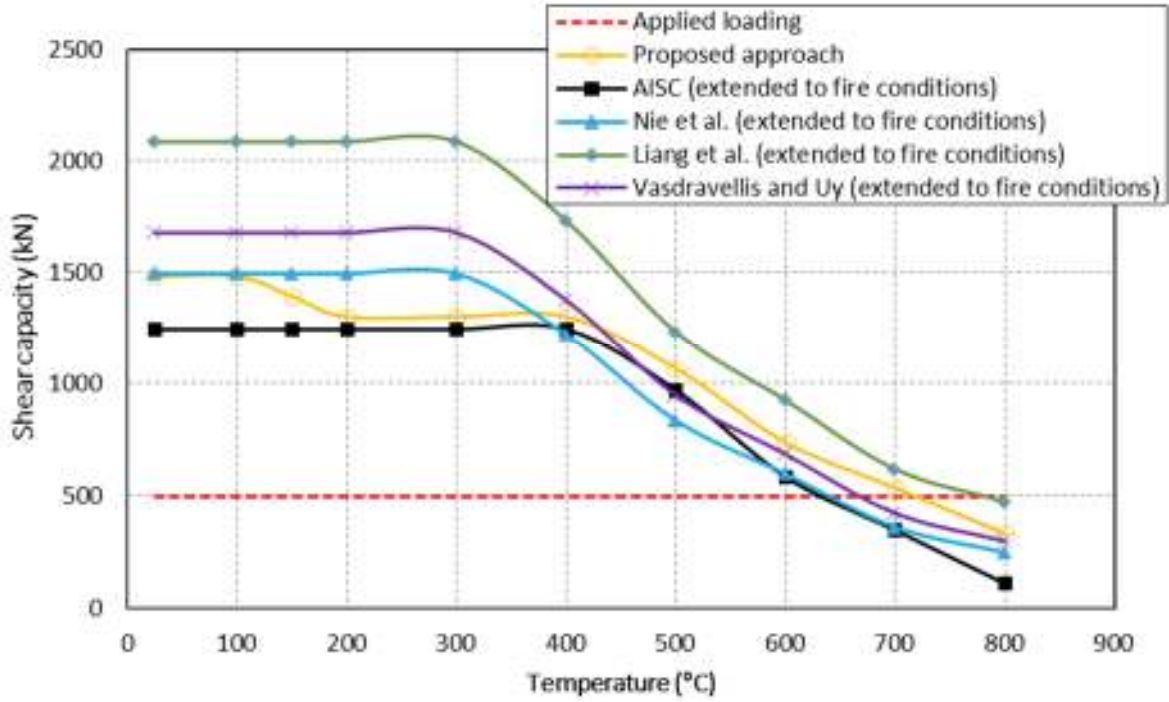

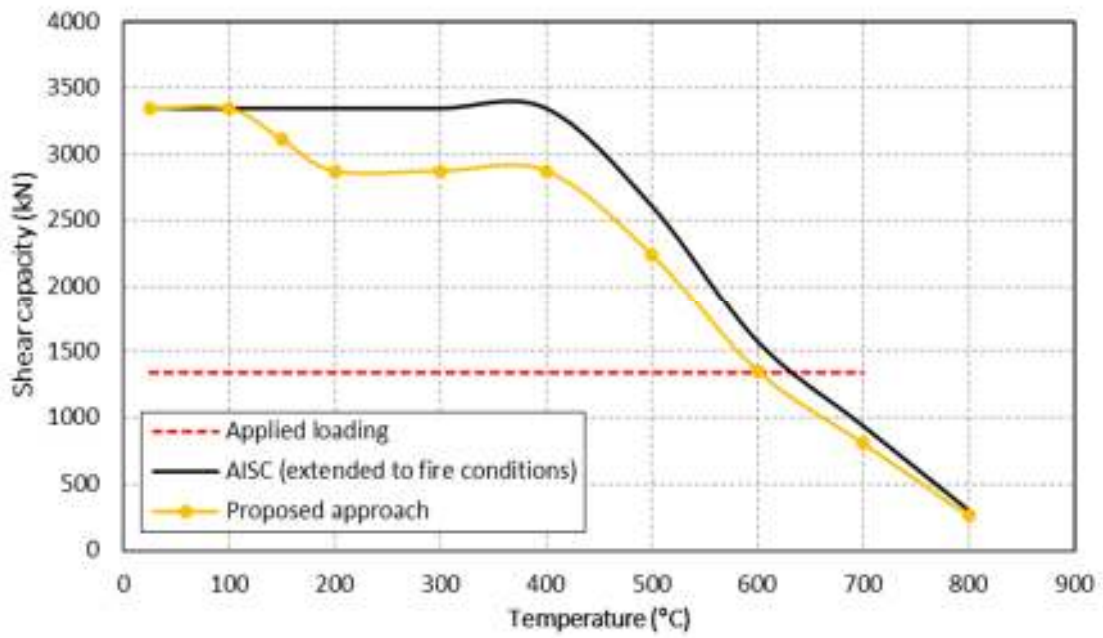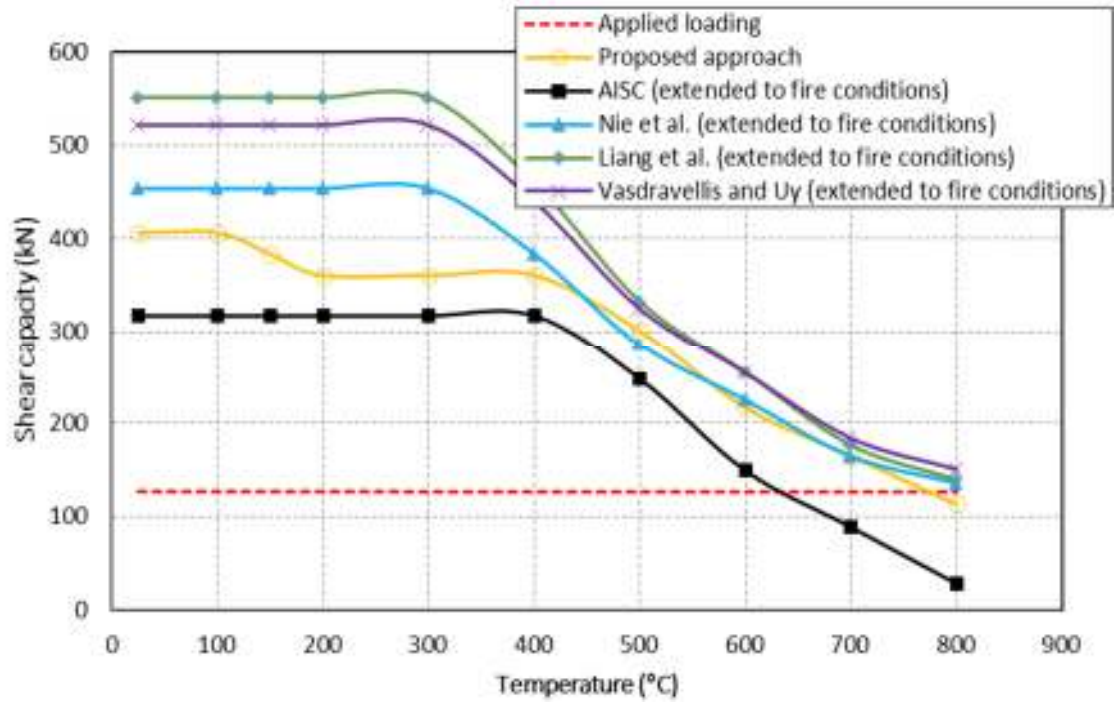(e) W24×55
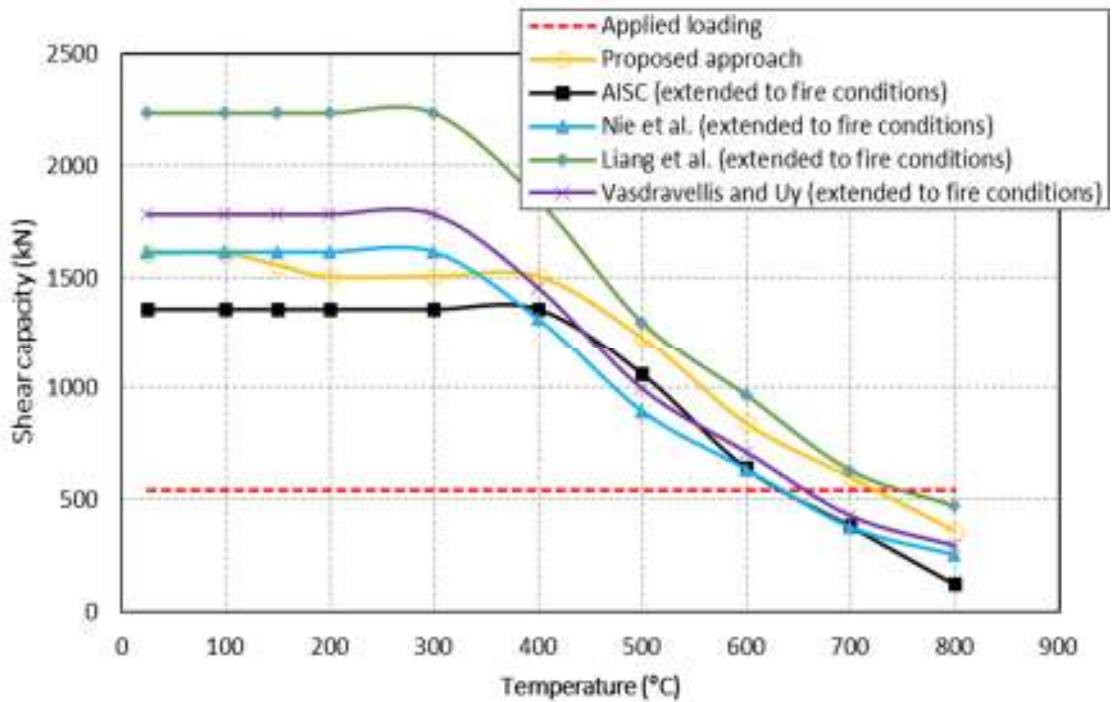
(f) W24×62

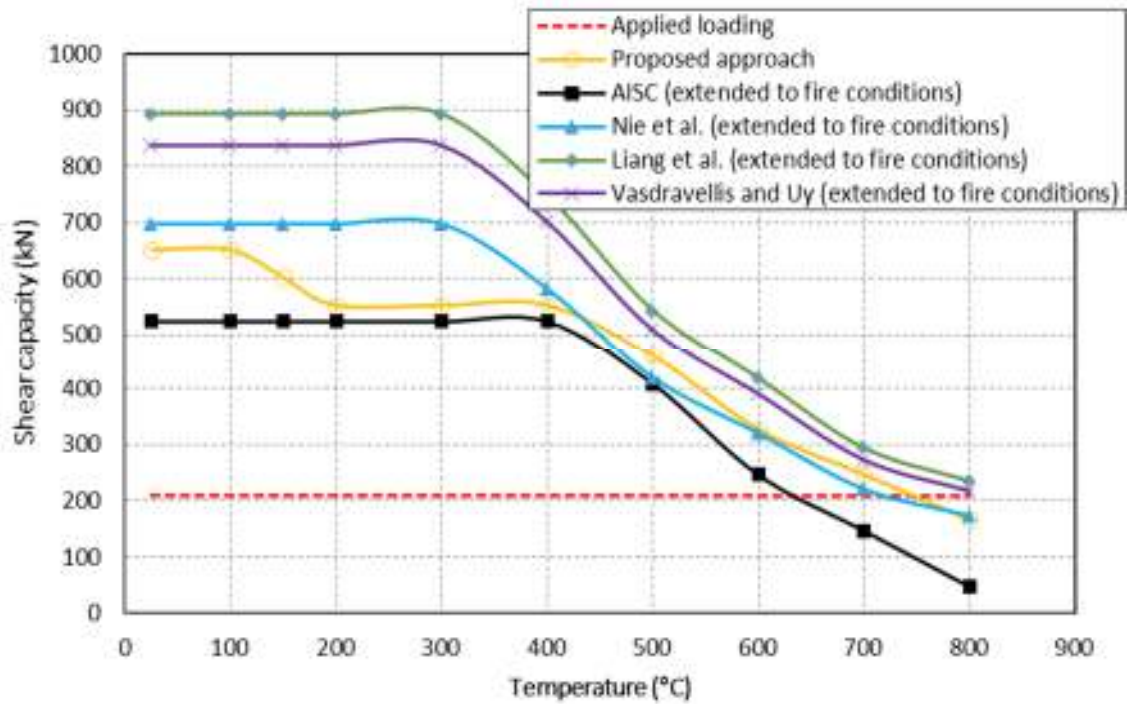Figure 6.13 (cont'd)

(g) W27×84

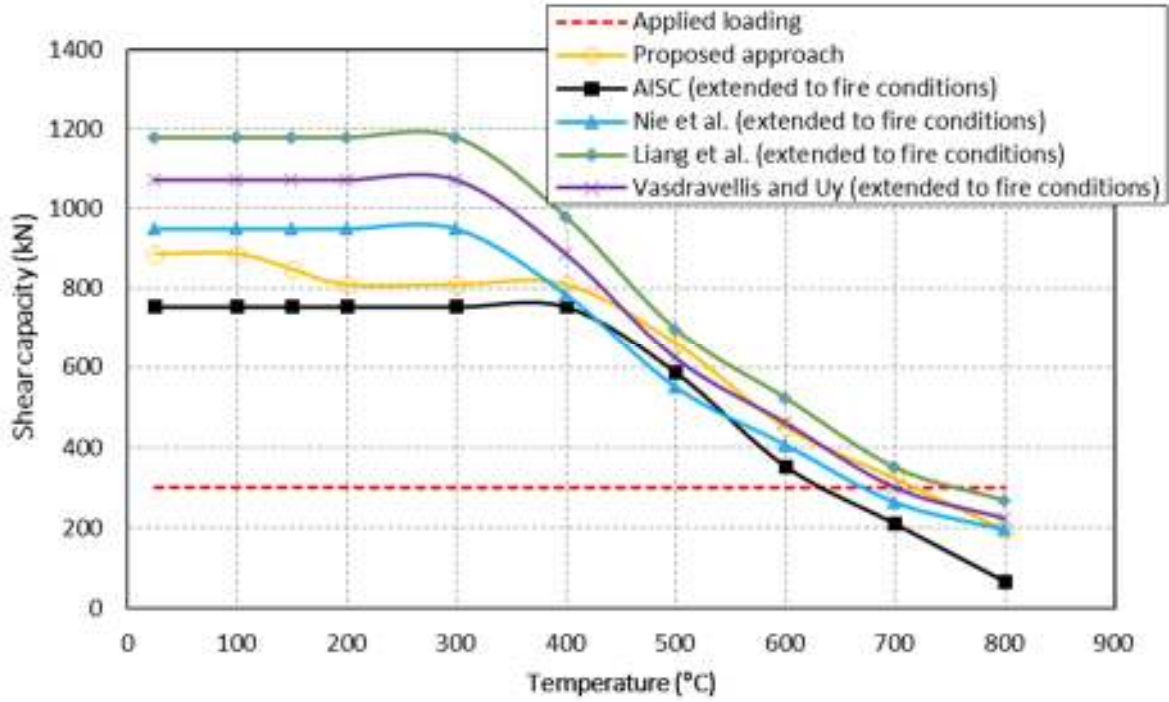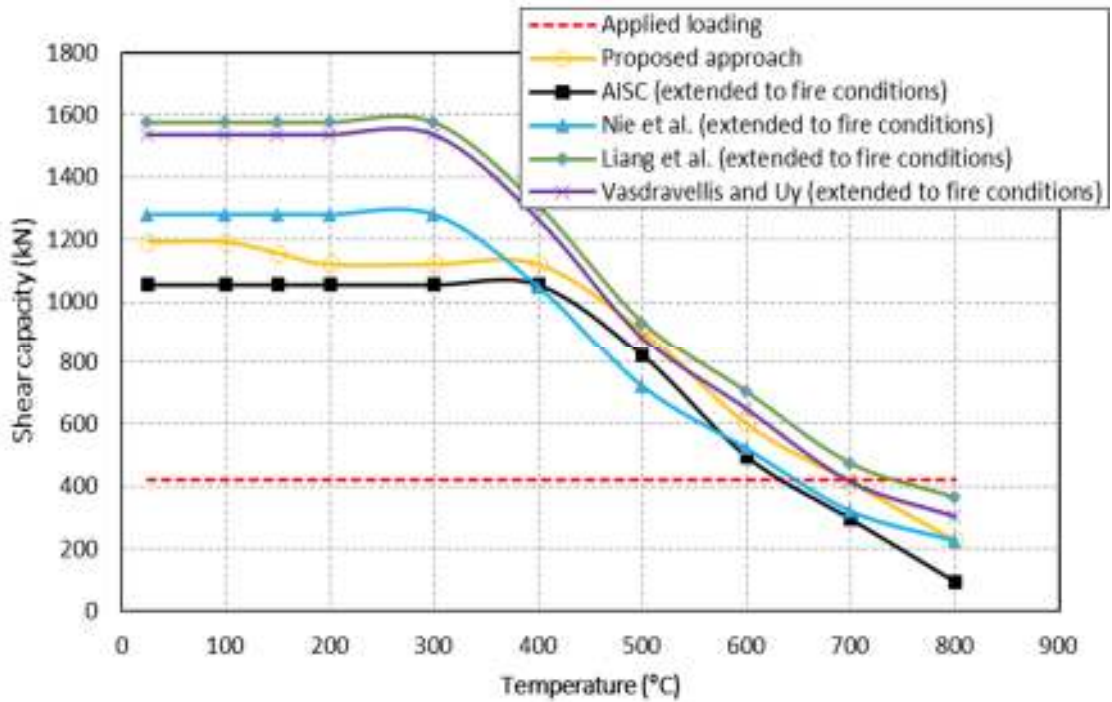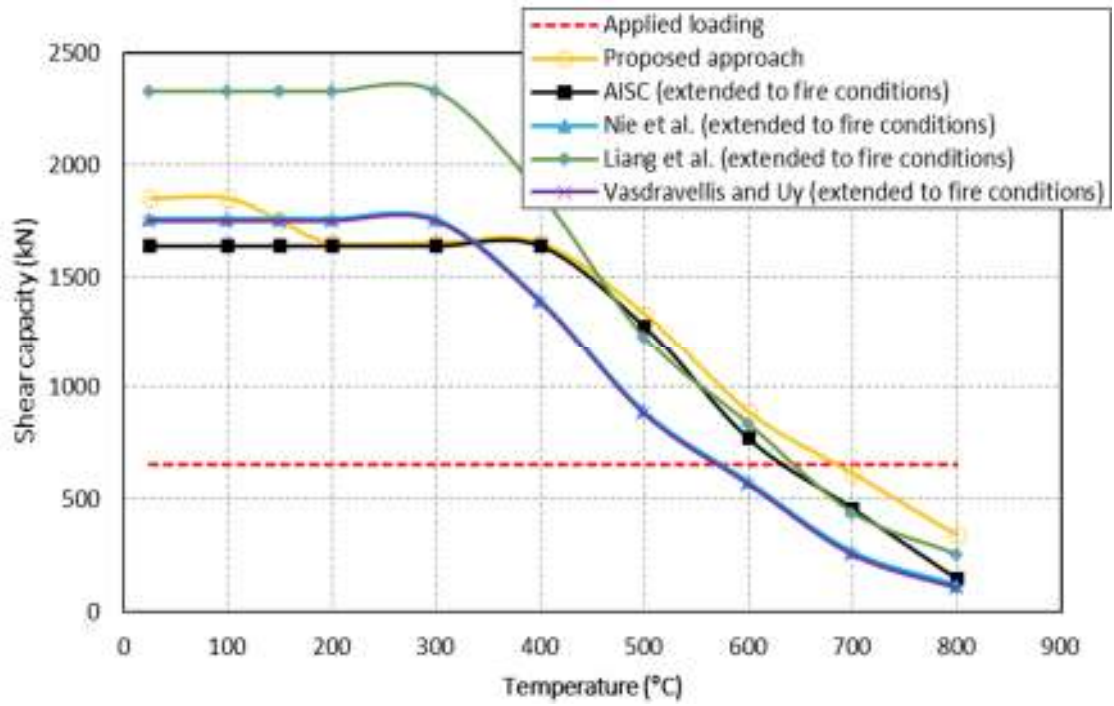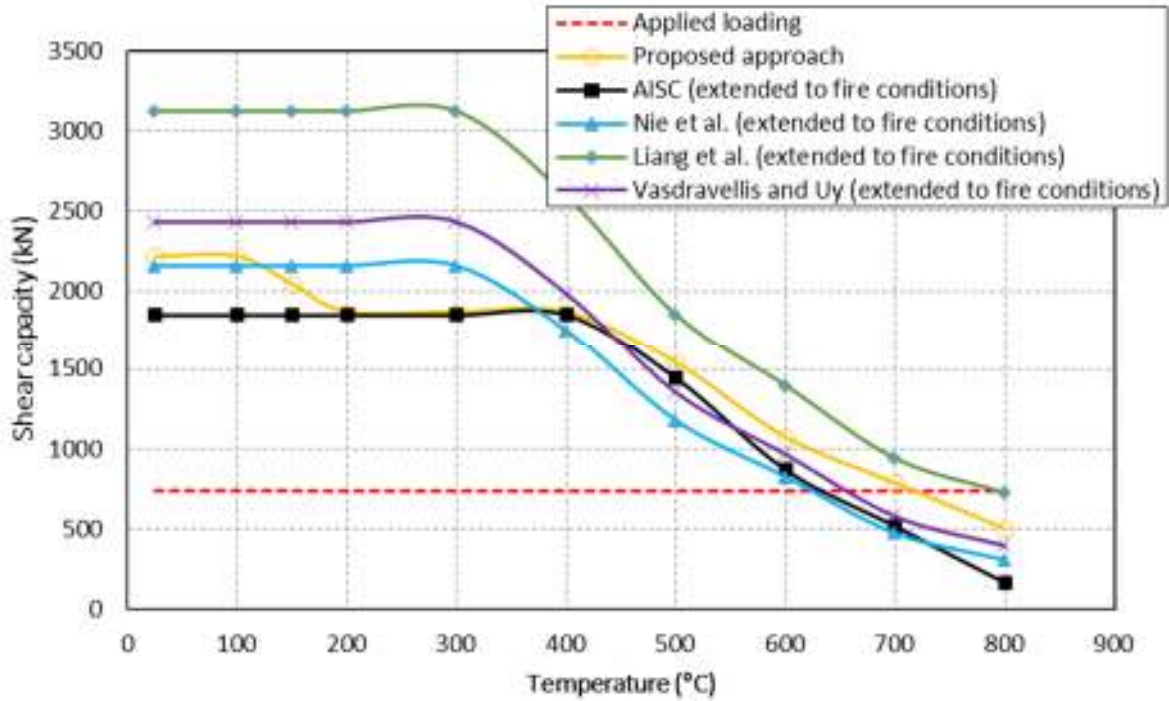

(h) W30×90

Figure 6.13 (cont'd)

(i) W33×130

(j) W40×167

213
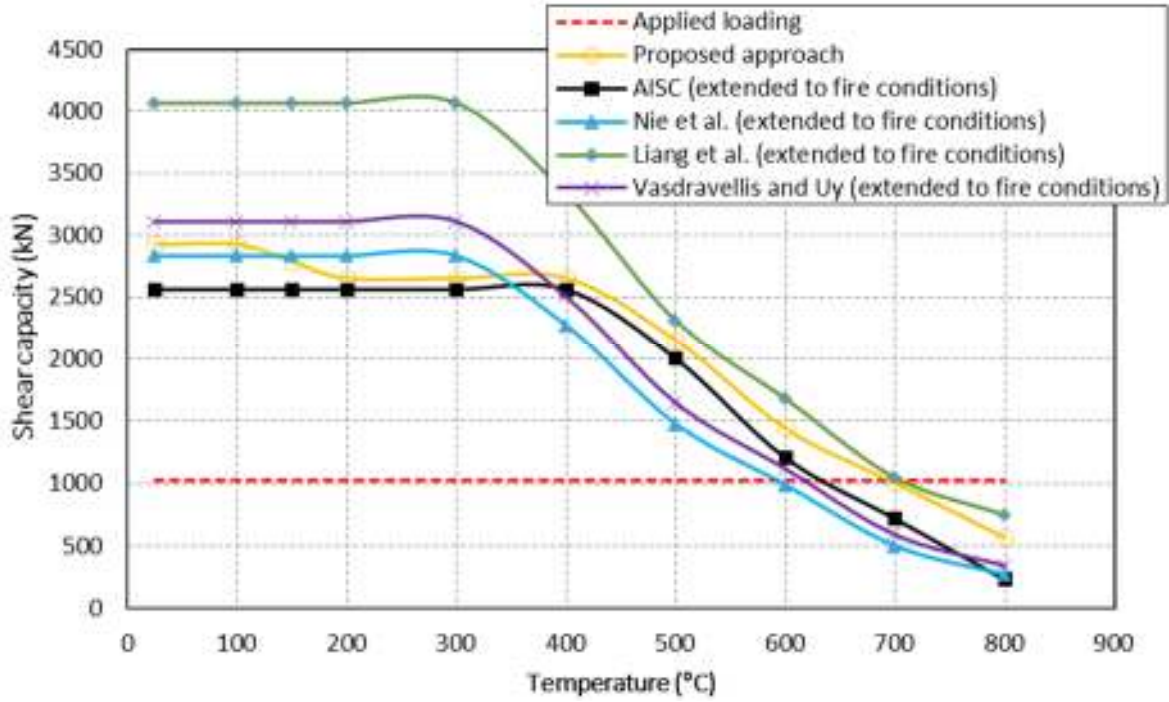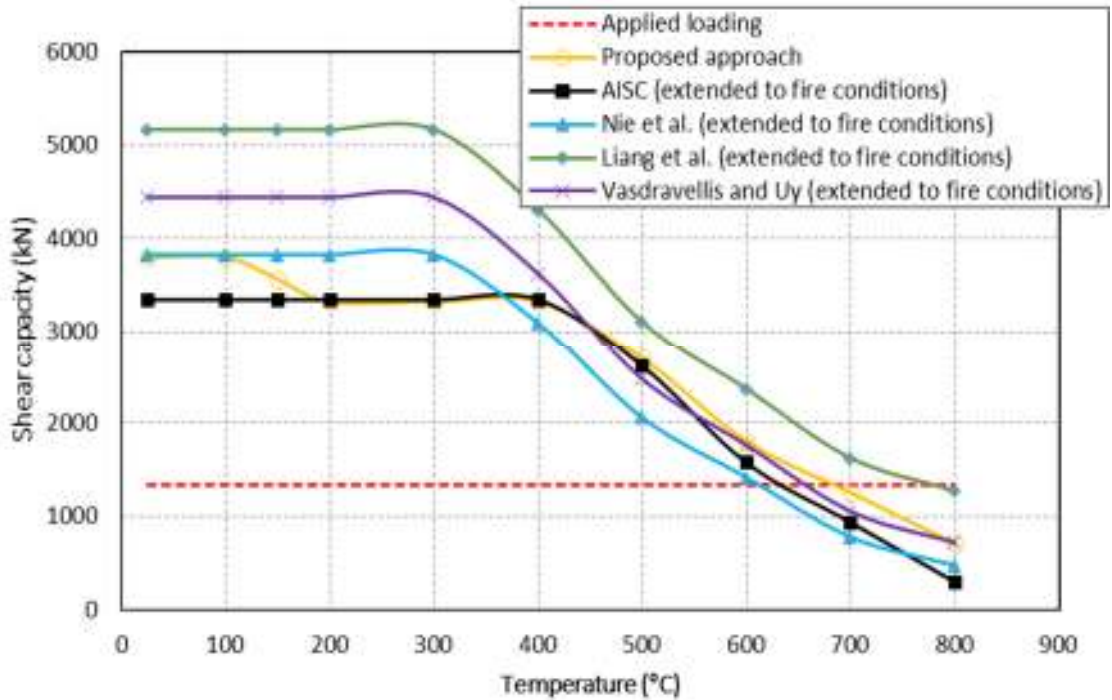
6.5 Summary

This chapter presents the development of a unified approach for evaluating flexural and shears capacity of steel and composite beams subjected to dominant shear and fire loading. This approach accounts for temperature-induced material degradation and web instability along with contribution of concrete slab to shear capacity. Through this approach, moment and shear capacity can be evaluated for steel and composite beams at any given fire exposure. The validity of the proposed approach is established by comparing moment and shear capacity as well as failure predictions with those obtained from fire tests and finite element analysis. The applicability of the proposed approach in design situations is also illustrated through a numerical example. Overall, the proposed approach provides a simple and rational method for evaluating fire response of steel and composite beams especially when subjected to high shear loading and fire exposure.

CHAPTER SEVEN

7. Conclusions and Recommendations

7.1 General

Response of steel and composite beams/girders[‡‡‡] subjected to high shear loading under fire conditions is evaluated to develop a fundamental understanding on the fire behavior of beams. As part of experimental studies, fire resistance tests were carried out on four composite beams in which the main test variables were shear loading and level of composite interaction. As part of numerical studies, a finite element model is developed to trace the response of beams under fire conditions. The developed model specifically accounts for geometric and material nonlinearities, temperature-dependent material properties, shear effect, sectional and global instability, composite action, and various failure limit states. The validity of the finite element model is established by comparing thermal and structural response parameters predicted from the analysis with measured data from fire tests. Then, this model was applied to perform a set of parametric studies on steel and composite beams at both room and under fire conditions. In these parametric studies, influence of various factors including sectional instability, web slenderness, load level, fire severity, loading configuration, level of composite action, shear stud stiffness and concrete slab thickness is studied.

Based on the results from experimental and numerical studies, an approach for evaluating shear capacity of steel and composite beams is derived. This methodology specifically accounts for property degradation of constituent materials, temperature-induced sectional instability and level of composite action offered by concrete slab in evaluating shear capacity in beams. This

---

[‡‡‡]The terms beam/girder are used interchangeably throughout this thesis.

approach is combined with flexural capacity calculations available in literature to developed a unified approach for design (and analysis) of fire-exposed beams. Predicted shear and flexural capacity of fire-exposed steel and composite beams from proposed equations are validated against measured data from fire tests, as well as predictions from current AISC design provisions. These comparisons show that the proposed unified approach design methodology leads to better fire response predictions, specifically for steel and composite beams subjected to dominant shear and fire loading.

7.2 Key Findings

Based on the information presented in this thesis, the following key conclusions can be drawn:

1. There is lack of data and understanding in the literature on the behavior of steel and composite beams under combined effects of dominant shear loading and fire exposure. In I-shaped (W-shaped) beams, temperature in slender web raises more rapidly than that in flanges. Hence, shear capacity can degrade at a higher pace than flexural capacity and this can lead to early failure of the beam under shear limiting state.

2. The degradation in shear capacity in steel and composite beams under fire conditions results not only from the effects of temperature-induced strength loss in steel, but also to temperature-induced sectional instability of web. Onset of local buckling in web can lead to significant degradation of shear capacity, which can lead to early failure under shear limiting capacity.

3. Current design philosophy of evaluating failure of beams based on flexural limit state may not be conservative in certain situations where steel and composite beams with slender webs, are subjected to high shear forces. In these scenarios, effect of shear

216

loading can dominate fire response and failure can occur under shear limit state earlier to that under flexural limit state.

4. Composite action arising from concrete slab, not only enhances sectional (shear) capacity but can minimize temperature-induced web local buckling (sectional instability) and thus influences (shear) overall response of composite beams under fire conditions.

5. The proposed finite element model is capable of tracing the response of isolated and composite beams under combined effects of structural loading and fire conditions. This model accounts for various critical parameters including material and geometrical nonlinearities, property degradation at elevated temperatures, shear effects, composite interaction between concrete slab and steel beam, and temperature-induced local buckling.

6. Results generated from experimental and numerical studies on the critical factors influencing the response of beams under fire conditions infer:

   • Steel and composite beams can experience failure in less than 30 minutes under different levels of fire severity. The fire resistance and failure mode is highly influenced by sectional instability, web slenderness, load level, fire severity, loading configuration, level of composite action, shear stud stiffness and concrete slab thickness.

   • Higher slenderness of web can lead to rapid degradation of shear capacity and at a higher pace than that of moment capacity, especially in fire-exposed steel and composite beams.

- The presence of concrete slab can enhance fire resistance of composite beams by transferring gravity load from the fire-weakened steel beam to cooler slab. Hence, the contribution of the concrete slab need to be accounted for in fire resistance analysis.

7. An approach for evaluating shear capacity of steel and composite beams is derived based on the results from experimental and numerical studies. The derived approach accounts for property degradation of constituent materials, temperature-induced sectional instability and level of composite action offered by concrete slab in evaluating shear capacity in beams.

8. The proposed unified methodology for evaluating flexural and shear capacity of fire-exposed steel and composite beams accounts for temperature-induced strength degradation, temperature-induced local buckling, as well as level of composite interaction. This methodology can be applied to evaluate fire response of wide range of steel and composite beams under fire conditions, including beams subjected to dominant shear loading where shear can be a governing limit state.

7.3 Recommendations for Future Research

While this study has developed fundamental understanding on the fire response of isolated steel and composite beams subjected to high shear loading, there is scope for further research to extend these principles to other practical situations in buildings, bridges and other infrastructure. The following are some of the key recommendations for further research in this area:

- Behavior of beams under high shear loading and fire conditions is quite complex, and these influences presented in this thesis does not cover all possible scenarios. Further

research, including fire tests and numerical modeling, on different states of shear web buckling (i.e., elastic and inelastic) and moment-shear interaction is recommended.

- In this study, the numerical analysis was carried out on an elemental level (i.e., steel and composite beams). The same principles applied here can be extended to conduct "system level" analysis in which structure is exposed to fire. More research is needed to develop better approaches and algorithms that can be used to enable feasible "system level analysis" simulations.

- The possibility of using fiber-reinforced concrete (FRC) in slabs is to be explored to evaluate beneficial contribution of FRP to enhance shear capacity in flexural and shear in composite beams.

7.4 Research Impact

Fires can pose a significant hazard to civil infrastructure. In a severe fire incident, the time to failure in steel and composite beams can be in the range of 20-45 minutes. This gives very short time for occupants to evacuate the fire-damaged structure and firefighters to tackle the fire. Such fires can cause failure of beams under different limiting states, including flexure, shear ore deflection limit state. At present, there are no specific guidelines in codes and standards to consider shear limit state. To overcome this fact, this thesis presents the derivation of an approach for evaluating shear capacity of steel and composite beams. This approach specifically accounts for property degradation of constituent materials, temperature-induced sectional instability and level of composite action offered by concrete slab in evaluating shear capacity in beams. The derived expressions can be combined with flexural capacity calculations available in literature to developed a unified approach for design (and analysis) of fire-exposed beams. The unified approach expresses shear capacity in terms of structural parameters and thus is attractive

for incorporation in codes and standards. Such a rational design approach will contribute to optimally design steel and composite beams which will contribute to reduced loss of life and property damage in fire incidents.

APPENDICES

Appendix A Calculation of flexural capacity in steel beam

Determine the flexural capacity of a W18×40 section made of Grade 50 (345 MPa) steel, at room and fire conditions (when $T = 500°C$). Assume the following parameters;

For W18×40 section,

$Z = 1280 \ mm^3$

$f_y = 345 \ MPa$

$f_{y,500°C} = 269.1 \ MPa$

Thus, the flexural capacity of W18×40 at room temperature is:

$\varphi M_n = \varphi \ M_p = \varphi \ f_y \ Z_x$

$\varphi M_n = 0.9 \times 345 \times 1280 = 397.4 \ kN.m$

Similarly, the flexural capacity of W18×40 at fire conditions (when $T = 500°C$) is:

$\varphi_f \ M_n = \varphi_f \ M_p = \varphi_f f_{y,T} \ Z_x$

$\varphi_f \ M_n = 1.0 \times 269.1 \times 1280 = 311 \ kN.m$

Figure A.1 shows degradation of moment capacity of this isolated steel beam with fire exposure time.
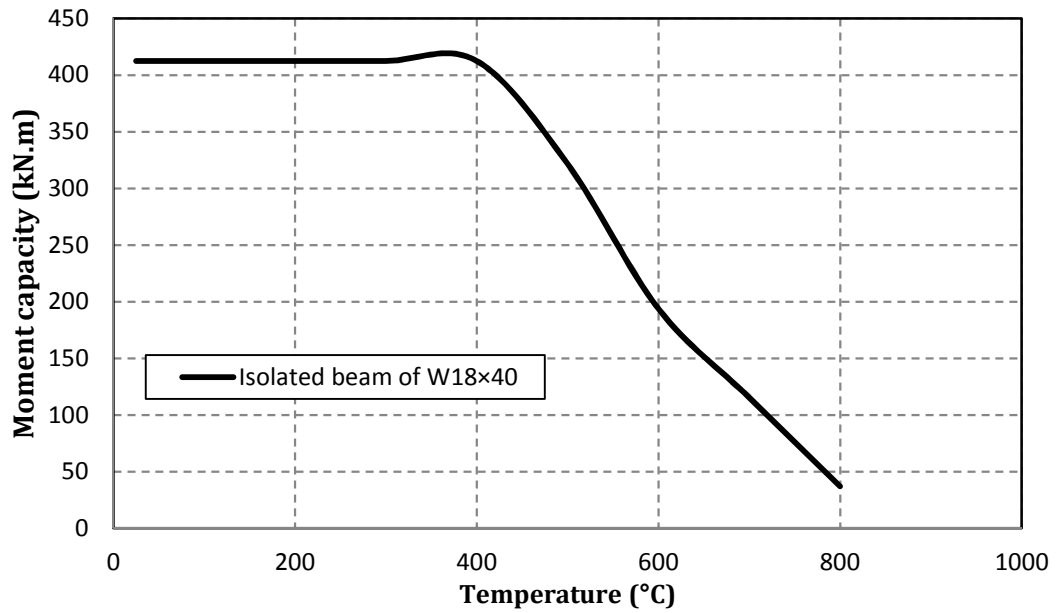
Figure A.1: Degradation of flexural capacity in steel beam of W18×40 section under fire exposure

Appendix B Calculation of flexural capacity in composite beam

Determine the flexural capacity of a W18×40 steel beam made of Grade 345 MPa and connected to a concrete slab made of concrete strength of 27.5 MPa and has a width and thickness of 1320 and 123 mm, respectively. In order to provide this composite beam with full composite action, twenty-four shear studs of 18.4 mm diameter and strength of 450 MPa are installed. Assume the following parameters;

For W18×40 section,	For concrete slab,	For shear studs,
$Z = 1280\ mm^3$	$b = 1320\ mm$	$D = 18.4\ mm$
$f_y = 345\ MPa$	$d = 123\ mm$	$F_u = 450\ MPa$
$f_{y,500°C} = 269.1\ MPa$	$f_c = 27.5\ MPa$	

In this composite beam;

- $0.85 f_c' A_c = 4076\ kN$

- $A_s f_y = 2691\ kN$

- $\sum Q_n = 2781\ kN$

It is clear that steel beam $(A_s f_y)$ controls the design of this section and the neutral axis lies within the slab (at room temperature). Thus, the flexural capacity of this composite beam can be evaluated by:

$$\varphi\,M_n = min\ of\ \varphi\{A_s f_y, 0.85 f_c' A_c\ or\ \sum Q_n\} \times y$$

$$\varphi\,M_n = 0.9 \times 2691 \times 279 = 675.8\ kN.m$$

Similarly, when steel beam temperature reaches 500°C, the average rise in concrete slab and shear stud is much lower than their critical temperature (of 400°C). Thus,

- $0.85 f'_{c,500°C} A_c = 4076 \ kN$

- $A_s f_{y,500°C} = 2043 \ kN$

- $\sum Q_{n,500°C} = 2781 \ kN$

Again, steel beam $(A_s f_{y,500°C})$ controls the design of this section and the neutral axis needs to shift upward to account for degradation in steel strength. Thus,

$$\varphi_f M_n = min \ of \ \varphi \left\{ A_s f_{y,T}, 0.85 f'_{c,T} A_c \ or \ \sum Q_{n,T} \right\} \times y$$

$$\varphi_f M_{n,500°C,} = 1.0 \times 2043 \times 288 = 610 \ kN.m$$

Figure B.1 shows degradation of moment capacity of this composite beam with fire exposure time. It is clear that this composite beam has larger flexural capacity than that of an isolated steel beam of W18×40.
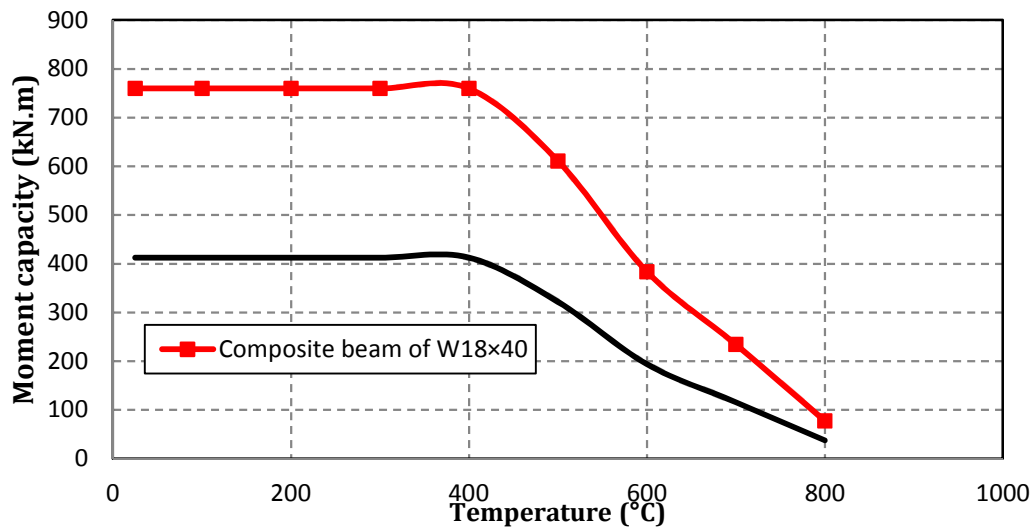

Figure B.1: Degradation of flexural capacity in isolated and composite beam of W18×40 section under fire exposure

225

REFERENCES

REFERENCES

1. American concrete institute (ACI) 318-99 (2011) building code requirements for structural concrete.

2. AISC (2011). "Steel Construction Manual." 14th Edition. American Institute of Steel Construction, Chicago, Illinois.

3. Alexander A., Clifford L., Bala T. (2009). "Experimental Investigation of the Ultimate Shear Resistance of End Web Panels in Steel Girder Bridges." Canadian Journal of Civil Engineering, vol. 36(2): pp. 267-279.

4. Alinia M., Shakiba M., Habashi, H. (2009). "Shear Failure Characteristics of Steel Plate Girders." Journal of Thin-Walled Structures, vol. 47: pp. 1498-1506.

5. Basler K., Yen B.T., Mueller J.A., Thürlimann B. (1960). "Web buckling tests on welded plate girders." Fritz Engineering Laboratory, Lehigh University, Bethlehem, Pennsylvania. Lehigh University Institute of Research, Report No. 251-11.

6. Reis, A., Lopes, N., Vila Real, P., (2016). "Numerical study of steel plate girders under shear loading at elevated temperatures." Journal of Constructional Steel Research, 117, pp. 1-12

7. ANSYS. ANSYS metaphysics. Version 14.5 ANSYS Inc. Canonsburg, PA, USA, 2013.

8. ASCE-07 (2005). "Minimum Design Loads for Buildings and Other Structures." American Society of Civil Engineers, Reston, VA.

9. ASTM E119a (2008). "Standard Methods of Fire Test of Building Construction and Materials." American Society for Testing and Materials, West Conshohocken, PA.

10. ASTM-A6/A6M. (2011). Standard specification for general requirements for rolled structural steel bars, plates, shapes, and sheet piling. American Society for Testing and Materials, West Conshohocken, PA

11. Aziz E.M., Kodur V.K.R., Glassman J. D., Garlock M.E.M. (2015) "Behavior of steel bridge girders under fire conditions". Journal of Constructional Steel Research, volume 106: pp. 11-22.

12. Bailey, C.G., Lennon, T., Moore, D.B. (1999). "The Behaviour of Full-Scale Steel-Framed Buildings Subjected to Compartment Fires." The Structural Engineering, vol. 77(8): pp. 15-21.

13. Bajwa, C.S., Easton, E.P., Adkins, H., Cuta, J., Klymyshyn, N., Suffield, S., "The MacArthur Maze fire and roadway collapse: a 'worst case scenario' for spent nuclear fuel

transportation?" in: Proceedings of the ASME 2012 Pressure Vessels & Piping Division Conference, Toronto, Ontario, Canada, 2012.

14. Bletzacker, R.W. (1966). "Effect of Structural Restraint on the Fire Resistance of Protected Steel Beam Floor and Roof Assemblies." Final Report. EES 246/266. Ohio State University, Columbus, Ohio.

15. British standard (1990). "BS-5950, Structural Use of Steelwork in Building." Part 8, Code of practice for fire resistant design.

16. British standard (1992). "BS-5950, Structural Use of Steelwork in Building." Part 2, Specification for materials, fabrication and erection: hot rolled sections.

17. BS 476-3:1987 (1987). "Fire Tests on Building Materials and Structures – Part 20: Method for Determination of the Fire Resistance of Elements of Construction (General Principles)." BSi, UK.

18. Chapman J.C., Balakrishnan S. (1964). "Experiments on Composite Beams". The Structural Engineering, vol. 42(11): pp. 369–83.

19. Comite Euro-International du Beton (CEB-FIP). CEB-FIP model code 1990. Bulletin D'Information No. 213/214 (Concrete Structures), Lausanne, Switzerland; 1993.

20. Dharma. R.B., Tan, K. (2007). "Rotational capacity of steel W-shape under fire conditions Part II: Numerical simulations." Engineering Structures 29, pp. 2403-2418.

21. Dwaikat, M.M.S and Kodur, V.K.R. (2010). "A Simplified Approach for Evaluating Plastic Axial and Moment Capacity Curves for Beam-Columns with Non-uniform Thermal Gradients." Journal of Engineering Structures, vol. 32(5): pp. 1423-1436.

22. EC1 (2002). "EN 1991-1-2: Actions on Structures. Part 1-2: General Actions - Actions on Structures Exposed to Fire", European Committee for Standardization, Brussels, Belgium.

23. EC2 (2004). "EN 1992-1-2: Design of Concrete Structures. Part1-2: General Rules-Structural Fire Design." European Committee for Standardization, Brussels, Belgium.

24. EC3 (2005). "EN 1993-1-2: Design of Steel Structures. Part 1-2: General Rules - Structural Fire Design." European Committee for Standardization, Brussels, Belgium.

25. EC4 (2003). "EN 1994-1-2: Design of Composite Steel and Concrete Structures. Part1-2: General Rules-Structural Fire Design." European Committee for Standardization, Brussels, Belgium.

26. Eldukair, A., Ayyub, B., (1991). "Analysis of recent U.S. structural and construction failures." J. Perform. Constr. Facil. Pp. 57-73.

27. "Experts Debate Future of the Skyscraper in Wake of Disaster". Engineering News-Record. September 24, 2001.

28. FEMA 403, World Trade Center Building Performance Study. (2002)

29. Fike R, and Kodur V.K.R. (2011). "Enhancing Fire Resistance of Composite Beam-Slab Assemblies Through Steel Fiber Reinforced Concrete." Journal of Engineering Structures, vol. 33(10): pp. 2870-2878.

30. Franssen J., Kodur V.K.R., Zaharia R. (2009). "Designing Steel Structures for Fire Safety." Taylor & Francis Group, London, UK.

31. Garlock, M., Payá-Zaforteza, I. , Kodur, V., Gu, L., (2012). "Fire Hazard in Bridges: Review, Assessment and Repair Strategies", Engineering Structures, Elsevier, V. 35, p. 89-98.

32. Glassman, J.D., Garlock, M.E.M., Aziz, E., Kodur, V. (2016). "Modeling parameters for predicting the postbuckling shear strength of steel plate girders." Journal of Constructional Steel Research 121, pp.136–143.

33. Gillie, M., Usmani, A., Rotter, M., O'Connor, M. (2001). "Modelling of heated composite floor slabs with reference to the Cardington experiments." Fire Safety Journal 36, pp. 745-767

34. Herzog, M.A., (1989). "Design formulas for unstiffened and stiffened plate girders in shear." J Struct Eng, 115: 2740–52.

35. Huber, M.T. (1904) Czasopismo Techniczne, Lemberg, Austria, Vol. 22, pp. 181.

36. Huang Z., Burgess I.W., Plank R.J. (1999). "The Influence of Shear Connectors on the Behaviour of Composite Steel-Framed Buildings in Fire." Journal of Constructional Steel Research, vol. 51: pp. 219–237.

37. IBC, (2015), "International Building Code." International Code Council, Inc. (ICC), Falls church, VA.

38. ISO, Fire Resistance Tests, Elements of Building Construction. ISO 834. International Organization for Standardization, Geneva, 1975.

39. Karter, M. (2012). "Fire loss in the United States during 2011". National Fire Protection Association.

40. Klasson, A., Crocetti, R., Hansson, E., (2016). "Slender steel columns: How they are affected by imperfections and bracing stiffness." Structures, pp. 35-43

41. Kirby B.R., Lapwood D.G., Thomson G. (1986). "The Reinstatement of Fire Damaged Steel and Iron Framed Structures." ISBN 900206 46 2, B.S.C, Swiden Laboratories. London.

42. Kirby B.R. British Steel data on the Cardington fire tests. Technical report, British Steel, 2000.

43. Kodur, V.K.R., Aziz, E.M., Dwaikat, M.M.S. (2013). "Evaluating Fire Resistance of Steel Girders in Bridges." ASCE Journal of Bridge Engineering, vol. 18: pp. 633-643.

44. Kodur, VKR, Fike, RS., (2009). "Guidelines for improving the standard fire resistance test specifications." Journal of ASTM International 2009;6:1-16.

45. Kodur V.K.R., Naser M.Z. (2013). "Importance Factor for Design of Bridges Against Fire." Engineering Structures, Vol. 54, pp. 207-220.

46. Kodur V., Naser M., Pakala P., Varma A. (2013). "Modeling the Response of Composite Beam-Slab Assemblies Exposed to Fire." Journal of Constructional Steel Research, Vol. 80, pp. 163–173.

47. Lamont, S., Gillie, M., Usmani, A.S. (2007). "Composite steel-framed structures in fire with protected and unprotected edge beams." Journal of Constructional Steel Research, 63, pp. 1138-1150.

48. Liang, Q., Uy, B., Bradford, M., Ronagh, H., (2005), "Strength Analysis of Steel–Concrete Composite Beams in Combined Bending and Shear." J. Struct. Eng. 131: pp. 1593-1600.

49. Naser M.Z., Kodur V.K.R. (2016). "Factors Governing onset of Local Instabilities in Fire Exposed Steel Beams." Journal of Thin-Walled Structures, Vol. 98, pp. 48-57.

50. Naser M.Z., Kodur V.K.R. (2015). "A Probabilistic Assessment for Classification of Bridges Against Fire Hazard." Fire Safety Journal, Vol. 76, pp. 65–73.

51. Naser M.Z., Kodur V.K.R. (2015). "A Probabilistic Assessment for Classification of Bridges Against Fire Hazard." Fire Safety Journal, Vol. 76, pp. 65–73.

52. NFPA 5000, (2015). "Building Construction and Safety Code." Edition 2015, Quincy, MA.

53. NFPA 502, (2011). "Standards for Road tunnels, Bridges, and Other limited Access Highways." Edition 2011, Quincy, MA.

54. Nie, J., Xiao, Y., Chen, L., (2004), "Experimental Studies on Shear Strength of Steel–Concrete Composite Beams." J. Struct. Eng., 130 pp. 1206-1213.

55. NIST GCR 02-843-1, Analysis of Needs and Existing Capabilities for Full-Scale Fire Resistance Testing, 2008.

56. National Institute of Standards and Technology (NIST), (2005). "Final Report on the Collapse of the World Trade Center Towers." Retrieved August 26, 2016.

57. Ollgaard, J.G., Slutter, R.G., Fisher, J.W., (1971). "Shear strength of stud connectors in lightweight and normal weight concrete." Eng J AISC, 8, pp. 55-64.

58. Payá-Zaforteza I., Garlock M.E.M. (2012). "A Numerical Investigation on the Fire Response of a Steel Girder Bridge. Journal of Constructional Steel Research, vol. 75: pp. 93-103.

59. Ramachandran, G. (1979). "Statistical methods in risk evaluation." Fire Saf J 80.

60. Rahikainen, J., Keski-Rahkonen, O. (2004). "Statistical determination of ignition frequencies of structural fires in different premises in Finland." Fire Technol, pp.335–53.

61. Rutstein, R. (1979). "The estimation of fire hazard in different occupancies." Fire Surv.

62. Rychlik, I., Rydén, J. Probability and risk analysis. An introduction for engineers. Berlin: Springer, 2006.

63. Rydén, J., I Rychlik, I., (2006). "A note on estimation of intensities of fire ignitions with incomplete data." Fire Safety Journal, 41. Pp. 399-405.

64. Romeijn, A., Sarkhosh, R., de Hoop, H., (2009). "Basic parametric study on corrugated web girders with cut outs." J Constr Steel Res, 65, pp.395–407.

65. Sagui W.T. (2013). "Steel Design" 5th Edition, Thompson Canada limited, Inc., Ontario.

66. Scandella, C., Knobloch, M., Neuenschwander, M., Fontana M., (2014). "Fire resistance of plate girders." EUROSTEEL 2014, September 10-12, 2014, Naples, Italy.

67. Scheer J. Failed Bridges: Case Studies, Causes and Consequences, John Wiley & Sons, 2010.

68. Shanmugam, N., Lian, V., Thevendran, V., (2002). "Finite element modeling of plate girders with web openings." Thin-Walled Struct, 40: pp. 443–64.

69. Shanmugam N. and Baskar K. (2003). "Steel–Concrete Composite Plate Girders Subject to Shear Loading." Journal of Structural Engineering, vol. 129(9): pp. 1230–1242.

70. Sinur, F., Beg, D., (2013). "Moment–shear interaction of stiffened plate girders—tests and numerical model verification." J Constr Steel Res, 85: pp. 116–29.

71. Standards Australia. (2003). "Composite structures. Part 1: Simply supported beams." AS2327.1, Standards Australia International, Sydney.

72. U.S. Fire Administration Fire Estimates, (2003), U.S. Department of Homeland Security • U.S. Fire Administration, National Fire Data Center, Emmitsburg, Maryland 21727.

73. U.S. Fire Administration/Technical Report Series, Highrise Office Building Fire One Meridian Plaza, Philadelphia, Pennsylvania, USFA-TR-049/February 1991

74. Vasdravellis, G., Uy, B., (2014). "Shear Strength and Moment-Shear Interaction in Steel-Concrete Composite Beams." J. Struct. Eng. ASCE, 140(11).

75. Vimonsatit V., Tan K., Qian Z. (2007). "Testing of Plate Girder Web Panel Loaded in Shear at Elevated Temperature." Journal of Structural Engineering, vol. 133(6): pp. 815-824.

76. Wainman D.E., Kirby B.R. (1989). "Compendium of UK Standard Fire Test Data for Unprotected Steel-1." Published by British Steel Technical and Swinden Laboratories, Rotherham, UK.

77. Wardhana, K., Hadipriono, F., (2003). "Analysis of Recent Bridge Failures in the United States." J. Perform. Constr. Facil., 17, pp. 144–150.

78. Wellman, E.I., Varma, A.H., Fike, R., Kodur, V., (2011) "Experimental Evaluation of Thin Composite Floor Assemblies under Fire Loading." ASCE Journal of Structural Engineering, 137, pp. 1002-1016.

79. White, D.W., Barker, M.G., (2008). "Shear resistance of transversely stiffened steel I-girders." J Struct Eng, 134: pp. 1425–36.

80. William, K., Warnke, E., (1975). "Constitutive model for the triaxial behavior of concrete." in International Association for bridge and Structural Engineering.

81. Wong V.Y.B., Burgess I.W., Plank R.J. (2010). "Experimental and Analytical Investigations of the Behaviour of Protected Composite Floor Beams with Web Opening in Fire." Proceedings of 6th International Conference on Structures in Fire, Michigan State University, East Lansing, USA.

82. Zeinoddini, VM., Schafer, BW., (2012). "Simulation of geometric imperfections in cold-formed steel members using spectral representation approach." Thin-Walled Structures, 60, pp. 105-117

83. Zhao, B., Kruppa, J. (1993). "Fire resistance of composite slabs with profiled steel sheet and of composite steel concrete beams Part 2: Composite beams." Centre technique industriel de la construction métallique.